University of the West of England
BRISTOL

Interaction of nitric oxide with auxin and ethylene signalling in Arabidopsis root gravitropism

Kannan Vembu

A thesis submitted in partial fulfilment of the requirements of the University of the West of England, Bristol for the degree of Doctor of Philosophy

Faculty of Health and Applied Sciences, University of the West of England, Frenchay Campus, Coldharbour Lane, Frenchay, Bristol, BS16 1QY
December 2016

Abstract

Gravitropism is required for the appropriate alignment of the plant root and shoot. According to the Cholodny-Went hypothesis, gravity induces asymmetric accumulation of auxin in the lower side of the root tissue. More recent studies on root gravitropism have also shown asymmetric accumulation of nitric oxide (NO) in response to gravity, and suggested the involvement of ethylene and NO signalling as well as auxin. Hence, this project aimed to investigate how NO, auxin and ethylene signalling interact in root growth, development and gravitropism. Arabidopsis mutants with defects in these hormonal signals were used in gravistimulation experiments. As expected, Col-0 (WT) plants displayed root bending 2 h after gravistimulation, but auxin mutants (*aux1*, *axr2* and *axr3*) did not exhibit any root bending in response to gravistimulation. Roots of ethylene mutants showed reduced root bending compared to WT. Nitrate reductase mutants *nia1* and *nia2* also revealed reduced root bending, and *nia1* showed slower bending than *nia2*. Exogenous application of the auxin NAA and the NO donor SNAP increased gravitropic bending. The application of the ethylene precursor ACC reduced root bending in the presence of NO, but increased bending in the absence of NO.

The localization of NO in response to gravitropism was investigated using confocal microscopy. Gravitropism induced asymmetric accumulation of NO in WT in the lower side of the bending zone of roots, whereas auxin mutants *aux1* and *axr2* localised NO ubiquitously in the root. NIA1 (nitrate reductase 1) transcript levels in WT root tips were measured using qPCR. The NIA1 transcript starts to accumulate after gravistimulation, reaching a two fold higher level after 2 h, before gradually subsiding. The findings suggested that functional auxin signalling is a prerequisite for NO signalling, and that *NIA1* mediated NO induces the root bending.

To ascertain the sub-cellular localization of NIA1 in response to gravity and other hormonal interactions, NIA1 transcriptional and translational mGFP4 reporter constructs were made and transformed into the WT and auxin, ethylene and NR mutant plants. Integration of the reporter construct in the plant genome was confirmed by PCR and sequencing. Initial confocal experiments showed the successful expression of NIA1-driven mGFP4 fluorescence in roots and stomatal guard cells. Further experiments with these transgenic lines will be needed to examine the role of NO in gravitropism and cross-talk with other phytohormones.

Acknowledgement

I take this great opportunity to thank everyone, who has rendered their valuable support both in my academic and personal life in and out of the university.

I wholeheartedly thank my supervisors Dr Heather Macdonald and Dr Ian Wilson for their sustained support and valuable guidance throughout my research programme. Copious thanks to Dr Iain Weir for his help in statistical analysis amidst his tight schedules.

I would also like to thank UWE for funding and the technical staff especially Dave Cory and Alison for training me to get hands-on with instruments and its supporting tools.

I would like to thank my friends Guru, Gopal, Bharani, CV karthikeyan, Riyaz, Mr&Mrs Nathan Ganapathi and Maithili, Vetriventhan, Ashokkumar, Nandakumar, Loganathan, Karthikeyan, Jey, Tharmaratnam Ratnakumar, for their advice, support, and help during my PhD. Without their moral support, I would have been distressed and lost track of my goals, they reminded me constantly of my responsibilities and encouraged me to move forward with a greater zeal.

I would like to thank my Family, primarily my Parents Mr&Mrs Vembu and Parvathi, My siblings Muthuramalingam and Ganesan, Miss Thambiratti and my loving wife Mrs Kumutha Kannan for their unconditional love, support and believing my abilities to accomplish my PhD.

I would like to thank all my teachers from my alma matter. Much deserving thanks to my master's supervisor Dr V. Udayasuriyan, Bt lab at CCMB, Tamil Nadu Agricultural University, where I had the opportunity to critically learn the basic molecular biology and cloning techniques.

I wish to make an Omnibus statement to thank everyone who have been incredible support during the past few years of my research, if I have left anyone its totally unintentional as I am completely into my thesis submission.

With complete honour and satisfaction, I dedicate this Thesis to my Parents and my new born daughter KavyaShree.

Contents

List of Figures

List of Tabels

List of abbreviations and units

bp	base pair
cm	centimetre
DNase I	deoxyribonuclease I
dNTP	deoxynucleotide triphosphate
EDTA	ethylenediaminetetraacetic acid
et al.	et alia (and others)
EtBr	ethidium bromide
g	gram
h	hour(s)
IPTG	isoprophyl-ß-D-thiogalactopyranoside
kb	kilobase
kDa	kiloDalton(s)
kV	kilovolts
λ	lambda
L	litre
M	molar
mg	milligram
min	minute(s)
ml	millilitre
mM	millimolar
µg	microgram
µs	microsecond
µM	micromolar
µm	micrometer
ng	nanogram
nm	nanometer
OD	optical density
Sec	second(s)
Temp	Temperature
TE	Tris, EDTA
U	unit(s) of enzyme activity
UV	ultraviolet
V	volts
v	volume
v/v	volume/volume
W	weight
WT	wildtype
w/v	weight/volume
xg	times gravity(s)

ABA	abscisic acid
ACC	1-aminocyclopropane-1-carboxylic acid
ACO	I-Aminocyclopropane-I-carboxy lie acid oxidase
AtNOA1	A. thaliana NITRIC OXIDE associated 1
AtNOS1	A.thaliana NITRIC OXIDE SYNTHASE 1
AUX1	AUXIN INSENSITIVE1
BLAST	Basic Local Alignment Search Tool
CaMV	Cauliflower mosaic virus
$CaCl_2$	calcium chloride
cDNA	complementary DNA
chl3	chlorate resistant mutant
Col-0	Columbia-0
cPTIO	2-(4-carboxyphenyl)-4,4,5,5-tetramethylimidazoline-1-oxyl-3-oxide
C_2H_4	ethylene
CI	confidence interval
cGMP	cyclic guanosine monophosphate
Ca_2^+	calcium chloride
Cys	cysteine
DAF-2D	4, 5-diaminofluorescein diacetate
DNA	deoxyribonucleic acid
dNTP	deoxyribonucleotide
dsDNA	double standard DNA
EC	Enzyme Commission
EDTA	Ethylenediaminetetraacetic acid
(eNOS)	endothelial NOS
FAD	flavin adenine dinucleotide
GSNO	S-Nitrosylated glutathione
GSSH	Glutathione disulphide
GFP	green fluorescent protein
gDNA	genomic DNA
GUS	beta-glucuronidase
HA	hydroxylamine
Hb	Haemoglobins
H_2O_2	Hydrogen peroxide
IAM	indole acetamide
IBA	Indole-3-butyric acid
IAOx	indole-3- acetaldoxime
(iNOS)	inducible NOS
L-NMMA	L-NG-Nitroarginine methyl ester
LB	Luria-Bertani
LUC	Luciferase

LRF	lateral root formation
MAPK	Mitogen- activated protein kinase
MTA	5'-methylthioadenosine
$MgCl_2$	Magnesium chloride
mGFP4	modified green fluorescent protein 4
MES	2(N-morpholino) ethanesulfonic acid
Mo-MPT	Mo-molybdopterin
NaCl	sodium chloride
NADH	nicotinamide adenine dinucleotide
NADPH	nicotinamide adenine dinucleotide phosphate
NCBI	National center for biotechnology information
NIA1pro-mGFP4	2.2 kb NIA1 promoter+mGFP4
NIA1pro-NIA1-mGFP4	2.2 kb NIA1 promoter+*NIA1* gene+mGFP4
NO	Nitric oxide
NO_3	nitrate
NO_2	nitrite
Ni-NOR	nitrite:NO oxidoreductase
nsHb	nonsymbiotic Haemoglobin
NH3	Ammonia
NR	nitrate reductase
NOS	nitric oxide synthases
nNOS	neuronal NOS
ONOO	Peroxynitrite.
OD	optical density
$O2^{\bullet}$	superoxide
PAT	polar auxin transport
PG	polygalacturonase
pH	potential of hydrogen
PIN	PIN-FORMED
PCR	Polymerase chain reaction
PTM	post translational modifications
QC	Quiescent center
Q-RT-PCR	Quantitative real time PCR
RNS	reactive nitrogen species
ROS	**r**eactive oxygen species
RHF	root hair formation
RNA	ribonucleic acid
RT-PCR	reverse transcription PCR
SAM	**(***S*-AdoMet) *S*-Adenosyl methionine
sGC	Soluble Guanylate cyclase
S-NO	S-nitrosothiol
SE	standard error
SNAP	S-nitroso-N-acety lpenicillamine
18 S	18 S ribosomal subunit

28 S	28 S ribosomal subunit
T-DNA	Transfer DNA
TRAF	Tumor necrosis Receptor Associate Factor
Taq	DNA polymerase from *Thermus aquaticus*
Trp	Tryptophan
WEI	WEAK ETHYLENE INSENSITIVE
WT	wildtype
X-gal	5-bromo-4-chloro3-indolyl-ß-D-galactopyranoside

A. thaliana	*Arabidopsis thaliana*
A. tumefaciens	*Agrobacterium tumefaciens*
E. coli	*Escherichia coli*
N. tabacum	*Nicotiana tabacum*
Z. mays	*Zea mays*

Chapter 1 Introduction

1.1 Overview

To date, scientists have focused mainly on shoot biomass and grain yield to increase food grain production. The first green revolution used more fertilizer to increase crop yield. Root traits are another important factor to increase food grain production. Plant root growth and development plays a central role in overall plant growth which could lead to better shoot biomass and greater yield. One way to increase the nutrient uptake capacity is by improving root system architecture (Den Herder *et al.,* 2010). Simulation studies by Hammer *et al.* (2009) showed that changes in root system architecture are responsible for increased biomass accumulation and historical yield of maize in the US corn belt.

Plant roots respond to many external signals. Gravity is one of the important external stimuli responsible for roots to grow downward (Gravitropism) and it's one of the critical processes in root development. Plant signalling molecules like auxin, ethylene and nitric oxide (NO) are involved in gravitropism (Hu *et al*., 2005; Ma and Ren, 2012). This introduction will discuss plant roots, gravitropism and hormones involved in gravitropism, focussing on NO and its interactions with auxin and ethylene.

1.2 The plant root

Plant roots play a vital role in anchorage of the plant to the soil and absorption of water and mineral nutrient from it. Root development is therefore a fundamental aspect of plant biology with great economic and ecological importance. Plant roots are susceptible to abiotic stresses like drought, waterlogging, salinity and heavy metals. A better understanding of the signalling pathway and hormone interaction in the root development will pave the way to improve the yield of food crops.

1.3 Basic root anatomy of Arabidopsis

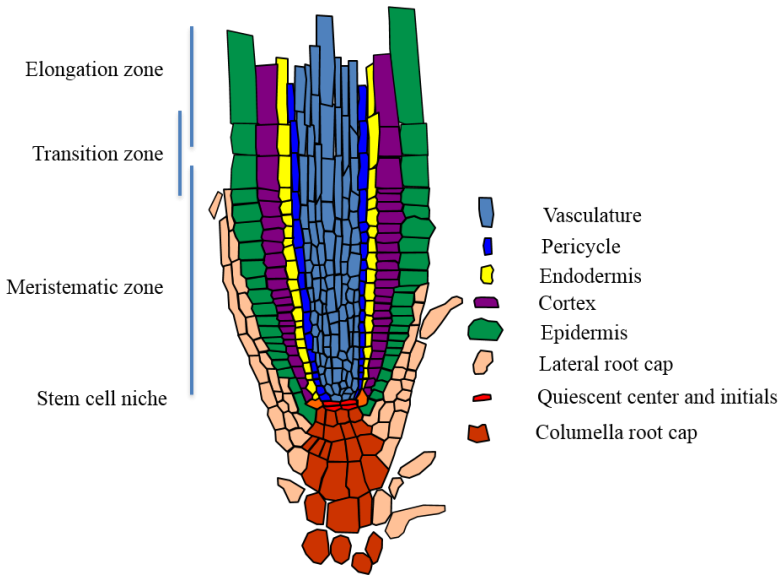

Figure 1-1: The Arabidopsis root tip (Source: Yvon Jaillais) -http://www.ens-lyon.fr/RDP/SiCE/Resources.html

Arabidopsis roots (from outside to inside) consist of epidermis, cortex, endodermis, pericycle and vasculature. Quiescent center (QC) and the columella root cap are located in the center of root tip.

The small size and simple anatomy of Arabidopsis is useful to study root traits. Arabidopsis cell layers (from outside to inside) consist of epidermis, cortex, endodermis, pericycle and vasculature (Figure. 1-1). The Quiescent center (QC) is present in the center of root tip. QC and initials forms the stem cell niche in the Arabidopsis root (Stahl and Simon, 2004). All the root cells such as epidermis, cortex, endodermis, pericycle, vasculature and columella are generated from the stem cells around the QC. The QC is mitotically inactive in Arabidopsis under optimal condition (Aichinger *et al.*, 2012), but stress-related phytohormones and DNA damage activate QC cell division (Heyman *et al.*, 2014). The root can be divided into four distinct zones, namely the meristematic zone, transition zone, elongation zone and growth terminating zone. The meristematic zone spreads up to 200 µm from the root cap. All cells in this zone are very active. The transition zone stretches from 200 µm to 520 µm away from the root cap and cells in this

zone grow slowly. Most of the cells in the distal portion of the transition zone participate in cell division. Proximal cells differentiate to enter the cell elongation zone. This zone is easily identifiable because of the presence of nuclei in the centre of the cell, small vacuoles, and the approximately equal length and width of the cells. The elongation zone covers the region from 520 µm to 850 µm. Cells in this zone elongate very fast; vacuoles become very large and push the nuclei to the side of the cell wall. Root hairs develop in this zone from the outer apical portion of the tricoblast (epidermal cells of roots which produces root hairs). The growth terminating zone spreads from 850 µm to 1500 µm from the root cap. Cells in the transition zone are the most sensitive towards external signals such as gravity, humidity, light and oxygen (Verbelen *et al.*, 2006).

1.3.1 Gravitropism

Plants respond to an array of environmental and developmental stimuli such as light, temperature and gravity. Gravity is one of the most significant cues to which plants must adapt to survive. Gravitropism is a process that dictates the growth of plant organs along a specific vector relative to gravity. It ensures that roots will grow down into the soil, where they take up water and nutrients whereas shoots will grow upwards, into the air, where they can photosynthesize, reproduce and disperse seed. In crop plants, gravitropism contributes to the optimal utilization of available resources and permits plants prostrated by wind and rain to straighten up.

1.3.2 Steps involved in gravitropism

Gravitropism involves several steps organized in a specific response pathway. These include the perception of a gravistimulus, the transduction of this mechanical stimulus into a physiological signal, the transmission of this signal from the site of sensing to the site of response, and a curvature-response which allows the organ tip to resume growth at a predefined set angle from the gravity vector. The primary sites for gravity sensing are

located in the cap for roots, and in the endodermis for shoots. The curvature response occurs in the elongation zones for each organ. Upon gravistimulation, a gradient of auxin appears to be generated across the stimulated organ, and be transmitted to the site of response where it promotes a differential growth response. Therefore, while the gravity-induced auxin gradient has to be transmitted from the cap to the elongation zones in roots, there is no need for a longitudinal transport in shoots, as sites for gravity sensing and response overlap in this organ (Masson *et al*., 2002). A combination of molecular genetics, physiology, biochemistry and cell biology, coupled with the utilization of *Arabidopsis thaliana* as a model system, have recently allowed the identification of a number of molecules involved in the regulation of each phase of gravitropism in shoots and roots of higher plants.

1.3.3 Hormones involved in gravitropism

Plant hormones are small organic molecules which influence many physiological functions at low concentrations. Hormones can be synthesized locally or transported over large distances to trigger an appropriate response. The hormones auxin, ethylene and nitric oxide have been shown to be involved in gravitropism. The synthesis, perception and physiological roles of these hormones and the interactions between them are discussed in the following sections.

1.4 Nitric oxide as a signalling molecule

Nitric oxide (NO) is a small, free radical, gaseous, multifunctional lipophilic signalling molecule easily able to diffuse through the plasma membrane. NO reacts rapidly with species containing unpaired electrons such as molecular oxygen, superoxide anions and metals (Mayer and Hemmens, 1997; Crawford, 2006). It was first described in mammals as an endothelium-derived relaxing factor and later shown to be an important signalling

molecule controlling many biological functions in humans. The biological importance of NO was widely recognized by the scientific community and to honour this NO was announced as a “Molecule of the year in 1992”. In 1998, the Nobel Prize for Physiology and Medicine was awarded to three scientists, Robert F. Furchgott, Louis J. Ignarro, and Ferid Murad for their contribution to the “discovery of NO signalling role in the cardiovascular and nervous systems.” Later it was found to be an important signalling molecule in plants (Arasimowicz and Floryszak-Wieczorek, 2007). It participates in all physiological, growth and developmental functions of plants, including seed dormancy, germination, root development, lateral root growth, root gravitropism, stomatal movement, leaf senescence, flowering, pollen tube growth, and fruit ripening. It is also involved in response to biotic and abiotic stress, such as viral and bacterial infections, drought and salt stress (Delledone et al., 1998; Qiao and Fan, 2008).

1.4.1 NO in plants

NO was the second gaseous signalling molecule discovered in plants after ethylene. The presence of NO in plants was reported much earlier than the discovery of NO as a signalling molecule in humans. The release of NO from herbicide-treated soybean leaves was first recorded by Klepper (1979). Once NO was identified as an important signalling molecule in an animal system it attracted more attention from plant scientists. The action of NO as a defence signalling molecule in response to bacterial and viral exposure in a plant was first reported by Delledone *et al*. (1998) and Durner *et al*. (1998). During the last two decades, NO biology in plants has been the subject of much research, but much of its signalling pathway remains unclear. Basic questions about how NO is synthesized and used in plants remain to be answered (Wilson *et al*., 2008), and how NO interacts with other plant hormones needs to be established.

1.4.2 Roles of NO signalling in plants

It is clear that NO is an important signalling molecule in plants (Freschi, 2013), controlling almost all physiological and developmental functions, either alone or by interacting with other plant hormones such as auxin, ethylene and abscisic acid. It plays a significant role in root growth and leaf expansion, photomorphogenesis and senescence (Beligni and Lamattina, 2001; Neill *et al*., 2003), as well as in rapid physiological reactions such as stomatal closure (Desikan *et al*., 2002, 2004). The involvement of NO in promoting root growth has been observed by Gouvea *et al*. (1997), who found that NO induces cell elongation in a similar way to auxin. A transient increase in NO concentration was shown to be involved in adventitious root development induced by indole acetic acid (Pagnussat *et al*., 2002). The authors suggest that NO could mediate the auxin response in this process. The participation of NO in gravitropic bending in soybean roots has been described by Hu *et al*. (2005). They found an asymmetric accumulation of NO in the primary root in response to gravistimulation. Similarly Pagnussat *et al*. (2002) observed that NO acts downstream of auxin leading to the accumulation of cGMP.

1.4.3 NO biosynthesis in plants.

The sources of NO in animal systems was well characterised, but the sources of NO in plants is not clearly understood; this needs to be investigated by further research. Two major enzymatic pathways have been proposed to be involved in NO synthesis in plants, the oxidative and reductive pathways (Moreau *et al.*, 2010). In addition, non-enzymatic pathways are also involved in NO synthesis. The oxidative pathway consists of oxidation of L-arginine, polyamine and hydroxylamine, whereas in the reductive pathway nitrate is reduced by nitrate reductase (NR), plasma membrane bound Ni-NOR (nitrite:NO oxidoreductase) and organelles such as mitochondria and chloroplasts (Figure 1-2).

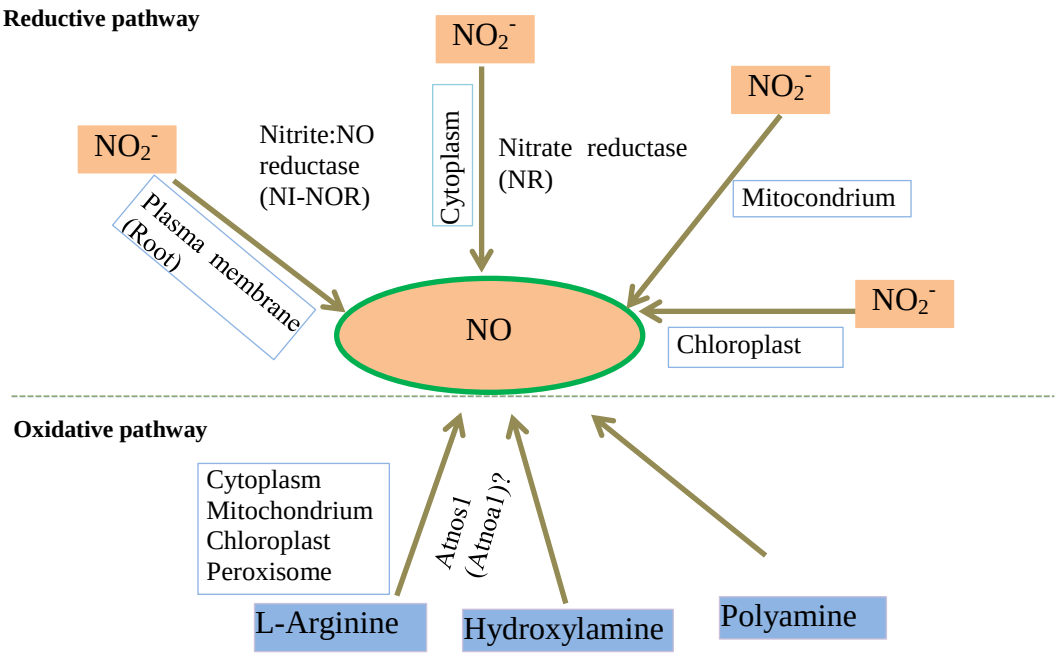

Figure 1-2: Various routes of nitric oxide production in plants (re-drawn from Wilson *et al.*, 2008). Copyright permission License Number-4237640475433.

In plants NO is synthesized by different pathways in accordance with specific condition and cell type. NO can be produced from nitrite in the cytoplasm, stomatal guard cells and in roots by NR enzyme and also in mitochondria and chloroplasts, by NI-NOR (nitrite: NO reductase) in root the exact mechanism of this pathway is not clearly understood. L-arginine-dependent NOSs (nitric oxide synthases)- mediated NO synthesis has been reported in plants but Atnos1 is not a NOSs. Alternative candidates for this role have not yet been found in plants. NO can also be synthesized from hydroxylamine and polyamine.

1.4.3.1 Do plants contain nitric oxide synthase?

In animals, NO is generated primarily by three homologous nitric oxide synthases (NOSs), namely neuronal NOS (nNOS), inducible NOS (iNOS) endothelial NOS (eNOS). NOSs are heme-containing proteins belonging to the cytochrome P450 family which oxidize L-arginine to L-citrulline and NO using NADPH as an electron donor and molecular oxygen (Mayer and Hemmens, 1997; Lamotte *et al.*, 2005; Crawford, 2006). The existence of NOS in plants is a topic of debate. NOS-like activity in plants has been inferred from studies using NOS inhibitors (L-arginine analogues) to inhibit NO-dependent processes in plant

extracts (Baudouin, 2011; Fancy *et al.*,2016). Guo *et al.* (2003) isolated AtNOS1 (*A. thaliana* NITRIC OXIDE SYNTHASE 1) which has 16% homology to a protein from snail (*Helix pomatia)*; this group reported arginine-dependent NO synthesis in plant's, and proposed that AtNOS be considered as a plant's NOS, behaves like mammalian eNOS and nNOS. Atnos1 T-DNA insertion mutants showed reduced NO accumulation and phenotypic defects (low fumarate, pale green leaves, slow growth and reduced chlorophyll content). In contrast, experiments carried out by Moreau *et al.* (2008) showed AtNOS1 did not bind arginine and failed to reproduce the earlier result of NO generation *via* oxidising arginine. They also failed to produce radiolabelled citrulline from [3H] arginine. Based on these results, the protein AtNOS1 is no longer considered to be a NOS; it has been renamed to AtNOA1 (*A. thaliana* NITRIC OXIDE associated 1). AtNOA1 contains a GTPase domain suggesting that it may participate in mitochondrial biogenesis and translation (Zemojtel *et al.,* 2006). So far no genetic evidence for the presence of NOS has been reported in Arabidopsis or in higher plants.

Recently Foresi *et al.* (2010) characterized two NOS sequence from a recently published genome of two photosynthetic green algae *Ostreococcus tauri* and *O. lucimarinus*. They found a sequence in *O. tauri* 45% similar to the mammalian NOS. They also expressed the recombinant *O. tauri* NOS in *E. coli* and found a 2.5 fold higher level of NO than in controls following application of L-Arginine. Cell viability was also increased. Frohilch and Durner (2011) have suggested that higher plants lost NOS during evolution. An intensive genome search in 1000 land plants carried out by Jeandroz *et al.* (2016) did not find any NOS-like enzyme and they concluded plants evolved to synthesize NO by a different mechanism. Arginine-dependent NO production takes place in peroxisomes, mitochondria and plastids (Baudouin, 2011), but the mechanism is unknown.

In animals, hydroxylamine also serves as a substrate for oxidative NO synthesis. Based on this Rumer *et al.* (2009) reported that, the external application of hydroxylamine (HA) to nia double mutant tobacco (*nia 30*) cell culture increased NO emission, but questioned the natural availability of HA in plants. Tun *et al.* (2006) reported polyamine-induced NO synthesis in specific tissues (elongation zone of Arabidopsis root tip and vein and trichomes of primary leaves) in Arabidopsis seedlings.

1.4.3.2 Nitrate reductase (NR)

NR (EC 1.6.6.1) is a flavoprotein, and a homodimer containing two identical subunits of approximately 100 kDa. Each subunit contains flavin adenine dinucleotide (FAD), heme-Fe, and Mo-molybdopterin (Mo-MPT). NR is a cytosolic enzyme primarily involved in nitrogen assimilation, which catalyzes nitrate (NO_3^-) into nitrite (NO_2^-) by NAD(P)H-dependent manner. NR can also further catalyse nitrite into NO by the following reaction: $NAD(P)H + 3H_2O^+ + 2NO_2^- \rightarrow NAD^+ + 2NO + 5H_2O$ (Yamasaki and Sakihama, 2000; Wilson *et al.,* 2008; Gupta *et al.*2011). This reaction has been demonstrated *in vivo* using soybean leaflets by Dean and Harper. (1986), and *in vitro* using purified NR from different plant species by Rockel *et al.* (2002). Both genetic (using *nia1, nia2* mutants in ABA induced stomatal closure) and pharmacological (using NR inhibitor tungstate) studies support the role of NR in NO generation in plants. Nitrite is used as the main substrate to generate NO by NR (Desikan *et al.,* 2002; Bright *et al.,* 2006).

1.4.3.3 Other sources of NO in plants

Apart from NR and NOS, other enzymatic NO synthesis pathways are also present in plants. The nitrite:NO reductase (ni:NOR) is a 310 kDa, plasma membrane-bound, nitrite-reducing enzyme converting nitrite into NO using cytochrome C as an electron donor in tobacco roots (Stohr and Stremlau, 2006). Studies in tobacco, pea and barley found that mitochondria are one of the major NO producing organelles, by nitrite reduction in the

presence of NADH under anoxic conditions in roots. (Gupta *et al.,* 2005; Gupta *et al.,* 2010). Soybean chloroplasts also synthesise NO via arginine or nitrite (Jasid *et al.,* 2006). Non-enzymatic synthesis of NO has also been reported by Bethke *et al.* (2004) in barley aleurone layer under low pH conditions.

1.4.3.4 NR is the most important source of NO in plants

As discussed in the previous section 1.4.3, many NO synthesis mechanisms function in plants, but recent studies support NR-mediated NO synthesis as one of the important mechanism in plants (Mur *et al*., 2013). The NR-mediated reductive pathway is one of the best characterised enzymatic sources of NO in plants (Gupta *et al.,* 2011). Pharmacological studies using the NOS inhibitor $_{L}$-NMMA, and genetic studies, using *Atnos1* and the NR double mutant *nia1 nia2* showed that Indole-3-butyric acid (IBA)-induced NO synthesis solely depends on NR activity. NO synthesis induced by auxin, ethylene, ABA, cytokinin, H_2O_2 and hypoxia is NR-mediated. *Arabidopsis thaliana* contains two NR genes, namely *NIA1* and *NIA2,* both located on chromosome 1. They have 83.5% amino acid sequence homology with sequence divergence in the N-terminal region. Both *NIA1* and *NIA2* genes are expressed in roots and leaves, but the expression is tissue specific and responds differently to signals (Cheng *et al.,* 1991). In guard cells, NO synthesis mediated by the NR isoform NIA1 plays a significant role in stomatal closure (Wilson *et al.,* 2008). Cytokinin-mediated increased NR activity in Arabidopsis seedlings is only due to the increased NIA1 transcript level (Yu *et al.,* 1998). NO-mediated lateral root development in Arabidopsis is based on modulation of NIA2 activity by H_2O_2 induced mitogen- activated protein kinase 6 (Wang *et al.,* 2010).

1.4.4 NO removal in plants

Once NO has triggered the initial signalling event, it is removed or scavenged by a number of different mechanisms. Increased NO accumulation can be due to reduced rate of

removal rather than a higher rate of synthesis (Misra *et al.,* 2010; Wilson *et al.,* 2008). There are four different NO removal mechanism functions in plants (Figure 1-3). First, NO is an unstable and reactive molecule, readily reacting with oxygen to form nitrite and nitrate. Second, NO reacts with reactive oxygen species (ROS) such as superoxide to produce peroxynitrite ($ONOO^-$). Another NO removal mechanism is via haemoglobin. Haemoglobins (Hb) have been identified in legumes, non-legumes, and actinorhizal plants. Four subfamilies of Hb are found in plants; symbiotic Hb, mainly found in legumes and a few nitrogen fixing species, and three types of non-symbiotic Hb (nsHb). The physiological functions of nsHb are not fully understood, but in maize and alfalfa classI nsHb (nsHbI) has been shown to convert NO to nitrate by an O_2 and NAD(P)H-dependent reaction. Removal of NO by nsHbI depends on signal specific NO synthesis (Gupta *et al.,* 2011). Finally, NO reacts with the tripeptide glutathione (GSH) to produce S-nitrosylated glutathione (GSNO). GSNO is considered as a NO reservoir, but it can also be further metabolized by GSNO reductase to form glutathione disulphide (GSSH) and ammonia (NH_3). Further investigation is needed to identify the exact NO removal mechanism during a specific plant condition (Neil *et al.,* 2008; Wilson *et al.,* 2008).

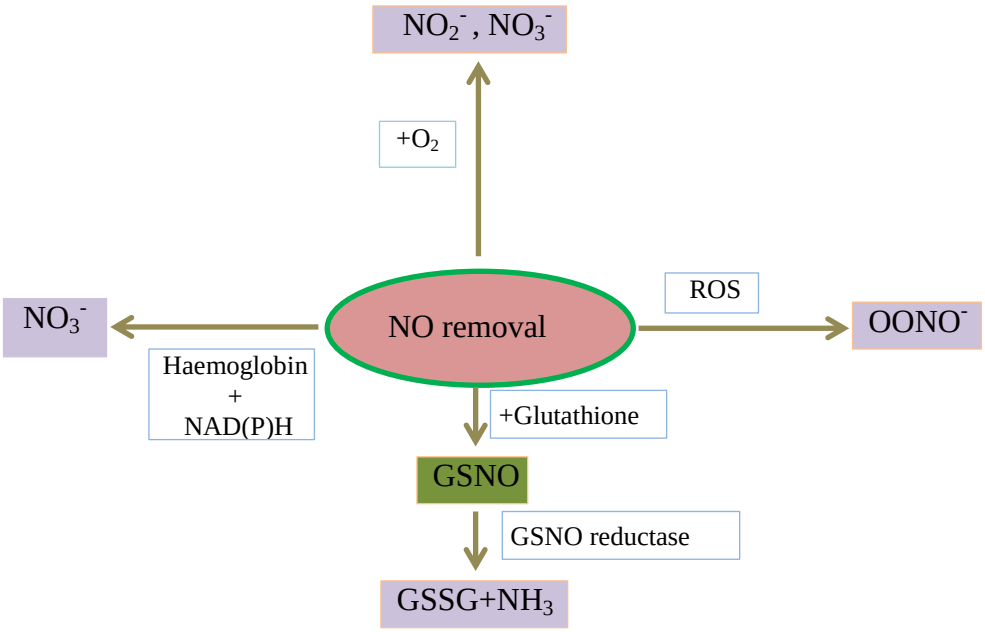

Figure 1-3: Nitric oxide removal mechanisms in plants

In plants, NO is removed after triggering specific signalling events by four different mechanisms. NO can be converted to nitrate or nitrite by oxygen or react with ROS to produce peroxynitrite or react with haemoglobin to form nitrite (NO_3^-) in an NAD(P)H dependent reaction, or reduced to S-nitrosylated glutathione (GSNO) by glutathione (GSH) which will be further reduced to glutathione disulphide (GSSG) and ammonia (NH_3) by GSNO reductase.

1.4.5 NO perception and signalling in plants

NO controls many important plant functions, which suggest plants perceive NO signals and respond accordingly. But the exact mechanism of NO perception is unclear and no plant NO receptor has been identified to date. Due to the reactive nature of NO it may have many NO perceptors (Neil *et al.*, 2008; Wilson *et al.*, 2008). External stimuli increase NO synthesis which further triggers physiological processes *via* second messengers such as cGMP, Ca^{2+}, activation of MAP kinase pathways, and modulation of gene expression. Apart from this, post-translational modifications (PTM) of target proteins such as S-nitrosylation, tyrosine nitrosylation and metal nitrosylation involve NO directly (Frohlich and Durner, 2011; Astier and Lindermayr, 2012).

Soluble guanylate cyclase (sGC) triggers the synthesis of cyclic guanosine monophosphate (cGMP). The cGMP will trigger a number of downstream signalling reactions. Hu *et al*. (2005) demonstrated asymmetric accumulation of cGMP in the bending zone of soybean roots during gravitropism in a similar way to the accumulation of auxin and NO. They also demonstrated that exogenous application of auxin or NO could increase the cGMP level.

NO also activates signalling through the MAP kinase signalling pathway, which is one of the important signalling cascades where by external stimuli are transduced into a cellular response in mammals, yeast and Fungi (Morris, 2001). MAP kinase genes have also been identified in several plant species. In tobacco, NO activates the salicylic acid induced MAP kinase signalling pathway during pathogen attack (Kumar and Klessig, 2000), and in cucumber NO activates the MAP kinase signalling pathway during IAA-induced adventitious rooting (Pagnussat *et al.*, 2004).

The NO signalling mechanism also functions through post-translational modification (PTM) of target proteins by either direct S-nitrosylation or indirect trans-nitrosylation and nitration of a tyrosine residue. S-nitrosylation is a prototypic redox-based signalling mechanism, involving the formation of S-nitrosothiol (S-NO) by reversible covalent attachment of a NO moiety to the thiol (R-SH) side chain of cysteine (Cys) residue of target protein. S-nitrosylation is one of the most studied NO-dependent PTM in plants, especially during plant defence against biotic and abiotic stress. Based on proteomic studies, more than 200 S-nitrosylated proteins have been identified so far. To date only 15 of the S-nitrosylated proteins were well characterised. (Astier and Lindermayr, 2012).

Tyrosine nitration is one of the PTM of proteins induced by NO, in a non-enzymatic reaction. NO interacts with superoxide ($O2^{\bullet-}$) to produces peroxynitrite ($ONOO^-$), one of the reactive nitrogen species (RNS) which acts as a nitrating agent, adding a nitro group to

the aromatic ring of tyrosine residues. In plants, tyrosine nitration can be detected using antibodies against 3-nitrotyrosine. Saito *et al.* (2006) in tobacco BY-2 cells treated with the 1NF1 elicitor from *Phytophthora infestans* reported tyrosine nitration in a defence response. Similarly Valderrama *et al.* (2007) found tyrosine nitration in response to salt stress in olive leaves.

Metal- nitrosylation is an another reversible PTM like S-nitrosylation. Being a free radical, NO reacts with transition metal centers like iron, copper, heme and zinc fingers. An example is soluble guanylate cyclase (sGC), which is one of the key players in animal NO signalling (Stasch and Evgenov, 2013). NO activates the sGC by binding with its heme domain, which further triggers the synthesis of cyclic guanosine monophosphate (cGMP). The cGMP will trigger a number of downstream signalling reactions. However, a NO-sensitive sGC homologue has not yet been identified in plants.

1.4.6 NO interaction with phytohormones.

In response to wide range of environmental and endogenous stimuli, NO is produced and interacts with all major classes of phytohormones. It also modulates the biosynthesis of other hormones leading to changes in physiological functions. Hormones like auxin, ethylene, abscisic acid, gibberellins, cytokinin and jasmonic acids also influence the endogenous level of NO (Freschi, 2013). Depending upon the signal, NO acts either upstream or downstream of the plant hormones. For example, during root growth and development NO acts downstream of auxin (Simontacchi *et al.,* 2013). In the case of salicylic acid accumulation, NO acts upstream of the signal. Even though NO interacts with many plant hormones, this thesis focusses on auxin and ethylene, and their interactions with NO.

1.5 Auxin

The first hormone discovered in plants was auxin. Auxin is a multifunctional plant hormone that controls almost all aspects of a plant life such as embryo and fruit development, organogenesis, vascular tissue differentiation, apical hook formation and apical dominance, root patterning, elongation and gravitropic growth. Auxin can stimulate or inhibit cell expansion depending on the concentration and on the sensitivity of the cells. This can result in different effects in different parts of the plant. Auxin promotes cell elongation in shoots and inhibits it in roots. This reflects a dramatic difference in sensitivity of these two organs to auxin (Kaufman *et al*., 1995).

1.5.1 Auxin biosynthesis

Indole-3-acetic acid is the predominant form of active auxin found in plants. Auxin is synthesized in young leaves and transported downward to the root tip (Goldsmith, 1977). Understanding of IAA biosynthesis is still incomplete. Stable isotope studies have revealed that IAA can derive from two major pathways: the tryptophan (Trp) dependent and Trp-independent pathways (Fig 1-4). Trp-independent pathway derives IAA from a precursor of Trp, anthranilate, but this pathway is not fully understood. Regulation of these biosynthetic pathways and crosstalk with other signals need to be further investigated (Tromas and Perrot-Rechemann, 2010). The Trp-dependent mechanism is well defined and it is the most important source of auxin. This is categorized into four different pathways based on the intermediates, namely indole acetamide (IAM), indole-3-pyruvic acid, tryptamine and indole-3-acetaldoxime (IAOx) (Saucer *et al*., 2013).

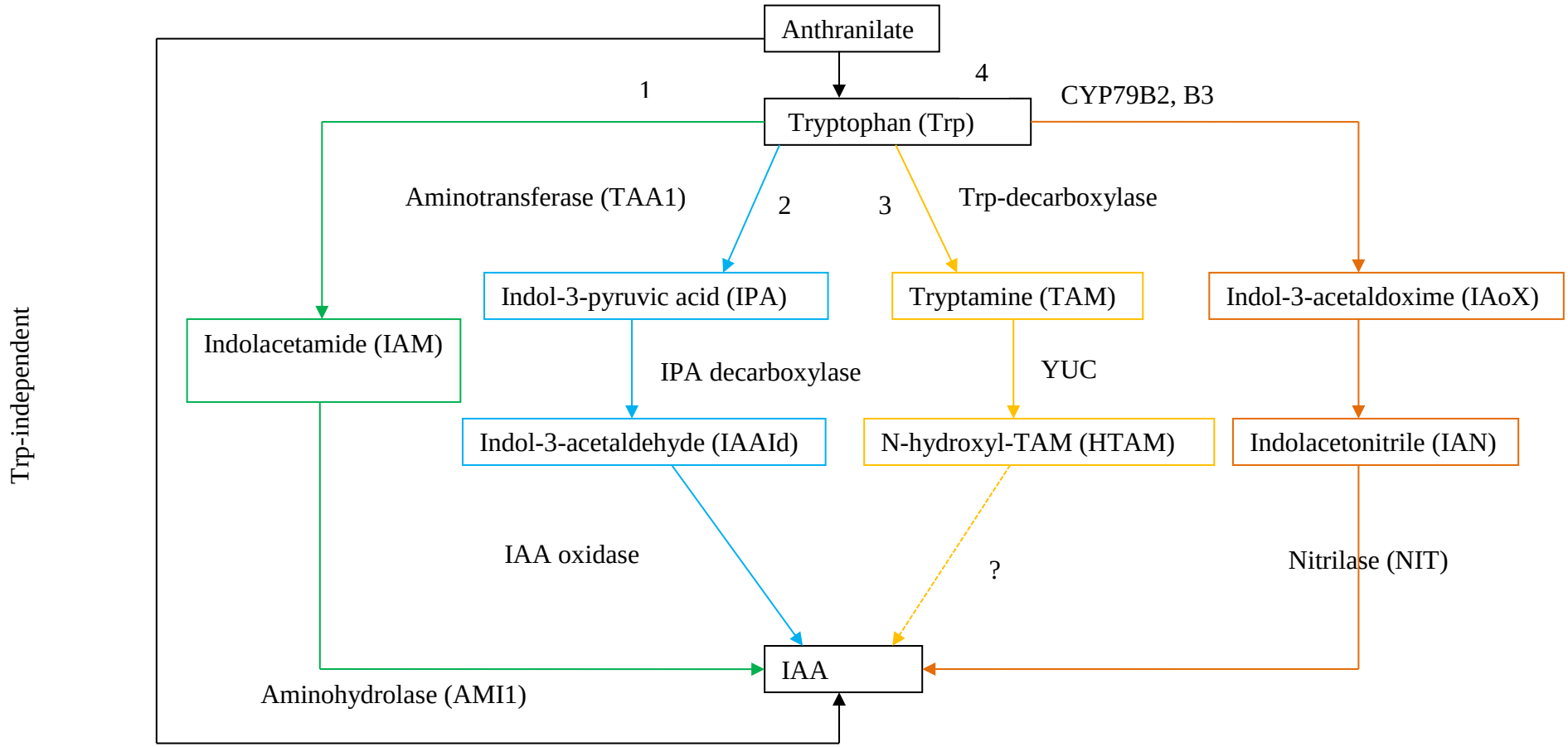

Figure 1-4: IAA biosynthesis pathways (Source: Tromas and Perrot-Rechemann, 2010) **Copyright permission obtained from ELSEVIER France.**

IAA can be synthesized from Trp-independent and Trp-dependent pathways. In the Trp-independent pathway the precursor of Trp, anthranilate, is converted into IAA. Incase of Trp-dependent pathway IAA is synthesized from four different routes. 1) Indolacetamide (IAM) as an intermediate which is transformed into IAA by an aminohydrolase (AMI1). 2) Trp is transformed into indole-3-pyruvic acid (IPA) by an aminotransferase (TAA1) and then IPA decarboxylase transforms IPA into indole-3-acetaldehyde (IAAId) which is then converted into IAA by an IAAId oxidase. 3) Trp is transformed into tryptamine (TAM) by Trp-decarboxylase then the YUCCA (YUC) protein convert, TAM to N-hydroxyl-TAM (HTAM) then subsequently HTAM is converted to IAA by an unknown mechanism. 4) Trp is converted to Indole-3-acetaldoxime (IAoX) by two cytochrome P_{450} (CYP79B2/CYP79B3) proteins. IAoX is then converted to indole acetonitrile (IAN) which is finally converted to IAA by nitrilases (NIT).

1.5.2 Auxin transport in the root

The mobile signal hormone auxin needs to be transported to accomplish its role of messenger between cells, tissues and organs. As previously mentioned auxin is mainly synthesized in young leaves and transported throughout the whole plant. There are two different types of auxin transport: long distance transport via phloem; and cell to cell auxin transport by polar auxin transport (PAT) through auxin transport proteins. Auxin transport in roots occurs in two distinct directions, acropetally and basipetally, spatially separated in two different tissues (Tanaka *et al*., 2006). The cell-to-cell PAT mechanism depends on active uptake through an influx carrier, such as AUXIN INSENSITIVE1 (AUX1), and facilitated efflux through a carrier such as a member of the PIN-FORMED (PIN) family of proteins. Different expression patterns of PIN proteins form a route for auxin flow and local distribution. Multidrug resistance p-glycoprotein is also involved as an auxin efflux carrier. The auxin transport network-mediated local auxin distribution requires the interaction of PIN proteins with other components to trigger different cellular responses in various developmental processes (Paciorek *et al*., 2006). The response pathway during gravitropism in roots has been separated into three sequential steps: gravity perception, signal transduction, and asymmetric growth leading to bending (Moulia and Fournier, 2009). The bending of the root is driven by formation of a differential auxin gradient between the upper and lower sides of the root and regulated by the polar transport of auxin (Muday and Rahman, 2008).

1.5.3 Auxin perception

In order to induce a biological response, auxin needs to be perceived by receptors. To date three auxin receptors/co-receptor systems have been identified in plants, namely 1) TIR1/AFB- Aux/IAA, 2) SKP2a and 3) ABP1. The former two systems regulate auxin dependent transcription in the nucleus, whereas ABP1 regulate auxin signalling at the

plasma membrane. Among these three receptor systems, TIR1/AFB-Aux/IAA is the best described sytem (Vanneste and Friml, 2012; Peer, 2013; Sauer *et al.*, 2013).

1.5.3.1 TIR1/AFB- *auxi*n- Aux/IAA system

Derepression of auxin response genes occurs during an increase in the intracellular auxin level. In this process auxin acts as molecular glue between domain II of AUX/IAA and Transport Inhibitor Response1/auxin related F-Box (TIR1/AFBs) subunits of the SCF complex, which adds multiple ubiquitins to the AUX/IAA substrate, thus targeting them for degradation by the proteasome (Figure1-5). This allows the derepression of ARF activators and transcription of auxin response genes (Tromas and Perrot-Rechemann, 2010). Arabidopsis contains 6 TIR1/AFBs and 29 AUX/IAA proteins. Experiments in the yeast-two hybrid system by Villalobos *et al.* (2012) showed that the interaction between specific pairs of TIR1/AFBs and AUX/IAAs depends on auxin concentration. This experiment also suggested that AUX/IAA is the determining factor for auxin affinity.

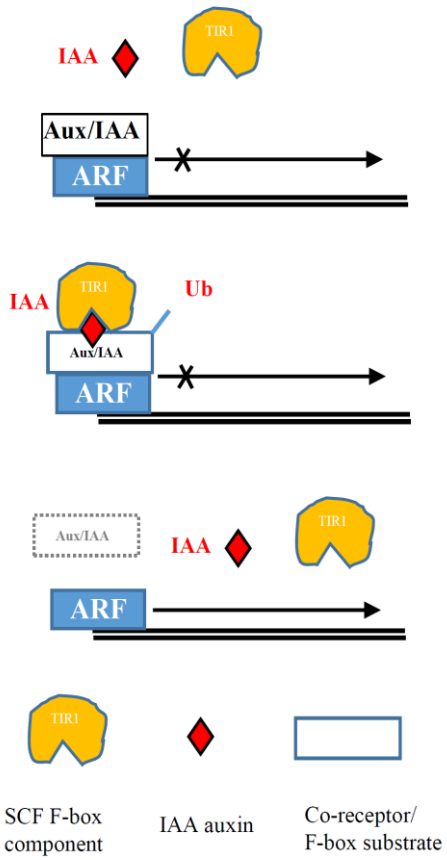

Figure 1-5: The model for the action of TIR1/AFBs-Aux/IAA (re-drawn from Peer, 2013). Copyright permission License Number: 4237611031191.

Auxin binds to the Aux/IAA and the F-box protein TIR1, leading to ubiqutinization and degradation of the Aux/IAA. This releases the transcription factor ARF allowing auxin-responsive gene expression.

1.5.4 Interaction of nitric oxide with auxin

NO and auxin function synergistically with each other. During the last decade, most of the NO and auxin interaction studies carried out were related to plant root development. Much less information is available about the role of NO in shoot and reproductive tissues (Freschi, 2013). Involvement of auxin during root development in response to nitrate has been demonstrated by Forde (2002). IAA-induced, NO-mediated adventitious rooting has been reported in cucumber; the authors suggested both NO and cGMP function downstream of auxin signalling (Pagnus *et al.,* 2003). Exogenous application of auxin has been shown to induce NO accumulation in soybean root tip and root protoplast (Hu *et al.*, 2005). These authors also found that unilateral application of auxin *via* agar blocks

increased the accumulation of NO near to the agar blocks. Auxin-induced, NO-mediated root hair initiation and elongation have been reported in both lettuce and Arabidopsis. Application of a NO scavenger reduces the root hair formation (Lombardo *et al.*, 2006). Exogenous application of indole-3-butyric acid (IBA) induces NO-mediated adventitious and lateral root formation in *A. thaliana* (Kolbert *et al.*, 2008). IBA is an inactive form of auxin which needs to be converted to the active form (IAA) for the lateral root formation. Conversion of IBA to IAA takes place in the peroxisome, where NO is synthesised and then induces lateral root formation (Schlicht *et al.*, 2013).

1.6 Ethylene

The phytohormone ethylene (C_2H_4) was the first example of a gaseous signalling molecule discovered in biological systems, which controls major plant growth and developmental responses. Ethylene is also a key regulator in response to biotic and abiotic stresses (Li and Guo, 2007). As a major plant hormone, it is involved in the regulation of essential physiological processes, such as seed germination, cell elongation, fruit ripening, senescence and abscission, root, shoot and flower development and root nodulation.

1.6.1 Ethylene biosynthesis in plants

Ethylene is synthesised via the methionine-*S*-Adomet-ACC cycle (Figure 1-6). Methionine is an amino acid, which acts as a building block for protein synthesis (Ravanel *et al*., 1998; Wang and Ecker, 2002). 80% of cellular methionine is converted to *S*-AdoMet by SAM synthase. *S*-AdoMet acts as a substrate for many biochemical pathways including polyamines and ethylene biosynthesis, and is also involved in methylation reactions to modify lipids, proteins and nucleic acids. Ethylene is synthesised from *S*-Adomet via 1-aminocyclopropane-1-carboxylic acid (ACC), in a two-step reaction catalysed by ACC synthase and ACC oxidase. The first step is the conversion of *S*-Adomet to ACC by ACC

synthase (ACS). This reaction also produces 5'-methylthioadenosine (MTA), which is converted back to methionine, which facilitates the continuous supply of methionine for the synthesis of ethylene. ACC is further oxidised by ACC oxidase to produce ethylene, CO_2 and cyanide. Cyanide is further oxidised to β-cyanoalanine to prevent toxicity during high rates of ethylene production (Wang and Ecker, 2002). Environmental and endogenous signals regulate ethylene biosynthesis through the differential expression of ACC synthase genes (Bleecker and Kende, 2000).

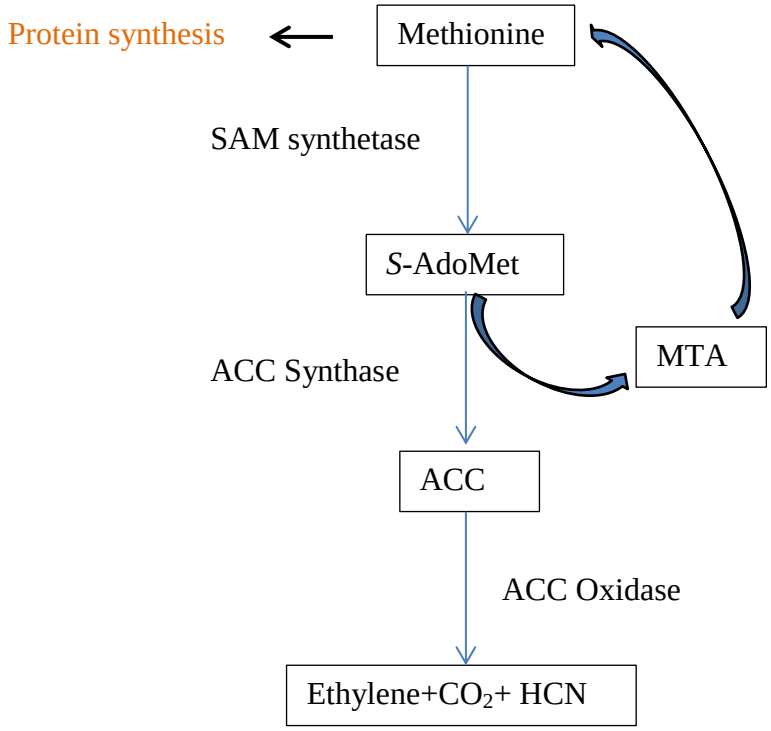

Figure 1-6: Ethylene biosynthetic pathway (Source: Wang *et al.*, 2002). Copyright permission License Number- 4237880779137.

Methionine was catalysed by SAM Synthetase to produce *S*-Adomet by consuming one molecule of ATP per molecule of *S*-AdoMet produced. *S*-AdoMet is the precursor of ACC , its also act as a precursor for polyamine synthesis pathway, ACC is synthesized from *S*-AdoMet by ACC synthase. MTA is the by product of ACC synthesis step, it will be converted back to methionine, this will help to maintain the constant methionine concentration. ACC is the immediate precursor of ethylene, ACC is further catalysed by ACC oxidase to produce ethylene and also generate carbon dioxide and cyanide.

1.6.2 Ethylene perception

Ethylene is perceived in the plasma membrane by a family of five ethylene receptors that includes ETR1, ERS1 ETR2, ERS2, and EIN4 (Figure 1-7). These receptors negatively regulate the ethylene signalling pathway. The ethylene signal is transduced from the membrane to the nucleus through a series of proteins including CTR1, EIN2, EIN5, EIN6, and EIN7. In the nucleus the EIN3/EIN3-like (EIL) family of proteins initiates the effector genes involved in the diverse responses to the hormone (Solano and Ecker, 1998).

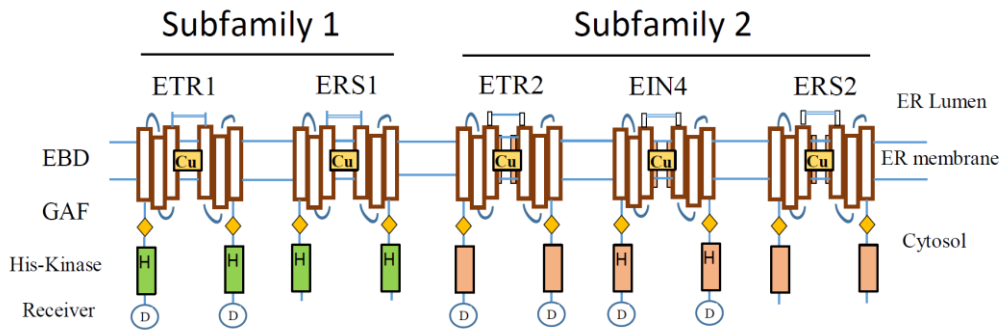

Figure 1-7: Ethylene receptors (re-drawn from Shakeel *et al.*, 2013)

Arabidopsis contains five ethylene receptors, further divided into two subfamilies based on phylogenetic analysis and structural difference. ETR1 and ERS1 belong to subfamily 1 and contain conserved His-kinase domains. ETR2, ERS2 and EIN4 belong to subfamily 2, and have a diverged His-kinase domain.

1.6.3 Ethylene signal transduction

The first step in the ethylene synthesis pathway is binding of ethylene to its receptors (Figure 1-8). Copper acts as a cofactor for ethylene binding and the receptor activity, which is supplied by intracellular copper transporter RAN1 (Hirayama *et al.*, 1999). RTE1 is located in the ER. In the absence of ethylene, RTE1 activates the ETR1 which acts as a negative regulator of the ethylene response. In the absence of ethylene, receptors activate the CTR1, which is a Ser/Thr protein kinase, thus suppressing the ethylene response (Clark *et al.*, 1998). Down stream of CTR1 is EIN2, which acts as a key player in ethylene synthesis. In the absence of ethylene, the C-terminal end of the EIN2 is phosporylated by CTR1 and will be in an inactive state. In the presence of ethylene, ethylene will bind to the receptor, inactivate the CTR1 and thus dephosphorylate the EIN2 and activate the downstream ethylene signalling events. Upon dephosphorylation C-terminal end of the EIN2 is cleaved and enters the nucleus, where it activates the EIN3 and EIN3 like (EIL1) transcription factor and further initiates the ethylene response (Merchante *et al.*, 2013; Shakeel *et al.*, 2013).

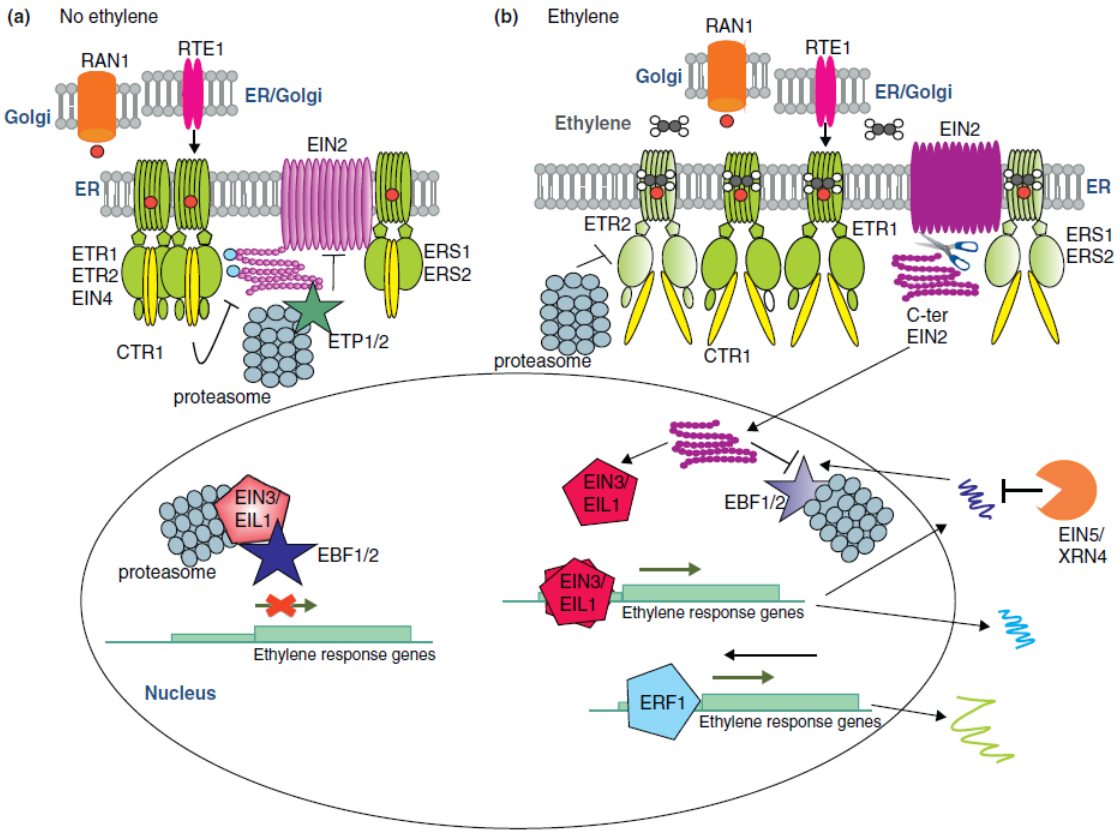

Figure 1-8: Ethylene signal transduction pathway (copied from Merchante *et al.*, 2013). Copyright permission License Number- 4237611362856.

In the current model of ethylene transduction pathway, ethylene is perceived by two subfamily of receptor with high affinity. Copper (red circles) act as a cofactor for ethylene binding. (a) In the absence of ethylene signal CTR1 (in yellow) inactivate the EIN2 (in purple) by phosphorylating its C-terminal end. (b) In the presence of ethylene, hormone will bind to the receptor and inactivate the CTR1. This further prevents the phosphorylation of EIN2, and thus C-Terminal end is cleaved by the unknown mechanism and moved into the nucleus and activate the EIN3/EIL1 and degrade the EBF1/2. Finally the transcription factors, EIN3/EIL1 dimerize and activate the ethylene response genes.

1.6.4 Interaction between NO and ethylene

Both NO and ethylene are gaseous signalling molecules. They interact antagonistically during ripening and leaf senescence and synergistically during biotic stress and Fe deficiency. NO may influence ethylene biosynthesis during the maturation and senescence of plant tissue (Arasimowicz and Floryszak-Wieczorek, 2007). Exogenous application of NO to plants decreased the ethylene synthesis by inhibiting ACC synthase activity (Zhu and Zhou, 2007). NO negatively regulates ethylene synthesis in fruits, This could be an useful technique in extending the shelf-life of fresh fruits. The first report on extending the

shelf-life of strawberry and kiwi fruits by NO fumigation has been demonstrated by Lesham and Wills (1998). After this discovery, many scientists used NO to delay the fruit ripening. Short time fumigation of vegetables like broccoli, green pea, and bok-choy with NO increased the shelf life, but the NO concentration required is unique to the vegetables (Soegiarto and Wills 2004). NO alleviates chilling injury and extends shelf life in Japanese plums (Singh *et al.,* 2009). NO fumigation in Kensington Pride mango reduce both ACS and ACO activity, which affects the ACC content and leads to less ethylene synthesis, also affects the fruit softening enzyme such as exo-PG (polygalacturonase), endo-PG and EGase enzyme (Zaharah and Sing, 2011). Apart from this, NO decreases ethylene synthesis by directly binding to the enzyme ACO to produce an ACO-NO complex which further binds with ACC to form a stable ACO-NO-ACC complex. Studies on NO treated peach fruit showed the irreversible conversion of ACC to MACC, a non-volatile metabolite of ACC, which limits the ACC-ethylene conversion (Zhu *et al.,* 2006). In contrast to the above antagonistic interactions, there are a few synergistic effects also reported. NO donors such as SNP and SNAP increase the ethylene production, which has earlier been reported to break the seed dormancy and germination by Gniazdowska *et al.* (2007). In Arabidopsis and cucumber roots, application of GSNO induces the expression of many genes involved in ethylene synthesis like SAM synthetase, ACO, ACS and the 5-methylthioribose kinase which in turn increase the NO synthesis (Garcia *et al.,* 2011). Further studies are needed to understand the cross talk between NO and ethylene, and how they regulate each other under specific conditions.

1.6.5 Interaction between auxin and ethylene

Synergistic effects of auxin and ethylene have been well defined in the regulation of hypocotyl elongation (Vandenbussche *et al*., 2003), root hair growth and differentiation (Pitts *et al*., 1998), apical hook formation (Lehman *et al*., 1996, Li *et al*., 2004), root

gravitropism (Lee *et al*., 1990; Buer *et al*., 2006), and root growth (Pickett *et al*., 1990; Rahman *et al*., 2001). This suggests that these two signaling pathways interact at the molecular level.

Although ethylene and auxin signalling pathways are relatively well characterized, the mechanisms of their interaction are still poorly understood. One interaction occurs at the hormone biosynthesis level; where auxin induces ethylene biosynthesis by upregulation of ACC synthase, the key enzyme in ethylene production (Abel *et al*., 1995). By contrast, ethylene might influence auxin levels because ethylene has been shown to regulate the expression of two genes (WEAK ETHYLENE INSENSITIVE WEI2 and WEI7) that encode subunits of anthranilate synthase, a rate-limiting enzyme in Trp biosynthesis (Stepanova *et al*., 2005), from which pathway auxin is at least partially derived (Woodward and Bartel, 2005).

Another process regulated by both hormones is gravitropic bending of the root. Asymmetric auxin redistribution in the basipetal (from the tip toward the base) direction mediated by the auxin influx (AUX1) and efflux carriers (PIN-FORMED3 [PIN3] and PIN2) is crucial for root gravitropism (Luschnig *et al*., 1998; Marchant *et al*., 1999; Friml *et al*., 2002). Exogenous application of ethylene reduces (Buer *et al*., 2006) or delays (Lee *et al*., 1990) the root gravitropic response. Although ethylene has been shown to down regulate lateral auxin movement in maize (*Zea mays*) root tips (Lee *et al*., 1990) and auxin transport in pea (*Pisum sativum*) epicotyls (Suttle, 1988), the mode of this auxin–ethylene interaction is not known.

1.6.6 ABA induces NR mediated NO synthesis in stomatal guard cells

The plant hormone abscisic acid (ABA) is mainly synthesized during abiotic stress such as drought, cold and temperature. It helps to regulate transpiration by closing the stomata hence preventing water loss. Desikan *et al.* (2002) showed that external application of ABA increased the NO in stomatal guard cells, and observed that ABA induces NO synthesis and stomatal closure in WT Arabidopsis, but not in NR mutant's. These experiments demonstrated the role of NR in guard cell NO synthesis and its closure. H_2O_2 also induced the guard cell NO synthesis (Bright *et al.*, 2006).

1.7 Use of mutants to explore signalling

Hormone response mutants were the key to elucidate a number of hormonal reaction mechanisms in plants. Further screening of the mutants will help to fill the blanks in hormonal transduction pathways. Plant hormone mutants can be classified into two categories: mutants that are impaired in hormone biosynthesis and mutants that are impaired in their response to hormones (Kende, 2001). The present study used NR, auxin, and ethylene mutants.

1.7.1 NR mutants (*nia1, nia2, nia1nia2*)

NR is involved in the first step of nitrate assimilation, and in Arabidopsis NR consists of two isoforms of genes, *NIA1* and *NIA2* (Wilson *et al.*, 2008). A single NR mutant does not show any phenotypic variation from Col-0, but showed less NO synthesis. When both the NR genes *NIA1* and *NIA2* are mutated, the importance of *NIA1* can be observed.

The nia1 mutation is a single nucleotide substitution that converts an alanine to a threonine in a highly conserved region of the molybdenum cofactor-binding domain of the NR protein. *NIA1* gene encodes a functional NR protein that contributes to the assimilation of nitrate in Arabidopsis. The *nia2* null mutant was isolated from a chlorate resistant mutant

chl3 and molecular analysis studies proved that the *CHL3* gene sequence is identical to the *NIA2* gene. *nia2* mutant showed less NR activity in the leaf and also are resistant to chlorate. The *nia1, nia2* double mutants shows only 0.5% of wild-type shoot NR activity also normal growth was affected on media with nitrate as the only form of nitrogen (Wilkinson and Crawford, 1993).

1.7.2 Auxin mutants

1.7.2.1 aux1

The *AUX1* gene primarily functions in the root and *aux1* mutations affect the gravitropic response of the seedling root. Plants with the *aux1* mutation were selected as resistant to both auxin and ethylene (Pickett *et al.,* 1990). AUX1 acts as an auxin influx carrier, which facilitates the uptake of auxin during the gravitropic root bending response (Marchant *et al*., 1999). Mutants in *aux1* are agravitropic but can be rescued by exogenous NAA, a membrane permeable auxin.

1.7.2.2 axr2-1

The *axr2-1* mutation is dominant and located on chromosome three. The mutant plants were isolated as resistant to the plant hormones auxin, ethylene and abcisic acid. Mutants have the phenotypic character of short hypocotyls, agravitropic root and shoot growth and no root hairs (Wilson *et al*., 1990). Timpte *et al*. (1994) proposed that *axr2-1* severely disrupts an early auxin response. It has subsequently been shown that AXR2 is an Aux/IAA7 protein (Nagpal *et al.,* 2000)

1.7.2.3 axr3

The axr3 mutation is semi-dominant and located on chromosome one. A mutant *axr3* plant shows enhanced apical dominance, reduced root elongation, increased adventitious rooting and no shoot and root gravitropism. AXR3 is an Aux/IAA17 protein (Rouse *et al.,* 1998).

1.7.3 Ethylene mutants

1.7.3.1 ein3-1

EIN3 (ethylene-insensitive3), is a nuclear transcription factor that initiates downstream transcriptional cascades for ethylene responses. The ein3-1 mutation is a loss-of-function mutation, leading to the suppression of ethylene-mediated effects including gene expression, the triple response (apical hook formation, thickening and shortening of hypocotyl), cell growth inhibition, and accelerated senescence.

1.7.3.2 ein3OX

The *EIN3OX* is a transgenic line which expresses the *EIN3-1* gene under the control of 35S promoter in an *ein3-1* mutant background. *EIN3OX* seedlings show the ethylene triple response phenotype in absence of ethylene.

1.8 Analysis of nitric oxide

1.8.1 Visualization of NO by confocal microscopy using specific dye DAF-2D

Real time visualization of the production and localisation of NO is achieved by confocal microscope using the fluorescent indicator DAF-2D. This method is useful to analyse the cellular function of NO. DAF-2D was originally designed and synthesized by Kojma *et al*. (1998). Non-fluorescent DAF-2D reacts with NO in the presence of oxygen and yields the highly fluorescent product triazolofluorescein (DAF-2T). Fluorescence intensity is directly proportional to the concentration of NO (Kojma *et al.,* 1998) and has been used frequently to demonstrate NO production in roots (Hu *et al.,* 2005; Stohr *et al.,* 2006; Kolbert *et al.,* 2008), and stomata (Desikan *et al*., 2002). The specificity of this dye to NO has been questioned by researchers, although it is accepted when used with the proper positive and negative controls.

1.8.2 Quantification of gene expression by Quantitative Real-Time PCR (Q-RT-PCR)

Q-RT-PCR can be used to measure changes in mRNA levels and therefore suggest possible changes in the protein level and function in response to the external stimuli. qPCR-based copy number quantification has advantages, such as high sensitivity, low cost and rapid screening, compared to other methods. Real time PCR measures the progress of DNA amplification in real time by using fluorescent probes, like SYBR green-I. SYBR green-I binds to double stranded DNA (dsDNA) and then emits 1000 fold greater fluorescence than when it is free in solution (Valasek and Repa, 2005). An increase in DNA product during PCR therefore leads to an increase in fluorescence intensity and is measured at each cycle, thus allowing DNA concentrations to be quantified.

1.9 Transgenic approach to visualize *NIA1*-mediated NO synthesis.

Although NO research has fascinated many plant scientists for two decades, the only method available to visualize NO, has been the cell permeable dye DAF-2DA viewed with a fluorescence microscope. Also this method allow visualization of the NO already synthesized in different parts of the plant tissues. However it cannot reveal which NR gene is responsible for the synthesis of NO in a particular plant tissue. Recent studies have shown NR mediated NO synthesis is the most important source of NO in plants, and that *NIA1* plays the major role in NO signalling. So producing transgenic plants expressing the *NIA1* gene tagged with a fluorescent marker will be a viable alternative tool to find the role of the *NIA1* gene in NO signalling. These plants will also be useful to find the location of the *NIA1* expression with particular external stimuli, and to study the hormonal interactions.

1.9.1 Use of green fluorescent protein (mGFP4) as a reporter system

The green fluorescent protein (GFP) has been used extensively by many scientists in both plant and animal systems. GFP is used for the direct visualization of gene expression and subcellular localization of fusion proteins in living cells (Siemering *et al*., 1996). GFP has two excitation peaks at 400 nm and 475 nm; the former excitation peak is useful to detect GFP fluorescence using a long wavelength UV lamp, the later one is used in the laser confocal microscope. This technique has several advantages over GUS reporter gene. In the present study *mGFP4* has been used to produce the *NIA1* construct. While expressing the original GFP from jellyfish *Aequorea victoria* in *A. thaliana*, the GFP coding sequence was cleaved because the sequence in GFP is similar to the plant intron recognition site. This cryptic intron was removed by using alternative codons and successfully expressed in Arabidopsis (Jim Haseloff *et al.*, 1997).

1.10 Aim of the project

It is clear that there is a considerable interaction between the different signalling pathways during the development of plants and it is likely that auxin, ethylene and NO signalling interact during the gravitropic responses of roots. The aim of this study was to investigate the effect of NO on gene expression in the bending zone of roots during response to gravity.

Specific objectives were

- To analyse the gravitropic curvature of roots in wild type and auxin, ethylene and NR mutants of Arabidopsis.
- To localise the production and accumulation of NO in the roots of Col-0, *aux1*, *axr2* and *axr3* Arabidopsis seedlings in response to gravity by using confocal microscopy.
- To quantify the changes in NIA1 transcript level in Col-0, *aux1*and *axr2* root zones (root tip, middle region and hypocotyl zones) in response to gravity by using Q-RT-PCR.
- To localise the *NIA1* gene expression during gravitropism, by using mGFP4 tagged *NIA1* transgenic plants.

2 Materials & Methods

2.1 Arabidopsis seeds

Arabidopsis thaliana (L.) Heynh, Colombia ecotype (Col-0) and auxin mutants (*aux1*, *axr2* and *axr3*), ethylene mutants (*ein3-1 and EIN3OX*) and nitrate reductase mutants (*nia1*, *nia2 and nia1nia2*) were obtained from Nottingham Arabidopsis Stock Centre (NASC), Nottingham, United Kingdom. All the Arabidopsis genotypes used in this study were in Columbia (Col-0) background.

2.2 Growth conditions for plants

Seed stocks were stratified by storage at 4^{o}C for at least three days before sowing. Plants were grown in a growth cabinet (MLR-351H, Sanyo Gallencamp, Loughborough, Leicestershire, UK) at 20^{o}C with 12 h of white light (Active Photon flux: 150 µEi/m^{2}/S) at 60% relative humidity.

2.2.1 Growth on compost

Plants were grown on Levingtons compost F2+sand (JFC Monro, Hayle, Cornwall, UK). Seeds were sown in trays and then transferred to individual pots (10 cm diameter x 15 cm depth). Plants were watered twice weekly.

2.2.2 Growth on MSR3

2.2.2.1 Surface sterlization

Prior to germination, seeds were surface sterilized to prevent contamination by immersing in 70% (v/v) ethanol for 15 min and 10% (v/v) household bleach for 15 min, followed by three rinses in sterile water, finally seeds were suspended in 1 ml sterile water.

2.2.2.2 MSR3 plates

In order to study the gravity bending, seedlings were grown in plant growth medium-MSR3 (Gamborg *et al.*, 1976) in a rectangular plates. MSR3 was prepared using bacteriological agar 0.8% (w/v), 2(N-morpholino) ethanesulfonic acid (MES) 0.05% (w/v), sucrose 0.15% (w/v). Murashige and Skoog basal salt mixture 0.44% (w/v), the pH was adjusted to 5.7 using NaOH. Medium was autoclaved at 121^{o}C for 20 min, then poured into a rectangular plates (120 x 120 x 17 mm) inside the laminar flow hood and allowed to set for 20 min. 5-10 surface sterilized seeds were placed in MSR3 plates using a micropipette (Figure 2-1). If the plants required antibiotic selection then MSR3 media was cooled to 60^{o}C before the addition of the relevant antibiotic. Kanamycin was used at 50 µg/ml and hygromycin was used at 30 µg/ml.

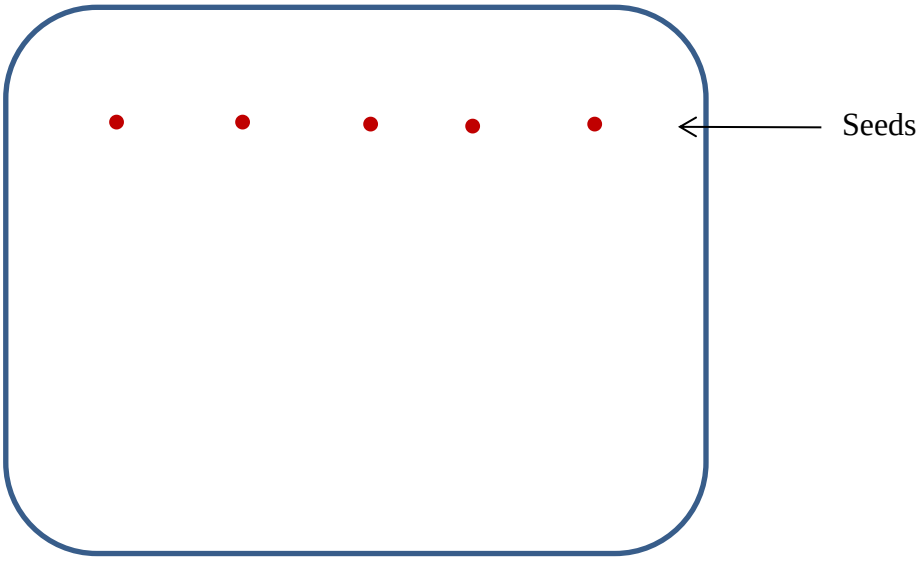

Figure 2-1: Schematic representation of MSR3 plates

2.3 Imaging of root development and gravitropic curvature

2.3.1 Measuring root gravitropism

In order to measure the gravity bending, Seeds shown in MSR3 plates were placed vertically in the growth champer in 12 h photoperiod at 20^{o}C and 60% humidity. After 5 days, the seedlings were gravistimulated for 2 h by changing the direction of the plate

(Horizantal orientation) by 90^{o} and then allowed to bend in a light proof cupboard. Gravity bending was measured in a five-day-old seedlings photographs. A camera (Canon 600D, 18-55 mm IS II Lens) was fixed above the sample. A millimetre-scale ruler is placed at the same focal depth as the subject to provide a scale reference. Plates were photographed at particular time intervals. Root bending curvature was measured from photographs using protractor and ruler.

2.3.2 Statistical methods:

Linear mixed-effects modelling was employed to assess the effect of various plant types on the change over time in the curvature of the individual samples. Analyses started with a model that incorporated:

- fixed effects of plant type interacting with a quadratic change in curvature over time;
- diagonal variance-covariance structure for random effects of quadratic time coefficients;
- weighting for varying plant type within sample variability;
- AR(1) correlation in residuals.

A backwards elimination approach was taken to find the minimal model that adequately represented the data. Models that differed in either the random effcts specification, plant type within sample variability or AR(1) correlation were compared by likelihood ratio tests. The significance of terms in the fixed-effcts specification was assessed by standard linear regression conditional t-tests. Visual inspection of residual plots of the final models did not reveal any obvious deviations from homogeneity of variance or normality.

All analyses were carried out in the R programming language and environment (R Development Core Team, 2014) using the nlme software package (Pinheiro *et al.*, 2016) for the linear mixed-effects modelling.

Two-way ANOVA was employed to analyse the overall difference between plants and treatments over time in terms of root bending. Turkey Post-hoc test was used to make a pairwise comparison. Normality was checked by Shapiro-Wilk test. Two-way ANOVA analyses were carried out in the IBM SPSS (IBM Corp. Released 2013. IBM SPSS Statistics for Windows, Version 23.0. Armonk, NY: IBM Corp.).

2.4 Detection of endogenous nitric oxide (NO) by confocal microscopy

Where indicated 50 µl of 100 µM specific NO scavenger 2-(4-carboxyphenyl)-4,4,5,5-tetramethylimidazoline-1-oxyl-3-oxide (cPTIO) was applied to 5 days old Arabidopsis seedling roots by micropipette and incubated for 15 min. Seedlings were gravistimulated for 2 h by changing the direction of the plate (Horizantal orientation) by 90^{o}. After 2 h of gravistimulation, 50 µl of a 20 µM solution of the cell-permeable fluorescent probe 4, 5-diaminofluorescein diacetate (DAF-2DA); (Calbiochem, San Diego) was applied to the root by micropipette and incubated in the dark for 20 min. Thereafter, roots were washed three times with fresh MES buffer and examined using laser confocal microscopy (DAF-2D excitation 495 nm, emission 515 nm). Slides were prepared by placing the seedling on a glass slide using forceps, the root was covered with immersion oil and coverslip placed on the sample. All micrographs were acquired under identical settings to indicate unadjusted fluorescence differences. Experiments were performed with and without cPTIO and gravistimulation.

2.5 ABA treatment for stomatal bioassay

Whole leaves from transformants and wilt type were incubated in MES-KCl buffer (10 mm 2-morpholino ethane sulfonic acid (MES), 5 mm KCl, 50 µm $CaCl_2$, pH 6.15) for 2 h under light condition in a growth chamber. After the incubation leef epitermal fragments were obtained from the leaves using a forceps, and they were further incubated

at 25^{o}C and 37^{o}C in light and dark for 4 h in MES buffer contains 150 µm ABA. Col-0 wild type treated with ABA was used as a control. After 4 h of incubation stomata was observed for mGFP4 fluorescence using confocal microscopy.

2.6 H_2O_2 treatment for root

Col-0 wild type and transgenic seedlings root were pre-treated with 100 µM of H_2O_2 and then gravistimulated for 6 h by chaning the direction of the plate (Horizantal orientation) by 90^{o}. After 6 h seedlings were placed on a glass slide using forceps, then the root was covered with immersion oil and coverslip. mGFP4 fluorescence was observed using confocal microscopy.

2.7 Bacterial growth medium & condition

Escherichia coli DH5-α and *Agrobacterium tumefaciens* (GV3101) were grown on solid Luria-Bertani (LB) agar plates consisting of tryptone 10 gl^{-1}, yeast extract 5 g l^{-1}, NaCl 10 g l^{-1} and agar 15 g l^{-1}. The medium was autoclaved at 121^{o}C for 20 min and cooled to approximately 60^{o}C before the addition of appropriate antibiotics.

2.7.1 Antibiotics

All antibiotics used in this study were purchased from Sigma Aldrich Ltd UK and are listed in the Table 2.1. Antibiotic stock solutions were filter sterilized using 0.22 µm filters (Millipore Corporation, USA). After autoclaving, MSR3 and LB media was cooled to 60^{o}C before the addition of the relevant antibiotics.

Table 2-1: Antibiotics solution used in this study

Antibiotics	Solvents	Stock concentration(mg/ml)	Working concentration(µg/ml)
Ampicillin	Water	100	100
Kanamycin	Water	100	50
Hygromycin	Water	100	30

Tetracyclin	Water	10	5
Rifampicin	Methanol	50	25

2.8 Extraction of nucleic acids

2.8.1 Extraction of total RNA from Arabidopsis root

Total RNA was extracted from Arabidopsis roots using Trizol reagent (Sigma Aldrich). Roots were collected from plants gravistimulated for 30 min, 1, 2, 4 and 6 h and non-gravistimulated plants. The whole root was separated into three parts (root tip, middle region and hypocotyl region) by using a scalpel blade and frozen in liquid nitrogen. Approximately 100 mg of tissues from the each of the three parts of the roots were ground separately to a fine powder using a pestle and mortar and homogenised with 1 ml of Trizol reagent. Samples were vortexed for 5 min and incubated at room temperature for 5 min. 200 µl of chloroform was added to the samples and tubes were shaken vigorously by hand for 15 s and incubated at room temperature for 5 min. Samples were centrifuged at 15000xg for 15 min at 4^{o}C and the clear aqueous phase was transferred to a fresh tube. RNA was precipitated by the addition of 0.5 ml of isopropanol and then further incubated at room temperature for 10 min. Samples were then centrifuged at 15000xg for 1 h at 4^{o}C. The supernatant was removed and the pellet was dissolved with 25 µl of RNase free water, 200 µl of 70% (v/v) ethanol, and then potassium acetate was added to the reaction mixture to a final concentration of 65 mM. The samples were kept at -80°C for 1 h then centrifuged at 15000xg for 1 h 30 min at 4^{o}C. The pellet was washed with 1 ml of 75% (v/v) then 95% (v/v) ethanol, and incubated at room temperature for 5 min. Tubes were centrifuged at 15000xg for 5 min at 4°C. The final RNA pellet was dried briefly under vacuum for 3-5 min and dissolved in 20 µl of RNase free water and stored at -80^{o}C until further use.

2.8.2 Extraction of plasmid DNA

Plasmid DNA was extracted from 1.5 ml overnight grown LB liquid cultures of *E. coli* transformants using GenElute^{TM} Plasmid miniprep kit (Sigma Aldrich, UK) following the manufacturer's instructions. The plasmid DNA was eluted from the column using 50 µl 1xTE pH 8.0. Plasmid DNA was stored in a freezer at -20^{o}C until further use.

2.8.3 Extraction of plant genomic DNA (gDNA)

Arabidopsis genomic DNA was extracted from 100 mg of young leaf tissues using a GeneJET Plant Genomic DNA purification kit (Thermo Scientific, UK) following the manufacturer's instructions. The final DNA pellet was dissolved in 100 µl of 1xTE buffer.

2.8.4 Quantification of nucleic acid by Nanodrop

Nucleic acid (DNA and RNA) concentration were determined by measuring the absorbance at 260 nm using a Nanodrop (Thermo scientific). The concentration of a 2 µl sample was calculated based on the absorbance measured at 260 nm x conversion factor (40 for RNA and 50 for DNA). Samples were checked for purity by measuring the absorbance ratio at 260 nm/280 nm for the presence of protein contamination and at 260 nm/230 nm for the presence of solvent or salt contamination.

2.8.5 Analysis of RNA samples by agarose gel electrophoresis (Sambrook *et al.*, 1989)

The quality of RNA was determined by agarose gel electrophoresis. Agarose (1.2% w/v) was mixed with 1X TAE buffer and melted in a microwave oven. The mixture was cooled to 60^{o}C and a final concentration of 30 ng ethidium bromide (EtBr) was added, and then mixed gently to avoid bubble formation. The mixture was poured into the gel mould containing comb and was allowed to solidify. 1X TAE buffer was poured into the gel buffer reservoir in the electrophoresis apparatus to about 2 mm above the gel surface. RNA

samples were mixed with a final concentration of 1x loading dye. Electrophoresis was carried out at 100 V. After the run, the gel was visualized on a UV (365 nm) transilluminator Fluorchem Q (Alpha Innotech, USA).

2.9 cDNA synthesis

2.9.1 DNase treatment

Removal of genomic DNA from total RNA samples was done using a DNA-*free*™ kit (Applied Biosystems) following the manufacturer's instructions. Two units of rDNase I and 0.1 volumes of 10x DNase I buffer was used for 20 µg of RNA in a 50 µL reaction. The mixture was incubated at 37°C for 30 min, and then 0.1 volume of DNase inactivation reagent was added to the tube and incubated for 2 min. After incubation, the tube was centrifuged at 10000xg for 2 min, and the supernatant, which contains the RNA, was transferred to a fresh tube and stored at -80°C.

2.9.2 First strand cDNA synthesis

First strand complementary DNA (cDNA) was synthesized from 5 µg of total RNA in a total reaction volume of 50 µl. 5 µg of RNA was mixed with 8 µl of anchored dT(18) primer, 1 ng of Human Tumour Necrosis Receptor Associating Factor 1 transcript (TRAF spike- NCBI gene bank accession number NM_005658.4) and 8.5 µl of sterile distilled water. The reaction was incubated at 70°C for 10 min, cooled on ice for few seconds, microfuged briefly and allowed to anneal at room temperature for 5 min. 5 µl of 10X RT buffer, 2.5 µl of 20 mM dNTP mix and 4 µl of 0.1M DTT was added and microfuged briefly. 2 µl of superscript III reverse transcriptase (200 U/µl, Invitrogen, United Kingdom) was added to the reaction mixture, briefly mixed and incubated at 42°C for 2 h 30 min. The reaction mixture was heat inactivated at 65°C for 10 min. Finally, the cDNA synthesis reaction was diluted ten times with sterile distilled water and used for RT-PCR.

2.10 Polymerase chain reaction

Polymerase chain reaction (PCR) was performed in a PTC200 Peltier Thermocycler (MJ Research). Genomic DNA or cDNA was used as template. The PCR products were analysed by agarose gel electrophoresis (see 2.65).

2.10.1 DNA polymerase

Taq DNA polymerase (Biolabs, UK) was used for general amplification. Amplification of PCR fragments for cloning was performed by using a proof reading polymerase (QIAGEN Long range PCR kit) with exonuclease activity.

2.10.2 Primer design

Primer pairs were designed to be between 18-25 base pair in length, with similar melting temperatures and a GC content of 40-60%. Primer pairs were designed using a primer design program (ABI-primer design 7000, Applied Biosystems). Primer pairs were selected in the final third of the cDNA sequence to give a product of 50-200 bp. All primer pairs were aligned with the Arabidopsis genome sequence from the NCBI database using the nucleotide BLAST search engine to determine their uniqueness. The chosen primers were synthesized by Eurofins Genomics, Germany (Table 2-2).

Table 2-2: Oligonucleotide primers

Primer Name	Primer sequence 5'-3'	Fragment size	Annealing Temp (^{o}C)
NIA1-F	AATCGCAAAGGAAGGTTGG	150 bp	60
NIA1-R	CTCTAGATTTGGCTGCAACG		
TrafRT1F	CATAAACTTTCCTCTTCCTGCC	150 bp	60
Trafrt1R	ACATTGCTCAGTGGCTTGG		
M13F	GTAAAACGACGGCCAGT	150 bp	60
M13R	GTAAAACGACGGCCAGT		
mGFP Cloning primers			
mGFP FP	GC**CTGCAG**ATGAGTAAAGGAGAAGAAC	717 bp	54
mGFP RN	**GCGGCCG**CTTATTTGTATAGTTCATCCAT		
mGFP Screening primers			
mGFP F	ATGAGTAAAGGAGAAGAACTTTTCAC	717 bp	54
mGFP R	TTATTTGTATAGTTCATCCATGCC		
Cloning primer for 2kb Nia1 promoter			
Nia1 FK	GC**GGTACC**GTGGGTTCATTTTGGTAGTTCGG	2 kb	54
Nia1 P RP	GC**CTGCAG**GGTTTAGTGATTGAACCGGTGATAA		
Cloning primer for 2kb Nia1 promoter with gene			
Nia1 FK	GC**GGTACC**GTGGGTTCATTTTGGTAGTTCGG	5.5 kb	54
Nia1 RP	GC**CTGCAG**GAAGATTAAGAGATCCTCCTTCACG		

Primer sequences containing restriction endonucleases recognization sites *KpnI* (GGTACC), *PstI* (CTGCAG), *NotI* (GCGGCCG) are in bold and underlined

2.10.3 PCR conditions

General PCR conditions are listed in Table 2-3. Annealing temperature was optimized for new DNA templates and primer pairs where they were used for the first time.

Table 2-3: PCR condition for amplification of *NIA1* gene

Step	Stage	Temperature (^{o}C)	Time (min)
1	Initial denaturation	94	10
2	Denaturation	94	1
3	Annealing	60	1
4	Extension	72	1 min/Kb
5	Step 2 to 4	34 cycles	
6	Final extension	72	10

2.10.4 Standard PCR

The polymerase chain reaction (PCR) mixture of 12.5 µl contained 2.5 µl of template (cDNA/gDNA/small amount of colony suspended in water), 2 µl of 10 µM oligonucleotide primers (Table 2-2), 0.25 µl of 20 mM dNTP mix, 1.25 µl of 10X PCR buffer (10 mM Tris-HCl; pH: 9.0, 50 mM KCl, 1.5 mM $MgCl_2$), 0.5 U of Taq DNA polymerase and 6 µl of sterile distilled water.

2.10.5 Quantitative Real-Time PCR (Q-RT-PCR)

Q-RT-PCR was performed using a *NIA1* gene specific primer with SYBR green (Primer Design). The reaction mixture of 20 µl contained 2X SYBR green master mix (10 µl), 300 nM of each gene specific primer NIA1F and NIA1R, template cDNA (5µl of diluted) and DNase free water. The reaction was carried out in duplicate in microamp optical 96 well plates (Ambion), which were sealed with a clear plastic adhesive cover (Ambion). Template control (without RNA), enzyme control (without RT enzyme) and sterile water samples were used as negative controls in this experiment. The reaction plate was centrifuged at 1000xg at room temperature. The reaction was performed in 7300 real time

PCR system (Applied Biosystems). Reaction conditions were as described in Table 2-4. To derive a standard curve, serially diluted (0.1 ng/µl to 0.00001 ng/µl) pBluescript II SK (+) plasmid was used in the reaction, and the reaction mixture was prepared as described earlier, with M13F and M13R primers (Table 2-2).

Table 2-4: Q-RT-PCR reaction condition

Stage	Temperature (^{o}C)	Time (min)	cycle
Activation	95	10	1
Denaturation	95	0.15	40
Annealing/Extension	60	1.0	
Melting curve analysis	95	0.15	1
	60	1.0	
	95	0.15	

2.10.6 Long range PCR

Long range PCR was performed to amplify larger DNA fragments (NIA1 promoter and gene) from BAC clone (T32E7), using a two-step PCR programme (Table 2.5). The long range PCR (Qiagen) high fidelity Taq DNA polymerase was used to avoid amplification errors. PCR mixture contains 10 ng of DNA, 10 µM of forward and reverse oligonucleotide cloning primers (Table 2-2), 1 µl of 20 mM dNTP mix, 5 µl of Q solution, 0.5 µl of 1.5 mM $MgCl_2$, 0.5 U of Long range Taq polymerase, made up to 15 µl with RNase free water. PCR amplification was carried out at 54^{o}C annealing Temp and an increased extension time (2 min for promoter and 6 min for promoter and gene, Table 2-5). The PCR products were then separated by agarose gel electrophoresis and visualized under UV light.

Table 2-5: Two step PCR reaction condition

Step	Stage	Temperature (^{o}C)	Time (min)
1	Initial denaturation	93	3
2	Denaturation	93	0. 45
3	Annealing	54	1
4	Extension	68	1 min/Kb
5	Step 2 to 4	9 cycles	
6	Denaturation	93	0. 40
7	Annealing	54	1
8	Extension	68	1 min/Kb then 10 s in each additional cycle
9	Go to 6	19 cycles	
10	Final extension	68	10

2.10.7 Inverse PCR

Inverse polymerase chain reaction (inverse PCR) was carried out to select a single copy transformants and also to know the insert location. The whole plant genomic DNA was isolated and digested with *kpn1*-HF restriction enzyme. This enzyme was chosen because this will give a single cleavage point in the T-DNA region and another cleavage point somewhere in the plant genomic region. Digested products were circularised by T4-DNA ligase enzyme. Primers designed in the known T-DNA regions were used in the long range PCR to amplify the circularised templates.

2.11 Cloning and transformation

2.12 Cloning strategy for PG35s-mGFP4 construct

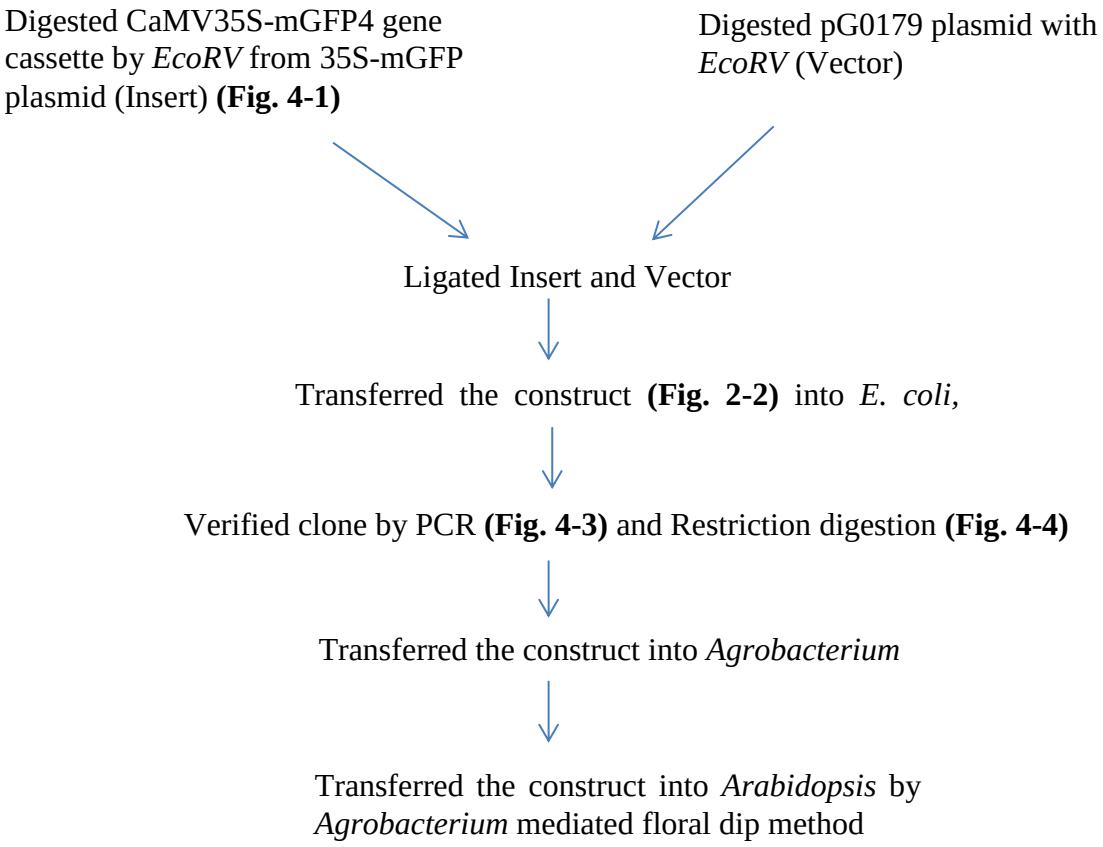

Figure 2-2: Overview of cloning strategy for PG35s-mGFP4

To make a PG35s-mGFP4 construct CaMV35S-mGFP4 cassette was released from the 35S-mGFP plasmid using *EcoRV* and then ligated with the pG0179 plasmid digested with the same enzyme. This construct was cloned into *E. coli* and then sub-cloned into *Agrobacterium*. CaMV35S-mGFP4 cassette was inserted into Col-0 wild type plants by using *Agrobacterium* harbouring PG35s-mGFP4 construct by floral tip method.

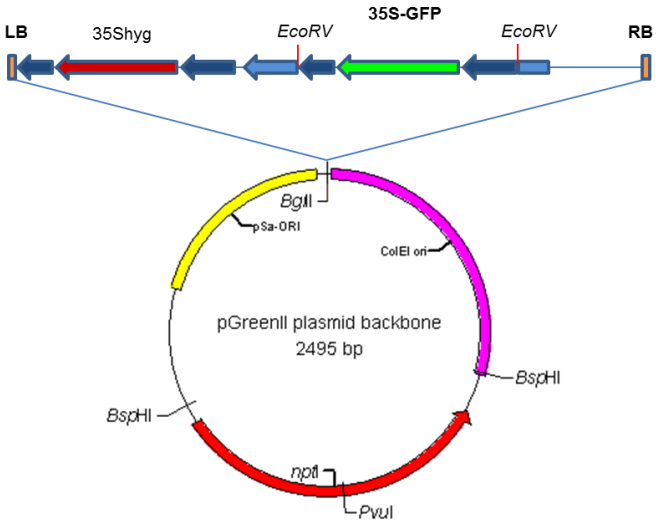

Figure 2-3: Schematic representation of pG35S-mGFP4 construct

CaMV35s-mGFP4 cassette was cleaved from the pGreen 35S-GFP plasmid by *EcoRV* restriction digestion. The purified cassette was then inserted into the *EcoRV* digested pG0179 plasmid vector. This construct was transferred to the wild type Arabidopsis (Col-0) by floral dip method. Transformed plant was confirmed for the insertion of mGFP4 and used as a control to check the 35S promoter driven GFP expression in plants.

LB- Left border, RB- Right border, hyg- Hygromycin resistance gene, 35S- CaMV35S promoter

2.13 Cloning strategy for NIA1pro-mGFP4 and NIA1pro-NIA1-mGFP4

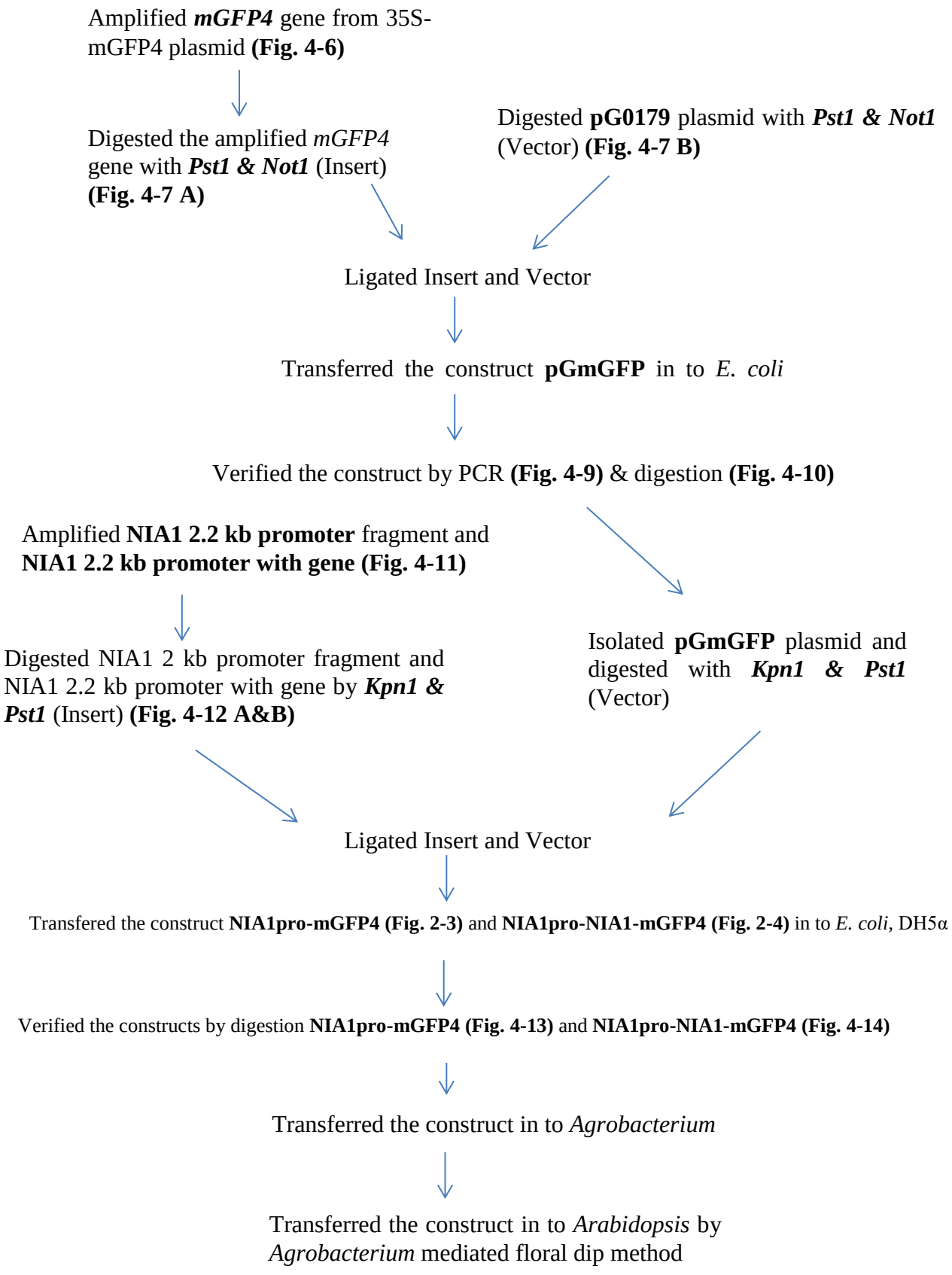

Figure 2-4: Overview of cloning strategy for NIA1pro-mGFP4 and NIA1pro-NIA1-mGFP4 constructs

To localise the *Nia1* gene expression during gravitropism NIA1pro-mGFP4 and NIA1pro-NIA1-mGFP4 constructs were made. First pGmGFP construct was made by inserting *mGFP4* gene into pG0179 plasmid in the *Pst1 & Not1* restriction site. Nia1 promoter and Nia1 promoter along with the *Nia1* gene was amplified using PCR and then inserted into pGmGFP construct in the *Kpn1 & Pst1* retriction site. This constructs was cloned into *E. coli* and then sub-cloned into *Agrobacterium*. Cloning was confirmed by colony PCR and restriction digestion. Inorder to produce transgenic plants NIA1pro-mGFP4 and NIA1pro-NIA1-mGFP4 cassetts were introduced into Col-0 wild type and auxin, ethylene and NR mutants by floral tip method.

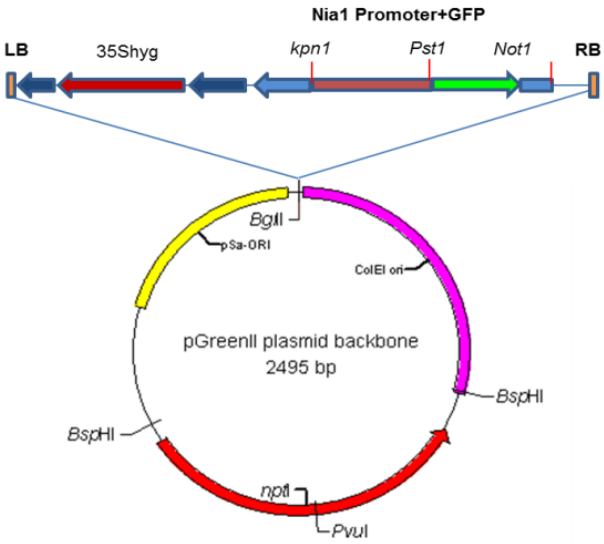

Figure 2-5: Schematic representation of NIA1pro-mGFP4 construct

The 2.2 kb NIA1 promoter fragment was amplified from the BAC clone (T32E7) using PCR long range Polymerase (Qiagen) and then further purified and digested with the restriction enzymes, *Kpn1 and Pst1.* This NIA1 promoter fragment was sub cloned into the pGmGFP4 vector. This construct was transferred to wild type *Arabidopsis* plant Col-0 and auxin, ethylene, NR mutant plants by floral dip method. Transformed plants were confirmed by PCR and used for further interaction studies.

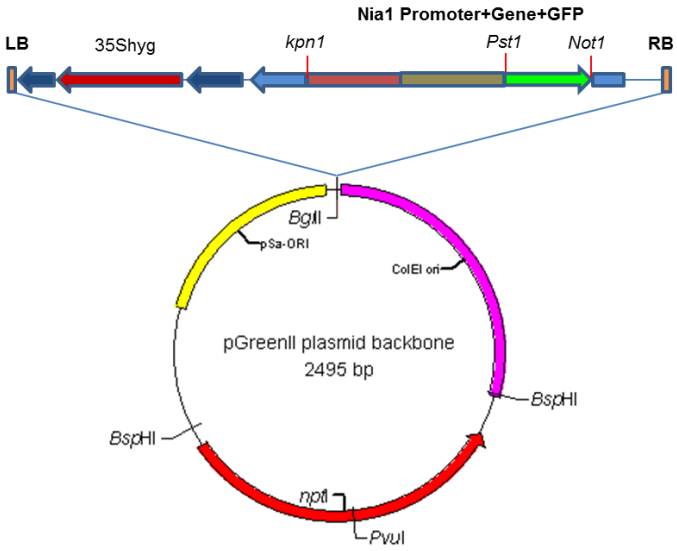

Figure 2-6: Schematic representation of NIA1pro-NIA1-mGFP4 construct

The 2.2 kb NIA1 promoter along with *NIA1* gene 3.5 kb (Total length of 5.7 kb) fragment was amplified from the BAC clone (T32E7) by using PCR long range polymerase (Qiagen) and then further purified and digested with the restriction enzymes, *Kpn1 and Pst1.* This 5.7 kb NIA1 fragment was sub cloned into the pGmGFP4 vector. This construct was transferred to the wild type *Arabidopsis* plant Col-0 and auxin, ethylene, NR mutant plants by floral dip method. Transformed plant were confirmed by PCR and used for further interaction studies.

2.13.1 Column purification of amplified DNA fragments

The amplicon (mGFP4, NIA1 2.2 kb promoter and NIA1 2.2 kb promoter with gene) obtained by long range PCR was separated on a 1.0 % (w/v) agarose gel. The PCR product was column purified with a PCR clean up kit (Sigma) following the manufacturer's instructions. The final concentration of the purified product was checked by resolving in a 0.8 % (w/v) agarose gel.

2.13.2 Restriction digestion of insert and vector

The plasmid DNA (pG0179 and pGmGFP) and purified PCR products (mGFP4, NIA1 2.2 kb promoter and NIA1 2.2 kb promoter with gene) were digested with restriction enzymes to obtain DNA fragments for cloning. Restriction digestion was carried out in 0.5 ml PCR tube containing 1-2 µg of plasmids or purified PCR products, 0.1 volume of buffer, 1-2 U of restriction enzymes and the volume made up to 20 µl using distilled water. Double digestion was performed using buffer in which both enzymes could function at their optimal activity. The digestion was carried out at 37^{o}C for 2-4 h.

2.13.3 Extraction of nucleic acid from agarose gel

Restriction digested plasmids (pG0179 and pGmGFP) and amplified DNA fragments (mGFP4, NIA1-2.2 kb promoter and NIA1-2.2 kb promoter with gene) separated by electrophoresis were extracted from agarose gel slices using the Qiaquick gel extraction kit (Qiagen Ltd, Crawley, West Sussex, UK), according to the manufacturers instructions. UV transilluminator was used to visualise DNA bands from agarose gels, which were excised using scalpel blades.

2.13.4 Ligation

DNA fragments were ligated into a linearized vector backbone using T4-DNA ligase (Sigma, UK) in the supplied ligase buffer, according to the manufacturer's instructions. The ligation was carried out in a 1:3 molar ratio of linearized plasmid and insert for every cloning. Reaction mixture was set up consisting of 2 U of T4-DNA ligase, 0.1 volume of ligase buffer and the volume made up to 20 µl using distilled water. Reaction was carried out in a PCR thermal cycler at 16^{o}C overnight. The amount of insert to include in the reaction mixture was calculated based on the following equation.

$$\text{Amount of insert (ng)} = \frac{\text{Amount of vector (ng) X size of insert (bp)}}{\text{Size of vector (bp)}} \text{ X } \text{Insert: vector molar ratio}$$

2.13.5 Preparation of *E. coli* competent cells

The *E. coli* strain [DH5α] to be transformed was inoculated into 4 ml LB broth and grown overnight. This was used as mother culture for competent cell preparation. 250 µl of the mother culture was inoculated into 25 ml of LB broth in a 250 ml flask and grown with vigorous shaking at 37°C for about 2 h (OD_{600} = ~ 0.6). The culture was transferred to a polypropylene tube and chilled on ice for 10 min. The cell suspension was pelleted by centrifugation at 5000xg for 10 min at 4°C. The supernatant was discarded and the cell pellet was suspended in ice cold 20 mM $CaCl_2$ (10 ml). The cell suspension was placed on ice for 20 min and centrifuged at 5000xg for 10 min at 4°C. The supernatant was discarded completely and the pellet was resuspended in sterile ice cold solution of 20 mM $CaCl_2$ (1.0 ml), followed by incubation in ice for 15 min. Competent cells were used immediately for transformation.

2.13.5.1 Transformation of vector into *E. coli*

10 µl of ligation mixture were added to the competent cells and incubated on ice for 30 min. The cells were then heat shocked for 1 min in a 42°C water bath, and rested immediately on ice for 5 min. To this, 1 ml LB broth was added to each tube, and the tubes were shaken gently to aerate (150 rpm) at 37°C for 1 h. Aliquots of 100 µl and 200 µl from cultures were then spread onto LB agar plates containing the appropriate antibiotics for selection of the plasmid. Plates were incubated at 37°C overnight to develop colonies, and kept at 4°C for longer term storage.

2.13.5.2 Blue white screening

To select the transformed colonies of *E. coli* carrying the insert DNA (mGFP4) and to eliminate the colonies with self-ligated vector, the α-complementation test was carried out as described by Sambrook *et al.* (1989). The XIA plates (X-Gal, IPTG and ampicillin) were prepared by spreading 40 µl of 0.1 M IPTG and 40 µl X-Gal (20 mg/ml) on LB agar medium containing ampicillin (100 µg/ml). The IPTG and X-Gal solutions were spread 30 min before inoculation. Recombinant colonies of *E. coli* were selected randomly from the LB amp plates and short streaked (Fig. 2-5) with a sterile tooth pick onto the XIA plates. The plates were wrapped with aluminium foil and incubated at 37°C for 12-16 h. The plates were stored at 4°C for 6 h to allow full colour development and the results were recorded.

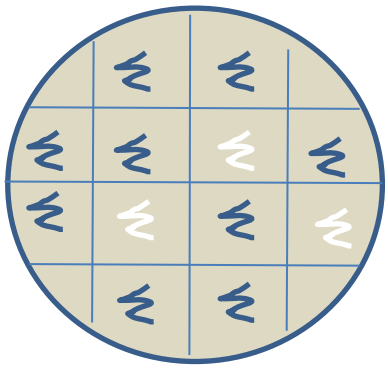

Figure 2-7: Schematic representation of short streaked plate

2.13.6 *Agrobacterium* competent cell preparation

A single colony of *Agrobacterium tumefaciens* strain was streaked onto a fresh LB plate with appropriate antibiotics, and incubated for 2 d at 28°C. From this plate, a single colony of *Agrobacterium* was picked and used to inoculate a 5 ml of LB with appropriate antibiotics. Cultures were grown overnight at 28°C in a shaking incubator. The next day, 5 ml of overnight culture were added to 500 ml of LB in a sterile 1000 ml flask and shaken vigorously (250 rpm) at 28^{o}C until the culture reached an OD_{600} of 0.5-0.6. Cultures were chilled on ice and centrifuged at 3000xg for 5 min at 4^{o}C to pellet the cells. The supernatant was discarded and cells were washed with 20 ml of ice cold TE (10 mM Tris-HCl, pH 7.5; 1 mM EDTA, pH 8.0) and then centrifuged at 3000xg for 5 min. The supernatant was discarded completely and the pellet was resuspended in 5ml of LB. Finally cells were pipetted in 0.1 ml aliquots into ice cold 1.5 ml eppendorf tubes. Competent cells were used immediately for transformation.

1.10.1.1 Transformation into *Agrobacterium* by freeze-thaw method

Aliquots of *A. tumefaciens* competent cells were placed on ice. 500 ng each of plasmid construct and pSoup helper plasmid was mixed with the *Agrobacterium* competent cells, the tube was then incubated on ice for 5 min and liquid nitrogen for 5 min. The cells were then heat shocked at 37^{o}C for 5 min using a water bath, and the tube rested on ice for 2

min. After addition of 1 ml LB medium, tubes were agitated for 4 h at 28^{o}C to allow cells to grow. Aliquots were spread on LB agar plates containing 50 µg/ml Rifampicin, 50 µg/ml kanamycin and 5 µg/ml tetracycline for vector selection. Plates were incubated at 28^{o}C for two days for colonies to develop.

2.13.6.1 Glycerol stock preparation

For long term storage, glycerol stocks were prepared from confirmed transformants of *E. coli* and *Agrobacterium*. Single colonies from the transformants were inoculated in 5 ml LB broth with appropriate antibiotics and allowed to grow overnight in the shaker at 37^{o}C and 28^{o}C. The next day, 500 µl of overnight grown bacterial culture was mixed with 40% (v/v) sterile glycerol solution in a 2 ml screw cap tube. Glycerol stocks were stored at -80^{o}C.

2.13.7 *Arabidopsis* floral dip transformation

Plant growth

Arabidopsis wild type Col-0 and mutant's were grown to flowering stage in the growth champer in 12 h photoperiod at 20^{0}C and 60% humidity. Plants were grown in an individual pot. 2-3 seeds were showed per pot and allowed to grow for few days, then only one healthy seedlings were allowed to grow until flowerescence stage. To obtain more floral buds per plant, primary inflorescences were clipped and allowed for 5-8 days to produce more secondary inflorescences.

Pre-culture

10 ml of LB medium (10 g l^{-1} tryptone, 5 g l^{-1} yeast extract, 10 g l^{-1} NaCl) containing kanamycin, rifampicin and tetracycline was inoculated with *A. tumefaciens* carrying binary vectors and incubated at 28°C with vigorous agitation. After 2 days, 500 ml of LB medium was inoculated with 5 ml of pre-culture and incubated for a further 24 h at 28°C. The

Agrobacterium culture was then pelleted by centrifugation at 1000xg for 10 min at room temperature. The pellet was suspended in 500 ml of infiltration medium (1x MS salts (Sigma). 1X Gamborg's B5 vitamins (Sigma), 5% w/v sucrose, 50 µl/L Silwet L-77 (Lehle Seeds, Round Rock, Texas, USA)). To prevent soil in pot from falling into infiltration medium, pot soil was covered with aluminium foil. *Arabidopsis* inflorescences with unopened floral buds were dipped into the medium and left to soak for 30 s. After dipping, plants were sealed in a bag and laid on their side for next 24 h. The covers were then removed and the plants rinsed with water and returned to their normal growing conditions. Seeds were collected from plants after 4-5 weeks.

2.13.8 Selection of transformants

Transformed lines were selected by sowing seeds in the MSR3 plates containing hygromycin (section 1.2.2.2 and 1.2.2.3) to select T-DNA insertion. Transformants which showed normal root development were then transferred to individual pots containing compost.

2.14 Sequencing

Plasmid DNA for sequencing was isolated by the mini prep method (Section 2.6.2). All sequencing reactions were performed by Eurofins Genomics, Germany. DNA sequence data was analysed using BLAST 2 sequencing tool (www.ncbi.nlm.nih.gov/blast/bl2seq).

Chapter 3 Role of NO in root growth and gravitropism

As discussed in the introduction (section 1.3.1), gravitropism plays a crucial role in causing plant organs to grow in the correct orientation during the early stage of seed germination. It facilitates the roots to grow downwards and the shoots upward. NO plays an important role in plant root development, so it is important to understand the role of NO in the important phenomenon of gravitropism. To achieve this, the following were investigated.

1. The gravitropic response of Wildtype (Col-0) and auxin, ethylene, NR mutants over different time intervals.
2. The pattern of NO accumulation in the bending zone of wildtype and auxin mutant roots.
3. The expression of *NIA1* gene in seedlings during gravitropism.
4. The gravitropic root bending response in Col-0 treated with auxin, ethylene and NO donors.

3.1 Gravitropic response in wild type and mutants

To examine the gravitropic response in the wildtype (Col-0) and auxin mutants (*aux1, axr2* and *axr3*), ethylene mutants (*ein3-1 and EIN3OX*) and NR mutants (*nia1, nia2*), seeds were sown on MSR3 plates and allowed to grow for five days in the growth chamber. After five days, plates were turned by 90^{o} vertically and allowed to gravistimulate in the dark. Photographs were taken at different times after gravistimulation (2, 4, 6, 8, 10 and 24 h), and root bending was measured and analysed.

3.1.1 Gravitropic response in wild type and auxin mutants (Col-0, *aux1*, *axr2* and *axr3*)

The effect of gravity on root bending in wildtype and auxin mutants were analysed, (Fig. 3-1 A). Col-0 seedling roots responded to gravity and bend towards the gravity vector, bending was visible after 2 h of gravistimulation and reached the maximum at 24 h. In contrast, auxin mutants *aux1, axr2* and *axr3* did not respond to the gravistimulation (Fig. 3-1 B, C and D). The *axr3* seedlings have a much shorter root length as compared to *aux1, axr2*. Even though *aux1, axr2* roots did not respond to gravity signals, root coiling was observed from the beginning, whereas Col-0 root grows downwards.

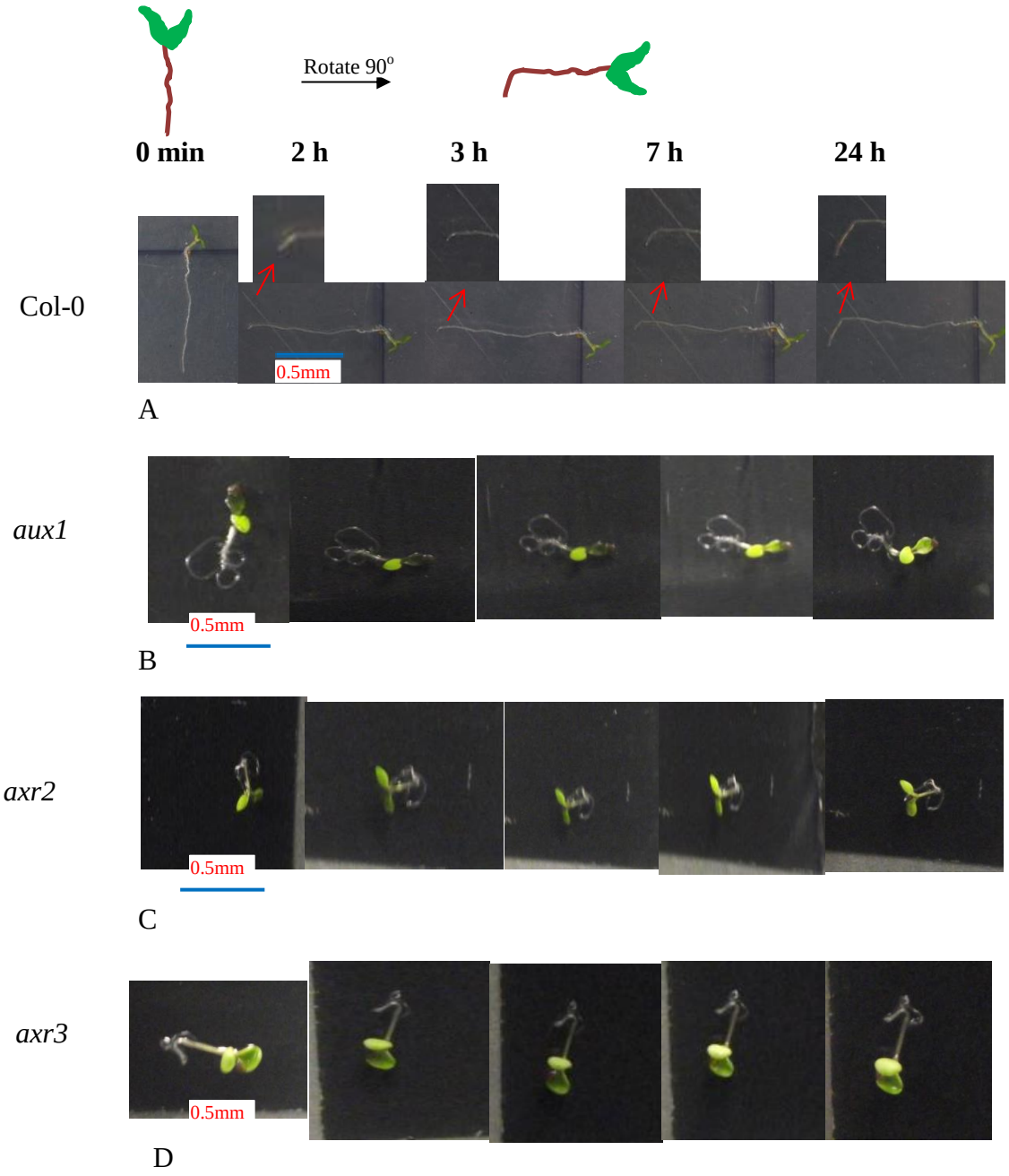

Figure 3-1: Col-0 Wild type root showed gravitropic bending but not the auxin mutants

(Scale bar – 0.5 mm). Col-0 wild type and auxin mutants (*aux1*, *axr*2 and *axr3*) were germinated on MSR3 plates in 12 h photoperiod at 20°C and 60% relative humidity. After 5 days past germination, seedlings were gravistimulated by changing the direction of the plate (Horizantal orientation) by 90°.

3.2 **Visualization of NO during gravitropism**

To observe the location of NO produced in plant roots, a NO-specific dye, DAF-2DA was used. This dye will bind with NO and emit fluorescence under the laser confocal microscope (excitation; 495 nm and emission; 515 nm). The fluorescence intensity was directly proportional to the cumulative amount of NO in the root during the gravistimulation. The experiment was designed in such a way to compare the NO synthesis and accumulation during gravitropism. To do that a set of seedlings were treated with cPTIO (NO scavenger) so that it will remove the already synthesized NO from the root. The experiment was done with both cPTIO treated and untreated, gravistimulated and non-gravistimulated roots.

3.2.1 Gravistimulation induces asymmetric accumulation of NO in Col-0

Gravistimulation induced the asymmetric accumulation of NO in the bending zone of the Col-0 root (Fig. 3-2 A and B). When the roots were pre-treated with the NO scavenger cPTIO and allowed to respond to gravity, the observed level of fluorescence was reduced throughout the root compared to cPTIO untreated gravistimulated root. In both cases, accumulation of NO was observed in the lower side of the bending region of the root (Fig. 3-2 B). Whereas in non-gravistimulated root (Fig. 3-2 C) and cPTIO pre-treated non-gravistimulated root (Fig. 3-2 D) asymmetric accumulation was not found. Equal amounts of fluorescence were observed in upper and lower side of the root. These results demonstrate that gravistimulation induced synthesis and asymmatric accumulation of NO in the lower side of the bending root.

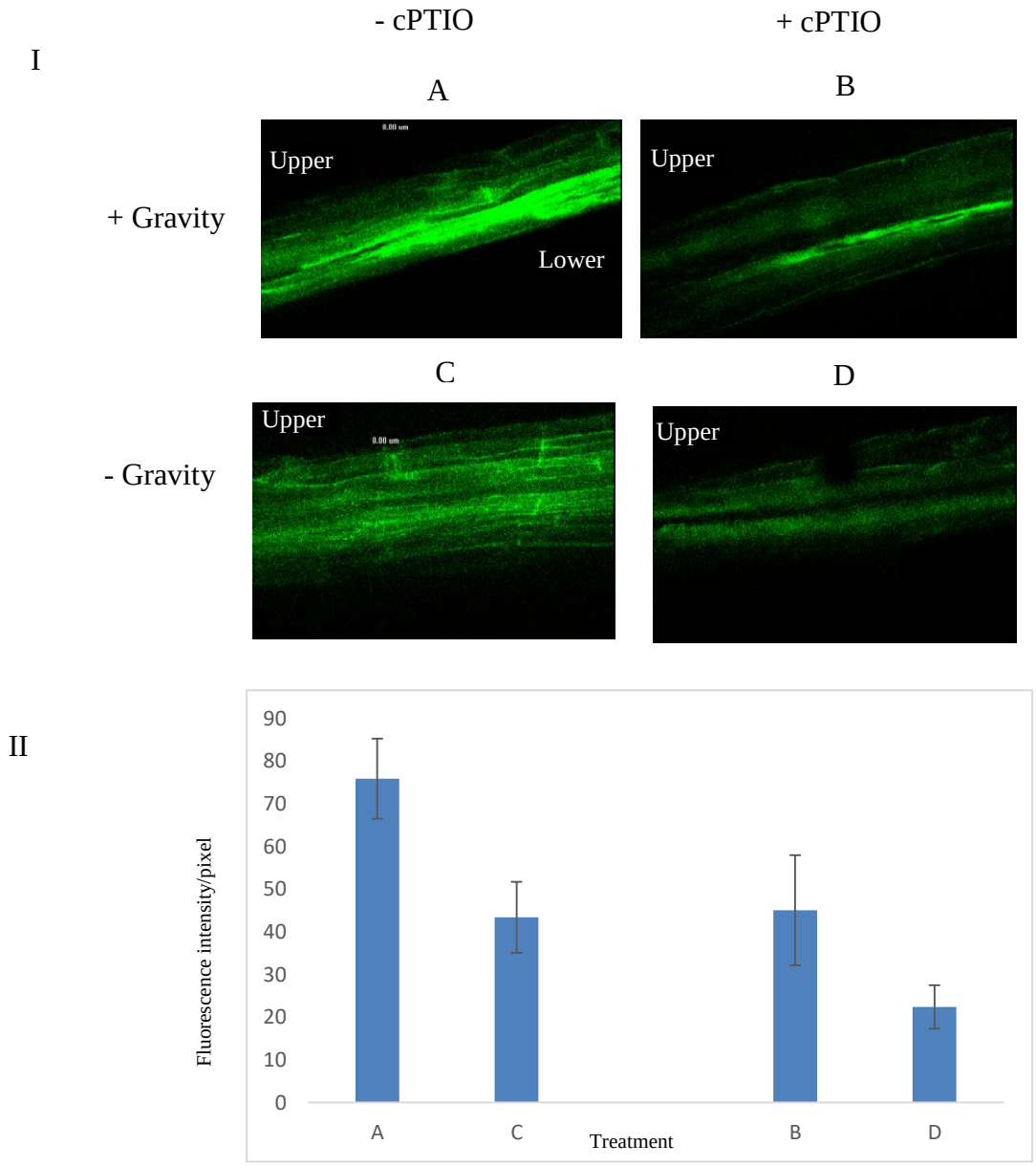

Figure 3-2: Gravistimulation induces accumulation of NO in bending zone

Seeds of Col-0 were germinated and grown in MSR3 plates placed vertically in the growth chamber in 12 h photoperiod at 20°C and 60% humidity. After 5 days, the seedlings were gravistimulated for 2 h by changing the direction of the plate (Horizantal orientation) by 90°. For control to remove the initial NO, 100 µM cPTIO was applied on the roots by using a micropipette and incubate at dark for 5 min, then gravistimulated for 2 h. Then 20 µM NO specific dye DAF-2DA was applied to the roots and incubated in dark for 20 min further, then seedlings were washed three times with fresh MES buffer and samples were observed by confocal microscopy for the presence of NO. Confocal images were obtained from root tip. Fig. 3-2 A gravistimulated Col-0 root. B, gravistimulated cPTIO pretreated Col-0 root. C, non-gravistimulated Col-0 root. D, non-gravistimulated cPTIO pretreated Col-0 root. Excitation 495 nm, emission 515 nm, gain- 4.5, exposures- 35 µs (Scale bar, 50.49 µm). (n=3). II. Fluorescence intensity/pixel was measured using Fiji image analysis software. All data are given as mean± SE; n=5/seedling.

3.2.2 *aux1* produced ubiquitous amount of NO

Gravistimulated agravitropic auxin mutant *aux1* root showed elevated levels of NO fluorescence in the root (Fig. 3-3 A). It did not show asymmetrical accumulation of NO upon gravistimulation like Col-0. cPTIO pre-treated gravistimulated root showed reduced level of NO (Fig. 3-3 B). Non-gravistimulated *aux1* root (Fig. 3-3 C) also showed the elevated level of NO fluorescence like *aux1* gravistimulated root. Non-gravistimulated cPTIO pre-treated root showed reduced level of NO (Fig. 3-3 D). These results demonstrate that *aux1* mutant root makes more NO at all the times, but NO does not accumulate asymmetrically in the lower side of the root in response to gravity.

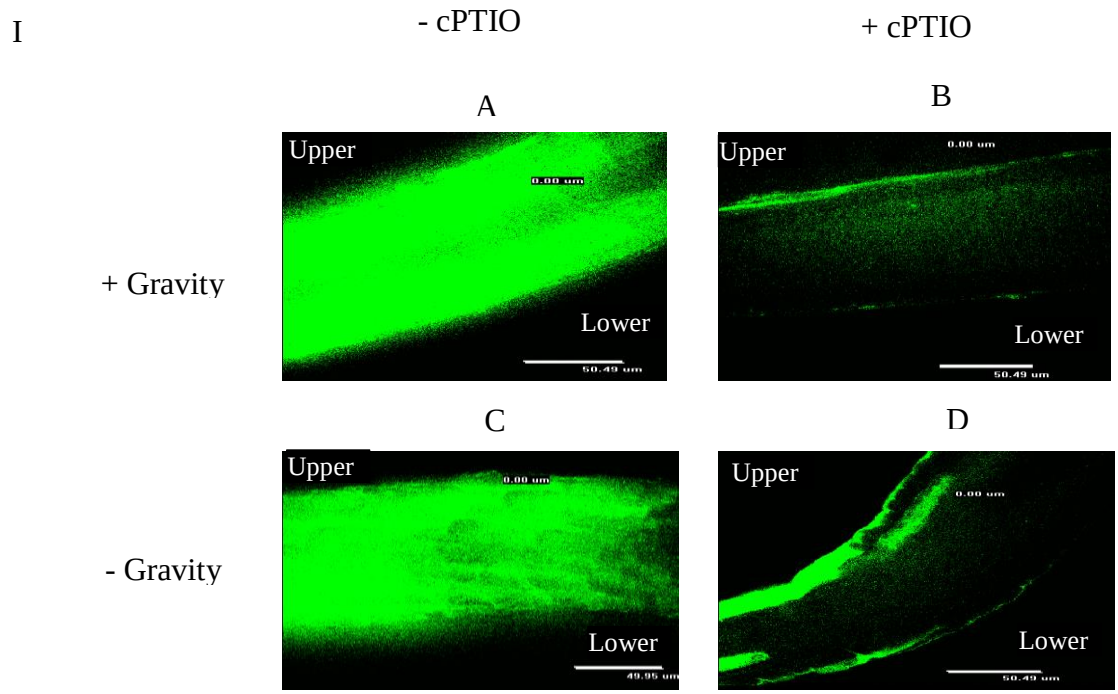

II

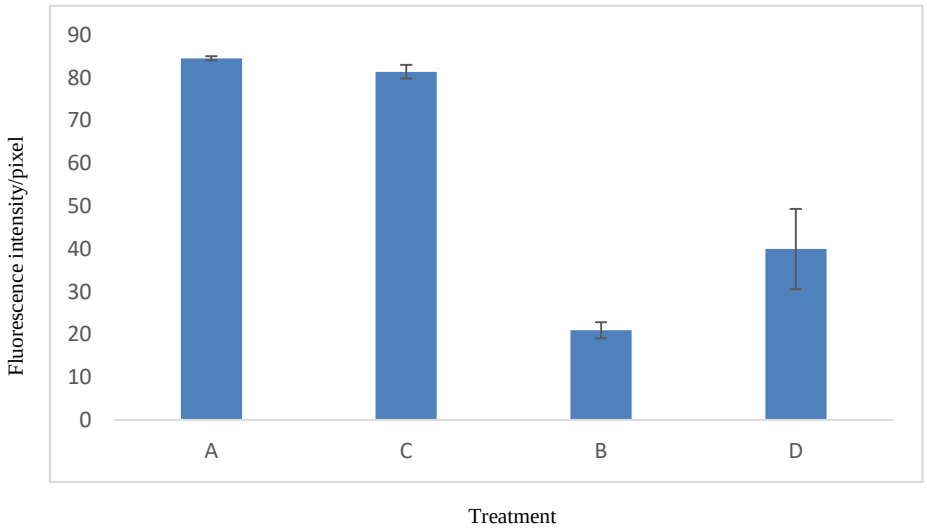

Figure 3-3: *aux1* root showed increased NO.

Seeds of *aux1* were germinated and grown in MSR3 plates placed vertically in the growth chamber in 12 h photoperiod at 20^{o}C and 60% humidity. After 5 days, the seedlings were gravistimulated for 2 h by changing the direction of the plate (Horizantal orientation) by 90^{O}. For control to remove the initial NO, 100 µM cPTIO was applied on the roots by using a micropipette and incubate at dark for 5 min, then gravistimulated for 2 h. then gravistimulated for 2 h. Then 20 µM NO specific dye DAF-2DA was applied to the roots and incubated in dark for 20 min further. Seedlings were washed three times with fresh MES buffer and samples were observed by confocal microscopy for the presence of NO. Fig. 3-3 A, gravistimulated *aux1* root. B, gravistimulated cPTIO pre-treated *aux1* root. C, non-gravistimulated *aux1* root. D, non-gravistimulated cPTIO pretreated *aux1* root. Excitation 495 nm, emission 515 nm, gain- 4.5, exposures- 35 µs (Scale bar, 50.49 µm). II. Fluorescence intensity/pixel was measured using Fiji image analysis software. All data are given as mean± SE; n=5/seedling.

3.2.3 *axr2* auxin mutant makes elevated amount of NO

Early auxin response mutant *axr2* also did not showed any difference in the level of NO fluorescence in gravistimulated and non-gravistimulated roots (Fig. 3-4 A and C). Both showed elevated level of fluorescence like *aux1* mutants. Gravistimulated cPTIO pre-treated *axr2* root showed reduced and equal level of fluorescence in the upper and lower side of the root (Fig. 3-4 B), whereas non-gravistimulated, cPTIO pre-treated *axr2* root showed greatly reduced level of NO fluorescence (Fig. 3-4 D, II).

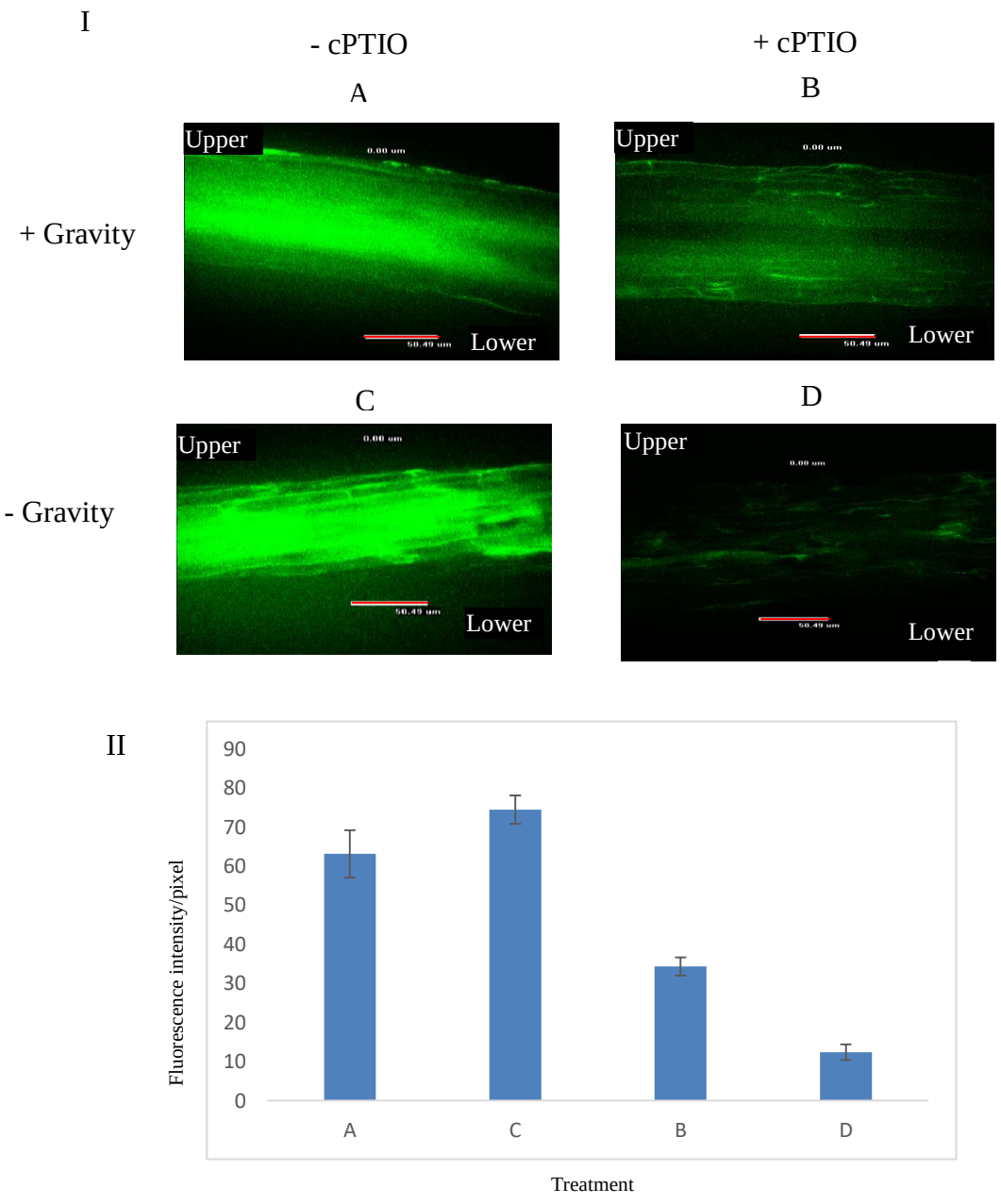

Figure 3-4: *axr2* root showed increased level of NO

Seeds of *axr2* was germinated and grown in MSR3 plates placed vertically in the growth chamber in 12 h photoperiod at 20°C and 60% relative humidity. After 5 days, the seedlings were gravistimulated for 2 h by changing the direction of the plate (Horizantal orientation) by 90°. For control to remove the initial NO, 100 µM cPTIO was applied on the roots by using a micropipette and incubate at dark for 5 min, then gravistimulated for 2 h. Then 20 µM NO specific dye DAF-2DA was applied to the roots and incubated in dark for 20 min further. Seedlings were washed three times with fresh MES buffer and samples were observed by confocal microscopy for the presence of NO. Fig. 3-4 A, gravistimulated *axr2*

root. B, gravistimulated cPTIO pretreated *axr2* root. C, non-gravistimulated *axr2* root. D, non-gravistimulated cPTIO pretreated *axr2* root excitation 495 nm, emission 515 nm, gain-4.5, exposures-35 µs (Scale bar, 50.49 µm). II. Fluorescence intensity/pixel was measured using Fiji image analysis software. All data are given as mean± SE; n=5/seedling.

3.2.4 Effect of gravistimulation in auxin mutant *axr3*

Gravistimulated *axr3* mutant root showed equal levels of NO fluorescence in the upper and lower side of root (Fig. 3-5 A). Non-gravistimulated root (Fig. 3-5 C), cPTIO pretreated gravistimulated and non-gravistimulated roots (Fig. 3-5 B and D) all showed very low levels of fluorescence.

I

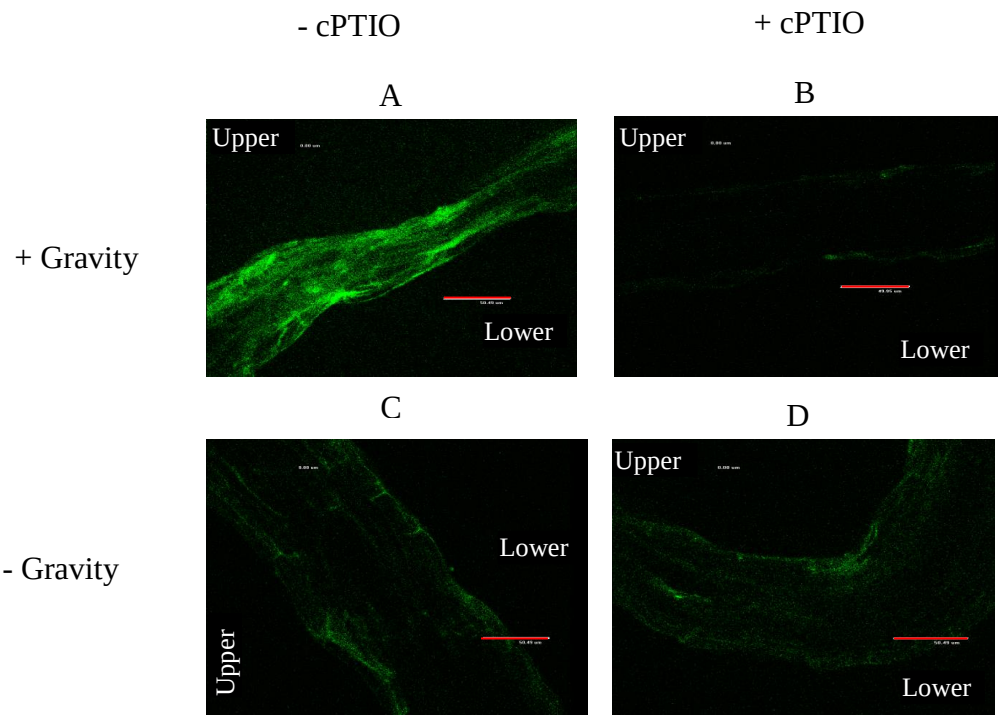

II

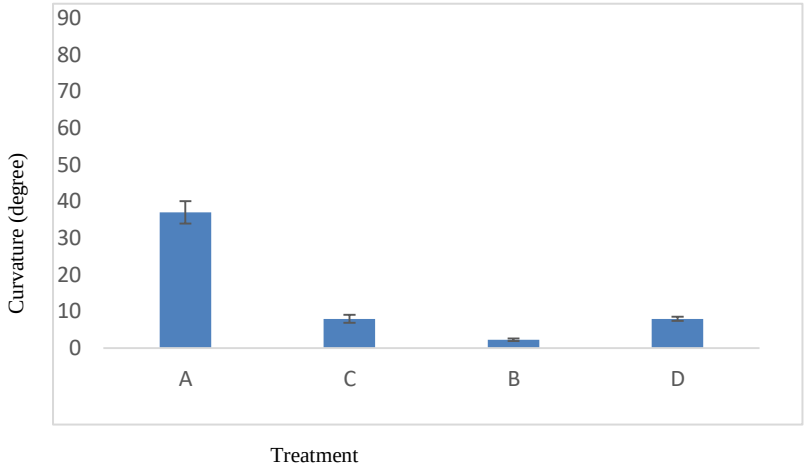

Figure 3-5: Confocal images of gravistimulated and non-gravistimulated *axr3* root

Seeds of *axr3* were germinated and grown in MSR3 plates placed vertically in the growth chamber in 12 h photoperiod at 20°C and 60% humidity. After 5 days, the seedlings were gravistimulated for 2 h by changing the direction of the plate (Horizantal orientation) by 90°. For control to remove the initial NO, 100 µM cPTIO was applied on the roots by using a micropipette and incubate at dark for 5 min, then gravistimulated for 2 h. Then 20 µM NO specific dye DAF-2DA was applied to the roots and incubated in dark for 20 min further. Seedlings were washed three times with fresh MES buffer and samples were observed by confocal microscopy for the presence of NO. Fig. 3-5 A, gravistimulated *axr3* root. B, gravistimulated cPTIO pretreated *axr3* root. C, non-gravistimulated *axr3* root. D, non-gravistimulated cPTIO pretreated *axr3* root. excitation 495 nm, emission 515 nm, gain- 4.5, exposures- 35 µs (Scale bar, 50.49 µm). II. Fluorescence intensity/pixel was measured using Fiji image analysis software. All data are given as mean± SE; n=5/seedling.

3.3 Quantification of *NIA1* gene expression during gravitropism

3.3.1 Isolation of RNA from Arabidopsis root (Col-0)

Total RNA was isolated from the root tip (I), middle region (II) and hypocotyls region (III) of Col-0, *aux1* and *axr2* seedlings and 3 µg of RNA was electrophoresed in a 1% (w/v) agarose gel (Fig. 3-6). Results showed good quality of intact RNA. RNA was quantified by measuring the absorbance at 260 nm using a Nanodrop machine.

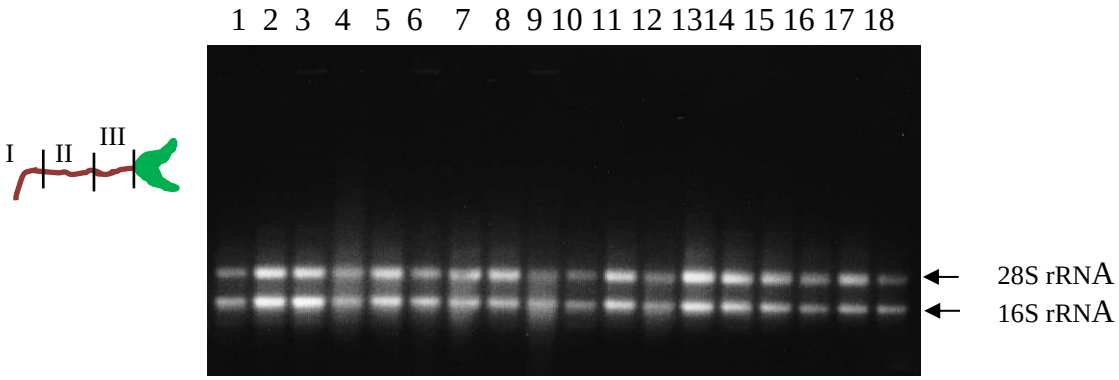

Figure 3-6: Agarose gel electrophoresis of Col-0 RNA samples

Lanes 1, 4, 7, 10, 13 and 16 represent the RNA from root tips (I), Lanes 2, 5, 8, 11, 14 and 17 represent the RNA from middle region (II). Lanes 3, 6, 9, 12, 15 and 18 represent the RNA from hypocotyls (III).

3.3.2 cDNA synthesis from Col-0, *aux1 and axr2* RNA samples

cDNA was synthesized from 5 µg of RNA sample (as described in 2.7) with negative controls (template control (without RNA) and enzyme control (without RT enzyme). 0.3 ng of TRAF (Tumor necrosis Receptor Associate Factor) RNA was mixed with each sample during the reverse transcription which was used as an external normalisation control. Ten times the product was diluted and used as a template for further PCR reactions.

3.3.3 PCR amplification of *NIA1* cDNA sequence from Col-0

cDNA from root tip, middle region and hypocotyl region of Col-0 non-gravistimulated and gravistimulated (30 min, 1, 2, 4 and 6 h) seedlings was used for the PCR amplification of a transcript encoded by the *NIA1* gene. Results showed that all the samples were positive for the expression of *NIA1* gene and gave the expected amplicon size of 150bp (Fig. 3-7).

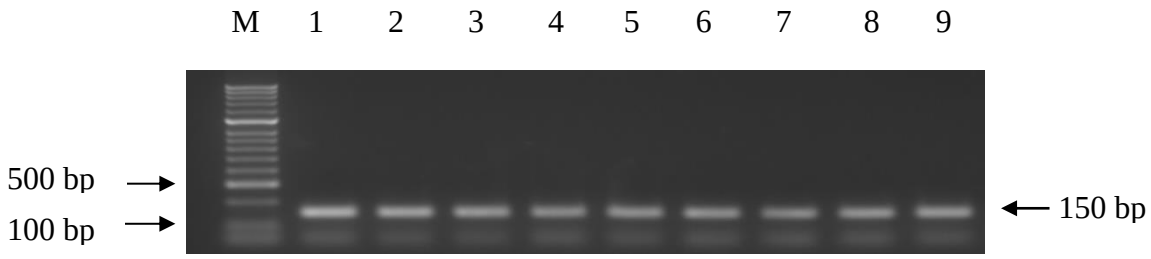

Figure 3-7: Agarose gel image of amplification of *NIA1* from cDNA of Col-0

cDNA from the Col-0 root samples were used to check the amplification for *NIA1* gene with *NIA1* primers. Lane M – 100 bp DNA ladder. Lanes 1-3 amplicons of NIA1 transcript from Col-0 non-gravistimulated and lanes 4-9 gravistimulated (30 min (4, 5, 6), 1 h (7, 8, 9)) roots (root tip (1, 4, 7), middle region (2, 5, 8) and hypocotyl region (3, 6, 9)).

3.3.4 Quantification of NIA1 transcript by Q-RT-PCR

To quantify the expression of *NIA1* gene transcript in roots during gravitropism, Q-RT-PCR was performed on total RNA extracted from the root regions (root tip, a middle region and hypocotyl region). RNA was extracted from Col-0, *aux1* and *axr2* non-gravistimulated and gravistimulated roots. 5 µg of RNA was reverse transcribed with oligo dT, and 1 ng TRAF spike (Human Tumour Necrosis Receptor Associating Factor 1) used as an internal control. A 10 fold serially diluted M13 pBluescriptSK(+) plasmid was used as a standard. Samples were amplified using *NIA1* gene specific primers, TRAF primers and M13 primers (see Table 2.1). Individual sample expression was normalised against the internal TRAF spikes.

3.3.4.1 Col-0 root tip shows a gradual increase in NIA1 transcript 2 h after gravistimulation

Gravistimulated Col-0 root tip Q-PCR analysis showed a gradual increase in NIA1 transcript over the first 2 h, NIA1 transcripts start to increase at 30 min after gravistimulation and showed a 3 fold increase at 2 h, where the gravity bending experiment also showed root bending at 2 h after gravistimulation (Fig. 3-1). After the initiation of root bending, the NIA1 transcript level starts to decrease (4 h) and after 6 h it showed 3.5 fold reduction in transcript level. In the elongation zone a similar NIA1 accumulation pattern was observed. This result clearly showed the accumulation NIA transcript in response to root gravitropism.

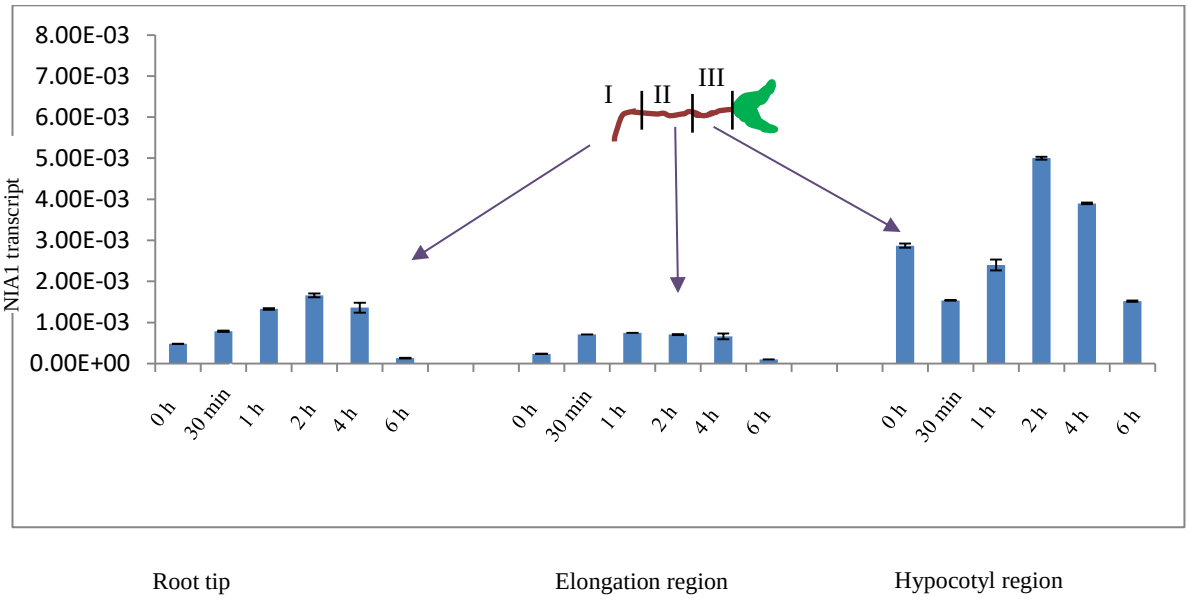

Figure 3-8: qPCR shows an increase in NIA1 transcript in Col-0 following gravistimulation

qPCR performed on RNA from Col-0 root tip (I), elongation (II) and hypocotyl regions (III). RNA was isolated from the seedlings with the different times of gravistimulation. Samples were analysed for the changes in NIA1 transcript level during the gravistimulation. All data are given as mean± SE; n=2.

3.3.4.2 *aux1* root shows reduction of NIA1 transcript in response to gravistimulation

The *aux1* root tip Q-PCR analysis showed non-gravistimulated *aux1* root has higher amount of NIA1 transcript. At 30 min after gravistimulation, a 2 fold reduction of NIA1 transcript level was observed but did not show major changes after the initial reduction. In contrast, elongation and hypocotyl regions did not show major changes in transcript level. In general, 3 fold higher NIA1 transcript levels were observed in the root tip, elongation zone and hypocotyl region than Col-0.

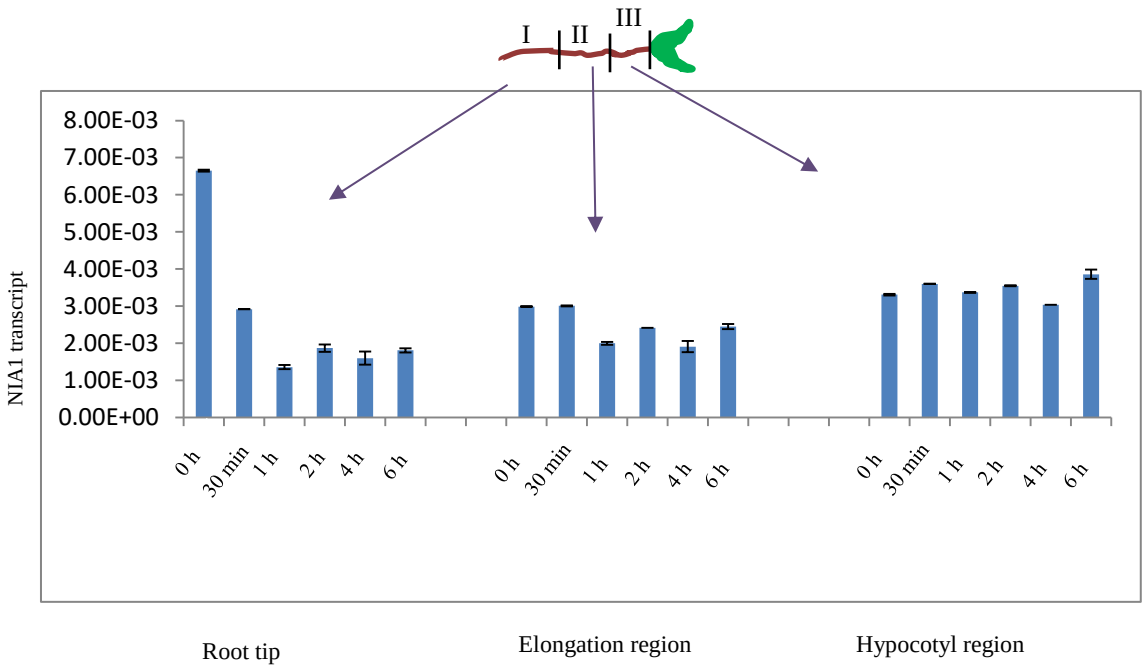

Figure 3-9: *aux1* qPCR shows initial reduction of NIA1 transcript in response to gravity

qPCR performed on RNA from *aux1* root tip (I), elongation (II) and hypocotyl regions (III). RNA was isolated from the seedlings with the different times of gravistimulation. Samples were analysed for the changes in NIA1 transcript level during the gravistimulation. All data are given as mean± SE; n=2.

3.3.4.3 *axr2* root shows negligible amount of NIA1 expression in response to gravistimulation

3.3.4.4 Gravistimulated *axr2* root tip Q-PCR analysis showed reduced amount of *NIA1* gene expression in root tip, where as in elongation zone transcript level was increased 5 fold at 30 min then it was decreased. In hypocotyl region NIA1 transcript level was increased at 2 h. In general *axr2* root tip, elongation and hypocotyl region NIA1 transcript level was 100 fold lower than *aux1*.

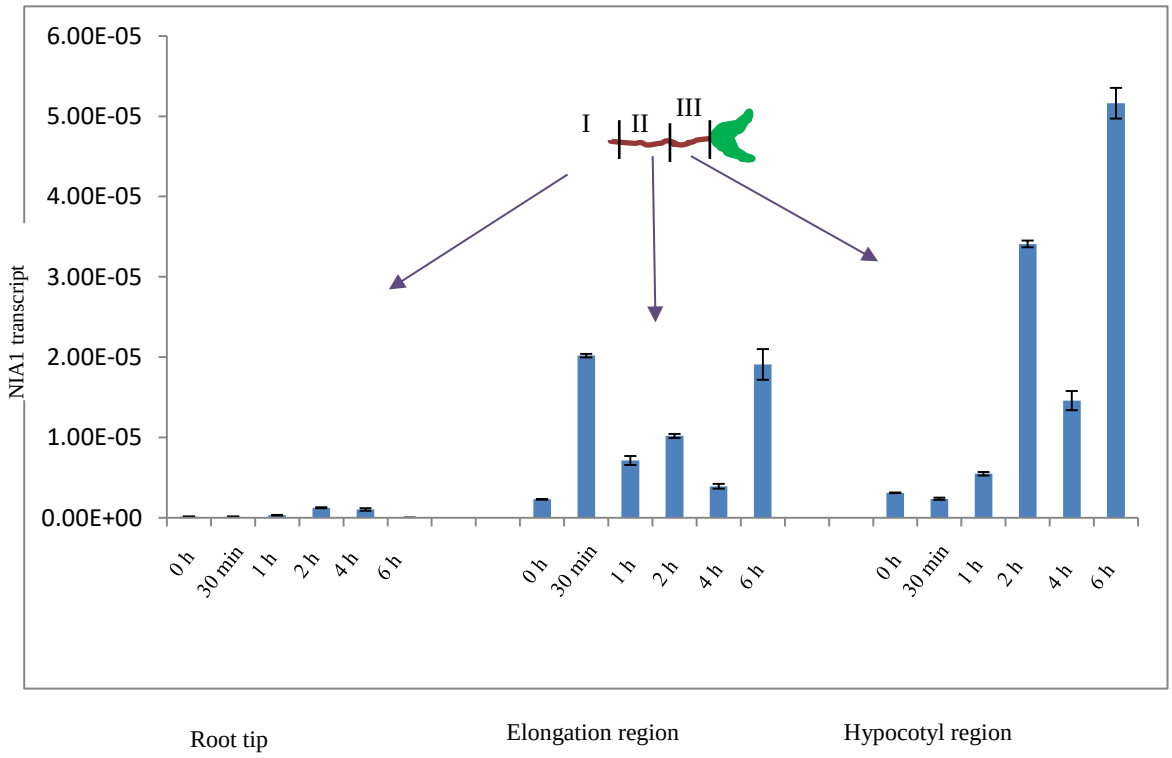

Figure 3-10: *axr2* showed lower levels of NIA1 transcript in root

qPCR performed on RNA from *axr2* root tip (I), elongation (II) and hypocotyl regions (III). RNA was isolated from the seedlings with the different times of gravistimulation. Samples were analysed for the changes in NIA1 transcript level during the gravistimulation. All data are given as mean± SE; n=2.

3.3.5 Roots of NR mutant *nia1* bend more slower than *nia2* and Col-0

To investigate the importance of NR genes in root bending following gravistimulation, root bending was compared in *nia1*, *nia2* and Col-0 seedlings. *nia1* roots showed slower root bending than *nia2*, and both *nia1* and *nia2* showed much slower bending compared to Col-0 (Fig. 3-11 A). Bending in Col-0 visible 2 h after gravistimulation, whereas in *nia1* and *nia2* bending visible only after 4 h (Fig. 3-11 B). Two-way ANOVA analysis results (Fig. 3-11 A) (Appendix 1) showed that Col-0, *nia1* and *nia2* were significantly different from each other's in terms of over all root bending, also root bending was significantly inteact during the course of time. All Pairwise comparison (Table 6) was carried out for each simple main effect to check exactly which time point Col-0, *nia1* and *nia2* were significantly different from each other. Col-0 and *nia1* was significantly different at all-time points. *nia1 and nia2* were only significantly different at 2, 8 10 and 24 h, and they are not significantly different at 4 and 6 h. Col-0 and *nia2* was significantly different at 2, 4, 6, 8 and 24 h except 10 h. Statistical analysis by linear mixed model also showed significant level of difference in gravity bending between Col-0 and *nia1* (Fig. 3-12), Col-0 and *nia2* (Fig. 3-13) and *nia1* and *nia2* (Fig. 3-14), (Appendix 2 to 4).

Table 6: Pairwise comparition between Col-0, *nia1* and *nia2*

Plant type	Over all	2hr	4hr	6hr	8hr	10hr	24hr
Col-0 vs *nia1*	*	*	*	*	*	*	*
nia1 vs *nia2*	*	*	-	-	*	*	*
Col-0 vs *nia2*	*	*	*	*	*	-	*

*- significantly different; - not significantly different.

I

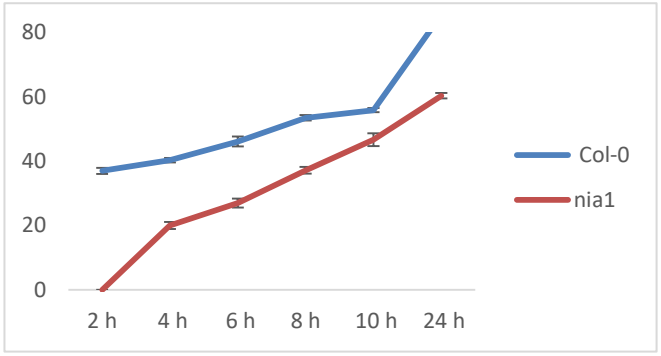

II

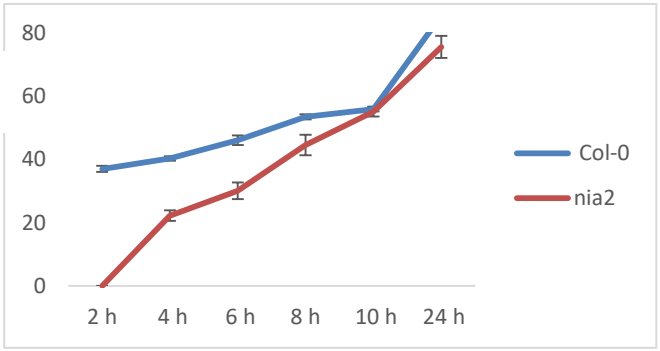

III

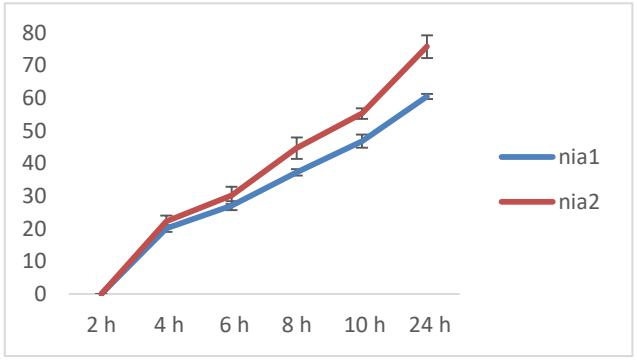

Figure 3-11. Pair wise comparision of root bending in Col-0, *nia1* and *nia2*

Over all root bending between Col-0 and *nia1* (I), Col-0 and *nia2* (II), *nia1* and *nia2* (III) were compared. Col-0, *nia1* and *nia2* were significantly different from each other in terms of root bending. All data are the mean of n=4 replicates ±SE.

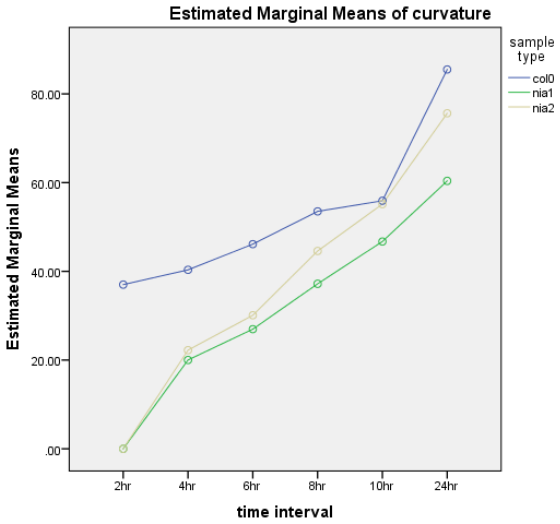

Figure 3-12: Overall root bending graph for Col-0, *nia1* and *nia2*

A two-way ANOVA was conducted to explore the difference between sample type (Col-0, *nia1* and *nia2*) and impact of time (2, 4, 6, 8, 10 and 24 h) on gravity bending. Normality was assessed using Shapiro-Wilks test, samples were normally distributed ($p > 0.05$). There was a statistically significant interaction between sample type and time interval on root bending $F(10, 54) = 14.169$, $p = 0.0005$. There was a statistically significant difference in main effect for sample type $F(2, 54) = 224.782$, $p = 0.0005$ and overall time $F(5, 54) = 429.712$, $p = 0.0005$.

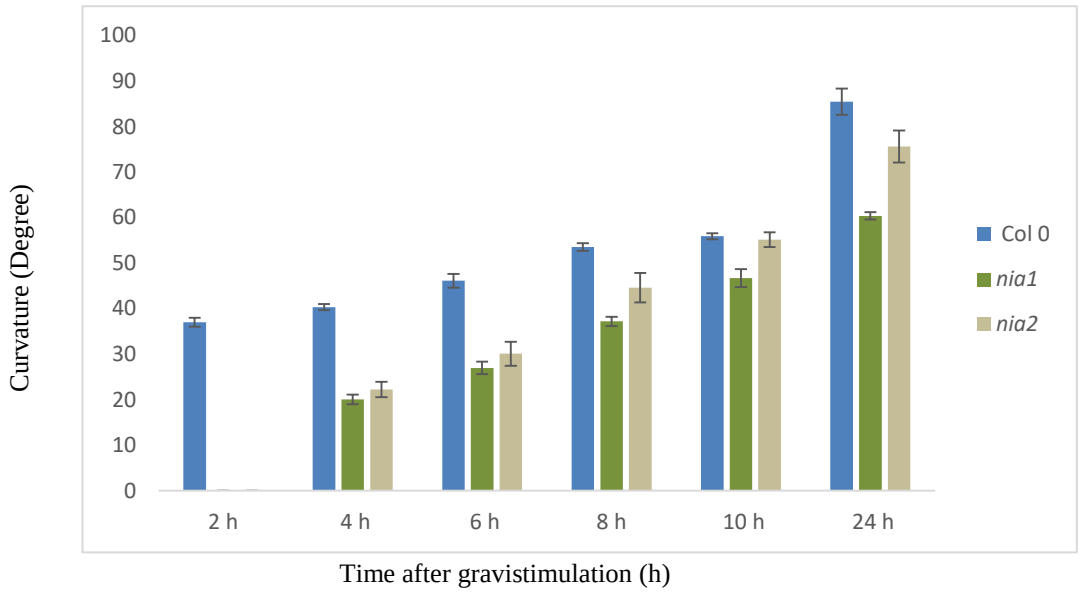

Figure 3-13: The *nia1* showed slower bending compared to the roots of Col-0 and *nia2*

Col-0 wild type and *nia1* seedlings were grown in MSR3 plates under a 12 h photoperiod at 20°C and 60% relative humidity. After 5 d seedlings were gravistimulated by changing the direction of the plate (Horizantal orientation) by 90°. Photographs were taken at different time intervals, root curvature was measured. All data are the mean of n=4 replicates ±SE.

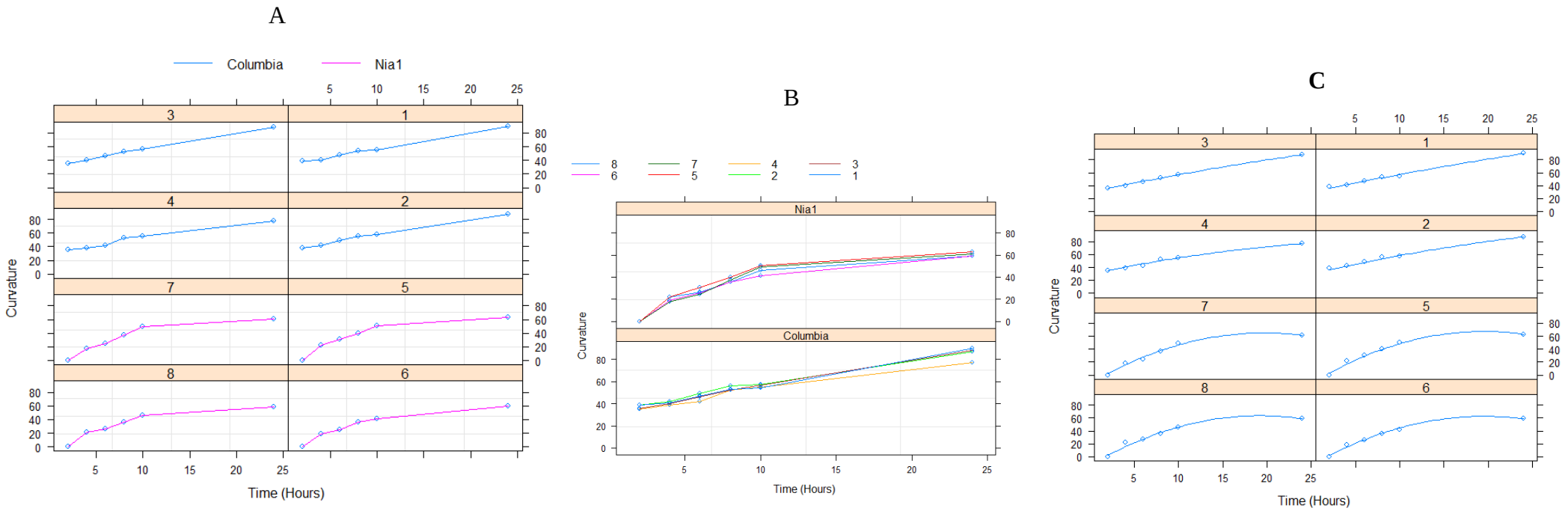

Figure 3-14: Comparison of root bending between Col-0 and *nia1*

Root bending between Col-0 and *nia1* was analysed statistically by Linear mixed-effects model. Curvature versus time for the 8 samples 1-4 are Col-0, 5-8 are *nia1*. The fitted relationships are shown from the minimum adequate mixed-effect model. These demonstrate that *nia1* roots bend slower that Col-0 and showed significant difference between Col-0 and *nia1* in terms of gravity bending. $p<0.05$. A and B raw data, C-fitted plot.

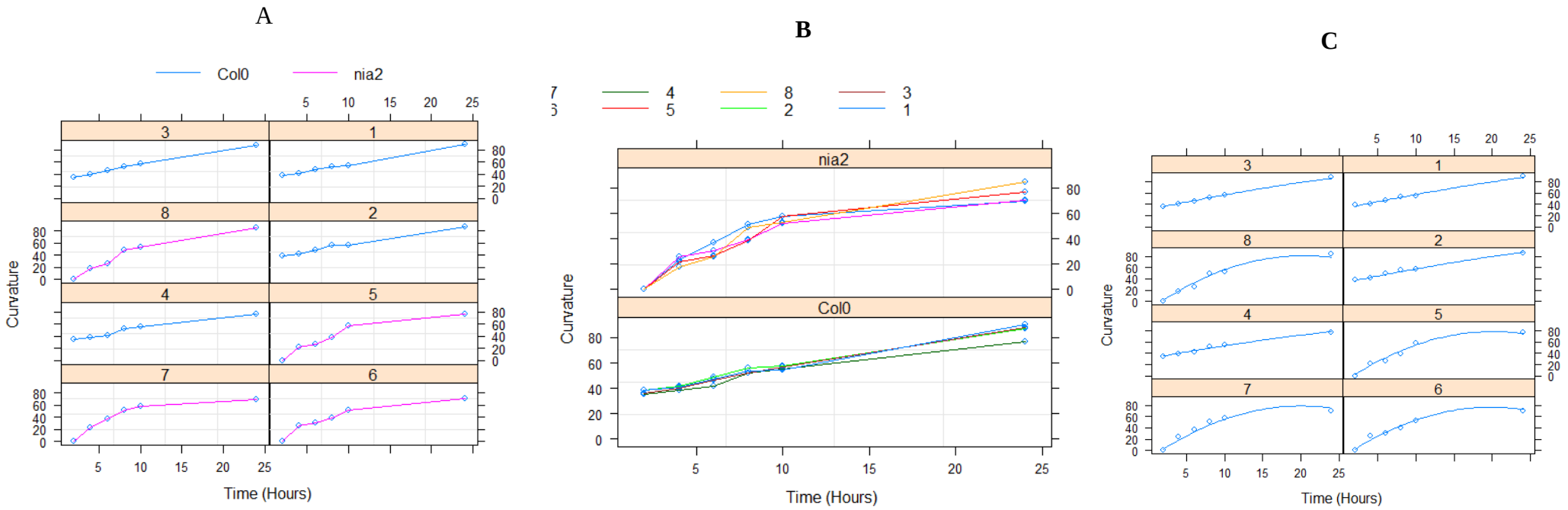

Figure 3-15: Comparison of root bending between Col-0 and *nia2*

Root bending between Col-0 and *nia2* was analysed statistically by Linear mixed-effects model. Curvature versus time for the 8 samples 1-4 are Col-0, 5-8 are *nia2*. The fitted relationships are shown from the minimum adequate mixed-effect model. These demonstrate that *nia2* roots showed lesser bending than Col-0 and showed significant difference between Col-0 and *nia2* in terms of gravity bending. $p<0.05$. A and B raw data, C-fitted plot.

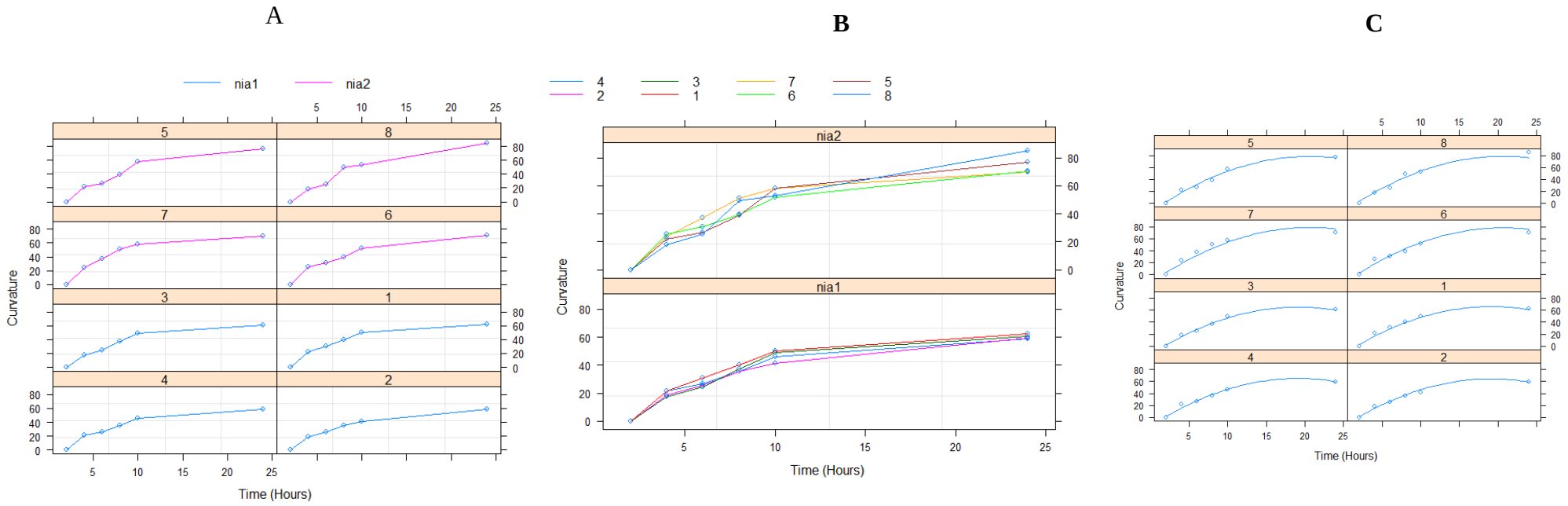

Figure 3-16: Comparison of root bending between *nia1* and *nia2*

Root bending between *nia1* and *nia2* were analysed statistically by Linear mixed-effects model. Curvature versus time for the 8 samples 1-4 are *nia1*, 5-8 are *nia2*. The fitted relationships are shown from the minimum adequate mixed-effect model. These demonstrate that *nia2* roots bends slower than *nia1*. This model showed significant difference between these two plants in terms of gravity bending. $p<0.05$ *nia1* n=4, *nia2* n=4. A and B raw data, C-fitted plot.

3.3.6 Ethylene mutant showed slower root bending than Col-0

To investigate the role of ethylene in root bending following gravistimulation, root bending was compared in ethylene mutants (*ein3-1* and *EIN3Ox*) and Col-0. Results showed both the ethylene mutants have a slower root bending than Col-0 (Fig. 3-15 A). When comparing the root bending between the mutants, ethylene over-expressing mutant *EIN3Ox* root showed slower and reduced root bending than ethylene insensitive mutant *ein3-1*. *EIN3Ox* mutant takes more than six hours to initiate root bending, hence the root bending starts around 8 h after gravistimulation, whereas in *ein3-1* mutant root bending started just 4 h after gravistimulation. Two-way ANOVA analysis results (Appendix 5) showed that Col-0, *ein3-1* and *EIN3Ox* were significantly different from each other's in terms of overall root bending, also root bending was significantly inteact during the course of time. All Pairwise comparison (Table 7) was carried out for each simple main effect to check exactly which time point Col-0, *ein3-1* and *EIN3Ox* significantly different from each other. Col-0 and *ein3-1* was significantly different at 2, 4, 6, 8 h not differ at 10 & 24 h. *ein3-1* and *ein30x* was significantly different at 4, 8, 10, 24 h. Col-0 and *EIN3Ox* was significantly different at all time points. Statistical analysis using a linear mixed effect model also showed a significant difference in bending between Col-0 and *ein3-1* (Fig. 3-16), Col-0 and EIN3Ox (Fig. 3-17) and *ein3-1* and EIN3Ox (Fig. 3-18), (Appendix 6 to 8).

Table 7: Pairwise comparition between Col-0, *ein3-1* and *EIN30X*

Plant type	Over all	2hr	4hr	6hr	8hr	10hr	24hr
Col-0 vs *ein3-1*	*	*	*	*	*	-	-
ein3-1 vs *EIN30X*	*	-	*	*	*	*	*
Col-0 vs *EIN30X*	*	*	*	*	*	*	*

*- significantly different; - not significantly different.

I

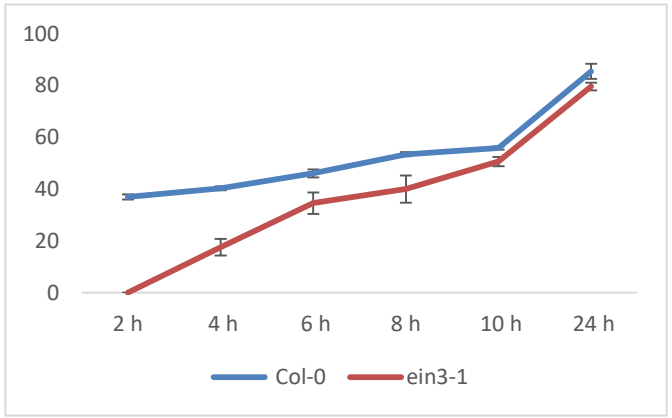

II

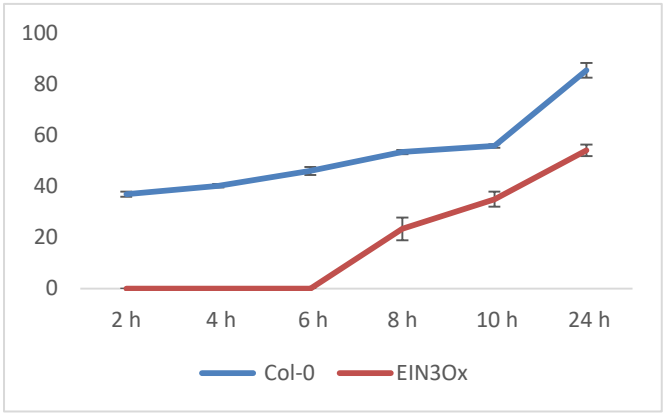

III

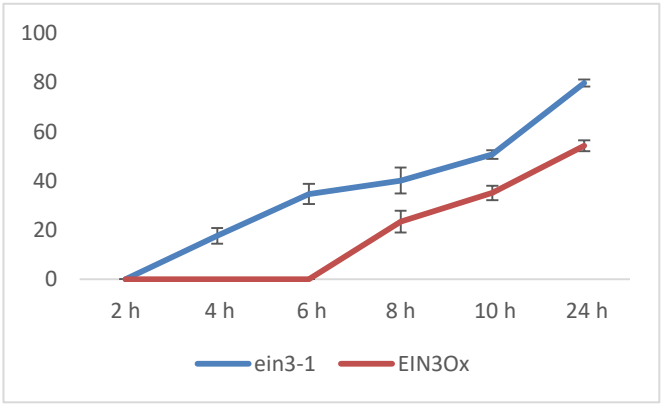

Figure 3-17. Pair wise comparision of root bending in Col-0, *ein3-1* and EIN3Ox

Over all root bending between Col-0 and *ein3-1* (I), Col-0 and EIN3Ox (II), *ein3-1* and EIN3Ox (III) were compared. Col-0, *ein3-1* and EIN3Ox were significantly different from each other in terms of root bending. All data are the mean of n=4 replicates ±SE.

A

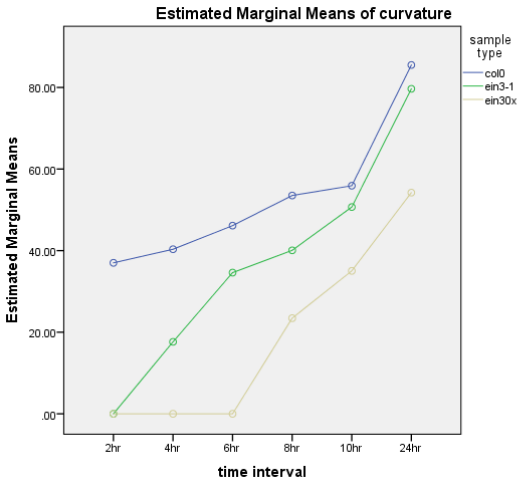

Figure 3-18: Overall root bending graph for Col-0, *ein3-1* and EIN30X

A two-way ANOVA was conducted to explore the difference between sample type (Col-0, *ein3-1* and EIN30X) and impact of time (2, 4, 6, 8, 10 and 24 h) on gravity bending. Normality was assessed using Shapiro wilks test, samples were normally distributed ($p > 0.05$). There was a statistically significant interaction between sample type and time interval on root bending $F(10, 42) = 11.34$, $p = 0.0005$. There was a statistically significant difference in main effect for sample type $F(2, 42) = 353.233$, $p = 0.0005$ and overall time $F(5, 42) = 278.723$, $p = 0.0005$.

B

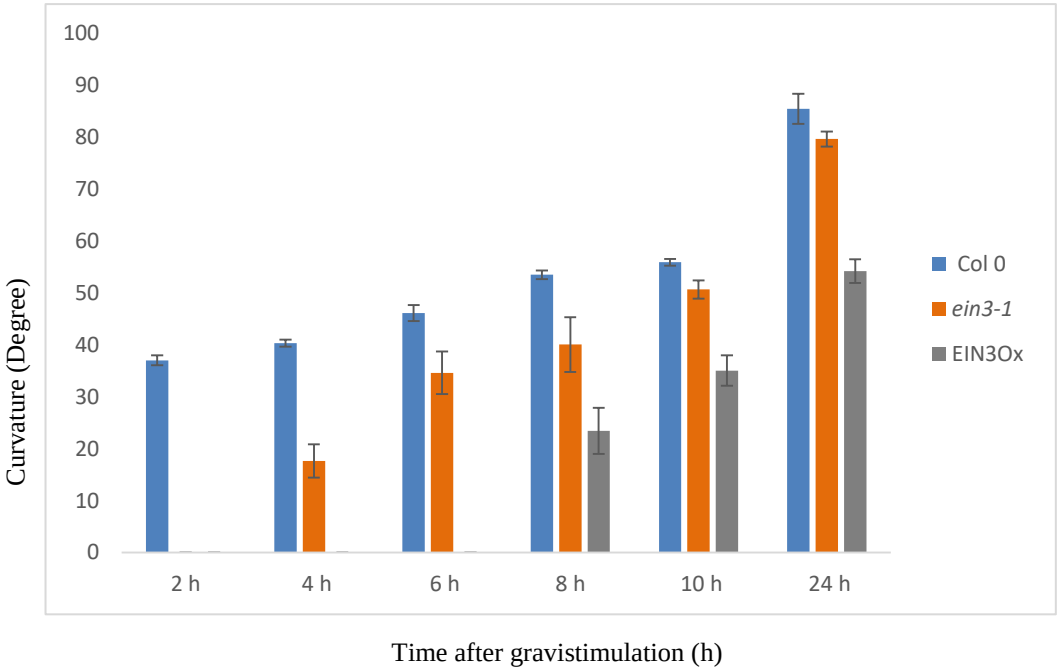

Figure 3-19: The roots of *EIN3Ox* showed slower bending than the roots of Col-0 and *ein3-1*

The *ein3-1* and *EIN3Ox* seedlings were grown in MSR3 plates in 12 h photoperiod at 20°C and 60% relative humidity. After 5 d seedlings were gravistimulated by changing the direction of the plate (Horizantal orientation) by 90°. Photographs were taken at different time intervals, root curvature was measured. All data are the mean of n=3 replicates ±SE.

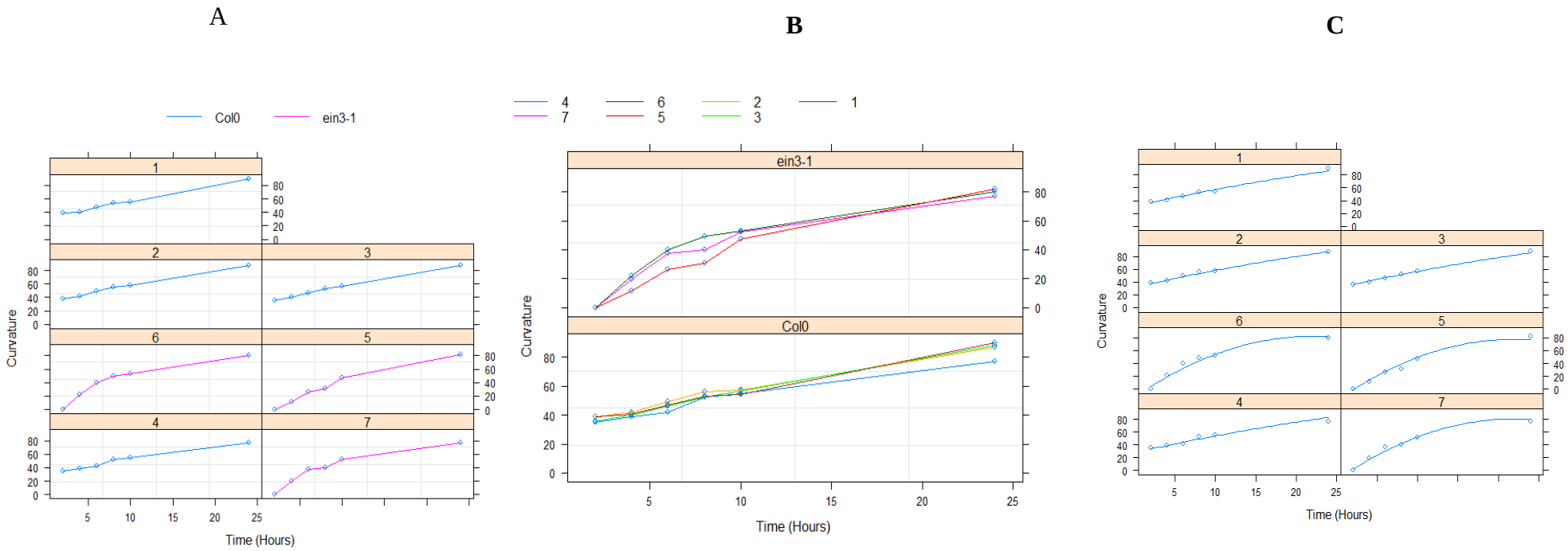

Figure 3-20: Comparison of root bending between Col-0 and *ein3-1*

Root bending between Col-0 and *ein3-1* were analysed statistically by Linear mixed-effects model. Curvature versus time for the 7 samples 1-4 are Col-0, 5-7 are *ein3-1*. The fitted relationships are shown from the minimum adequate mixed-effect model. These demonstrate that *ein3-1* roots bend slower than Col-0. This model showed significant difference between these two plants in terms of gravity bending. $p<0.05$. A and B raw data, C-fitted plot

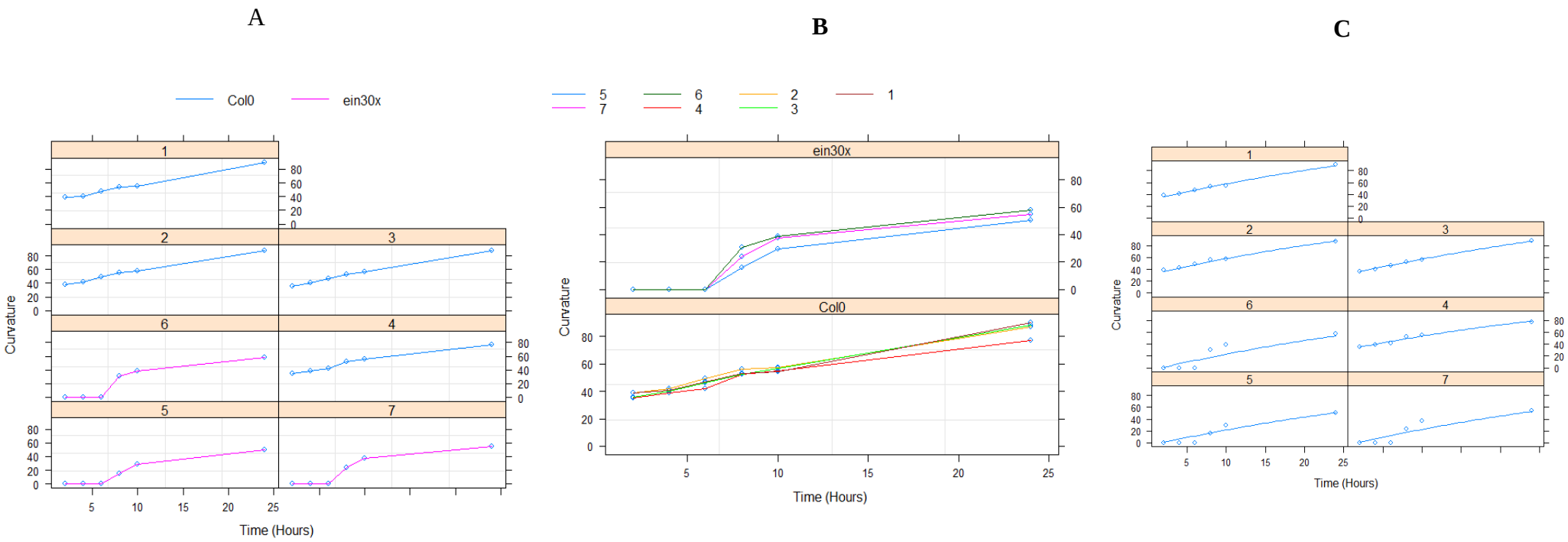

Figure 3-21: Comparison of root bending between Col-0 and *EIN3Ox*

Root bending between Col-0 and *EIN3Ox* were analysed statistically by Linear mixed-effects model. Curvature versus time for the 7 samples 1-4 are Col-0, 5-7 are *EIN3Ox*. The fitted relationships are shown from the minimum adequate mixed-effect model. These demonstrate that *EIN3Ox* roots bend slower than Col-0. This model showed significant difference between these two plants in terms of gravity bending. $p<0.05$. A and B raw data, C-fitted plot

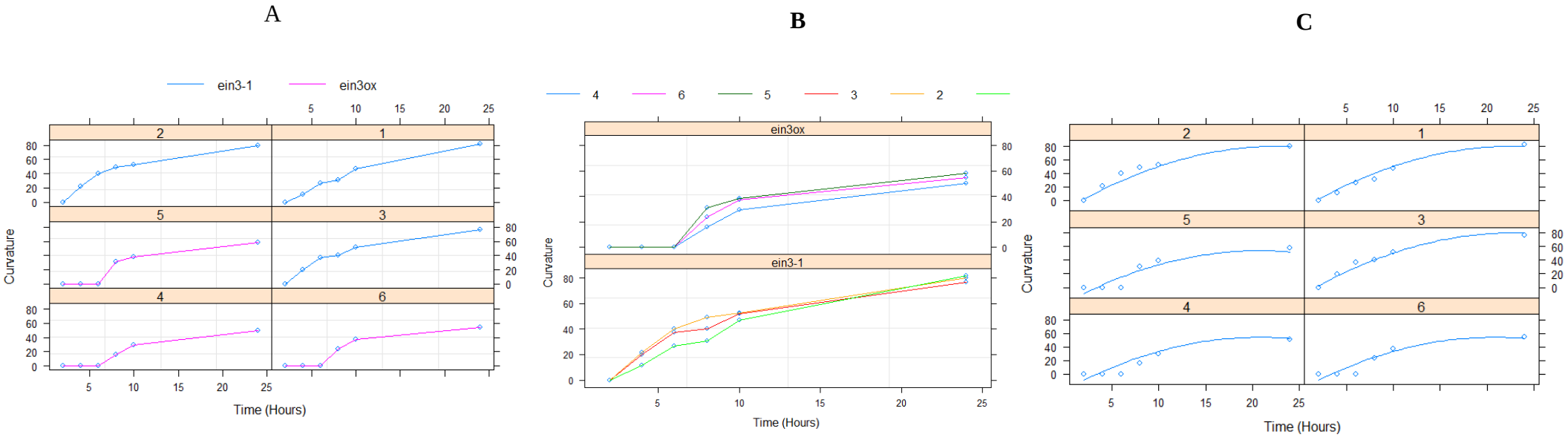

Figure 3-22: Comparison of root bending between *ein3-1* and *EIN3Ox*

Root bending between ein3-1and *ein3ox* were analysed statistically by Linear mixed-effects model. Curvature versus time for the 6 samples 1-3 are *ein3-1*, 5-7 are *EIN3Ox*. The fitted relationships are shown from the minimum adequate mixed-effect model. These demonstrate that *EIN3Ox* roots bend slower than ein3-1. This model showed significant difference between these two plants in terms of gravity bending. $p<0.05$. A and B raw data, C-fitted plot

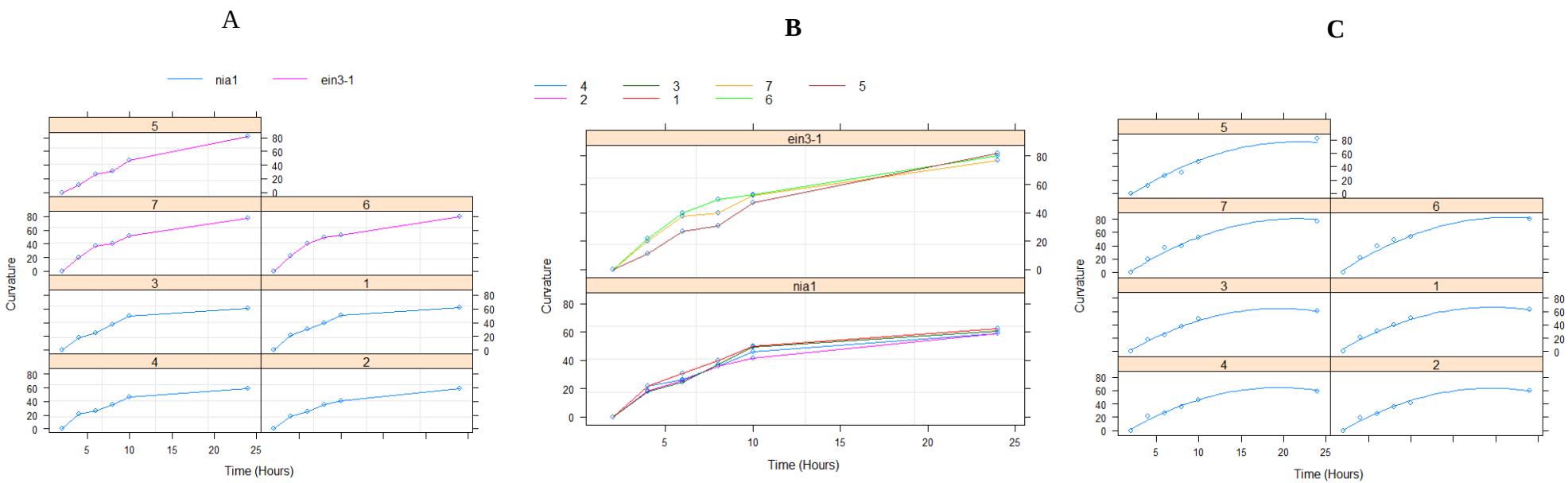

Figure 3-23: Comparison of root bending between *nia1* and *ein3-1*

Root bending between *ein3-1* and *nia1*were analysed statistically by Linear mixed-effects model. Curvature versus time for the 7 samples 1-4 are *nia1*, 5-7 are *ein3-1*. The fitted relationships are shown from the minimum adequate mixed-effect model. These demonstrate that *ein3-1* roots bend slower than *nia1* initially, but later bending was faster than nia1. This model showed significant difference between these two plants in terms of gravity bending. $p<0.05$ A and B raw data, C-fitted plot

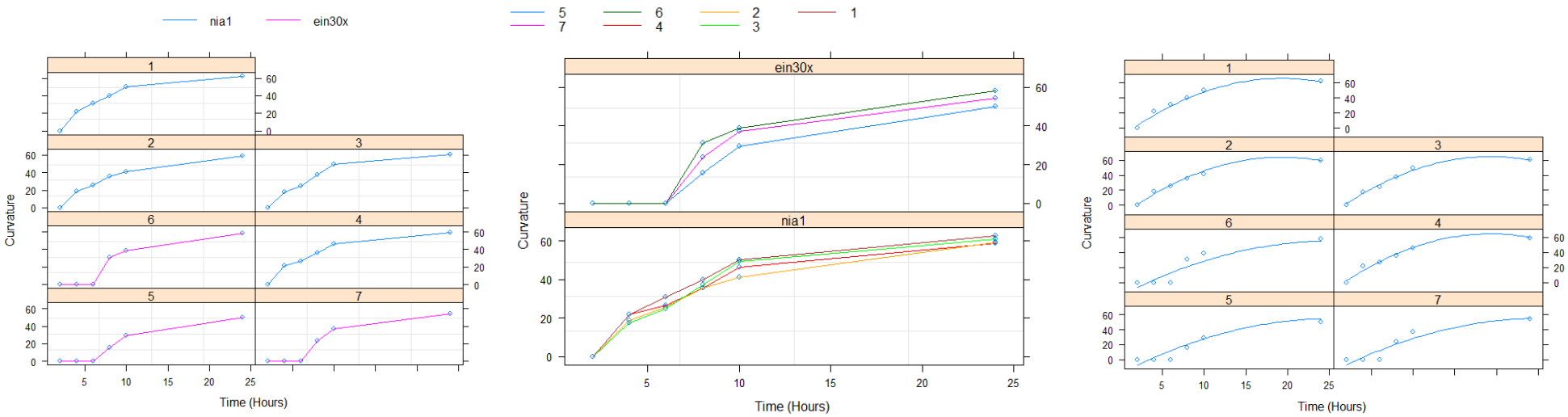

Figure 3-24: Comparison of root bending between *nia1* and *EIN3Ox*

Root bending between *ein3-1* and *ein3ox* were analysed statistically by Linear mixed-effects model. Curvature versus time for the 7 samples 1-4 are *nia1*, 5-7 are *EIN3Ox*. The fitted relationships are shown from the minimum adequate mixed-effect model. These demonstrate that *EIN3Ox* roots bend slower than *nia1*. This model showed significant difference between these two plants in terms of gravity bending. $p<0.05$. A and B raw data, C-fitted plot

3.4 Effect of exogenous application of hormone in gravitropism

3.4.1 NAA increases the rate of gravitropic bending in Col-0

To investigate the effect of auxin during gravitropism, Col-0 seedlings root were pre-treated with 0.1 µM of membrane permeable auxin NAA, NAA was applied on the root by micro-pipette, and then seedlings were subjected to gravistimulation. Photographs were taken at different time intervals (2, 4, 6, 8, 24 h). In this experiment the root bending was measured in Col-0, Col-0 pre-treated with the NO scavenger cPTIO, Col-0 pre-treated with NAA and Col-0 pre-treated with cPTIO and NAA. The results (Fig. 3-21 B) showed gravity induced root bending in Col-0, with a rate of bending that was increased in response to time. Bending starts at 2 h after the gravistimulation and reaches 90^{o} around 24 h. Removal of NO by cPTIO reduced the root bending but did not completely inhibit, suggest that NO is not required to initiate root bending, but increases the rate of root bending. Following external application of 0.1 µm NAA, root bending was not observed at 2 h, but the root started to bend around 4 h and was increased at 6 h compared to control after gravistimulation. Application of NAA after removing the initial endogenous NO by cPTIO led to greater degree of root bending compared to treatment with cPTIO alone. Roots that had been treated with NAA produced more root hairs (Fig. 3-25 A) in the bending region.

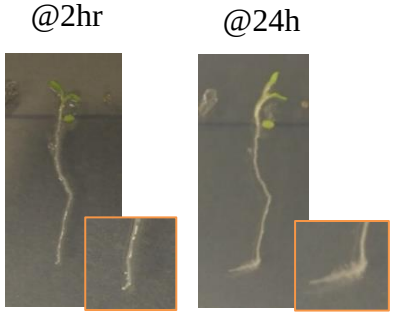

Figure 3-25 A: Application of NAA produced more root hairs in bending zone.

Table 8: Pairwise wise comparison for Col-0 treated with NAA, cPTIO and NAA+cPTIO

Treatment	pairwise	@2 h	@4 h	@6 h	@8 h	@24 h
Col-0 vs cPTIO treated	*	*	-	-	-	*
Col-0 vs NAA treated	-	*	-	-	*	-
Col-0 vs cPTIO+NAA treated	*	*	-	-	-	-
cPTIO treated vs NAA treated	*	*	-	*	*	-
cPTIO treated vs cPTIO+NAA treated	-	*	-	-	-	-
NAA treated vs cPTIO+NAA treated	-	*	-	-	*	-

*- significantly different; - not significantly different.

Two-way ANOVA analysis results (Fig. 3-21 B) (Appendix 11) showed that Col-0, Col-0 treated with NAA, Col-0 treated with cPTIO and Col-0 treated with NAA and cPTIO were significantly different from each other's in terms of overall root bending, also root bending was significantly inteact at certain time poins. All Pairwise comparison (Table 8) was carried out for each simple main effect to check exactly which time point Col-0, NAA treated, cPTIO treated and both cPTIO and NAA treated significantly different from each other. Col-0 significantly different from cPTIO treated and both cPTIO and NAA treated, but not different from NAA treated alone. cPTIO treated is significantly different from NAA treated but not different from both cPTIO and NAA treated, NAA treated is not significantly different from both cPTIO and NAA treated. At 2 h all pairs were significantly different. At 4 h none of the pairs were significantly different. At 6 h cPTIO treated was significantly different from NAA treated. At 8 h NAA treated was significantly different from Col-0, cPTIO treated, and both NAA and cPTIO treated. At 24 h Col-0 was significantly different from cPTIO treated, all other pairs were not significantly different. Linear mixed effect model analysis also showed significant differences in gravity bending among the treatments (Fig. 3-22), (Appendix 12).

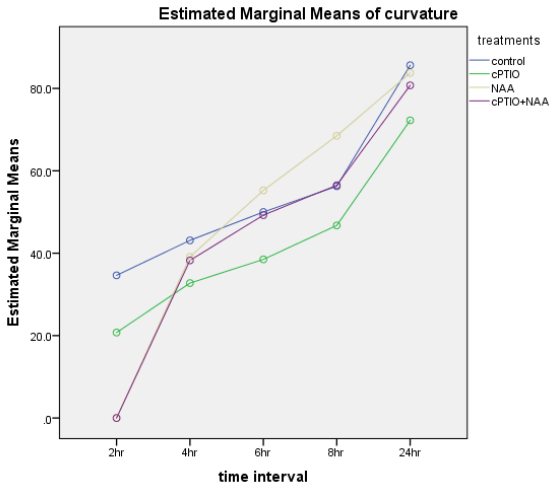

Figure 3-26 B: Overall root bending graph for Col-0 treated with NAA, cPTIO and NAA+cPTIO

A two-way ANOVA was conducted to explore the difference between treatments (Col-0(control), cPTIO treated, NAA treated, cPTIO+NAA treated samples) and impact of time (2, 4, 6, 8, 10 and 24 h) treatment on gravity bending. Normality was assessed using Shapiro wilks test, samples were normally distributed ($p > 0.05$). There was a statistically significant interaction between treatment and time interval on root bending $F(12, 60) = 9.288$, $p = 0.0005$. There was a statistically significant difference in main effect for treatment $F(3, 60) = 14.517$, $p = 0.0005$ and overall time $F(4, 60) = 264.411$, $p = 0.0005$.

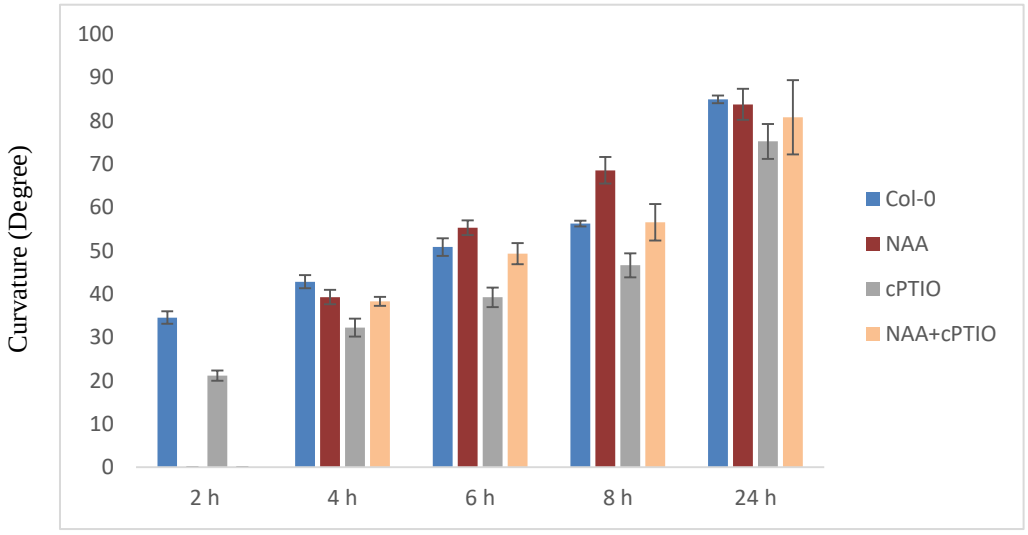

Figure 3-27: External application of NAA increased the root bending

Col-0 seedlings were germinated and grown in MSR3 plates in 12 h photoperiod at 20°C and 60% relative humidity. Five days after germination, roots were incubated with 0.1 µM NAA, and then seedlings were gravistimulated by changing the direction of the plate (Horizontal orientation) by 90°. Photographs were taken at time intervals and root curvature was measured. All data are the mean ±SE of n=4 replicates.

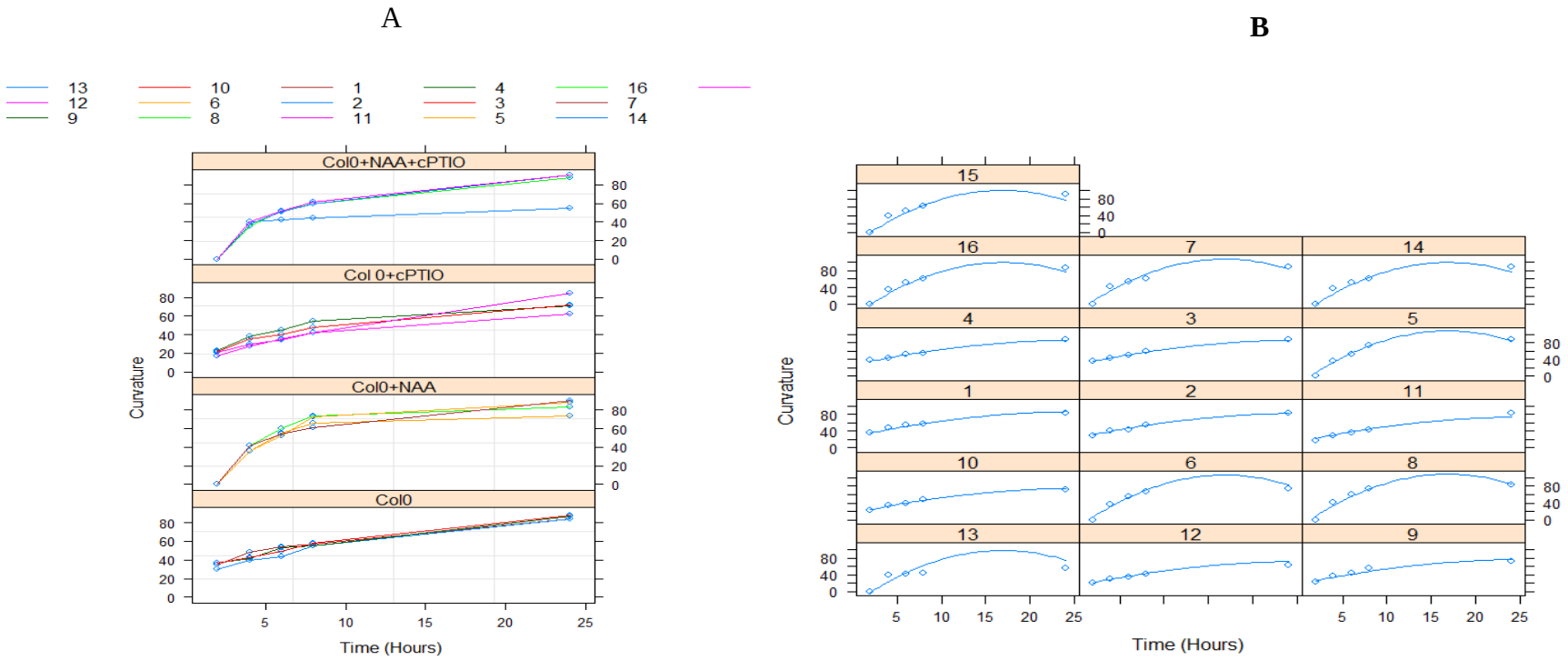

Figure 3-28: Analysis of the effect of externally applied NAA on root gravitropism

Effect of external application of NAA on Col-0 root gravitropic bending in the presence and absence of NO scavenger cPTIO were analysed statistically by Linear mixed-effects model. Curvature versus time for the 16 samples 1-4 are Col-0, 5-8 Col-0+NAA 9-12 are Col-0+cPTIO 13-16 are Col-0+cPTIO+NAA. The fitted relationships are shown from the minimum adequate mixed-effect model. These demonstrate that significant difference in root bending in the cPTIO applied Col-0, NAA applied Col-0 and both cPTIO and NAA applied Col-0 seedlings. A-raw data, B-fitted plot.

3.4.2 ACC increases the root gravitropic response

To investigate the effect of ethylene during gravitropism, seedlings root were treated with 25 µM of the ethylene precursor ACC and then subjected to gravistimulation. ACC was applied on the root by micro-pipette, and then seedlings were subjected to gravistimulation. Photographs were taken at time intervals (2, 4, 6, 8, 24 h). In this experiment the root bending curvature was measured in Col-0, Col-0 pre-treated with cPTIO, Col-0 pre-treated with ACC and Col-0 pre-treated with cPTIO and ACC. The results (Fig. 3-23 A & B) showed that roots treated with ACC did not start bending at 2 h, but increased the root bending around 4 h and subsequently slowed down at 6, 8, 24 h. External application of ACC reduced the most of root bending, whereas application of ACC after removing the initial endogenous NO using cPTIO showed increased root bending compared to wildtype treatment with cPTIO alone or with ACC alone (except at 24 h). These results showed that application of both cPTIO and ACC increased root bending (except at 24 h). This suggests that in the presence of NO, ethylene negatively regulates root gravitropism, whereas in the absence of NO, ethylene positively regulates gravitropism.

Table 9: Pairwise wise comparison for Col-0 treated with ACC, cPTIO and ACC+cPTIO

Treatment	overall	@2 h	@4 h	@6 h	@8 h	@24 h
Col-0 vs cPTIO treated	*	*	-	-	-	*
Col-0 vs ACC treated	*	*	-	-	-	*
Col-0 vs cPTIO+ACC treated	*	*	-	-	-	*
cPTIO treated vs ACC treated	-	*	*	-	-	-
cPTIO treated vs cPTIO+ACC treated	-	*	*	*	*	-
ACC treated vs cPTIO+ACC treated	*	*	-	-	-	-

*- significantly different; - not significantly different.

Two-way ANOVA analysis results (Appendix 13) showed that Col-0, Col-0 treated with ACC, Col-0 treated with cPTIO and Col-0 treated with both ACC and cPTIO were significantly different from each other's in terms of overall root bending, also root bending was significantly inteact at certain time poins. All Pairwise comparison was carried out for each simple main effect to check exactly which time point Col-0, ACC treated, cPTIO treated and both cPTIO and ACC treated significantly different from each other. Col-0 significantly different from cPTIO treated, ACC treated and both cPTIO and NAA treated. But cPTIO treated was not different from ACC treated and both ACC and cPTIO treated. ACC treated was significantly different from both ACC and cPTIO treated. At 2 h all pairs were significantly different. At 4 h cPTIO treated was significantly different from ACC treated and both ACC and cPTIO treated. At 6 h and 8 h only cPTIO treated was significantly different from ACC treated, both ACC and cPTIO treated. At 24 h Col-0 was significantly different from cPTIO treated, ACC treated, and both ACC and cPTIO treated. Linear mixed effect model analysis also showed significant difference in gravity bending among the treatments (Fig. 3-24), (Appendix 14).

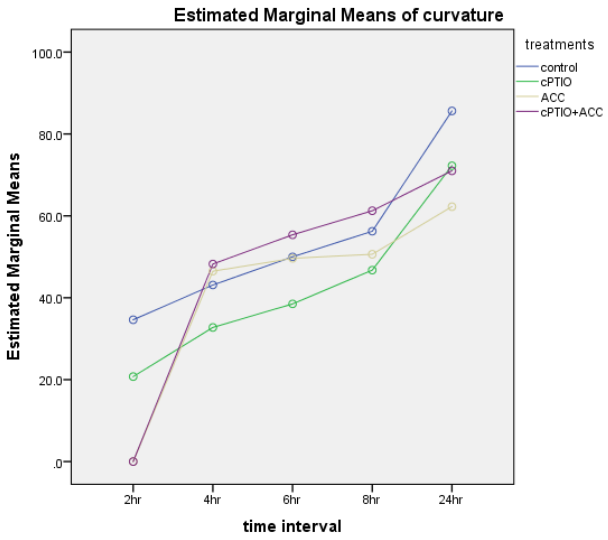

Figure 3-29: Overall root bending graph for Col-0 treated with ACC, cPTIO and ACC+cPTIO

A two-way ANOVA was conducted to explore the difference between treatments (Col-0(control), cPTIO treated, ACC treated, cPTIO+ACC treated samples) and impact of time (2, 4, 6, 8, 10 and 24 h) treatment on gravity bending. Normality was assessed using Shapiro wilks test, samples were normally distributed ($p > 0.05$). There was a statistically significant interaction between treatment and time interval on root bending $F(12, 60) = 8.818$, $p = 0.0005$. There was a statistically significant difference in main effect for treatment $F(3, 60) = 15.689$, $p = 0.0005$ and overall time $F(4, 60) = 179.246$, $p = 0.0005$.

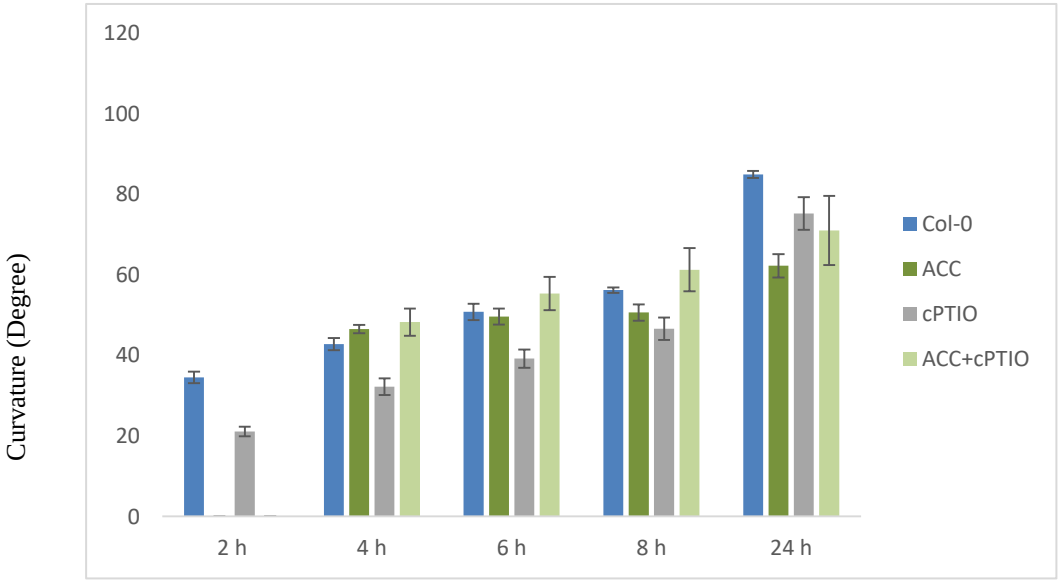

Time after gravistimulation (h)

Figure 3-30: External application of ACC alone slows root bending. However in the presence of NO scavenger cPTIO, ACC increases the root gravitropic response

Col-0 seedlings were germinated and grown in MSR3 plates in 12 h photoperiod at 20°C and 60% relative humidity. Five days after germination, roots were incubated with 25 µM ACC, and then seedlings were gravistimulated by changing the direction of the plate (Horizantal orientation) by 90°. Photographs were taken at time intervals and root curvature was measured. All data are the mean ±SE of n=4 replicates.

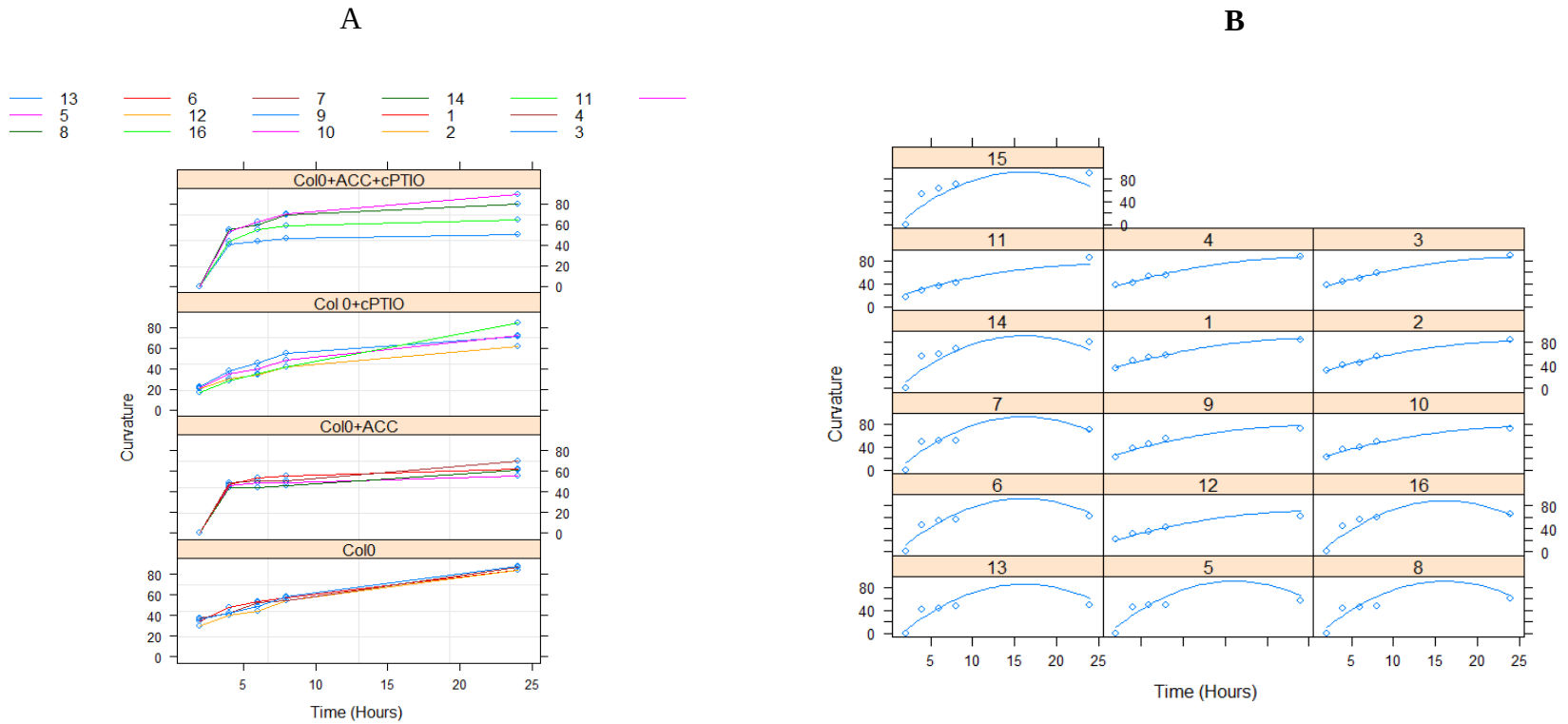

Figure 3-31: Analysis of the effect of externally applied ACC on root gravitropism

Effect of external application of ACC on Col-0 root gravitropic bending in the presence and absence of NO scavenger cPTIO were analysed statistically by Linear mixed-effects model. Curvature versus time for the 16 samples 1-4 are Col-0, 5-8 Col-0+ACC 9-12 are Col-0+cPTIO 13-16 are Col-0+cPTIO+ACC. The fitted relationships are shown from the minimum adequate mixed-effect model. These demonstrate that significant difference in root bending in the cPTIO applied Col-0, ACC applied Col-0 and both cPTIO and ACC applied Col-0 seedlings. A-raw data, B-fitted plot.

3.4.3 The NO donor SNAP increases the root gravitropic response

To investigate the effect of NO during gravitropism, seedlings roots were treated with the 50 µM of NO donor SNAP. SNAP was applied on the root by micro-pipette, and then seedlings were subjected to gravistimulation. Photographs were taken at time intervals (2, 4, 6, 8, 24 h). External application of 50 µm SNAP increased the degree of root bending during gravistimulation (Fig. 3-25). Initially NO increases root bending (4, 6, 8 h) and then decrease root bending (at 24 h). Application of SNAP after removing the initial endogenous NO by using cPTIO showed faster root bending compared to roots treated with cPTIO alone. but slower than roots treated with SNAP alone.

Table 10: Pairwise wise comparison for Col-0 treated with SNAP, cPTIO and SNAP+cPTIO

Treatment	overall	@2 h	@4 h	@6 h	@8 h	@24 h
Col-0 vs cPTIO treated	*	*	*	-	-	*
Col-0 vs SNAP treated	*	-	*	*	*	-
Col-0 vs cPTIO+SNAP treated	-	*	-	*	*	-
cPTIO treated vs SNAP treated	*	-	*	*	*	-
cPTIO treated vs cPTIO+SNAP treated	*	-	*	*	*	-
SNAP treated vs cPTIO+SNAP treated	-	-	-	-	-	-

*- significantly different; - not significantly different.

Two-way ANOVA analysis results (Appendix 15) showed that Col-0, Col-0 treated with SNAP, Col-0 treated with cPTIO and Col-0 treated with both SNAP and cPTIO were significantly different from each other's in terms of overall root bending, also root bending was significantly inteact at certain time poins. All Pairwise comparison was carried out for each simple main effect to check exactly which time point Col-0, SNAP treated, cPTIO treated and both cPTIO and SNAP treated significantly different from each other. Col-0 significantly different from cPTIO treated, SNAP treated but not different from both cPTIO and SNAP treated. cPTIO treated was significantly different from SNAP treated and both SNAP and cPTIO treated. SNAP treated was not significantly different from both SNAP and cPTIO treated. At 2 h Col-0 significantly different from cPTIO treated and both SNAP and cPTIO treated. At 4 h Col-0 significantly different from cPTIO treated and SNAP treated alone. But not different from both SNAP and cPTIO treated. cPTIO treated was significantly different from SNAP treated and both SNAP and cPTIO treated. At 6 h and 8 h Col-0 is significantly different from SNAP treated and both SNAP and cPTIO treated but not in cPTIO

alone treated, cPTIO treated is significantly different from SNAP treated alone and both cPTIO and SNAP treated, SNAP treated is not different from both cPTIO and SNAP treated. At 24 h Col-0 was significantly different from cPTIO treated, all other pairs were not significantly different. Linear mixed effect model analysis also showed significant difference in gravity bending among the treatments (Fig 3-26), (Appendix 16).

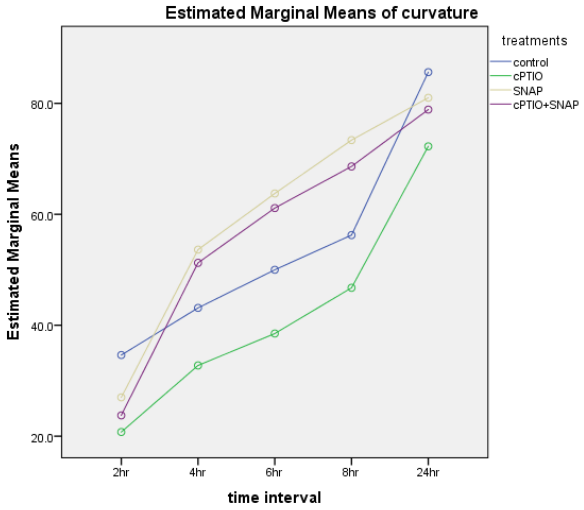

Figure 3-32: Overall root bending graph for Col-0 treated with SNAP, cPTIO and SNAP+cPTIO

A two-way ANOVA was conducted to explore the difference between treatments (Col-0 (control), cPTIO treated, SNAP treated, cPTIO+SNAP treated samples) and impact of time (2, 4, 6, 8, 10 and 24 h) treatment on gravity bending. Normality was assessed using Shapiro wilks test, samples were normally distributed ($p > 0.05$). There was a statistically significant interaction between treatment and time interval on root bending $F(12, 60) = 6.198$, $p = 0.0005$. There was a statistically significant difference in main effect for treatment $F(3, 60) = 15.282$, $p = 0.0005$ and overall time $F(4, 60) = 271.156$, $p = 0.0005$.

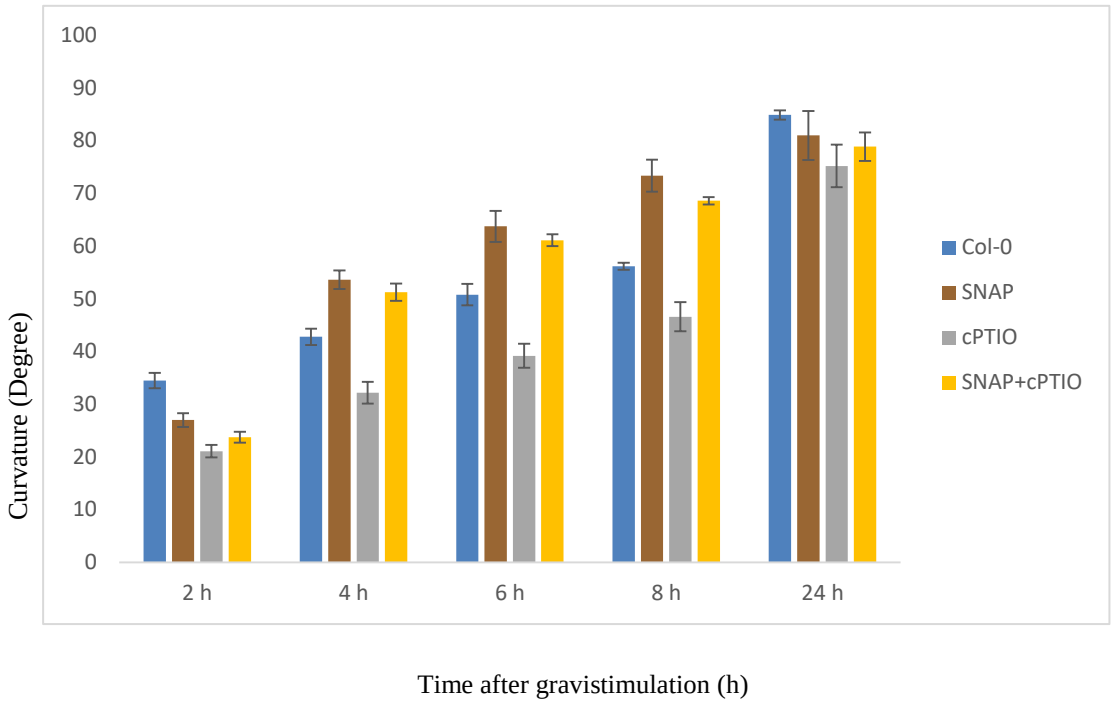

Figure 3-33: External application of NO donor SNAP increases the degree of root bending

Col-0 seedlings were germinated and grown in MSR3 plates in 12 h photoperiod at 20°C and 60% relative humidity. Five days after germination, roots were incubated with 50 µM SNAP and then seedlings were gravistimulated by changing the direction of the plate (Horizantal orientation) by 90°. Photographs were taken at time intervals and root curvature was measured. All data are the mean ± SE of n=4 replicates.

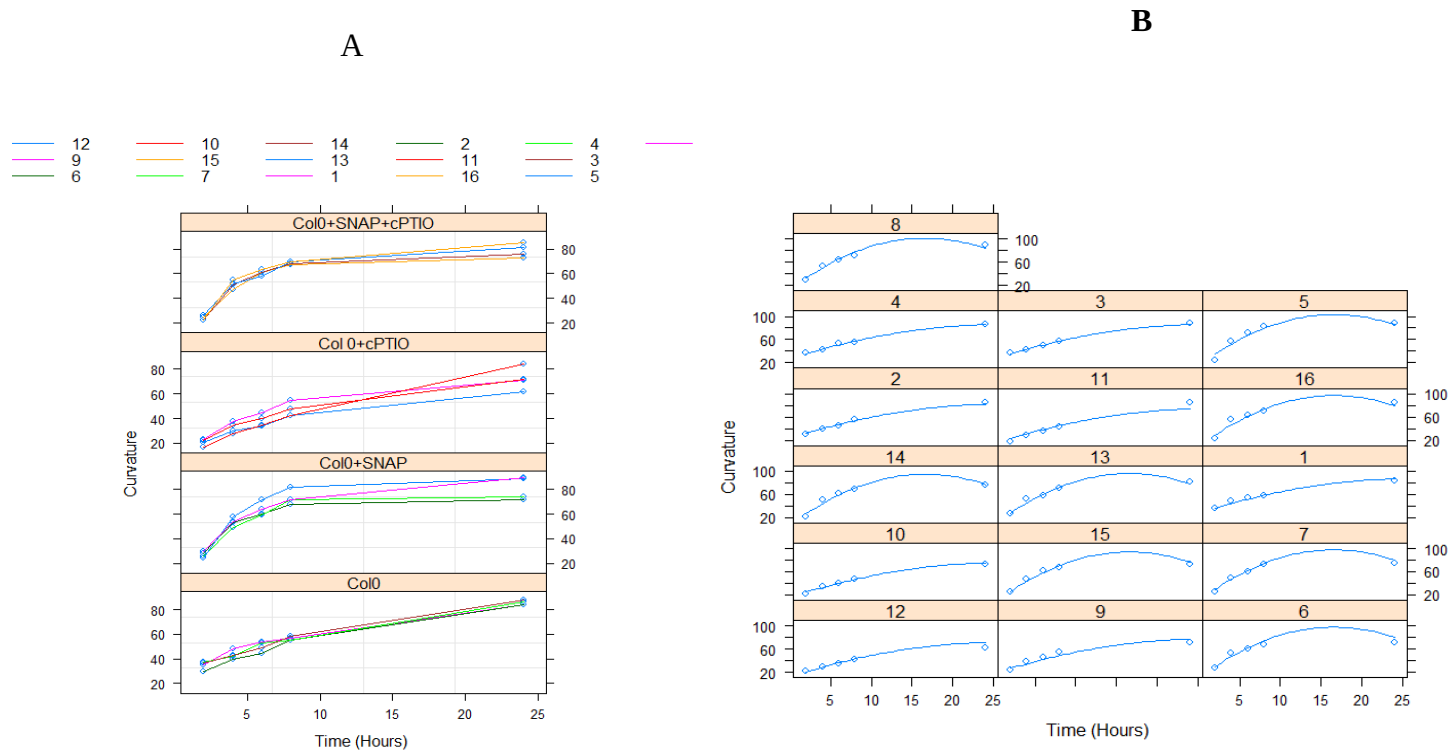

Figure 3-34: Analysis of the effect of externally applied ACC on root gravitropism

Effect of external application of ACC on Col-0 root gravitropic bending in the presence and absence of NO scavenger cPTIO were analysed statistically by Linear mixed-effects model. Curvature versus time for the 16 samples 1-4 are Col-0, 5-8 Col-0+SNAP 9-12 are Col-0+cPTIO 13-16 are Col-0+cPTIO+SNAP. The fitted relationships are shown from the minimum adequate mixed-effect model. These demonstrate that significant difference in root bending in the cPTIO applied Col-0, ACC applied Col-0 and both cPTIO and ACC applied Col-0 seedlings. A-raw data, B-fitted plot

3.5 **Discussion**

Roots are a vital part of the plant since these aid the uptake of water and nutrients from the soil, as well as providing anchorage to the plant. A full understanding of the developmental and signalling mechanism of the root will help us to improve the yield and biotic and abiotic stress tolerance in plants by modifying the genetic makeup of the plant.

Nitric oxide plays many important physiological roles in the plant development. It also interacts with the other plant hormones like auxin, ethylene and abscisic acid. Through understanding of the exact mechanism of nitric oxide signalling and interaction, understanding of its role in the plant root development can be improved.

3.5.1 Defects in auxin transport signal affects gravity sensing and response

Gravistimulation experiments clearly showed Col-0 roots respond to gravity and start to bend upon receiving the gravity signals. Bending was visible to the naked eye after around 2 h, and reached nearly 90^{o} angle around 24 h after gravistimulation. As expected (Bennett *et al.*, 1996; Timpte *et al.*, 1994; Leyser *et al.*, 1996) roots of the auxin mutants *aux1* (auxin transport mutant), *axr2*, and *axr3* (auxin signalling mutant) did not respond to gravity signals. The *axr3* root was short and slow growing as compared to *aux1* and *axr2*. *axr3* root also did not respond to gravitropic signals. Non-gravity response of auxin mutants *aux1*, *axr2* and *axr3* were already reported by Marchant *et al.*, 1999; Wilson *et al.*, 1990; Leyser *et al.*, 1996, present study result also supports that mutation in auxin signalling severely affects the gravity sensing and response. Other than the agravitropic phenotype, *aux1* and *axr2* roots were coiled during the early growth period. This experiment suggests that *aux1* and *axr2* roots also do bend continuously to make a root coil, and this root bending is not related to gravity, and the direction of bending was very random. Also, the time required for each coiling was unknown. This coiling in the auxin

mutant raises questions about the role of auxin in root bending. Ethylene-induced root coiling has been demonstrated in tomato seedlings by Woods *et al.* (1994), who also reported an increased number of coils with increased ethylene concentration. However they failed to induce root coiling in the agravitropic mutant *dgt,* even at a higher ethylene concentration. They concluded that the coiling of roots is not related to gravitropism. *dgt* is less sensitive to auxin. They also found no root coiling in *dgt* in the absence of ethylene. In the experiments reported here, agravitropic auxin mutants exhibited root coiling. This may be because a defect in auxin transport/synthesis induces root coiling or it increases endogenous ethylene levels.

3.5.2 Gravitropism induces asymmetric accumulation of NO

Detection of NO using confocal microscopy showed gravistimulation induces the asymmetric accumulation of NO in the lower side of the bending zone of Col-0 roots. Gravity induced asymmetric accumulation of NO in the lower side of the bending zone of the root has been demonstrated by Hu *et al.* (2005) in maize and soybean root. Non-gravitropic auxin mutants *aux1, axr2 and axr3* did not show asymmetric accumulation of NO in the bending zone, but *aux1* and *axr2* showed elevated level of NO in both gravistimulated and non-gravistimulated roots, whereas *axr3* did not produce much NO in their roots. This study suggests that defects in auxin transport, signalling or response affect NO synthesis during gravitropism and there is a strong interaction between nitric oxide signalling and auxin signalling in plant roots. Hu *et al.* (2005) also suggest that auxin induces the asymmetric accumulation of nitric oxide. current experiments showed gravity induced the accumulation of NO in the lower side of *Arabidopsis* root.

3.5.3 NIA1 transcript levels increase during gravistimulation

Nitrate reductase (NR) mediated NO synthesis occurs in roots (Kolbert and Erdei, 2008). Amplification of *NIA1* transcript from the mRNA of gravistimulated and non-

gravistimulated Col-0 root samples demonstrated the expression of *NIA1* gene in the root tip, middle region of roots. These results suggest that the *NIA1* gene is expressed in all the parts of the root. Expression of the *NIA1* gene in the non-gravistimulated root revealed that NO is not only involved in the gravitropic response, it is likely to have other basic physiological roles in the development of roots. Few example, Pagnussat *et al.* (2002) demonstrated that NO induces adventitious root formation in cucumber.

Q-PCR results from non-gravistimulated and gravistimulated Col-0 root tips showed a gradual increase in the NIA1 transcript level of about 3 fold after 2 h of gravistimilation. Confocal experiments also showed asymmetric accumulation of NO in the lower side of the Col-0 root at 2 h after gravistimulation. This increased NO accumulation initiates gravitropic root bending at 2 h. After initiating bending, the NIA1 transcript level gradually decreased 3.5 fold after 6 h. Taken together these result support the involvement of *NIA1*-mediated NO synthesis during gravitropic root bending.

The *aux1* root tip contains higher levels of NIA1 transcript than Col-0 at 0 h, NIA1 transcript was attenuated two fold at 30 min and remaining constant till 24 h. Elongation and hypocotyl root zones did not show much change in response to gravity. *aux1* NO levels were higher at all times than in Col-0 and *aux1* seedlings produced 3 fold more NIA1 transcript than Col-0. In contrast, in *axr2* the level of NIA1 transcript was 100 fold lower than *aux1*. At the same time, *axr2* root confocal images showed equal fluorescence to *aux1* root, which suggests that there is a weak correlation between the transcript level and the protein level. There is a possibility that a low level of mRNA is more preferentially translated to an abundant level of functional protein, or the protein has increased stability or a reduced rate of degradation or greater activity in *axr2* than in *aux1*.

3.5.4 *NIA1* is involved in gravity mediated root bending

The degree of root bending in gravistimulated Col-0, *nia1* and *nia2 Arabidopsis* seedlings were measured and analysed. The results showed *nia1* seedling bend more slowly in response to gravity than Col-0 and *nia2*. Results from confocal and QPCR also demonstrate the NIA1 mediated NO role in gravity bending.

3.5.5 Ethylene response reduces degree of root bending

The degree of root bending in gravistimulated Col-0, *ein3-1* and *EIN3OX* was investigated. Ethylene insensitive mutant e*in3-1* showed reduced root bending than wild type, whereas the ein3 over producing transgenic line *EIN3OX* showed severely reduced root bending and slower gravity response. Ethylene insensitivity and ethylene response lines showed a similar effect, reduced root bending compared to Col-0, but the intensity of gravity bending was was very less incase of *EIN3OX*.

3.5.6 Externally applied NAA, SNAP increase root bending but not ACC

To determine the effect of auxin, NO and ethylene on gravity bending, curvature of roots after application of NAA, SNAP and ACC was analysed. Application of NAA and SNAP increased root bending, whereas ACC decreased the root bending. However the application of ACC after removing the NO increased the gravity bending. Buer *et al.* (2006) also reported that the external application of the ethylene precursor ACC to Col-0 seedlings reduced the root elongation and gravitropic curvature. The current experiment also showed external application of ACC reduced the gravitropic curvature. These results suggest that in the presence of NO, ethylene negatively regulates the gravity stimulated bending and in the absence of NO, ethylene positively regulates the root bending.

The aim of the next chapter is to make a NIA1 transcriptional and translational reporter construct with mGFP4 reporter gene to study the expression pattern and subcellular

localization of *NIA1* gene in Arabidopsis wild type and mutant seedlings in response to gravity.

Chapter 4 Transgenic approach to investigate *NIA1* gene expression

Nitric oxide (NO) plays numerous physiological and developmental roles in plants. NO is synthesized in both an enzymatic and non-enzymatic way. In Arabidopsis, nitrate reductase (NR) activity is one of the enzymatic sources. This enzyme is encoded by two isoform genes namely *Nia1* and *Nia2*. Studies by Kolbert *et al.* (2008) showed that NR genes are the main source of NO for lateral root development. Of these two isoforms, *NIA1* plays the most significant role in NO synthesis (Wilson *et al.*, 2008). Experiments in guard cells have shown the importance of the *NIA1*-mediated NO response during stomatal closure. Most studies the localization of NO in plants is detected by treating the samples with the cell-permeable dye DAF-2DA, which binds NO and is then visualized using a fluorescence microscope. Experiments by Planchet and Kaiser (2006) questioned the specificity of DAF-2DA fluorescence for NO and suggested that other DAF reactive compounds may be present in cells. Another way to understand the expression pattern and localization of individual genes is by making reporter constucts in transgenic plants. Transcriptional and translational fusion of *NIA1-mGFP4* reporter construct was made to study the expression pattern, localization of NO and its interaction with other plant hormones auxin and ethylene.

To achieve this aim, the following cloning work was carried out and presented in this chapter.

1. Cloning of the CaMV35S-mGFP4 construct
2. Cloning of mGFP4 gene in frame with 2.2 kb NIA1 promoter and 2.2 kb NIA1 promoter with 3.5 kb gene.
3. Floral tip transformation of these constructs with Arabidopsis wild type, auxin, ethylene and NR mutants.
4. Analysis of the transgenic plants to detect expression of the mGFP4 gene.

4.1 Making of 35S-mGFP4 construct

4.1.1 Transformation of pGreen35S-mGFP4 plasmid into competent cells of *E. coli*

pGreen plasmid DNA containing the 35S-mGFP4 cassette (Fig. 4-1) was received from John Innescentre (Norwich, UK). Plasmid DNA was diluted 1/100 times and 2 µl was used to transform competent cells of *E. coli*, DH5α. Transformed colonies were short streaked (See Fig. 2-5 in M&M) on LB ampicillin plates. Plasmid DNA was isolated from a single colony of transformed *E. coli* grown in LB ampicillin broth. Quantification of plasmid was done by measuring the absorbance at 260 nm using a Nanodrop.

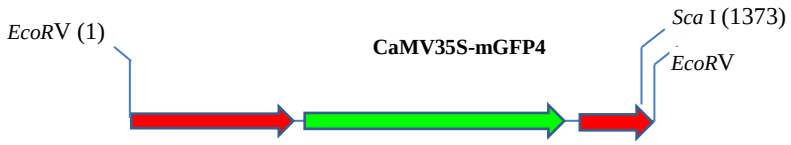

Figure 4-1: 35S mGFP4 cassette from pGreen 35S-GFP plasmid

The mGFP4 gene shown here in the cassette was a modified GFP developed by Haseloff *et al.* (1997). While expressing the wild type GFP from jellyfish (*Aequorea victoria*) in *A. thaliana*, GFP coding sequence was cleaved, because sequence of GFP is similar to the plant introns recognition site. These cryptic introns in the wild type GFP was removed by codon usage and successfully expressed in the model plant *Arabidopsis.*

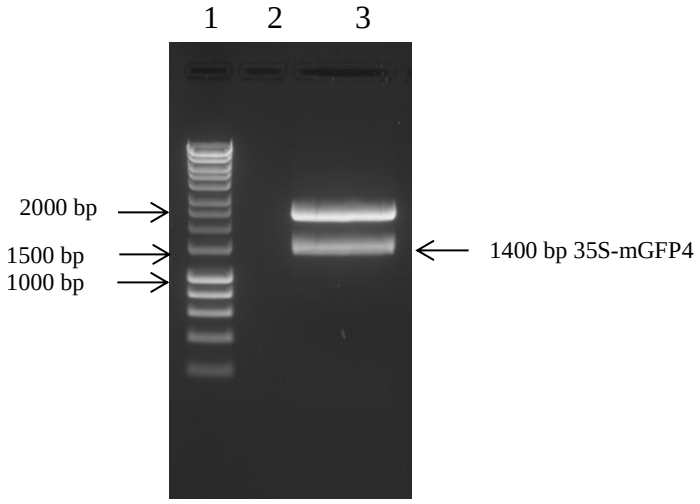

Figure 4-2: Restriction digestion to release 35S-mGFP4 fragment

2 µg of pGreen 35S-mGFP4 plasmid were digested with 20 U of *EcoRV* - HF™ enzyme at 37°C for 1 h and then digested products were separated in 0.8% (w/v) agarose gel. The CaMV35S-mGFP4 band was purified using QIAquick Gel Extraction Kit (Qiagen) for further cloning. Lane 1, HyperLadder-1 (Bioline); lane 2, blank; lane 3, *EcoRV* digested PGreen 35S-mGFP4 Plasmid showed the cleaved cassette.

4.1.2 Cloning of pGreen35S-mGFP4 cassette into pG0179 Vector

pGreen 35S-mGFP4 plasmid DNA was digested with *EcoRV* and the cleaved product separated by 0.8% (w/v) agarose gel electrophoresis. The 1400 bp 35S-mGFP4 cassette and plasmid backbone can be seen in (Fig. 4-2).

The 35S-mGFP4 fragment was purified from the gel and then ligated with pG0179 vector digested with *EcoRV* (1:1 molar ratio). 10 µl of ligated product was transformed into DH5-α *E. coli* competent cells by the heat shock method and spread onto LB Kan X-Gal-IPTG plates for blue white screening. Recombinant colonies appeared white, whereas non-recombinant formed blue colonies. White colonies were selected and short streaked on LB Kanamycin plates.

4.1.3 Selection of *E. coli* transformants harbouring pG35S-mGFP4

4.1.3.1 Screening of *E. coli* transformants by colony PCR

The presence of the 35S-mGFP4 cassette in pG0179 plasmid in the recombinant *E. coli* colonies was confirmed by colony PCR using forward and reverse primers specific to the *mGFP4* gene. Agarose gel electrophoresis showed amplification of the expected size of *mGFP4* (Fig. 4-3).

.

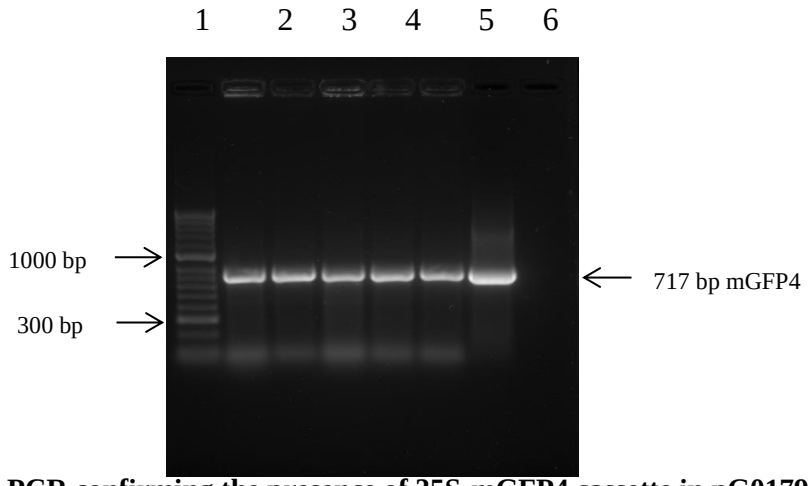

Figure 4-3: Colony PCR confirming the presence of 35S-mGFP4 cassette in pG0179.

A small amount of each single *E. coli* transformant colonies suspended in 15 µl of sterile water was used as a template for PCR to confirm the insertion of 35S-mGFP4 fragment in pG0179 vector. PCR was performed by using the Taq DNA polymerase in the presence of dNTPs using mGFP4 screening primers at 54^0C annealing temp. Lane1, HyperLadder 1; 2, lane (2-5), recombinant colonies; lane 6, positive control (35S-mGFP4 plasmid).

4.1.3.2 Isolation of transformant plasmid for restriction analysis

Plasmid DNA was isolated from the PCR positive colonies of *E. coli* grown in LB Kanamycin broth. Plasmid concentration was determined by measuring the absorbance at 260 nm using a Nanodrop.

4.1.3.3 Restriction analysis pG35S-mGFP4

One of the recombinant clones was named as pG35S-mGFP4. The recombinant plasmid, pG35S-mGFP4 (Fig. 4-4) on restriction digestion with *EcoRV* released fragments of the expected size, viz., ~1.4 kb (35S-mGFP4) and ~5.1 kb (vector) (Fig. 4-4).

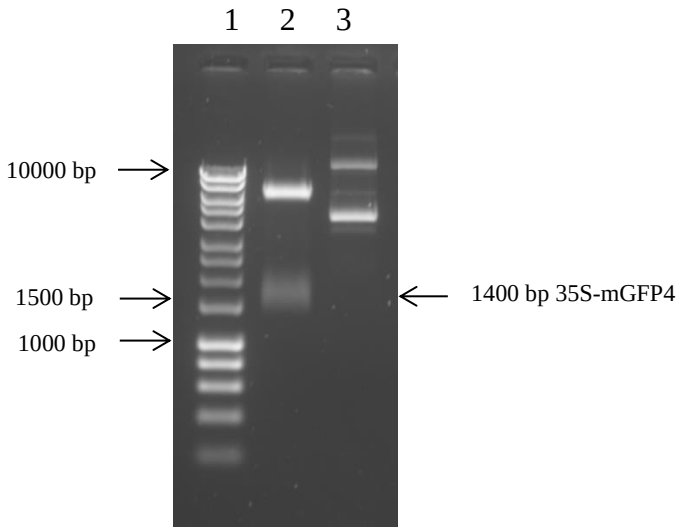

Figure 4-4: Restriction digestion confirming the presence of 35S-mGFP4 cassette in pG35S-mGFP4

Plasmid DNA (0.3 µg) isolated from pG35S-mGFP4 clone was digested with 10 U of *EcoRV*-HF™ restriction enzyme at 37^0C for 1 h. Cleaved product separated in a 0.8% (w/v) agarose gel shows the presence of the 1.4 kb 35S-mGFP4 in pG0179 vector. Lane 1, HyperLadder 1; lane 2, pG35S-mGFP4 plasmid digested with *EcoRV*; lane 3, undigested plasmid as a control.

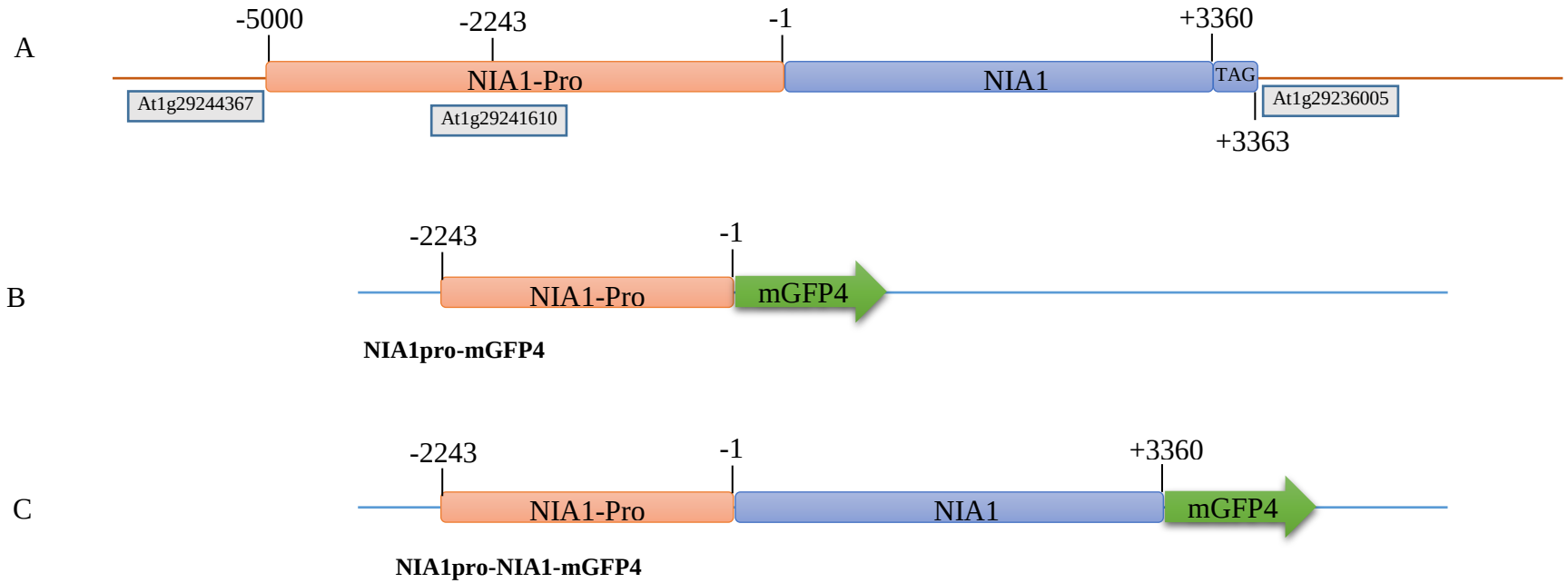

Figure 4-5: Schematic representation of NIA1 locus and mGFP4 reporter construct

A) The structure of NIA1 locus in chromosome 1 (Sequence id: CP002684.1). B & C) Graphical representation of NIA1pro-mGFP4 and NIA1pro-NIA1-mGFP4 constructs. Numbers represents nucleotide position relative to the translational start codon

4.2 Making pGmGFP4 (pG0179+mGFP4) construct

4.2.1 Cloning of mGFP4 gene into the pG0179 Plasmid

4.2.1.1 Amplification of mGFP4 from pGreen 35S-mGFP4 plasmid

pGreen 35S-mGFP4 plasmid was used as a template for amplification of the *mGFP4* gene fragment to use in future constructs. The *mGFP4* gene of about 717bp was amplified by PCR, using a set of forward and reverse primers (Table 2-2). The forward primer (mGFP FP) and reverse primer (mGFP RN) introduce *PstI* and *NotI* sites at 5'and 3' ends of the product respectively. An intact band of 717 bp was amplified from the plasmid with mGFP FP and mGFP RN primers by PCR (Fig. 4-6).

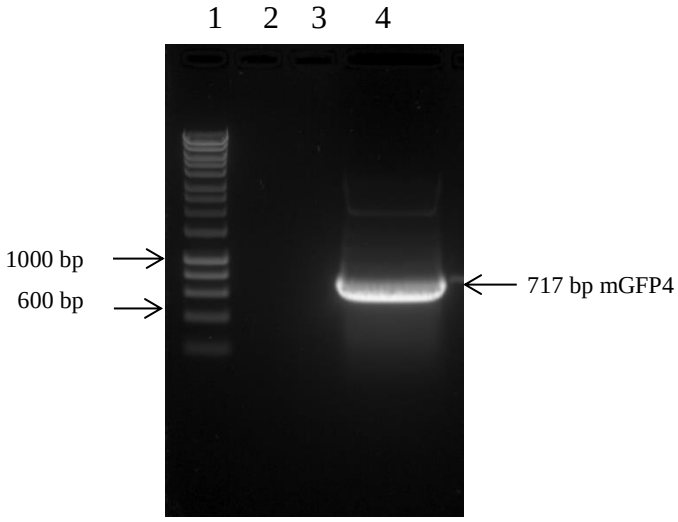

Figure 4-6: PCR amplification of *mGFP4* gene

10 ng of pG35S-mGFP4 plasmid was used as a template for the amplification of the mGFP4 coding sequence. The *mGFP4* gene was amplified by using Qiagen Longrange polymerase with mGFP FP & mGFP RN primers annealed at 54^{o}C. These forward and reverse primers introduce *Pst1* and *Not1* restriction sites for further cloning. Amplification was verified by gel electrophoresis and visualized under UV light. Lane 1, HyperLadder 1 (Bioline); lane 2&3, blank; lane 4, mGFP4 amplicon.

4.2.1.2 Restriction digestion of mGFP4 gene fragment with Pst1 and Not1

The PCR amplified *mGFP4* gene fragment was excised from the gel and eluted using a Sigma gel purification kit. The resulting product was quantified using the Nanodrop and

1 µg of the *mGFP4* gene fragment was used for further digestion with *Pst1 and Not1* together. Restriction digestion was carried out at 37°C for 1 h. The product was separated in a 0.8% (w/v) agarose gel (Fig. 4-9 A) then the digested gene fragment was excised from the gel and purified by the Sigma gel purification kit.

4.2.1.3 Restriction digestion pG0179 plasmid with Pst1 and Not1

The pG0179 plasmid (1 µg) was digested with *Pst1* and *Not1* together. Restriction digestion was carried out at 37°C for 1 h and the product was loaded on an 0.8% (w/v) agarose gel (Fig. 4-7 B). Digested plasmid was excised from the gel and purified by the Sigma gel purification kit.

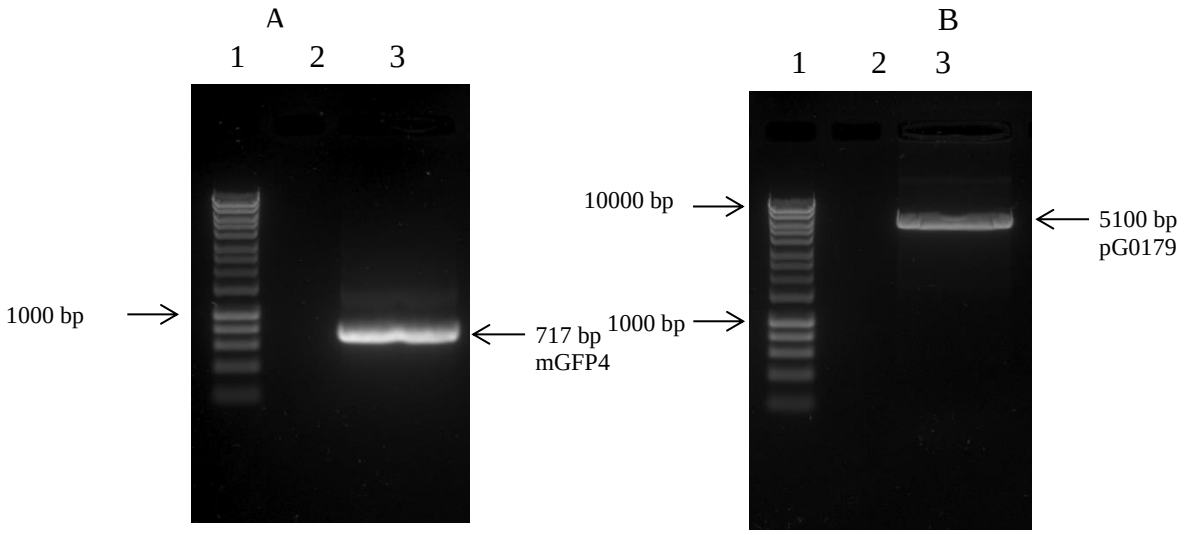

Figure 4-7: Linearised fragment of mGFP4 gene (A) and pG0179 vector (B).

2 µg of PCR amplified, purified mGFP4 gene and 1 µg pG0179 vector was double digested with 20 U of *Pst1*- HF™ and *Not1*- HF™ restriction enzymes at 37°C for 1 h. Digested fragments were separated by gel electrophoresis and the band was excised from the gel and purified by QIAquick Gel Extraction Kit (Qiagen) and used for ligation. Lane 1, Hyper Ladder 1 (Bioline); lane 2, blank; lane 3, mGFP4/pG0179 digested with *Pst1 and Not1.*

4.2.1.4 Cloning of mGFP4 into pG0179 Vector

Quantification of *Pst1* and *Not1* digested and purified *mGFP4* gene (insert) and pG0179 vector was performed by comparing with a known concentration of HyperLadder I (Fig. 4-8). A 1:3 insert:vector molar ratio was used for the ligation. Ligation was carried out at

16^{o}C overnight. 10 µl of ligated product was transformed into *E. coli* competent cells by the heat shock method and spread onto LB Kanamycin X-Gal-IPTG plates. White colonies were selected and short streaked on LB Kanamycin plates.

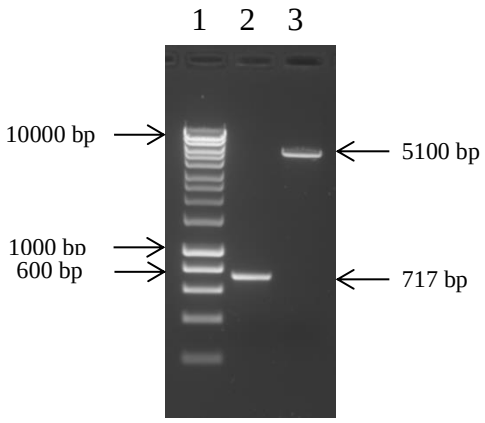

Figure 4-8: Gel to determine the concentration of insert and vector

2 µl of purified *mGFP4* (insert) and (pG0179) vector were separated by agarose gel electrophoresis and visualized under UV light. The concentration was determined in comparison with the known concentration of hyperlader and also by Nanodrop. Lane 1, HyperLadder1 (Bioline); Lane 2, mGFP4 ; Lane 3, pG0179.

4.2.1.5 Confirmation of pGmGFP4 in *E. coli* transformants by colony PCR

Cloning of *mGFP4* in the pG0179 vector was confirmed by colony PCR with mGFP forward and reverse screening primers. Agarose gel (Fig. 4-9) showed amplification of a band of the expected size for *mGFP4*.

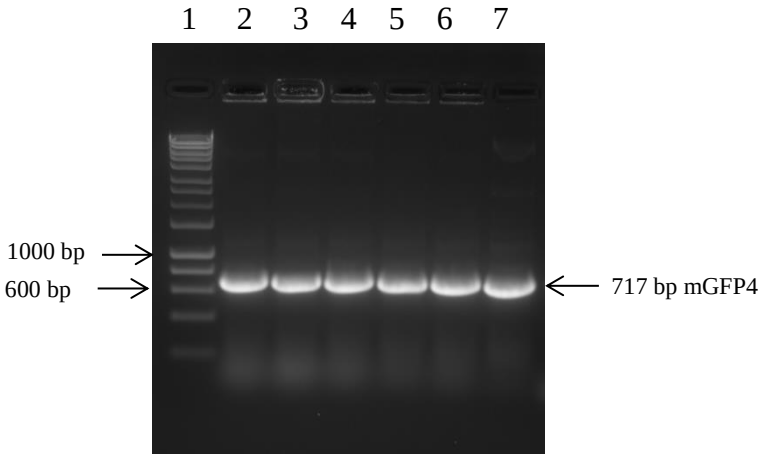

Figure 4-9: Colony PCR confirms pGmGFP4 construct.

Small amounts of each single *E. coli* recombinant colonies were diluted in 15 µl of sterile water and used as template to confirm the insertion of mGFP4 gene in pG0179 vector. PCR was performed by using the Taq DNA polymerase in the presence of dNTPs with the help of set of mGFP screening primers at 54^{o}C annealing temp. Lane 1, HyperLadder1 (Bioline); lane 2-6, transformant colonies; Lane 7, Positive control 35S-GFP4 Plasmid.

4.2.1.6 Restriction analysis of recombinant plasmid pGmGFP4

Plasmid DNA was isolated and quantified from the PCR positive white colonies of *E. coli* grown in LB Kanamycin broth. The selected recombinant clone was named as pGmGFP4. The recombinant plasmid pGmGFP4 was double digested with *Pst1 and Not1* and released the expected fragments of 717 bp (mGFP4) and 5.1 kb (vector) (Fig. 4-10).

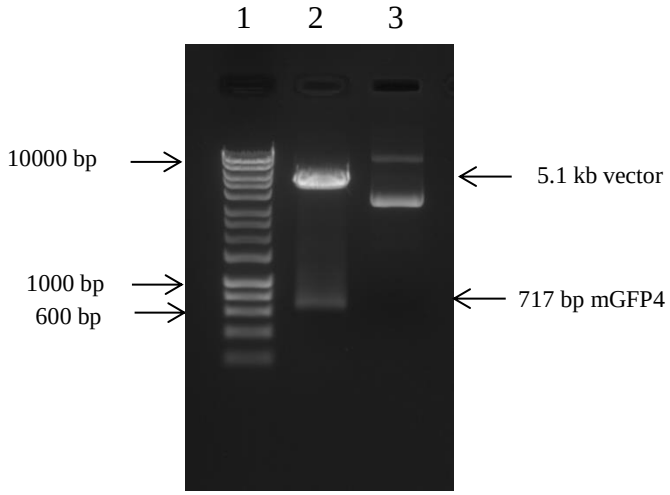

Figure 4-10: Restriction digestion confirms the insertion of the mGFP4 gene in pG0179.

Plasmid DNA was isolated from one of the PCR positive *E. coli* colonies and then digested with *Pst1*-HF™ *and Not1*-HF™ restriction enzyme. Release of a 717 bp band shows the presence of mGFP4 gene in the pG0179 plasmid. This plasmid was named as pGmGFP4. Lane1, HyperLadder1(Bioline); lane 2, pGmGFP4 digested with *Pst1 and Not1;* lane 3, undigested pGmGFP plasmid.

4.3 Making NIA1pro-mGFP4 and NIA1pro-NIA1-mGFP4

4.3.1 Amplification of 2.2 kb NIA1 promoter and 2.2 kb promoter with 3.5 kb *NIA1* gene

The 2.2 kb NIA1 promoter alone and promoter with its 3.5 kb gene were amplified from bacterial artificial chromosome (BAC) T32E7. Nia1P FK and Nia1P RP primers (Table 2-2) were used for the amplification of the 2.2 kb NIA1 promoter region. Nia1P FK and Nia1R P primers were used for the amplification of the 5.7 kb fragment of promoter and gene. The forward primer (Nia1P FK) and reverse primer (Nia1P RP & Nia1RP) introduce *Kpn1* and *PstI* sites at 5'and 3' ends of produts respectively. The amplified PCR product was checked by agarose gel electrophoresis (Fig. 4-11). The band was excised from the gel and purified for further cloning.

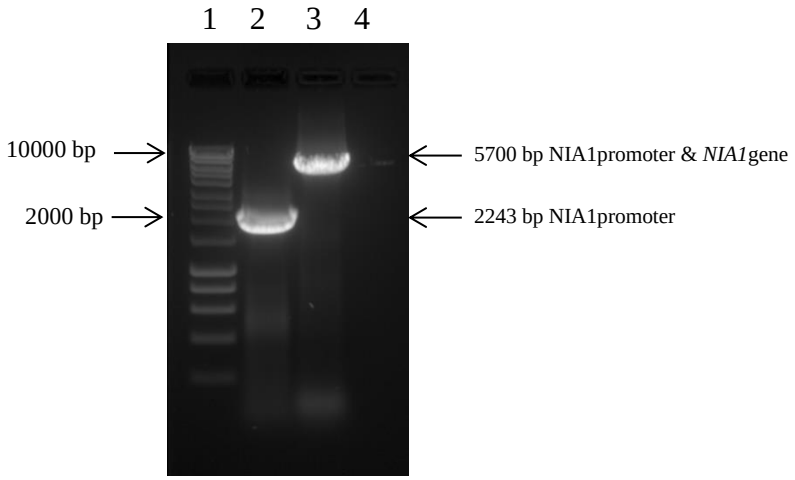

Figure 4-11: PCR amplification of 2.2 kb NIA1 promoter and 2.2 kb NIA1 promoter with 3.5 kb *NIA1* gene.

T32E7 BAC clone was used as a template to amplify the 2.2 kb NIA1 promoter fragment alone and 2.2 kb promoter with *NIA1* gene (2.2 kb promoter and 3.5 kb gene = 5.7 kb). In order to amplify the larger PCR product, a two step PCR programme was used. The long range PCR (Qiagen) high fidelity Taq DNA polymerase was used to avoid amplification errors. PCR amplification was carried out in the presence of dNTPs , Q-solution and $MgCl_2$ at 54^0C annealing temp and an increased extension time (2 min for promoter and 6 min for promoter and gene). The PCR products were then separated by agarose gel electrophoresis and visualized under UV light. Lane 1, HyperLadder1(Bioline); lane 2, 2.2 kb NIA1 promoter amplicon; lane 3, (5.7 kb) 2.2 kb NIA1 promoter with 3.5 kb *NIA1* gene amplicon; lane 4, blank

4.3.2 Restriction digestion of 2.2 kb NIA1 promoter and 2.2 kb promoter with 3.5 kb *NIA1* gene fragment with *Kpn1* and *Pst1*.

Amplified PCR product of 2.2 kb NIA1 promoter and 2.2 kb NIA1 promoter with 3.5 kb gene fragment was excised from the gel and purified. The resulting product was quantified using the Nanodrop and 2 ug of each gene fragment was used for digestion with *Kpn1* and *Pst1* restriction enzymes. Restriction digestion was carried out at 37^0C for 1 h. The digested product was loaded in the 0.8% (w/v) agarose gel (Fig. 4-12 A&B) then the gene fragment was excised from the gel and eluted using the Sigma gel purification kit.

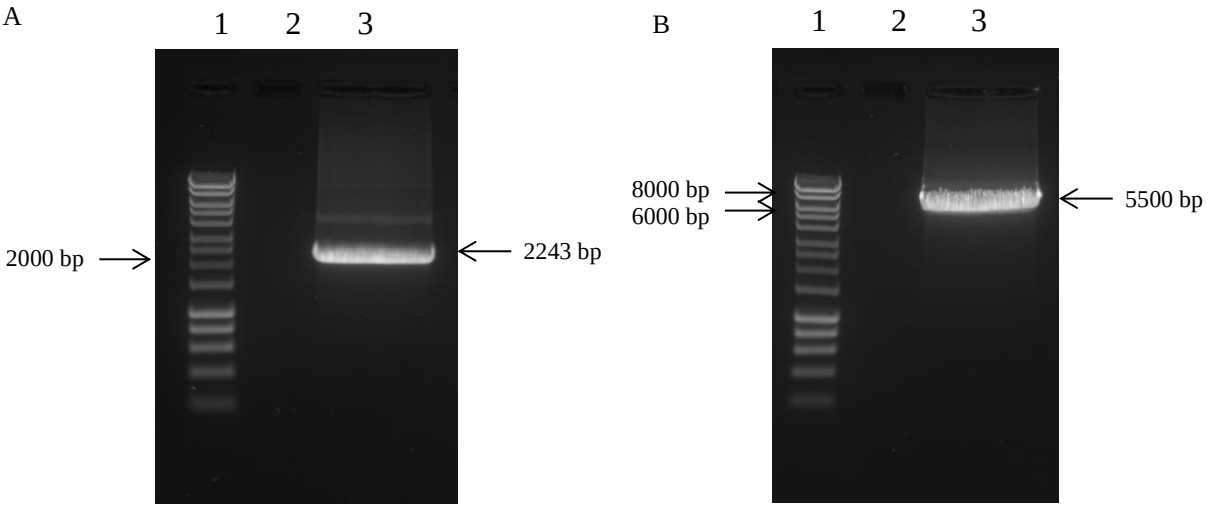

Figure 4-12: Restriction digestion of 2.2 kb NIA1 promoter (A) and 2.2 kb NIA1 promoter with 3.5 kb *NIA1* gene amplicon (B) with *Kpn1* and *Pst1*.

2 µg of PCR amplified and purified 2.2 kb NIA1 promoter and 2.2 kb NIA1 promoter with 3.5 kb *NIA1* gene fragments was digested with *Kpn1*-HF™ and *Pst1*-HF™ restriction enzymes at 37°C for 1 h. Digested products were separated by agarose gel electrophoresis and further purified and ligated with *Kpn1*-HF™ and *Pst1*-HF™ digested pGmGFP4 vector. Lane 1- HyperLadder1(Bioline); lane 2, blank; lane 3- 2.2 kb NIA1 promoter/2.2 kb NIA1 promoter with 3.5 kb *NIA1* gene.

4.3.3 Cloning of 2.2 kb promoter and 2.2 kb promoter with 3.5 kb gene into pGmGFP4

Quantification of *Kpn1* and *Pst1* digested and purified NIA1 promoter, NIA1 promoter with gene (insert) and pGmGFP4 vector was done with the Nanodrop. A 1:3 insert vector molar ratio was used for the ligation. Ligation was carried out at 16°C overnight. 10 µl of

ligated product was transformed into *E. coli* competent cells by heat shock method and spread onto LB Kanamycin plates. Transformed colonies were confirmed by colony PCR.

4.3.4 Restriction analysis of recombinant plasmid NIA1pro-mGFP4

Plasmid DNA was isolated from the PCR positive colony of *E. coli* grown in LB Kanamycin broth. Quantification of the plasmid was done using the Nanodrop. The selected recombinant clone was named as NIA1pro-mGFP4. The recombinant plasmid NIA1pro-mGFP4 was digested with *Kpn1* and *Pst1* (Fig. 4-13: lane 2), *Pst1 and Not1* (Fig. 4-13: lane 3), to release the expected fragments of 2243 bp (NIA1 promoter) and ~5.1 kb (vector), 7.1 kb (promoter+vector) and 717 bp *mGFP*4 respectively.

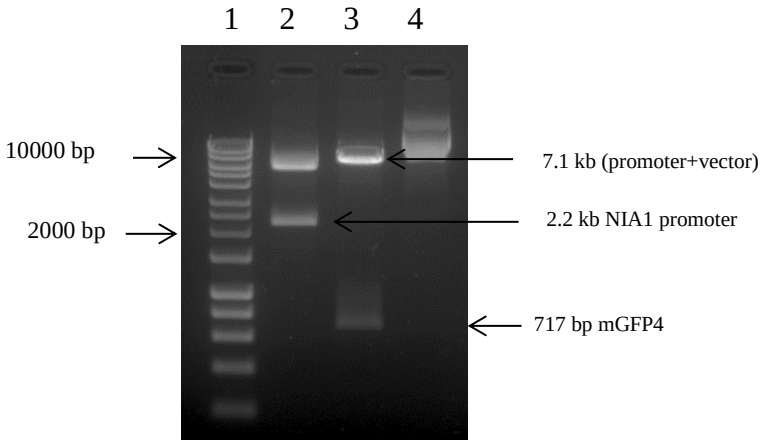

Figure 4-13: Restriction digestion confirmation of NIA1pro-mGFP4.

0.5 µg of plasmid DNA isolated from a NIA1pro-mGFP4 transformant was digested with different enzyme combinations to verify the construct. Digestion was carried out at 37^0C for 1 h. Upon digestion the products were separated by agarose gel electrophoresis. Lane 1, Hyperladder1 (Bioline); lane 2, NIA1pro-mGFP4 plasmid digested with *Kpn1 and Pst1*; lane 3, NIA1pro-mGFP4 Plasmid digested with *Pst1 & Not1*; lane 4, undigested NIA1pro-mGFP4.

4.3.5 Restriction analysis of recombinant plasmid NIA1pro-NIA1-mGFP4

Plasmid DNA was isolated from the PCR positive colonies of *E. coli* grown in LB+Kan broth. Quantification of plasmid was done by Nanodrop. The recombinant clone was named as NIA1pro-NIA1-mGFP4. The recombinant plasmid NIA1pro-NIA1-mGFP4 was

digested with *Kpn1* and *Pst1* (Fig. 4-14 lane 2), *Pst1 and Not1* (Fig. 4-14 lane 3), released the expected fragments size of 5.7 kb (NIA1 promoter and gene) and ~5.1 kb (vector), 10.6 kb (promoter+gene+ vector) and 717 bp mGFP4 respectively.

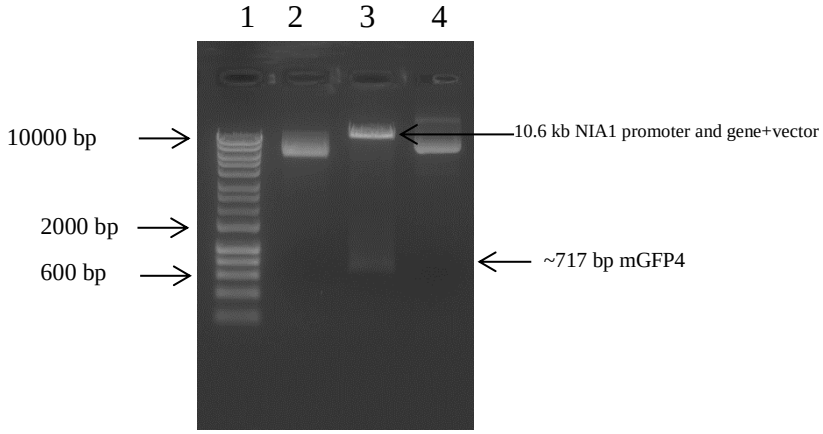

Figure 4-14: Restriction digestion confirmation of NIA1pro-NIA1-mGFP4

0.5 µg of Plasmid DNA isolated from NIA1pro-NIA1-mGFP4 transformant was digested with different enzyme combination to verify the construct. Digestion was carried out at 37^0C for 1 h. Upon digestion product was separated by agarose gel electrophoresis. *Kpn1 and Pst1* enzyme was used to release the 5.7 kb NIA1 promoter and gene and *Pst1 & Not1* was used to release the *mGFP4* gene. Above gel shows the release of correct size of the product corresponding to the enzyme digestion. Lane 1, Hyperladder1; lane 2, NIA1pro-NIA1-mGFP4 plasmid digested with *Kpn1 and Pst1* (released approximately equal size of NIA1 promoter+gene (5.7 kb) and vector (5. kb)); lane 3, NIA1pro-NIA1-mGFP4 Plasmid digested with *Pst1 & Not1*; lane 4, undigested NIA1pro-NIA1-mGFP4.

4.4 Transformation of pG35SmGFP4, NIA1pro-mGFP4 and NIA1pro-NIA1-mGFP4 constructs into *Agrobacterium* strain

0.5 µg of each construct (pG35SmGFP4, NIA1pro-mGFP4 and NIA1pro-NIA1-mGFP4) was transformed into the three separate lot of *Agrobacterium* competent cells with the help of helper plasmid pSoup by a freeze and thaw method (Weigel and Glazebrook, 2006). Cells were spread on LB *Rif+Kan+Tet* plates after 3 h incubation at 28^oC. Recombinant colonies were developed after 48 h incubation at 28^oC. Transformed colonies were further confirmed by colony PCR.

4.5 Making transgenic plants expressing GFP driven by NIA1

Arabidopsis wild type (Col-0), auxin mutants *aux1* and *axr2*, ethylene mutants *ein3-1* and *EIN3OX* and NR gene mutants *nia1* and *nia2* were transformed by the floral dip method. During the unopened flowerbud stage the inforescence was dipped into the transformation media containing *Agrobacterium* carrying the NIA1pro-mGFP4 and NIA1pro-NIA1-mGFP4 construct. To make a control, the 35S-mGFP4 construct was transformed into the WT plant Col-0. Seeds from these plants were collected and transformed plants were selected by allowing them to grow on plates containing ½ MS media with 30 µg/ml of hygromycin. The T-DNA contains the hygromycin resistance gene, so the transformed plants containing the cassette grow normally and produce roots and shoots. In contrast, wild type plants failed to grow on the hygromycin plate. Once the transformed seeds had produced healthy plants with long roots (Fig. 4-15), they were transferred to soil and grown to produce seeds for further analysis.

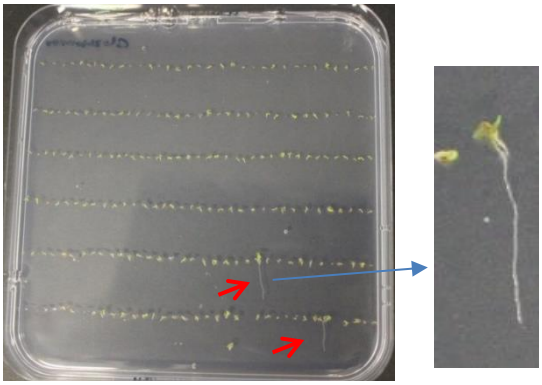

Figure 4-15: Selection of promising transgenic lines.

T_0 seeds were surface sterilized and germinated on an MSR3 plate containing 30 mg/ml hygromycin in a 12 h photoperiod at 20°C and 60% relative humidity. Hygromycin resistant seedlings (red arrows) were transferred to soil.

4.6 Confirmation of transgenic plants by PCR

Genomic DNA from young leaves of transgenic plants were isolated and quality of the DNA was analysed by agarose gel electrophoresis (Fig. 4-16). After the hygromycin selection, presence of construct in the transgenic line was confirmed by PCR using mGFP4 screening primers. 10 ng of plant genomic DNA was used as a template to verify transgenic plants. PCR results showed the presence of 717 bp *mGFP4* gene fragments in transgenic plants (Fig. 4-17) and further confirmed by sequencing.

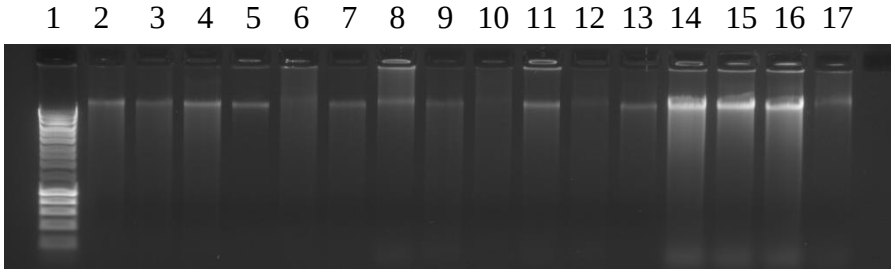

Figure 4-16: Plant genomic DNA isolated from transgenic plants.

Total plant genomic DNA was isolated from the leaves of transgenic plants, and 2 µl was loaded in the agarose gel and visualized under UV to check the quality of the DNA. Lane 1, HyperLadder1 (Bioline); lanes 2-17, genomic DNA samples.

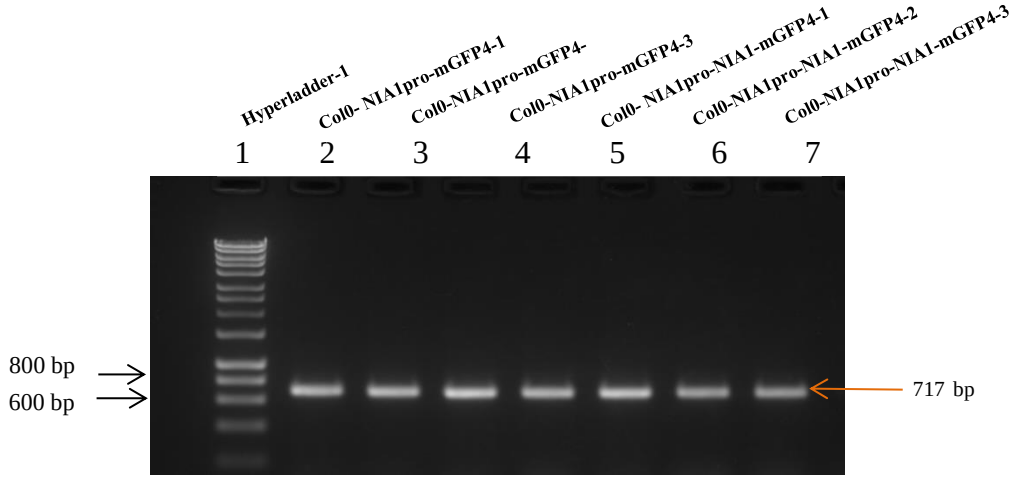

Figure 4-17: Transgenic plants showed the presence of *mGFP4* gene.

Genomic DNA isolated from transgenic plants was used as a template for PCR. mGFP4 screening primers were used to check the presence of mGFP4 in the transgenic plants. PCR result showed all the transgenic lines harbouring the mGFP4 reporter constructs.
Lane1, HyperLadder1 (Bioline); lane 2-7, transgenic plants. Image showed here is the representative image of transgenic plants screening.

4.7 Screening for single copy transgenic lines by inverse PCR

For each construct, a single copy insertion transgenic line was selected by performing inverse PCR. Total genomic DNA from the young leaves of transgenic plants were isolated and digested with *Kpn1*-HF^{TM} restriction enzyme, which cleaved one position in the T-DNA region and another one will be somewhere in the unknown plant genomic region (Fig. 4-18). Restriction digested DNA fragments were ligated by T4-DNA ligase; this circularised the cleaved DNA fragments. Primers were designed in the known T-DNA region (forward primer in the 5' end of mGFP4 region and reverse primer in the 3' region of the 2.2 kb promoter) and used to amplify the unknown genomic region. Sequencing of this PCR product showed the insertion region. A single copy insertion line gave a single PCR band in the agarose gel electrophoresis. The size of the PCR products being amplified from the circularised T-DNA will vary, because the cleavage site of *Kpn1* in the plant genome is depending upon where T-DNA integrates. To amplify the unknown size of the product, Qiagen long range PCR polymerase was used, as it allows the amplification of PCR product up to 40 kb in length. The PCR product was run through a 1.5% (w/v) agarose gel (Fig. 4-19). Wild type plant DNA digested with *Kpn1* was used as a control for a PCR which did not give any amplification.

To determine the location of the T-DNA insertion in the independent lines, the PCR fragment was excised and purified using QIAquick Gel Extraction Kit (Qiagen) and sequenced. This sequence was analysed through NCBI BLAST. The final analysed result will showed the insertion region of the T-DNA. These single copy lines were used for further studies.

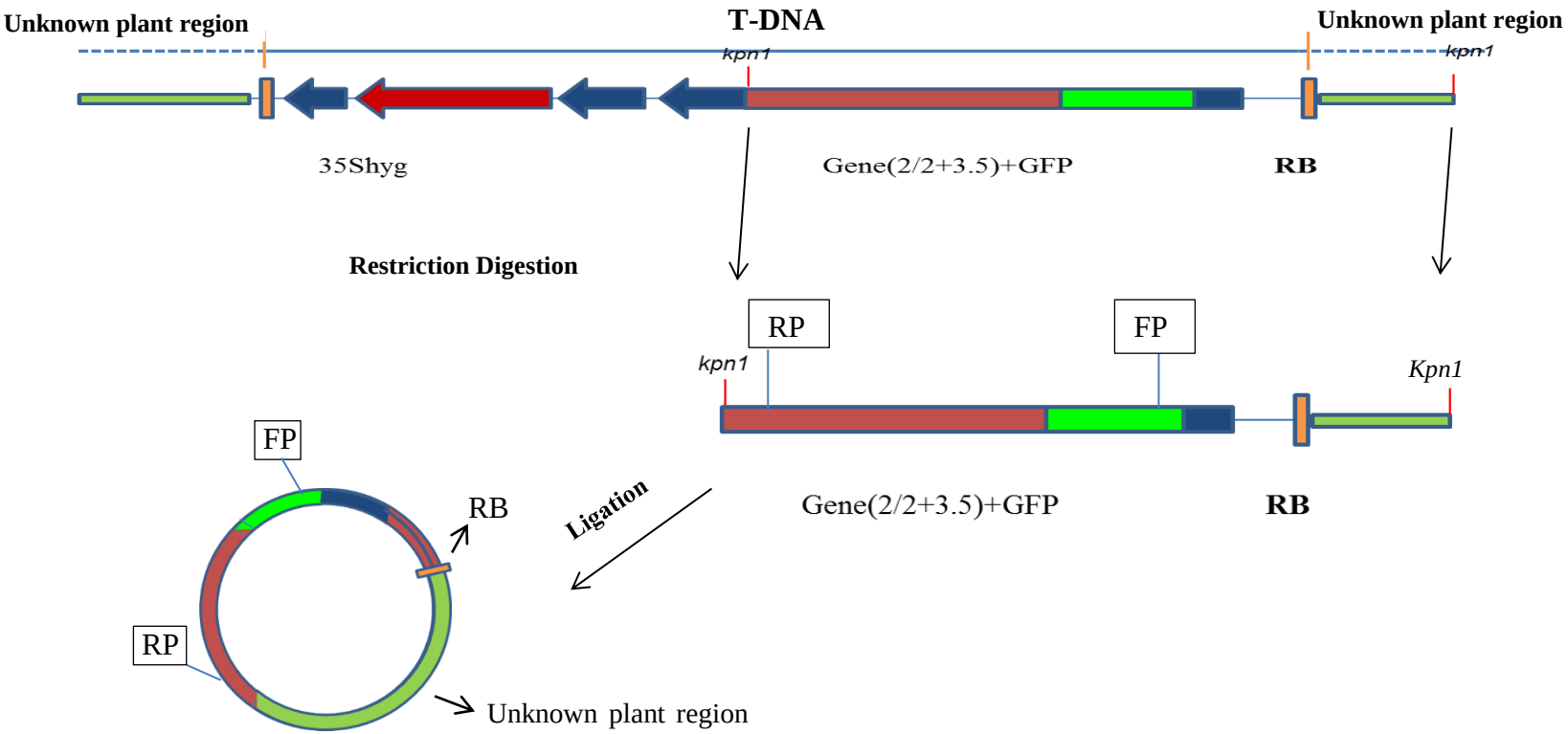

Figure 4-18: Schematic representation of inverse PCR steps to find the single copy insertion line.

First transgenic plant total genomic DNA was digested with *Kpn*1-HF restriction enzyme and then the digested product was circularised by using T4-DNA ligase. Primers in the known T-DNA region were used to amplify the circularised template by long range PCR. FP, forward primer; RP, reverse primer; RB, right border.

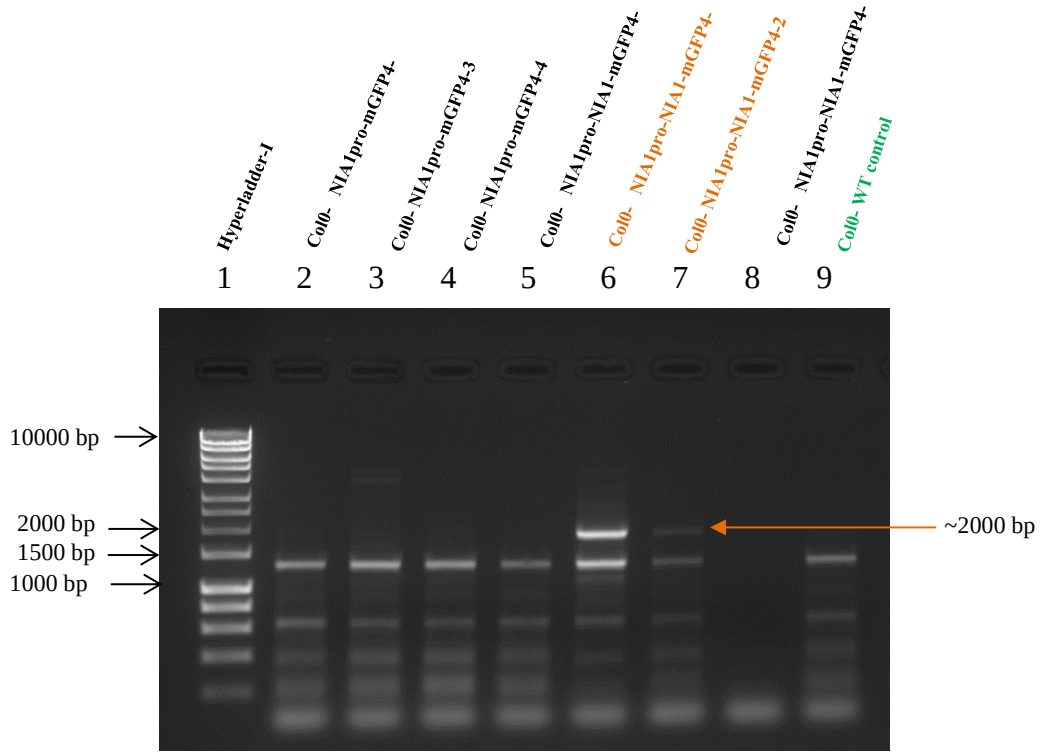

Figure 4-19: Gel electrophoresis to detect single copy insertion lines.

10 µl ligated and circularised *Kpn1*-digested genomic DNA of transgenic lines was used as a template to select single-copy-insertion lines. Long range PCR was used to amplify the unknown length of the PCR fragment. Lanes 2, 3, 4 and 5 showed random circularised fragments like the WT control (lane 9). Lanes 6 and 7 showed amplified single copy PCR fragments. These band was excised from the gel and used for sequencing.

Gel electrophoresis (Fig. 4-19) showed amplification in lanes 6 and 7 from Col-0 harbouring NIA1Pro-NIA1-mGFP4 transgenic line 2. The amplified fragment (~2 kb) from lanes 6 and 7 was purified from the gel and sent for sequencing. All other lanes showed a similar pattern of fragments to the WT control. These fragments are random circularised DNA fragments from the plant genome. Sequence analysis from Col-0 NIA1Pro-NIA1-mGFP4 transgenic line 2 revealed that T-DNA is located in chromosome 5 at position 24,250,885 (Appendix 12).

4.8 Discussion

Cloning a gene of interest, in-frame with the GFP reporter gene is a useful tool to understand the role of the gene in a biological process as well as its detailed spatial and temporal gene expression profile, and the subcellular localization of the corresponding protein (Zhou *et al.*, 2011). In order to find out the role and function of the *NIA1* gene in gravitropism, the *NIA1*-mGFP4 reporter construct was made. The wild type Col-0, auxin mutants (*aux1*, *axr2* and *axr3*), NR mutants (*nia1*, and *nia2*), ethylene mutants *ein3-1* and ethylene transgenic line *EIN3OX* were transformed with NIA1pro-mGFP4 and NIA1pro-NIA1-mGFP4 constructs. In addition Col-0 was transformed with the pG0179 containing 35S-mGFP4, which can be utilized as a positive control. Transgenic efficiency varied among mutants, Col-0, auxin and ethylene mutant showed low transgenic efficiency, whereas the NR mutant harbouring NIA1pro-NIA1-mGFP4 constructs produced high transformation efficiency (data not shown). Lower transformation efficiency may be due to NO toxicity.

T_0 plants were allowed to self and produce T_1 seeds. Further homozygous T1 transgenic lines were selected by germinating them on an MSR3 plate containing 30 mg/ml hygromycin. This is the optimal concentration of hygromycin to decrease the hypocotyl length, produce cholorotic tiny leaves and no root growth in non-transformant plants (Ee *et al.*, 2014). Plants containing the construct produced healthy roots and leaves, whereas the growth of non-transformants was inhibited. A transgenic line with a single copy number was selected based on inverse PCR (Fig. 4-20, 4-21). Insertional position was identified by further sequencing (Appendix 12).

Chapter 5 Optimization of mGFP4 expression in transgenic plants

In the previous chapter, the cloning of 35S-mGFP4, mGFP4 in-frame with the NIA1 promoter and NIA1 promoter along with the *NIA1* gene was described, together with transformation of these cassettes into the WT, NR, auxin and ethylene mutants. Successful integration of these cassettes into the plant genome was confirmed by PCR and inverse PCR followed by sequencing.

GFP has been used as a reporter system in many animal cells and plant species, but while expressing in Arabidopsis wild-type GFP failed to express, because Arabidopsis recognises sequence in the coding region of WT-GFP as a plant intron and undergoes inappropriate splicing (Haseloff *et al.,* 1997). Wild-type GFP requires a strong promoter and low incubation temperature. whereas modified GFP (mGFP) requires higher temperature for fluorescence. GFP protein is highly stable after chromophore maturation and the fluorescence was unaffected up to 65^0C (Ward and Bokman, 1982). After expression of GFP it has to undergo folding followed by cyclisation, oxidation and dehydration to become a fully functional fluorescence protein (Craggs, 2009). These processes together are called maturation.

ABA and H_2O_2 have been shown to induce NIA1-mediated NO synthesis in stomatal guard cells. Hence to optimize the expression of mGFP4, experiments were carried out in ABA and H_2O_2 treated stomatal guard cells. The results from these experiments are discussed in this chapter.

5.1 Expression of 35S driven mGFP4 in transgenic plants

In order to examine the expression of mGFP4 in transformed plants, roots and stomatal peels of Col-0 harbouring the 35S-mGFP4 construct along with the negative control were observed by confocal microscopy. Roots showed bright mGFP4 fluroscence, and leaf peels (Fig. 5-1 A&D) showed fluorescence throughout, especially in the guard cells. Images were compared with WT Col-0 plants (Fig. 5-1 B&E). Bright fluorescence from the 35S-mGFP4 indicates the successful expression of mGFP4 under the control of the CaMV35S promoter. Quantitative measurement of mGFP4 total fluoresence was carried out using Fiji image analysis software and the results showed the difference in fluorescence level between the root and stomata in the Col-0:35S-mGFP4 and WT plants. Insignificant auto fluorescence was observed in the Col-0 WT plant.

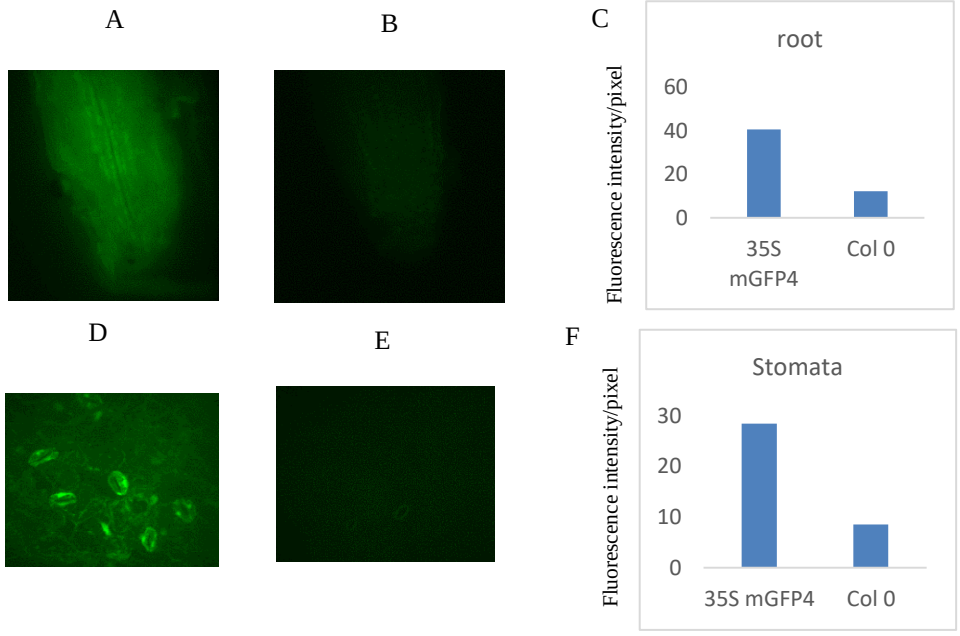

Figure 5-1: Expression of 35S-driven mGFP4 in roots and stomata of Col-0.

Five day old WT seedlings and transformants harbouring 35S-mGFP4 were used to observe the functional expression of mGFP4. Transgenic plant root (A) and young leaf peel (D) showed bright fluorescence compared to the WT Col-0 root (B) and leaf peel (E). Imaging conditions (excitation, 475 nm; emission, 510 nm; gain, 4.5; exposure, 35 µs) were identical for all the plants in the experiments. Graph C and F showed the difference in the fluorescence intensity (measured by Fiji image analysis software) between the transgenic and control plants (n=3).

5.2 Optimization of time and temperature for mGFP4 expression in transgenic lines

5.2.1 mGFP4 did not fluorescence at 25^{o}C after 4 h of incubation

In order to find the temperature and time required for optimal mGFP4 expression, fluorescence was measured in ABA-treated (section 2.5) stomata at 25^{o}C in both light and dark conditions. After 4 h of incubation samples were observed using the confocal microscopy, but no expression of mGFP4 was detected in Col-0 harbouring NIA1pro-mGFP4 and NIA1pro-NIA1-mGFP4 (Fig. 5-2 I); in both the transgenic lines, stomata look similar to WT Col-0, only auto fluorescence in stomatal pore was visible. (due to lack of control at 25^{o}C, images were compared to control at 37^{o}C in Fig. 5-2 II).

5.2.2 mGFP4 expression starts at 37^{o}C after 4 h of incubation

ABA treated samples were incubated at 37^{o}C for 4 h in light and dark environments were imaged using the confocal microscopy, WT Col-0 showed auto-fluorescence from the cell wall of the stomatal pore, whereas, Col-0 harbouring NIA1pro-mGFP4 (Light and dark incubated) and NIA1pro-NIA1-mGFP4 (Light incubated) stomatal guard cells showed some mGFP4 fluorescence in the guard cells (Fig. 5-2 II).

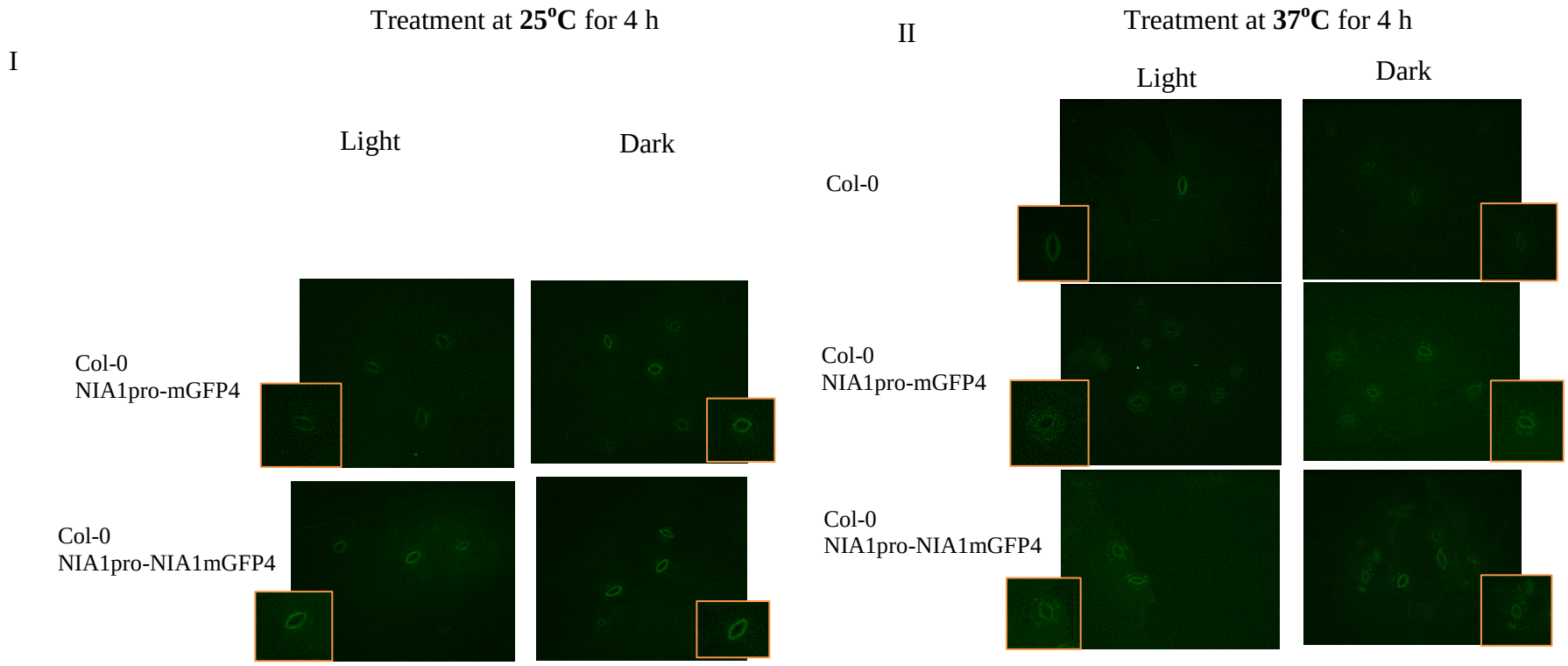

Figure 5-2: mGFP4 was not visible after 4 h at 25°C, but visible at 37°C

Epidermal fragments from Col-0 harbouring NIA1pro-mGFP4 and NIA1pro-NIA1-mGFP4 stomata were treated with 150 µM ABA and then incubated at 25 °C and 37°C in both light and dark conditions. samples were observed after 4 h of incubation. Imaging conditions (excitation 475 nm; emission 510 nm; gain, 4.5; exposures, 35 µs) were identical for all the plants in the experiments. The images displayed here were from representative samples (n=3).

5.2.3 Bright mGFP4 fluorescence was observed at 37°C after 6 and 10 h of incubation

After observing the initiation of mGFP4 expression in stomatal guard cells after 4 h, samples were further incubated up to 10 h and visualized using the confocal microscopy. Col-0 harbouring NIA1pro-mGFP4 guard cells showed NIA1-promoter-mediated mGFP4 fluorescence in both light and dark incubated samples, but the sample incubated in the light showed brighter fluorescence than the sample incubated in the dark (Fig. 5-4). In contrast, Col-0 guard cells harbouring NIA1pro-NIA1-mGFP4 showed NIA1-promoter and gene mediated mGFP4 expression only in the light incubated sample. In the case of *nia1* harbouring NIA1pro-NIA1-mGFP4, mGFP4 fluorescence was observed in both dark and light after 6 h of incubation. The sample incubated in light showed brighter fluorescence than the sample incubated in the dark.

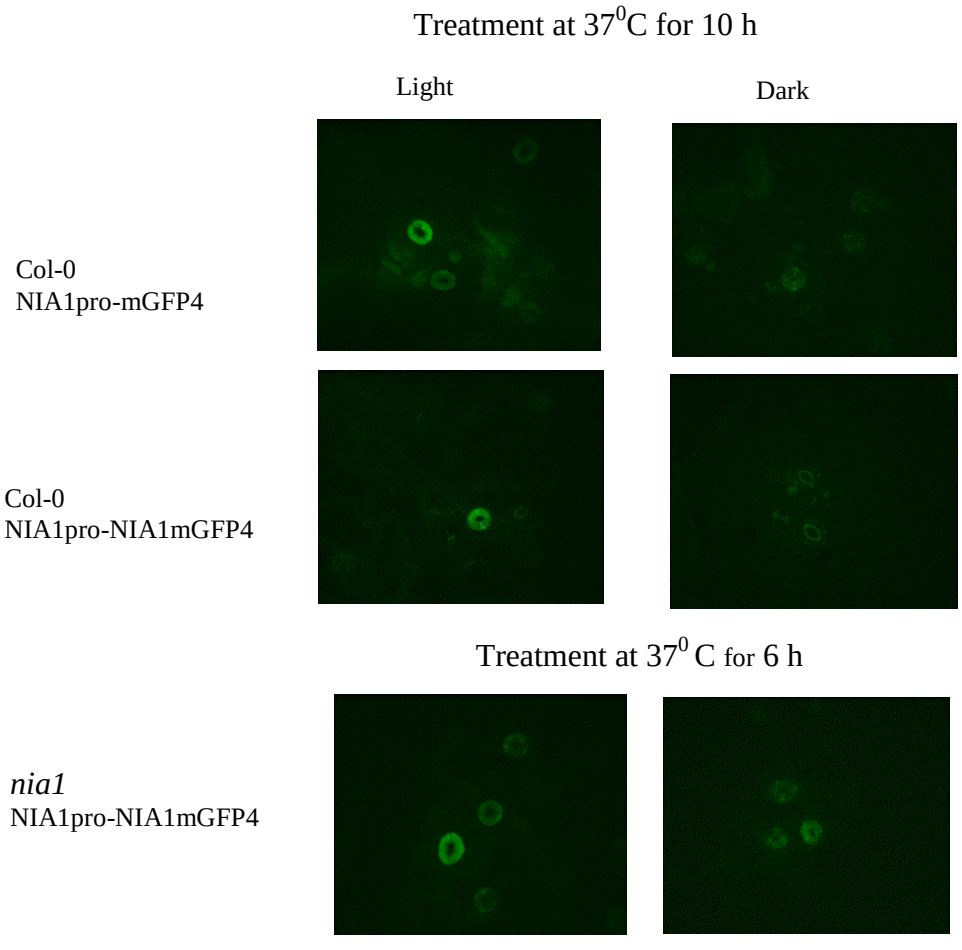

Figure 5-2: mGFP4 fluorescence found after longer incubation at 37°C

Epidermal fragments from Col-0 and *nia1* harbouring NIA1pro-mGFP4 and NIA1pro-NIA1-mGFP4 stomata were treated with 150 µM ABA and incubated at 37°C in both light and dark conditions. Samples were observed after 6 h and 10 h of incubation. Imaging conditions (excitation 475 nm; emission 510 nm; gain, 4.5; exposure, 35 µs) were identical for all the plants in the experiments. The images displayed here were from representative samples (n=3).

5.3 Expression of mGFP4 in transgenic root

To demonstrate *NIA1*- promoter and gene mediated mGFP4 expression in roots, Col-0 transgenic seedlings harbouring NIA1pro-mGFP4 and NIA1pro-NIA1-mGFP4 were incubated with 100 µM H_2O_2 (section 2.6) and then gravistimulated for 6 h. After 6 h, roots were observed using laser scanning confocal microscopy (Fig. 5-5). In both the transgenic lines, roots showed bright fluorescence compared to control (Col-0) roots. These images represent the expression of NIA1-promoter and NIA1-promoter and gene mediated mGFP4 fluorescence during gravitropism. mGFP4 fluorescence was observed in the lower side of the root, which shows gravity induces the expression of *nia1* gene in the lower side of the root.

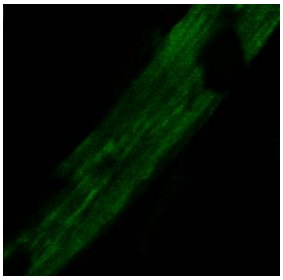

Col-0 WT

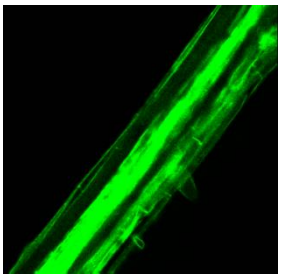

Col-0-NIA1pro-mGFP4

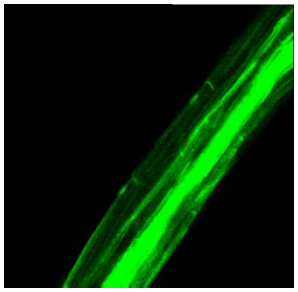

Col-0-NIA1pro-NIA1mGFP4

Figure 5-3: mGFP4 fluorescence in root induced by gravitropism

Col-0 seedlings harbouring NIA1pro-mGFP4 and NIA1pro-NIA1-mGFP4 were pre-treated with 100 µM of H_2O_2 and then gravistimulated for 6 h. After 6 h, roots were mounted on slides and images were taken. Transgenic seedling roots showed bright mGFP4 fluorescence. All the images were taken at identical settings (excitation 475 nm; emission 510 nm; gain, 4.5; exposure, 35 µs). The images displayed here were from representative samples (n=3).

5.4 **Discussion**

Reporter proteins are useful to monitor cellular events in plants and other organisms. In the past, two important reporter proteins, beta-glucuronidase (GUS) and luciferase (LUC) were used extensively in plants, but they do have limitations. They need an additional substrate to express inside the biological system, and they are not suitable to test primary transformant seedlings because of the destructive nature of the assay. The green fluorescent protein (GFP) from *Aequorea victoria* is being widely used as a standard reporter system in both animal and plant systems. GFP does not require an exogenous substrate and can be used in living cells. Wild-type GFP was successfully expressed in tobacco (dicot), and some monocot plants, but when expressed in *Arabidopsis thaliana* GFP failed to fluorescence. This is because the wild-type GFP mRNA undergoes abberant splicing within its coding sequence, due to a sequence similarity to the plant intron splice site. This splicing limits the use of wild type GFP in Arabidopsis plants. The cryptic intron of the wildtype GFP was modified by altering the codon, and then named as mGFP4 (modified GFP4) (Haseloff *et al.*, 1997). Arabidopsis callus expressing mGFP4 showed a brighter green fluorescence using a handheld 100 W long-wavelength UV lamp and also showed a major peak of fluorescence at 395 nm (excitation) and 509 nm (emission) in the confocal microscopy (Haseloff *et al.*, 1997). Therefore mGFP4 was used in this investigation.

The cauliflower mosaic virus promoter (CaMV35S) is one of the widely used constitutive promoters in plant transformation. Stable integration of 35S gene fused upstream of a GUS reporter gene into the plant chromosome showed GUS expression in all the cells (Jefferson *et al.,* 1987). Dutt *et al.* (2014) reported expression of 35S promoter is species specific with diverse levels of expression found in strawberry, tomato and petunia plants. In the present study, mGFP4 driven by CaMV35S was constitutively expressed in root and leaf cells of transformed Col-0 plants.

Hu *et al.* (2006) have already demonstrated the asymmetric accumulation of NO in soybean and maize root and Desikan *et al.* (2002) demonstrated ABA-induced NO synthesis in stomatal guard cells, but in this current study transgenic plants harbouring NIA1pro-mGFP4 and NIA1pro-NIA1-mGFP4 construct did not show any fluorescence in H_2O_2 pre-treated gravistimulated root or in ABA pre-treated stomatal guard cells at room temperature. Lin *et al.* (1994) showed 1.5 kb sequence of 5' flanking region of *NIA1* promoter is enough for nitrate response induction by expressing the native promoter fused with the reporter gene in tobacco plants. In contrast Konishi *et al.* (2011) failed to find 1.9 kb *NIA1* promoter response to nitrate in Arabidopsis. Also, they have reported the downstream sequence of *NIA1* gene along with the promoter was required for the nitrate response. Most of the plant promoters contains its regulatory region within the 2 kb upstream sequence. These 2 kb regions are enough to provide critical information about the gene expression pattern (Xiao *et al.,* 2010). In the present study 2.2 kb NIA1 promoter sequence was used to drive the *mGFP4* expression, however failed to see the mGFP4 expression at room temperature. In addition, expression of modified GFP has been shown to be temperature sensitive and the maturation of GFP protein is depends on time (Haseloff, *et al.,* 1997). To optimise the temperature and time required for the expression of mGFP4, experiments were performed at 25^oC and 37^oC in both light and dark

conditions. These results showed bright mGFP4 fluorescence at 37^{o}C in gravistimulated root and ABA-induced stomatal guard cells. The maturation of mGFP4 takes 6-10 h. Hence, all experiments need to be carried out at 37^{o}C. This result demonstrates that the 2.2 kb *NIA1* promoter region is sufficient for expression of the *NIA1* gene, gravity and ABA induces NIA1-promoter, NIA1-promoter and gene mediated expression of mGFP4 in roots and in stomatal guard cells respectively. The mGFP4 fluorescence in the lower side of the root especially in the lower epidermal cells, shows the localisation of *nia1 gene* in gravity bending. Even though several NO synthesis mechanism exist in the plants NR-mediated NO synthesis in the root was reported earlier. Hu *et al.* (2006) also demonstrated the asymmetric synthesis and accumulation of NO in the lower half of the gravistimulated soybean root, induced the gravitropic response, they have also reported putative NR inhibitor (sodium azide) reduces both NO synthesis and gravity bending. This suggested that NR (either *NIA1* or *NIA2*) plays important role in the NO synthesis and root bending. In the present study, most of the *NIA1*-mediated mGFP4 fluorescence was also observed in the lower side of the gravistimulated root, which shows that gravity induces the expression of NIA1 promoter and gene, especially in the lower side of the root. This experiment results could support the role of *NIA1*-mediated asymmetric accumulation of NO in the lower half of the root during gravity bending. Further studies are required to investigate the role of NIA1 in NO synthesis in root and light to dark induction of NO synthesis in stomatal guard cells. Function, synthesis and interaction of the gene of interest can be thoroughly studied when GFP is cloned in frame with the particular gene or protein (Tian, 1999). With the availability of mutants (auxin, ethylene and NR mutants) harbouring the NIA1pro-mGFP4 or NIApro-NIA1-mGFP4 cassette, further experiments could be performed to study the role of *nia1* in NO synthesis and the interaction between NO, auxin

and ethylene during root gravitropism and stomatal opening and closure in response to biotic and abiotic stress.

Chapter 6 Summary and future work

6.1 Summary

The aim of this investigation was to identify the role of *NIA1* mediated NO synthesis and signalling in root growth and development. Experiment results demonstrating the localisation of *NIA1* during gravitropic bending.

Gravitropic analysis of Col-0 and auxin mutants confirmed that Col-0 responds to gravity and starts to bend towards the gravity signal, whereas auxin mutants did not respond to gravity. Confocal analysis also showed that gravity induced the synthesis and accumulation of NO in the lower side of the bending region of the Col-0 root, whereas auxin mutants did not show any accumulation in the lower side of the root. Quantitative analysis of *NIA1* by qPCR also demonstrate that NIA transcript accumulation increased 2 h after gravistimulation in Col-0 root. It was therefore concluded that gravity induces NIA1-mediated NO synthesis and accumulation, which further induces root bending.

Analysis of root bending in NIA mutants showed that *nia1* bends significantly slower than *nia2* and Col-0. This result suggest that *NIA1* has more prominent role in root bending than *NIA2*. The ethylene mutant *ein3-1* and the over expression line *EIN3OX* both showed slower root bending than Col-0. *EIN3OX* showed significantly reduced and slower root bending than *ein3-1* and Col-0. These results suggest that ethylene negatively regulates root bending. External application of NAA and SNAP significantly increased the root bending, whereas external application of ACC significantly decreased the root bending. Removal of NO using a NO scavenger also significantly reduced gravitropic bending. All these results suggest that NO and auxin positively regulate root bending, whilst ethylene negatively regulates root bending.

Arabidopsis ecotype Col-0 and auxin, ethylene and *NIA* mutants were successfully transformed with *NIA1* transcriptional (NIA1pro-mGFP4) and translational (NIA1pro-NIA1-mGFP4) reporter construct. These transgenic lines were optimized for mGFP4 expression. Successful expression of ABA and H_2O_2 induced *NIA1*-mediated mGFP4 fluorescence was detected by confocal microscopy in the stomata and root respectively. Further experiments would be carried out to find out the role of *NIA1* in root development and possible NO interaction with other phytohormones during biotic and abiotic stress.

6.2 **Conclusion**

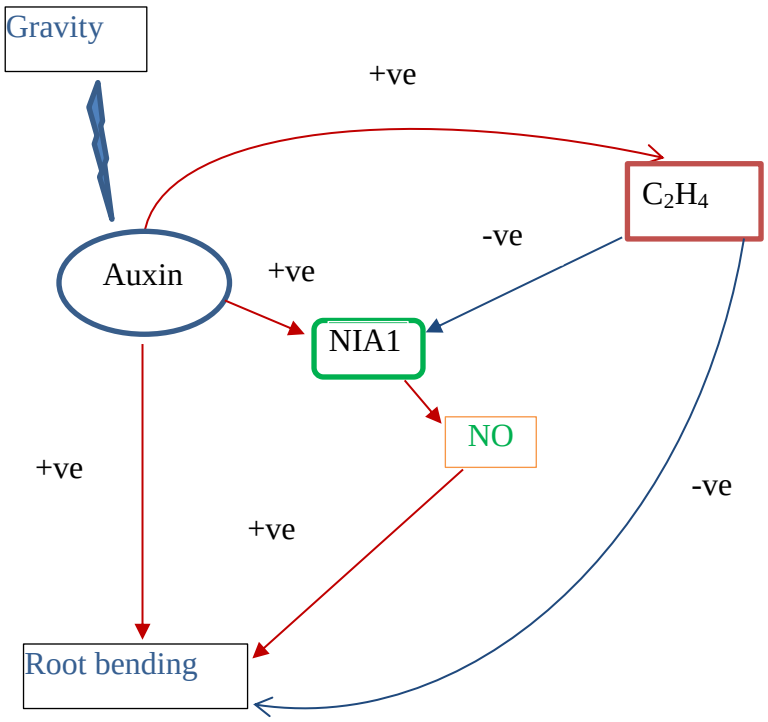

Figure 6-1: Model for NO, auxin and ethylene interaction

Initial stage of gravity perception induces auxin and NIA1 mediated NO signalling, which will produce and differential distribution/accumulation of auxin and NO in the lower side of root. Increased accumulation of auxin and NO in the lower part of cells in the root inhibit cell elongation and initiate gravity bending. After the initiation of gravity bending later stage auxin positively regulated ethylene signalling which produces and accumulates ethylene and negatively regulate the root bending.

6.2.1 Proposed model for NO, auxin and ethylene interaction

Based on the results from current experiments, here proposed a model for interaction between NO, auxin and ethylene signalling during root bending (Figure 6.1). Gravity signals positively regulate auxin signalling which induces the synthesis of *NIA1*-mediated NO signalling, which further induces root bending. Intial gravity perception switches on auxin and *NIA1* mediated NO signalling, which leads to the asymmetric accumulation of auxin and NO in the lower side of the root. Low concentration of auxin and NO in the upper side of the root induces cell elongation, whereas high auxin and NO in the lower side of the root inhibits cell elongation leading to root bending. Later stage auxin positively regulate ethylene signalling, which negatively regulate the NO signalling and decrease the gravity bending. Exposure to ethylene has been shown to rapidly reduce cell elongation (Le *et al.,* 2001). Hence auxin and NO positively regulate root bending, whereas ethylene negatively regulates the root bending.

6.3 Future work

Further work with NIA1pro-mGFP4 and NIA1pro-NIA1-mGFP4 transgenic lines would focus on the importance of role of NIA1 in NO synthesis, also to investigate the expression and localisation of *NIA1* and NO in response to gravistimulation, drought, nutrient availability, light and temperature.

Interaction of NO with other phytohormones like auxin, ethylene, ABA, cytokinin and gibberellic acid would be investigated by the external application of IAA, NAA, ACC, ABA and other phytohormones cytokinin, GA. Also it would be possible to study the interactions by crossing the NIA1pro-mGFP4 and NIA1pro-NIA1-mGFP4 transgenic lines with the relavant hormone mutant lines.

The interaction of NO and ABA signalling in stomatal closure would be further investigated with the help of transgenic lines.

Experiments based on the promoter-report-system has provided significant insight in auxin signalling. Spatial and temporal expression of auxin genes during root development, other physiological development and interaction with phytohormones has been demonstrated using a DR5 reporter construct (Chen *et al.*, 2003).

NO is also an important plant signalling molecule that participates in many physiological functions. However, NO research in plants is at an early stage. To date, no receptor for NO has been identified. Therefore, further experiments with the transgenic lines could be a useful tool to explore the importance of NO signalling in plants.

References:

Abel, S., Nguyen, M.D., Chow, W. and Theologis, A., (1995). ACS4, a primary indoleacetic acid-responsive gene encoding 1-aminocyclopropane-1-carboxylate synthase in *Arabidopsis thaliana*. Structural characterization, expression in Escherichia coli, and expression characteristics in response to auxin. *The Journal of Biological Chemistry*. 270 (32), 19093-19099.

Aichinger, E., Kornet, N., Friedrich, T. and Laux, T., (2012). Plant stem cell niches. *Annual Review of Plant Biology*. 63 615-636.

Arasimowicz, M. and Floryszak-Wieczorek, J., (2007). Nitric oxide as a bioactive signalling molecule in plant stress responses. *Plant Science*. 172 (5), 876-887.

Astier, J. and Lindermayr, C., (2012). Nitric oxide-dependent posttranslational modification in plants: an update. *International Journal of Molecular Sciences*. 13 (11), 15193-15208.

Baudouin, E., (2011). The language of nitric oxide signalling. *Plant Biology*. 13 (2), 233-242.

Beligni, M. and Lamattina, L., (2001). Nitric oxide in plants: the history is just beginning. *Plant, Cell & Environment*. 24 (3), 267-278.

Bennett, M.J., Marchant, A., Green, H.G. and May, S.T. (1996) Arabidopsis AUX1 gene: a permease-like regulator of root gravitropism. *Science*. 273 (5277), 948.

Bethke, P.C., Badger, M.R. and Jones, R.L., (2004). Apoplastic synthesis of nitric oxide by plant tissues. *The Plant Cell*. 16 (2), 332-341.

Bleecker, A. and Kende, H., (2000). Ethylene: A gaseous signal molecule in plants. *Annual Review of Cell and Developmental Biology*. 16, 1-18.

Bright, J., Desikan, R., Hancock, J.T., Weir, I.S. and Neill, S.J., (2006). ABA-induced NO generation and stomatal closure in Arabidopsis are dependent on H_2O_2 synthesis. *The Plant Journal*. 45 (1), 113-122.

Buer, C.S., Sukumar, P. and Muday, G.K., (2006). Ethylene modulates flavonoid accumulation and gravitropic responses in roots of Arabidopsis. *Plant Physiology*. 140 (4), 1384-1396.

Chen, Y., Yordanov, Y.S., Ma, C., Strauss, S. and Busov, V.B., 2013. DR5 as a reporter system to study auxin response in Populus. Plant cell reports, 32(3), 453-463.

Cheng, C.L., Acedo, G.N., Dewdney, J., Goodman, H.M. and Conkling, M.A., (1991). Differential expression of the two Arabidopsis nitrate reductase genes. *Plant Physiology*. 96 (1), 275-279.

Clark, K.L., Larsen, P.B., Wang, X. and Chang, C., (1998). Association of the Arabidopsis CTR1 Raf-like kinase with the ETR1 and ERS ethylene receptors. *Proceedings of the National Academy of Sciences of the United States of America*. 95 (9), 5401-5406.

Craggs, T.D., (2009). Green fluorescent protein: structure, folding and chromophore maturation. *Chemical Society Reviews*. 38 (10), 2865-2875.

Crawford, N.M., (2006). Mechanisms for nitric oxide synthesis in plants. *Journal of Experimental Botany*. 57 (3), 471-478.

Dean, J.V. and Harper, J.E., (1986). Nitric Oxide and Nitrous Oxide Production by Soybean and Winged Bean during the in Vivo Nitrate Reductase Assay. *Plant Physiology*. 82 (3), 718-723.

Delledonne, M., Xia, Y., Dixon, R.A. and Lamb, C., (1998). Nitric oxide functions as a signal in plant disease resistance. *Nature*. 394 (6693), 585-588.

Den Herder, G., Van Isterdael, G., Beeckman, T. and De Smet, I., (2010). The roots of a new green revolution. *Trends in Plant Science*. 15 (11), 600-607.

Desikan, R., Cheung, M.K., Bright, J., Henson, D., Hancock, J.T. and Neill, S.J. (2004) ABA, hydrogen peroxide and nitric oxide signalling in stomatal guard cells. *Journal of Experimental Botany*. 55 (395), 205-212.

Desikan, R., Griffiths, R., Hancock, J. and Neill, S., (2002). A new role for an old enzyme: nitrate reductase-mediated nitric oxide generation is required for abscisic acid-induced stomatal closure in *Arabidopsis thaliana*. *Proceedings of the National Academy of Sciences of the United States of America*. 99 (25), 16314-16318.

Durner, J., Wendehenne, D. and Klessig, D.F., (1998). Defense gene induction in tobacco by nitric oxide, cyclic GMP, and cyclic ADP-ribose. *Proceedings of the National Academy of Sciences of the United States of America*. 95 (17), 10328-10333.

Dutt, M., Dhekney, S.A., Soriano, L., Kandel, R. and Grosser, J.W., (2014). Temporal and spatial control of gene expression in horticultural crops. *Horticulture Research*. (1), 1-17.

Ee, S., Khairunnisa, M., Hussein, Z.A.M., Noor Azmi, S. and Zainal, Z., (2014). Effective hygromycin concentration for selection of Agrobacterium-mediated transgenic Arabidopsis thaliana. *Malaysian Applied Biology*. 43 (1), 119-123.

Fancy, N.N., Bahlmann, A. and Loake, G.J., (2016). Nitric oxide function in plant abiotic stress. *Plant, Cell & Environment*. 40 (4), 462-472.

Forde, B.G., (2002). Local and long-range signaling pathways regulating plant responses to nitrate. *Annual Review of Plant Biology*. 53 (1), 203-224.

Foresi, N., Correa-Aragunde, N., Parisi, G., Calo, G., Salerno, G. and Lamattina, L., (2010). Characterization of a nitric oxide synthase from the plant kingdom: NO generation from the green alga *Ostreococcus tauri* is light irradiance and growth phase dependent. *The Plant Cell*. 22 (11), 3816-3830.

Freschi, L., (2013). Nitric oxide and phytohormone interactions: current status and perspectives. *Frontiers in Plant Science*. (4), 1-22.

Friml, J., Wiśniewska, J., Benková, E., Mendgen, K. and Palme, K., (2002). Lateral relocation of auxin efflux regulator PIN3 mediates tropism in Arabidopsis. *Nature*. 415 (6873), 806-809.

Fröhlich, A. and Durner, J., (2011). The hunt for plant nitric oxide synthase (NOS): is one really needed? *Plant Science*. 181 (4), 401-404.

García, M.J., Suárez, V., Romera, F.J., Alcántara, E. and Pérez-Vicente, R., (2011). A new model involving ethylene, nitric oxide and Fe to explain the regulation of Fe-acquisition genes in Strategy I plants. *Plant Physiology and Biochemistry*. 49 (5), 537-544.

Gniazdowska, A., Dobrzyńska, U., Babańczyk, T. and Bogatek, R., (2007). Breaking the apple embryo dormancy by nitric oxide involves the stimulation of ethylene production. *Planta*. 225 (4), 1051-1057.

Goldsmith, M., (1977). The polar transport of auxin. *Annual Review of Plant Physiology*. 28 (1), 439-478.

Gouvea, C., Souza, J., Magalhaes, A. and Martins, I., (1997). NO-releasing substances that induce growth elongation in maize root segments. *Plant Growth Regulation*. 21 (3), 183-187.

Guo, F.Q., Okamoto, M. and Crawford, N.M., (2003). Identification of a plant nitric oxide synthase gene involved in hormonal signaling. *Science (New York, N.Y.)*. 302 (5642), 100-103.

Gupta, K.J., Fernie, A.R., Kaiser, W.M. and van Dongen, J.T., (2011). On the origins of nitric oxide. *Trends in Plant Science*. 16 (3), 160-168.

Gupta, K.J. and Kaiser, W.M., (2010). Production and scavenging of nitric oxide by barley root mitochondria. *Plant & Cell Physiology*. 51 (4), 576-584.

Gupta, K.J., Stoimenova, M. and Kaiser, W.M., (2005). In higher plants, only root mitochondria, but not leaf mitochondria reduce nitrite to NO, in vitro and in situ. *Journal of Experimental Botany*. 56 (420), 2601-2609.

Hammer, G.L., Dong, Z., McLean, G., Doherty, A., Messina, C., Schussler, J., Zinselmeier, C., Paszkiewicz, S. and Cooper, M., (2009). Can changes in canopy and/or root system architecture explain historical maize yield trends in the US Corn Belt? *Crop Science*. 49 (1), 299-312.

Haseloff, J., Siemering, K.R., Prasher, D.C. and Hodge, S., (1997). Removal of a cryptic intron and subcellular localization of green fluorescent protein are required to mark transgenic Arabidopsis plants brightly. *Proceedings of the National Academy of Sciences of the United States of America*. 94 (6), 2122-2127.

Haseloff, J., Siemering, K.R., Prasher, D.C. and Hodge, S., (1997). Removal of a cryptic intron and subcellular localization of green fluorescent protein are required to mark transgenic Arabidopsis plants brightly. *Proceedings of the National Academy of Sciences of the United States of America*. 94 (6), 2122-2127.

Heyman, J., Kumpf, R.P. and De Veylder, L., (2014). A quiescent path to plant longevity. *Trends in Cell Biology*. 24 (8), 443-448.

Hirayama, T., Kieber, J.J., Hirayama, N., Kogan, M., Guzman, P., Nourizadeh, S., Alonso, J.M., Dailey, W.P., Dancis, A. and Ecker, J.R., (1999). RESPONSIVE-TO-ANTAGONIST1, a Menkes/Wilson Disease-Related Copper Transporter, is required for ethylene signaling in Arabidopsis. *Cell*. 97 (3), 383-393.

Hu, X., Neill, S.J., Tang, Z. and Cai, W., (2005). Nitric oxide mediates gravitropic bending in soybean roots. *Plant Physiology*. 137 (2), 663-670.

Jasid, S., Simontacchi, M., Bartoli, C.G. and Puntarulo, S., (2006). Chloroplasts as a nitric oxide cellular source. Effect of reactive nitrogen species on chloroplastic lipids and proteins. *Plant Physiology*. 142 (3), 1246-1255.

Jeandroz, S., Wipf, D., Stuehr, D.J., Lamattina, L., Melkonian, M., Tian, Z., Zhu, Y., Carpenter, E.J., Wong, G.K. and Wendehenne, D., (2016). Occurrence, structure, and evolution of nitric oxide synthase-like proteins in the plant kingdom. *ScienceSignaling*. 9 (417), 1-10.

Jefferson, R.A., Kavanagh, T.A. and Bevan, M.W., (1987). GUS fusions: beta-glucuronidase as a sensitive and versatile gene fusion marker in higher plants. *The EMBO Journal*. 6 (13), 3901-3907.

Kaufman, P.B., Wu, L., Brock, T.G. and Kim, D., (1995). Hormones and the orientation of growth. *Plant Hormones*. Springer, 547-571.

Kende, H., (2001). Hormone response mutants. A plethora of surprises. *Plant Physiology*. 125 (1), 81-84.

Klepper, L., (1979). Nitric oxide (NO) and nitrogen dioxide (NO 2) emissions from herbicide-treated soybean plants. *Atmospheric Environment*. 13 (4), 537-542.

Kojima, H., Sakurai, K., Kikuchi, K., KAWAHARA, S., KIRINO, Y., NAGOSHI, H., HIRATA, Y. and NAGANO, T., (1998). Development of a fluorescent indicator for nitric oxide based on the fluorescein chromophore. *Chemical and Pharmaceutical Bulletin*. 46 (2), 373-375.

Kolbert, Z., Bartha, B. and Erdei, L., (2008). Exogenous auxin-induced NO synthesis is nitrate reductase-associated in *Arabidopsis thaliana* root primordia. *Journal of Plant Physiology*. 165 (9), 967-975.

Konishi, M. and Yanagisawa, S., (2011). The regulatory region controlling the nitrate-responsive expression of a nitrate reductase gene, NIA1, in Arabidopsis. *Plant & Cell Physiology*. 52 (5), 824-836.

Kumar, D. and Klessig, D.F., (2000). Differential induction of tobacco MAP kinases by the defense signals nitric oxide, salicylic acid, ethylene, and jasmonic acid. *Molecular Plant-Microbe Interactions*. 13 (3), 347-351.

Lamotte, O., Courtois, C., Barnavon, L., Pugin, A. and Wendehenne, D., (2005). Nitric oxide in plants: the biosynthesis and cell signalling properties of a fascinating molecule. *Planta*. 221 (1), 1-4.

Le, J., Vandenbussche, F., Van Der Straeten, D. and Verbelen, J.P., (2001). In the early response of Arabidopsis roots to ethylene, cell elongation is up- and down-regulated and uncoupled from differentiation. *Plant Physiology*. 125 (2), 519-522.

Lee, J.S., Chang, W and Evans, M.L., (1990). Effects of ethylene on the kinetics of curvature and auxin redistribution in gravistimulated roots of Zea mays. *Plant Physiology*. 94, 1770-1775.

Lehman, A., Black, R. and Ecker, J.R., (1996). HOOKLESS1, an ethylene response gene, is required for differential cell elongation in the Arabidopsis hypocotyl. *Cell*. 85 (2), 183-194.

Leshem, Y. and Wills, R., (1998). Harnessing senescence delaying gases nitric oxide and nitrous oxide: a novel approach to postharvest control of fresh horticultural produce. *Biologia Plantarum*. 41 (1), 1-10.

Leyser, H., Pickett, F.B., Dharmasiri, S. and Estelle, M., (1996). Mutations in the AXR3 gene of Arabidopsis result in altered auxin response including ectopic expression from the SAUR-AC1 promoter. *The Plant Journal*. 10 (3), 403-413.

Li, H., Johnson, P., Stepanova, A., Alonso, J.M. and Ecker, J.R., (2004). Convergence of signaling pathways in the control of differential cell growth in Arabidopsis. *Developmental Cell*. 7 (2), 193-204.

Li, H. and Guo, H., (2007). Molecular basis of the ethylene signaling and response pathway in Arabidopsis. *Journal of Plant Growth Regulation*. 26 (2), 106-117.

Lin, Y., Hwang, C.F., Brown, J.B. and Cheng, C.L., (1994). 5' proximal regions of Arabidopsis nitrate reductase genes direct nitrate-induced transcription in transgenic tobacco. *Plant Physiology*. 106 (2), 477-484.

Lombardo, M.C., Graziano, M., Polacco, J.C. and Lamattina, L., (2006). Nitric oxide functions as a positive regulator of root hair development. *Plant Signaling & Behavior*. 1 (1), 28-33.

Luschnig, C., Gaxiola, R.A., Grisafi, P. and Fink, G.R., (1998). EIR1, a root-specific protein involved in auxin transport, is required for gravitropism in *Arabidopsis thaliana*. *Genes & Development*. 12 (14), 2175-2187.

Marchant, A., Kargul, J., May, S.T., Muller, P., Delbarre, A., Perrot-Rechenmann, C. and Bennett, M.J., (1999). AUX1 regulates root gravitropism in Arabidopsis by facilitating auxin uptake within root apical tissues. *The EMBO Journal*. 18 (8), 2066-2073.

Masson, P.H., Tasaka, M., Morita, M.T., Guan, C., Chen, R. and Boonsirichai, K., (2002). *Arabidopsis thaliana*: a model for the study of root and shoot gravitropism. *The Arabidopsis Book*. 2-23.

Mayer, B. and Hemmens, B., (1997). Biosynthesis and action of nitric oxide in mammalian cells. *Trends in Biochemical Sciences*. 22 (12), 477-481.

Merchante, C., Alonso, J.M. and Stepanova, A.N., (2013). Ethylene signaling: simple ligand, complex regulation. *Current Opinion in Plant Biology*. 16 (5), 554-560.

Misra, A., Misra, M. and Singh, R., (2010). Nitric oxide biochemistry, mode of action and signaling in plants. *Journal of Medicinal Plants Research*. 4 (25), 2729-2739.

Moreau, M., Lindermayr, C., Durner, J. and Klessig, D.F., (2010). NO synthesis and signaling in plants-where do we stand? *Physiologia Plantarum*. 138 (4), 372-383.

Moreau, M., Lee, G.I., Wang, Y., Crane, B.R. and Klessig, D.F., (2008). AtNOS/AtNOA1 is a functional *Arabidopsis thaliana* cGTPase and not a nitric-oxide synthase. *The Journal of Biological Chemistry*. 283 (47), 32957-32967.

Morris, P.C., 2001. MAP kinase signal transduction pathways in plants. *New Phytologist*. 151(1), 67-89.

Moulia, B. and Fournier, M., (2009). The power and control of gravitropic movements in plants: a biomechanical and systems biology view. *Journal of Experimental Botany*. 60 (2), 461-486.

Muday, G.K. and Rahman, A., (2008). Auxin transport and the integration of gravitropic growth. *Plant Tropisms.* 47-78.

Mur, L.A.J., Mandon, J., Persijn, S., Cristescu, S.M., Moshkov, I.E., Novikova, G.V., Hall, M.A., Harren, F.J.M., Hebelstrup, K.H. and Gupta, K.J., (2013). Nitric oxide in plants: an assessment of the current state of knowledge. *AoB Plants*. 5, 1-17.

Nagpal, P., Walker, L.M., Young, J.C., Sonawala, A., Timpte, C., Estelle, M. and Reed, J.W., (2000). AXR2 encodes a member of the Aux/IAA protein family. *Plant Physiology*. 123 (2), 563-574.

Neill, S.J., Desikan, R. and Hancock, J.T., (2003). Nitric oxide signalling in plants. *New Phytologist*. 159 (1), 11-35.

Neill, S., Bright, J., Desikan, R., Hancock, J., Harrison, J. and Wilson, I., (2008). Nitric oxide evolution and perception. *Journal of Experimental Botany*. 59 (1), 25-35.

Paciorek, T. and Friml, J., (2006). Auxin signaling. *Journal of Cell Science*. 119 (7), 1199-1202.

Pagnussat, G.C., Lanteri, M.L. and Lamattina, L., (2003). Nitric oxide and cyclic GMP are messengers in the indole acetic acid-induced adventitious rooting process. *Plant Physiology*. 132 (3), 1241-1248.

Pagnussat, G.C., Lanteri, M.L., Lombardo, M.C. and Lamattina, L., (2004). Nitric oxide mediates the indole acetic acid induction activation of a mitogen-activated protein kinase cascade involved in adventitious root development. *Plant Physiology*. 135 (1), 279-286.

Pagnussat, G.C., Simontacchi, M., Puntarulo, S. and Lamattina, L., (2002). Nitric oxide is required for root organogenesis. *Plant Physiology*. 129 (3), 954-956.

Peer, W.A., 2013. From perception to attenuation: auxin signalling and responses. *Current opinion in plant biology*, 16(5), 561-568.

Pickett, F.B., Wilson, A.K. and Estelle, M., (1990). The aux1 Mutation of Arabidopsis Confers Both Auxin and Ethylene Resistance. *Plant Physiology*. 94 (3), 1462-1466.

Pinheiro, J., Bates, D., DebRoy, S. and Sarkar, D., (2014). R Core Team (2014) nlme: linear and nonlinear mixed effects models. R package version 3.1-117. *See Http://CRAN.R-Project.org/package= Nlme*.

Pitts, R.J., Cernac, A. and Estelle, M., (1998). Auxin and ethylene promote root hair elongation inArabidopsis. *The Plant Journal*. 16 (5), 553-560.

Planchet, E. and Kaiser, W.M., (2006). Nitric oxide (NO) detection by DAF fluorescence and chemiluminescence: a comparison using abiotic and biotic NO sources. *Journal of Experimental Botany*. 57 (12), 3043-3055.

Qiao, W. and Fan, L.M., 2008. Nitric oxide signaling in plant responses to abiotic stresses. *Journal of Integrative Plant Biology*, 50 (10), 1238-1246.

Rahman, A., Amakawa, T., Goto, N. and Tsurumi, S., (2001). Auxin is a positive regulator for ethylene-mediated response in the growth of Arabidopsis roots. *Plant & Cell Physiology*. 42 (3), 301-307.

Ravanel, S., Gakiere, B., Job, D. and Douce, R., (1998). The specific features of methionine biosynthesis and metabolism in plants. *Proceedings of the National Academy of Sciences of the United States of America*. 95 (13), 7805-7812.

Rockel, P., Strube, F., Rockel, A., Wildt, J. and Kaiser, W.M., (2002). Regulation of nitric oxide (NO) production by plant nitrate reductase in vivo and in vitro. *Journal of Experimental Botany*. 53 (366), 103-110.

Rouse, D., Mackay, P., Stirnberg, P., Estelle, M. and Leyser, O., (1998). Changes in auxin response from mutations in an AUX/IAA gene. *Science (New York, N.Y.)*. 279 (5355), 1371-1373.

Rumer, S., Gupta, K.J. and Kaiser, W.M., (2009). Plant cells oxidize hydroxylamines to NO. *Journal of Experimental Botany*. 60 (7), 2065-2072.

Stasch, J.P. and Evgenov, O.V., 2013. Soluble guanylate cyclase stimulators in pulmonary hypertension. *Pharmacotherapy of Pulmonary Hypertension*. 279-313

Saito, S., Yamamoto-Katou, A., Yoshioka, H., Doke, N. and Kawakita, K., (2006). Peroxynitrite generation and tyrosine nitration in defense responses in tobacco BY-2 cells. *Plant & Cell Physiology*. 47 (6), 689-697.

Sambrook, J., Fritsch, E.F. and Maniatis, T., (1989). *Molecular Cloning*. *Cold Spring Harbor Laboratory press.* New York.

Saucer, T.W. and Sih, V., (2013). Optimizing nanophotonic cavity designs with the gravitational search algorithm. *Optics Express*. 21 (18), 20831-20836.

Sauer, M., Robert, S. and Kleine-Vehn, J., (2013). Auxin: simply complicated. *Journal of Experimental Botany*. 64 (9), 2565-2577.

Schlicht, M., Ludwig-Müller, J., Burbach, C., Volkmann, D. and Baluska, F., (2013). Indole-3-butyric acid induces lateral root formation via peroxisome-derived indole-3-acetic acid and nitric oxide. *New Phytologist*. 200 (2), 473-482.

Shakeel, S.N., Wang, X., Binder, B.M. and Schaller, G.E., (2013). Mechanisms of signal transduction by ethylene: overlapping and non-overlapping signalling roles in a receptor family. *AoB Plants*. 5, (1-16).

Siemering, K.R., Golbik, R., Sever, R. and Haseloff, J., (1996). Mutations that suppress the thermosensitivity of green fluorescent protein. *Current Biology*. 6 (12), 1653-1663.

Simontacchi, M., García-Mata, C., Bartoli, C.G., Santa-María, G.E. and Lamattina, L., (2013). Nitric oxide as a key component in hormone-regulated processes. *Plant Cell Reports*. 32 (6), 853-866.

Singh, S., Singh, Z. and Swinny, E., (2009). Postharvest nitric oxide fumigation delays fruit ripening and alleviates chilling injury during cold storage of Japanese plums (*Prunus salicina* Lindell). *Postharvest Biology and Technology*. 53 (3), 101-108.

Soegiarto, L. and Wills, R., (2004). Short term fumigation with nitric oxide gas in air to extend the postharvest life of broccoli, green bean, and bok choy. *HortTechnology*. 14 (4), 538-540.

Solano, R. and Ecker, J.R., (1998). Ethylene gas: perception, signaling and response. *Current Opinion in Plant Biology*. 1 (5), 393-398.

Stahl, Y. and Simon, R., (2005). Plant stem cell niches. *The International Journal of Developmental Biology*. 49 (5-6), 479-489.

Stepanova, A.N., Hoyt, J.M., Hamilton, A.A. and Alonso, J.M., (2005). A Link between ethylene and auxin uncovered by the characterization of two root-specific ethylene-insensitive mutants in Arabidopsis. *The Plant Cell*. 17 (8), 2230-2242.

Stohr, C. and Stremlau, S., (2006). Formation and possible roles of nitric oxide in plant roots. *Journal of Experimental Botany*. 57 (3), 463-470.

Suttle, J.C., (1988). Effect of Ethylene Treatment on Polar IAA Transport, Net IAA Uptake and Specific Binding of N-1-Naphthylphthalamic Acid in Tissues and Microsomes Isolated from Etiolated Pea Epicotyls. *Plant Physiology*. 88 (3), 795-799.

Tanaka, H., Dhonukshe, P., Brewer, P. and Friml, J., (2006). Spatiotemporal asymmetric auxin distribution: a means to coordinate plant development. *Cellular and Molecular Life Sciences CMLS*. 63 (23), 2738-2754.

Team, R.C., (2014). *R: A Language and Environment for Statistical Computing.R Foundation for Statistical Computing, Vienna, Austria.2013*.

Tian, L., Levee, V., Mentag, R., Charest, P.J. and Seguin, A., (1999). Green fluorescent protein as a tool for monitoring transgene expression in forest tree species. *Tree Physiology*. 19 (8), 541-546.

Timpte, C., Wilson, A.K. and Estelle, M., (1994). The axr2-1 mutation of *Arabidopsis thaliana* is a gain-of-function mutation that disrupts an early step in auxin response. *Genetics*. 138 (4), 1239-1249.

Tromas, A. and Perrot-Rechenmann, C., (2010). Recent progress in auxin biology. *Comptes Rendus Biologies*. 333 (4), 297-306.

Tun, N.N., Santa-Catarina, C., Begum, T., Silveira, V., Handro, W., Floh, E.I. and Scherer, G.F., (2006). Polyamines induce rapid biosynthesis of nitric oxide (NO) in *Arabidopsis thaliana* seedlings. *Plant & Cell Physiology*. 47 (3), 346-354.

Valasek, M.A. and Repa, J.J., (2005). The power of real-time PCR. *Advances in Physiology Education*. 29 (3), 151-159.

Valderrama, R., Corpas, F.J., Carreras, A., Fernández-Ocaña, A., Chaki, M., Luque, F., Gómez-Rodríguez, M.V., Colmenero-Varea, P., del Río, L.A. and Barroso, J.B., (2007). Nitrosative stress in plants. *FEBS Letters*. 581 (3), 453-461.

Vandenbussche, F., Vriezen, W.H., Smalle, J., Laarhoven, L.J., Harren, F.J. and Van Der Straeten, D., (2003). Ethylene and auxin control the Arabidopsis response to decreased light intensity. *Plant Physiology*. 133 (2), 517-527.

Vanneste, S. and Friml, J., (2012). Plant signaling: Deconstructing auxin sensing. *Nature Chemical Biology*. 8 (5), 415-416.

Verbelen, J., Cnodder, T.D., Le, J., Vissenberg, K. and Baluška, F., (2006). The root apex of *Arabidopsis thaliana* consists of four distinct zones of growth activities: meristematic zone, transition zone, fast elongation zone and growth terminating zone. *Plant Signaling & Behavior*. 1 (6), 296-304.

Villalobos, Luz Irina A Calderón, Lee, S., De Oliveira, C., Ivetac, A., Brandt, W., Armitage, L., Sheard, L.B., Tan, X., Parry, G. and Mao, H., (2012). A combinatorial TIR1/AFB–Aux/IAA co-receptor system for differential sensing of auxin. *Nature Chemical Biology*. 8 (5), 477-485.

Wang, K.L., Li, H. and Ecker, J.R., (2002). Ethylene biosynthesis and signaling networks. *The Plant Cell*. 14, 131-51.

Wang, P., Du, Y., Li, Y., Ren, D. and Song, C.P., (2010). Hydrogen peroxide-mediated activation of MAP kinase 6 modulates nitric oxide biosynthesis and signal transduction in Arabidopsis. *The Plant Cell*. 22 (9), 2981-2998.

Ward, W.W. and Bokman, S.H., (1982). Reversible denaturation of *Aequorea* green-fluorescent protein: physical separation and characterization of the renatured protein. *Biochemistry*. 21 (19), 4535-4540.

Weigel, D. and Glazebrook, J., 2006. Transformation of agrobacterium using the freeze-thaw method. *CSH protocols*. 7, 1031-1036.

Wilkinson, J.Q. and Crawford, N.M., (1993). Identification and characterization of a chlorate-resistant mutant of *Arabidopsis thaliana* with mutations in both nitrate reductase structural genes NIA1 and NIA2. *Molecular and General Genetics MGG*. 239 (1-2), 289-297.

Wilson, A.K., Pickett, F.B., Turner, J.C. and Estelle, M., (1990). A dominant mutation in *Arabidopsis* confers resistance to auxin, ethylene and abscisic acid. *Molecular and General Genetics MGG*. 222 (2-3), 377-383.

Wilson, I.D., Neill, S.J. and Hancock, J.T., (2008). Nitric oxide synthesis and signalling in plants. *Plant, Cell & Environment*. 31 (5), 622-631.

Woods, S., Roberts, J. and Taylor, I., (1984). Ethylene-induced root coiling in tomato seedlings. *Plant Growth Regulation*. 2 (3), 217-225.

Woodward, A.W. and Bartel, B., (2005). Auxin: regulation, action, and interaction. *Annals of Botany*. 95 (5), 707-735.

Xiao, Y., Redman, J.C., Monaghan, E.L., Zhuang, J., Underwood, B.A., Moskal, W.A., Wang, W., Wu, H.C. and Town, C.D., (2010). High throughput generation of promoter reporter (GFP) transgenic lines of low expressing genes in Arabidopsis and analysis of their expression patterns. *Plant Methods*. 6 (1), 1.

Yamasaki, H. and Sakihama, Y., (2000). Simultaneous production of nitric oxide and peroxynitrite by plant nitrate reductase: in vitro evidence for the NR-dependent formation of active nitrogen species. *FEBS Letters*. 468 (1), 89-92.

Yu, X., Sukumaran, S. and Marton, L., (1998). Differential expression of the arabidopsis nia1 and nia2 genes cytokinin-induced nitrate reductase activity is correlated with increased nia1 transcription and mrna levels. *Plant Physiology*. 116 (3), 1091-1096.

Zaharah, S. and Singh, Z., (2011). Mode of action of nitric oxide in inhibiting ethylene biosynthesis and fruit softening during ripening and cool storage of ‘Kensington Pride’mango. *Postharvest Biology and Technology*. 62 (3), 258-266.

Zemojtel, T., Kolanczyk, M., Kossler, N., Stricker, S., Lurz, R., Mikula, I., Duchniewicz, M., Schuelke, M., Ghafourifar, P. and Martasek, P., (2006). Mammalian mitochondrial nitric oxide synthase: characterization of a novel candidate. *FEBS Letters*. 580 (2), 455-462.

Zhou, R., Benavente, L.M., Stepanova, A.N. and Alonso, J.M., (2011). A recombineering-based gene tagging system for Arabidopsis. *The Plant Journal*. 66 (4), 712-723.

Zhu, S., Liu, M. and Zhou, J., (2006). Inhibition by nitric oxide of ethylene biosynthesis and lipoxygenase activity in peach fruit during storage. *Postharvest Biology and Technology*. 42 (1), 41-48.

Zhu, S. and Zhou, J., (2007). Effect of nitric oxide on ethylene production in strawberry fruit during storage. *Food Chemistry*. 100 (4), 1517-1522.

Chapter 7 Appendix

1. Two-way ANOVA result for Col-0 vs *nia1* vs *nia2*

Tests of Normality

plant		Shapiro-Wilk		
		Statistic	df	Sig.
2hr	col 0	.813	4	.129
4hr	col 0	.998	4	.993
	nia1	.831	4	.170
	nia2	.966	4	.814
6hr	col 0	.998	4	.993
	nia1	.863	4	.270
	nia2	.901	4	.434
8hr	col 0	.783	4	.075
	nia1	.832	4	.173
	nia2	.821	4	.147
10hr	col 0	.950	4	.716
	nia1	.914	4	.505
	nia2	.790	4	.085
24hr	col 0	.820	4	.143
	nia1	.911	4	.489
	nia2	.878	4	.332

b. 2hr is constant when plant = nia1. It has been omitted.

c. 2hr is constant when plant = nia2. It has been omitted.

Descriptive Statistics

Dependent Variable: curvature

time interval	sample type	Mean	Std. Deviation	N
2hr	Col-0	37.0100	1.91896	4
	nia1	.0000	.00000	4
	nia2	.0000	.00000	4
	Total	12.3367	18.25000	12
4hr	Col-0	40.3375	1.38615	4
	nia1	20.0175	2.10410	4
	nia2	22.2325	3.38051	4
	Total	27.5292	9.75827	12
6hr	Col-0	46.1325	3.05382	4

	nia1	26.9650	2.76947	4
	nia2	30.0975	5.29149	4
	Total	34.3983	9.44244	12
8hr	Col-0	53.5175	1.66820	4
	nia1	37.1900	2.01779	4
	nia2	44.5825	6.49745	4
	Total	45.0967	7.87386	12
10hr	Col-0	55.9150	1.30926	4
	nia1	46.7200	3.98520	4
	nia2	55.1625	3.17998	4
	Total	52.5992	5.14909	12
24hr	Col-0	85.5000	5.80230	4
	nia1	60.3850	1.64371	4
	nia2	75.6250	7.01635	4
	Total	73.8367	11.82258	12
Total	Col-0	53.0688	16.51344	24
	nia1	31.8796	19.86140	24
	nia2	37.9500	25.07141	24
	Total	40.9661	22.36615	72

Tests of Between-Subjects Effects

Dependent Variable: curvature

Source	Type III Sum of Squares	df	Mean Square	F	Sig.	Partial Eta Squared
Corrected Model	34830.880[a]	17	2048.875	161.165	.000	.981
Intercept	120832.003	1	120832.003	9504.699	.000	.994
timeinterval	27314.342	5	5462.868	429.712	.000	.975
sampletype	5715.259	2	2857.629	224.782	.000	.893
timeinterval * sampletype	1801.280	10	180.128	14.169	.000	.724
Error	686.495	54	12.713			
Total	156349.378	72				
Corrected Total	35517.375	71				

a. R Squared = .981 (Adjusted R Squared = .975)

Estimates

Dependent Variable: curvature

time interval	sample type	Mean	Std. Error	95% Confidence Interval	
				Lower Bound	Upper Bound
2hr	Col-0	37.010	1.783	33.436	40.584
	nia1	.000	1.783	-3.574	3.574
	nia2	-1.421E-14	1.783	-3.574	3.574
4hr	Col-0	40.337	1.783	36.763	43.912
	nia1	20.017	1.783	16.443	23.592
	nia2	22.232	1.783	18.658	25.807
6hr	Col-0	46.132	1.783	42.558	49.707
	nia1	26.965	1.783	23.391	30.539
	nia2	30.097	1.783	26.523	33.672
8hr	Col-0	53.518	1.783	49.943	57.092
	nia1	37.190	1.783	33.616	40.764
	nia2	44.583	1.783	41.008	48.157
10hr	Col-0	55.915	1.783	52.341	59.489
	nia1	46.720	1.783	43.146	50.294
	nia2	55.163	1.783	51.588	58.737
24hr	Col-0	85.500	1.783	81.926	89.074
	nia1	60.385	1.783	56.811	63.959
	nia2	75.625	1.783	72.051	79.199

Pairwise Comparisons

Dependent Variable: curvature

time interval	(I) sample type	(J) sample type	Mean Difference (I-J)	Std. Error	Sig.[b]	95% Confidence Interval for Difference[b]	
						Lower Bound	Upper Bound
2hr	Col-0	nia1	37.010*	2.521	.000	30.781	43.239
		nia2	37.010*	2.521	.000	30.781	43.239
	nia1	Col-0	-37.010*	2.521	.000	-43.239	-30.781
		nia2	1.776E-14	2.521	1.000	-6.229	6.229
	nia2	Col-0	-37.010*	2.521	.000	-43.239	-30.781
		nia1	-1.776E-14	2.521	1.000	-6.229	6.229
4hr	Col-0	nia1	20.320*	2.521	.000	14.091	26.549
		nia2	18.105*	2.521	.000	11.876	24.334

	nia1	Col-0	-20.320*	2.521	.000	-26.549	-14.091
		nia2	-2.215	2.521	1.000	-8.444	4.014
	nia2	Col-0	-18.105*	2.521	.000	-24.334	-11.876
		nia1	2.215	2.521	1.000	-4.014	8.444
6hr	Col-0	nia1	19.167*	2.521	.000	12.938	25.397
		nia2	16.035*	2.521	.000	9.806	22.264
	nia1	Col-0	-19.167*	2.521	.000	-25.397	-12.938
		nia2	-3.132	2.521	.658	-9.362	3.097
	nia2	Col-0	-16.035*	2.521	.000	-22.264	-9.806
		nia1	3.132	2.521	.658	-3.097	9.362
8hr	Col-0	nia1	16.328*	2.521	.000	10.098	22.557
		nia2	8.935*	2.521	.002	2.706	15.164
	nia1	Col-0	-16.328*	2.521	.000	-22.557	-10.098
		nia2	-7.393*	2.521	.015	-13.622	-1.163
	nia2	Col-0	-8.935*	2.521	.002	-15.164	-2.706
		nia1	7.393*	2.521	.015	1.163	13.622
10hr	Col-0	nia1	9.195*	2.521	.002	2.966	15.424
		nia2	.752	2.521	1.000	-5.477	6.982
	nia1	Col-0	-9.195*	2.521	.002	-15.424	-2.966
		nia2	-8.443*	2.521	.004	-14.672	-2.213
	nia2	Col-0	-.752	2.521	1.000	-6.982	5.477
		nia1	8.443*	2.521	.004	2.213	14.672
24hr	Col-0	nia1	25.115*	2.521	.000	18.886	31.344
		nia2	9.875*	2.521	.001	3.646	16.104
	nia1	Col-0	-25.115*	2.521	.000	-31.344	-18.886
		nia2	-15.240*	2.521	.000	-21.469	-9.011
	nia2	Col-0	-9.875*	2.521	.001	-16.104	-3.646
		nia1	15.240*	2.521	.000	9.011	21.469

Based on estimated marginal means

*. The mean difference is significant at the .05 level.

b. Adjustment for multiple comparisons: Bonferroni.

curvature

Tukey HSD[a,b]

sample type	N	Subset 1	Subset 2	Subset 3
nia1	24	31.8796		
nia2	24		37.9500	
Col-0	24			53.0688
Sig.		1.000	1.000	1.000

Means for groups in homogeneous subsets are displayed.

Based on observed means.

The error term is Mean Square(Error) = 12.713.

a. Uses Harmonic Mean Sample Size = 24.000.

b. Alpha = .05.

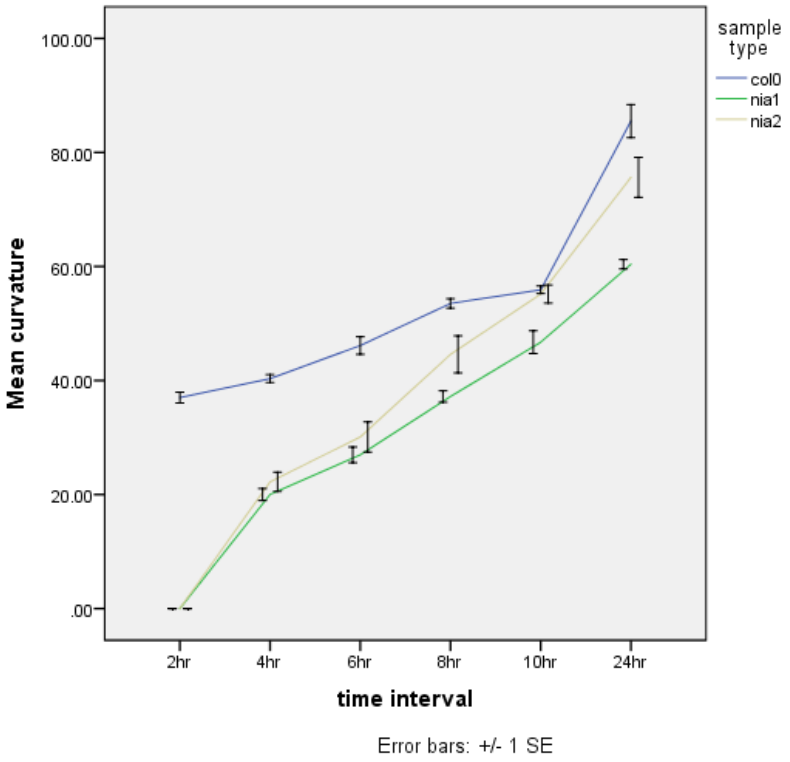

2. Linear mixed-effects model fit by REML for Col-0 vs *nia1*

"Best" fitted model:

Random effects:

Formula: ~-1 + time + I(time^2) | Sample

Structure: Diagonal

	time	I(time^2)	Residual
StdDev:	0.2561972	0.09533836	2.481843

Fixed effects: Curvature ~ time * plant + I(time^2)

	Value	Std.Error	DF	t-value	p-value
(Intercept)	30.09153	1.5488639	37	19.428131	0.000
time	2.95351	0.3506545	37	8.422839	0.000
plantNia1	-42.52309	2.1664747	6	-19.627780	0.000
I(time^2)	-0.11537	0.0347335	37	-3.321505	0.002
time:plantNia1	4.97068	0.4897197	37	10.150049	0.000

Approximate 95% confidence intervals

Fixed effects:

	Lower	Est.	upper
(Intercept)	26.9532331	30.0915294	33.22982570
time	2.2430131	2.9535067	3.66400028
plantNia1	-47.8242599	-42.5230874	-37.22191488
I(time^2)	-0.1857444	-0.1153676	-0.04499077
time:plantNia1	3.9784122	4.9706785	5.96294478

Within-group standard error:

lower	est.	upper
1.920000	2.481843	3.208096

LRT of fixed effects:

	numDF	denDF	F-value	p-value
(Intercept)	1	37	2708.7482	<.0001
time	1	37	460.6789	<.0001
plant	1	6	441.8329	<.0001
I(time^2)	1	37	11.0324	0.002
time:plant	1	37	103.0235	<.0001

Significance of need of quadratic random effect:

	Model	df	AIC	BIC	logLik	Test	L.Ratio	p-value
mod update(mod, random = pdDiag(~-1 + time))	1	8	292.6681	306.7577	-138.334	1 vs 2	18.74186	<.0001
	2	7	309.4100	321.7384	-147.7050			

Approaching significance in differences of plant within variability:

	Model	df	AIC	BIC	logLik	Test	L.Ratio	p-value
mod update(mod,weights=varIdent (form =~1| plant))	1	8	292.6681	306.7577	-138.3341	1 vs 2	3.176238	0.0747
	2	9	291.4919	307.3427	-136.7459			

No signs of AR(1) correlation in residuals:

	Model	df	AIC	BIC	logLik	Test	L.Ratio	p-value
Mod update(mod, correlation = corAR1())	1	8	292.6681	306.7577	-138.3341	1 vs 2	0.5374411	0.4635
	2	9	294.1307	309.9815	-138.0653			

3. Linear mixed-effects model fit by REML for Col-0 vs *nia2*

"Best" fitted model:
Random effects:
Formula: ~time | Sample
Structure: Diagonal

	(Intercept)	time	Residual
StdDev:	0.8021707	0.1731107	4.840363

Variance function:
Structure: Different standard deviations per stratum
Formula: ~1 | plant
Parameter estimates:

nia2	Col-0
1.000000	0.401897

Fixed effects: Curvature ~ (time + I(time^2)) * plant

	Value	Std.Error	DF	t-value	p-value
(Intercept)	30.70740	1.291049	36	23.784843	0.0000
time	2.80470	0.273542	36	10.253281	0.0000
plantNia1	-0.02172	0.009290	36	-2.337427	0.0251
I(time^2)	-46.81511	3.339334	6	-14.019297	0.0000
time:plantnia2	6.68189	0.706531	36	9.457332	0.0000
I(time^2):plantnia2	-0.21438	0.024913	36	-8.604901	0.0000

Approximate 95% confidence intervals
Fixed effects:

	Lower	Est.	upper
(Intercept)	28.08903332	30.70740247	33.325771619
time	2.24993016	2.80469807	3.359465982
I(time^2)	-0.04055736	-0.02171559	-0.002873822
plantnia2	-54.98616506	-46.81510996	-38.644054870
time:plantnia2	5.24898347	6.68189386	8.114804244
I(time^2):plantnia2	-0.26490366	-0.21437702	-0.163850378

attr(,"label")
[1] "Fixed effects:"

Random Effects:
Level: Sample

	Lower	Est.	upper
sd((Intercept))	0.06793005	0.8021707	9.472652
sd(time)	0.07735155	0.1731107	0.387417

Variance function:

	lower	est.	upper
Col-0	0.2505205	0.401897	0.6447426

attr(,"label")
[1] "Variance function:"
Within-group standard error:

lower	est.	upper
3.512413	4.840363	6.670375

LRT of fixed effects:

	numDF	denDF	F-value	p-value
(Intercept)	1	36	3607.726	<.0001
time	1	36	682.086	<.0001
I(time^2)	1	36	35.730	<.0001
plant	1	6	151.410	<.0001
time:plant	1	36	18.721	1e-04
I(time^2):plant	1	36	74.044	<.0001

plant within variability:

> anova(mod,update(mod,weights=NULL))

	Model	df	AIC	BIC	logLik	Test	L.Ratio	p-value
mod	1	10	284.9281	302.3048	-132.4640	1 vs 2	12.81665	3e-04
update(mod, weights = NULL)	2	9	295.7447	311.3838	-138.8724			

No signs of AR(1) correlation in residuals:

	Model	df	AIC	BIC	logLik	Test	L.Ratio	p-value
mod	1	10	284.9281	302.3048	-132.4640	1 vs 2	0.1370398	0.7112
update(mod, correlation = corAR1())	2	11	286.7910	305.9054	-132.3955			

4. Linear mixed-effects model fit by REML for *nia1* vs *nia2*

"Best" fitted model:
Random effects:
Formula: ~1 | Sample

	(Intercept)	Residual
StdDev:	0.9309631	2.879836

Variance function:
Structure: Different standard deviations per stratum
Formula: ~1 | plant
Parameter estimates:

nia1	nia2
1.000000	1.708996

Fixed effects: Curvature ~ time:plant + I(time^2)

	Value	Std.Error	DF	t-value	p-value
(Intercept)	-13.828048	1.6093505	37	-8.592316	0
I(time^2)	-0.215925	0.0118705	37	-18.190001	0
time:plantnia1	8.261477	0.3327250	37	24.829747	0
time:plantnia2	8.936094	0.3414345	37	26.172207	0

Approximate 95% confidence intervals
Approximate 95% confidence intervals

Fixed effects:

	Lower	Est.	upper
(Intercept)	-17.0889018	-13.8280479	-10.5671941
I(time^2)	-0.2399767	-0.2159248	-0.1918728
time:plantnia1	7.5873125	8.2614774	8.9356422
time:plantnia2	8.2442820	8.9360940	9.6279060

attr(,"label")
[1] "Fixed effects:"

Random Effects:
Level: Sample

	Lower	Est.	upper
sd((Intercept))	0.1109245	0.9309631	7.813352

Variance function

	Lower	Est.	upper
nia2	1.085958	1.708996	2.689486

attr(,"label")
[1] "Variance function:"
Within-group standard error:

lower	est.	upper
2.047539	2.879836	4.050452

significance in differences of plant within variability:

	Model	df	AIC	BIC	logLik	Test	L.Ratio	p-value
mod	1	7	288.4040	300.8934	-137.2020	1 vs 2	0.01553615	0.9008
update(mod, weights = NULL)	2	6	291.6529	302.3580	-139.8265			

No signs of AR(1) correlation in residuals:

	Model	df	AIC	BIC	logLik	Test	L.Ratio	p-value
mod	1	7	288.4040	300.8934	-137.2020	1 vs 2	0.01553615	0.9008
update(mod, correlation = corAR1())	2	8	290.3885	304.6620	-137.1943			

5. Two-way ANOVA result for Col-0, *ein3-1* and *ein30x*

Tests of Normality

plant		Shapiro-Wilk		
		Statistic	df	Sig.
2hr	Col-0	.813	4	.129
4hr	Col-0	.998	4	.993
	ein3-1	.887	3	.347
6hr	Col-0	.998	4	.993
	ein3-1	.898	3	.379
8hr	Col-0	.783	4	.075
	ein3-1	1.000	3	.992
	ein3ox	.999	3	.937
10hr	Col-0	.950	4	.716
	ein3-1	.860	3	.267
	ein3ox	.861	3	.270
24hr	Col-0	.820	4	.143
	ein3-1	.987	3	.780
	ein3ox	.997	3	.895

a. Lilliefors Significance Correction

b. 2hr is constant when plant = ein3-1. It has been omitted.

c. 2hr is constant when plant = ein3ox. It has been omitted.

d. 4hr is constant when plant = ein3ox. It has been omitted.

e. 6hr is constant when plant = ein3ox. It has been omitted.

Descriptive Statistics

Dependent Variable: curvature

time interval	sample type	Mean	Std. Deviation	N
2hr	Col-0	37.0100	1.91896	4
	ein3-1	.0000	.00000	3
	ein30x	.0000	.00000	3
	Total	14.8040	19.14397	10
4hr	Col-0	40.3375	1.38615	4
	ein3-1	17.6333	5.56762	3
	ein30x	.0000	.00000	3
	Total	21.4250	18.00837	10
6hr	Col-0	46.1325	3.05382	4
	ein3-1	34.6067	7.10786	3
	ein30x	.0000	.00000	3
	Total	28.8350	20.87035	10
8hr	Col-0	53.5175	1.66820	4
	ein3-1	40.0733	9.13508	3

	ein30x	23.4467	7.66421	3
	Total	40.4630	14.31212	10
10hr	Col-0	55.9150	1.30926	4
	ein3-1	50.6833	3.04645	3
	ein30x	35.0433	5.07644	3
	Total	48.0840	9.72391	10
24hr	Col-0	85.5000	5.80230	4
	ein3-1	79.6667	2.51661	3
	ein30x	54.2133	3.90585	3
	Total	74.3640	14.69211	10
Total	Col-0	53.0688	16.51344	24
	ein3-1	37.1106	26.19127	18
	ein30x	18.7839	21.69184	18
	Total	37.9958	25.39294	60

Tests of Between-Subjects Effects

Dependent Variable: curvature

Source	Type III Sum of Squares	df	Mean Square	F	Sig.	Partial Eta Squared
Corrected Model	37323.304[a]	17	2195.488	128.074	.000	.981
Intercept	77714.036	1	77714.036	4533.446	.000	.991
timeinterval	23889.847	5	4777.969	278.723	.000	.971
sampletype	12110.513	2	6055.257	353.233	.000	.944
timeinterval * sampletype	1944.030	10	194.403	11.340	.000	.730
Error	719.980	42	17.142			
Total	124664.285	60				
Corrected Total	38043.284	59				

a. R Squared = .981 (Adjusted R Squared = .973)

Pairwise Comparisons

Dependent Variable: curvature

(I) sample type	(J) sample type	Mean Difference (I-J)	Std. Error	Sig.[b]	95% Confidence Interval for Difference[b]	
					Lower Bound	Upper Bound
Col-0	ein3-1	15.958*	1.291	.000	12.739	19.177
	ein30x	34.285*	1.291	.000	31.066	37.504
ein3-1	Col-0	-15.958*	1.291	.000	-19.177	-12.739
	ein30x	18.327*	1.380	.000	14.885	21.768
ein30x	Col-0	-34.285*	1.291	.000	-37.504	-31.066
	ein3-1	-18.327*	1.380	.000	-21.768	-14.885

Based on estimated marginal means

*. The mean difference is significant at the .05 level.

b. Adjustment for multiple comparisons: Bonferroni.

Pairwise Comparisons

Dependent Variable: curvature

time interval	(I) sample type	(J) sample type	Mean Difference (I-J)	Std. Error	Sig.[b]	95% Confidence Interval for Difference[b]	
						Lower Bound	Upper Bound
2hr	Col-0	ein3-1	37.010*	3.162	.000	29.124	44.896
		ein30x	37.010*	3.162	.000	29.124	44.896
	ein3-1	Col-0	-37.010*	3.162	.000	-44.896	-29.124
		ein30x	-1.421E-14	3.381	1.000	-8.430	8.430
	ein30x	Col-0	-37.010*	3.162	.000	-44.896	-29.124
		ein3-1	1.421E-14	3.381	1.000	-8.430	8.430
4hr	Col-0	ein3-1	22.704*	3.162	.000	14.819	30.590
		ein30x	40.337*	3.162	.000	32.452	48.223
	ein3-1	Col-0	-22.704*	3.162	.000	-30.590	-14.819
		ein30x	17.633*	3.381	.000	9.203	26.063
	ein30x	Col-0	-40.337*	3.162	.000	-48.223	-32.452
		ein3-1	-17.633*	3.381	.000	-26.063	-9.203
6hr	Col-0	ein3-1	11.526*	3.162	.002	3.640	19.411
		ein30x	46.132*	3.162	.000	38.247	54.018
	ein3-1	Col-0	-11.526*	3.162	.002	-19.411	-3.640
		ein30x	34.607*	3.381	.000	26.177	43.037

	ein30x	Col-0	-46.132*	3.162	.000	-54.018	-38.247
		ein3-1	-34.607*	3.381	.000	-43.037	-26.177
8hr	Col-0	ein3-1	13.444*	3.162	.000	5.559	21.330
		ein30x	30.071*	3.162	.000	22.185	37.956
	ein3-1	Col-0	-13.444*	3.162	.000	-21.330	-5.559
		ein30x	16.627*	3.381	.000	8.197	25.057
	ein30x	Col-0	-30.071*	3.162	.000	-37.956	-22.185
		ein3-1	-16.627*	3.381	.000	-25.057	-8.197
10hr	Col-0	ein3-1	5.232	3.162	.316	-2.654	13.117
		ein30x	20.872*	3.162	.000	12.986	28.757
	ein3-1	Col-0	-5.232	3.162	.316	-13.117	2.654
		ein30x	15.640*	3.381	.000	7.210	24.070
	ein30x	Col-0	-20.872*	3.162	.000	-28.757	-12.986
		ein3-1	-15.640*	3.381	.000	-24.070	-7.210
24hr	Col-0	ein3-1	5.833	3.162	.216	-2.052	13.719
		ein30x	31.287*	3.162	.000	23.401	39.172
	ein3-1	Col-0	-5.833	3.162	.216	-13.719	2.052
		ein30x	25.453*	3.381	.000	17.023	33.883
	ein30x	Col-0	-31.287*	3.162	.000	-39.172	-23.401
		ein3-1	-25.453*	3.381	.000	-33.883	-17.023

Based on estimated marginal means

*. The mean difference is significant at the .05 level.

b. Adjustment for multiple comparisons: Bonferroni.

curvature

Tukey HSDa,b,c

		Subset		
sample type	N	1	2	3
ein30x	18	18.7839		
ein3-1	18		37.1106	
Col-0	24			53.0688
Sig.		1.000	1.000	1.000

Means for groups in homogeneous subsets are displayed.

Based on observed means.

The error term is Mean Square(Error) = 17.142.

a. Uses Harmonic Mean Sample Size = 19.636.

b. The group sizes are unequal. The harmonic mean of the group sizes is used.

Type I error levels are not guaranteed.

c. Alpha = .05.

6. Linear mixed-effects model fit by REML for Col-0 vs *ein3-1*

"Best" fitted model:

Random effects:

Formula: ~1 | Sample

	(Intercept)	Residual
StdDev:	2.366761	2.350185

Variance function:

Structure: Different standard deviations per stratum

Formula: ~1 | plant

Parameter estimates:

Col-0	ein3-1
1.000000	1.982251

Fixed effects: Curvature ~ (time + I(time^2)) * plant

	Value	Std.Error	DF	t-value	p-value
(Intercept)	30.70740	1.896940	31	16.187863	0.0000
time	2.80470	0.313490	31	8.946689	0.0000
I(time^2)	-0.02172	0.011224	31	-1.934767	0.0622
plantein3-1	-45.21066	4.120807	5	-10.971312	0.0000
time:plantein3-1	5.82569	0.783041	31	7.439832	0.0000
I(time^2):plantein3-1	-0.17471	0.028035	31	-6.231967	0.0000

Approximate 95% confidence intervals

Fixed effects:

	Lower	Est.	upper
(Intercept)	26.83856817	30.70740247	34.576236761
time	2.16533091	2.80469807	3.444065235
I(time^2)	-0.04460684	-0.02171559	0.001175658
plantein3-1	-55.80352794	-45.21065657	-34.617785202
time:plantein3-1	4.22867145	5.82569418	7.422716917
I(time^2):plantein3-1	-0.23189264	-0.17471446	-0.117536291

attr(,"label")

[1] "Fixed effects:"

Random Effects:

Level: Sample

	Lower	Est.	upper
sd((Intercept))	0.9826139	2.366761	5.70067

Variance function:

	Lower	Est.	upper
ein3-1	1.189733	1.982251	3.302691

attr(,"label")

[1] "Variance function:"

Within-group standard error:

Lower	Est.	upper
1.699085	2.350185	3.250790

LRT of fixed effects:

plant within variability:

	Model	df	AIC	BIC	logLik	Test	L.Ratio	p-value
mod	1	9	251.0748	265.3264	-116.5374	1 vs 2	7.012493	0.0081
update(mod, weights = NULL)	2	8	256.0873	268.7554	-120.0436			

No signs of AR(1) correlation in residuals:

	Model	df	AIC	BIC	logLik	Test	L.Ratio	p-value
mod	1	9	251.0748	265.3264	-116.5374	1 vs 2	1.411543	0.2348
update(mod, correlation = corAR1())	2	10	251.6632	267.4984	-115.8316			

7. Linear mixed-effects model fit by REML for Col-0 vs EIN*3OX*

"Best" fitted model:

Random effects:
Formula: ~time | Sample
Structure: Diagonal

	(Intercept)	time	Residual
StdDev:	0.8402527	0.1878045	9.030223

Variance function:
Structure: Different standard deviations per stratum
Formula: ~1 | plant
Parameter estimates:

ein30x	Col-0
1.000000	0.2152903

Fixed effects: Curvature ~ plant + time + I(time^2)

	Value	Std.Error	DF	t-value	p-value
(Intercept)	30.25376	1.2794023	33	23.646792	0.0000
plantein30x	-35.03110	2.5412758	5	-13.784848	0.0000
time	2.93541	0.2695281	33	10.890941	0.0000
I(time^2)	-0.02475	0.0091273	33	-2.711991	0.0105

Approximate 95% confidence intervals
Fixed effects:

	Lower	Est.	upper
(Intercept)	27.6507964	30.25375995	32.856723520
plantein30x	-41.5636573	-35.03109978	-28.498542314
time	2.3870558	2.93541487	3.483773938
I(time^2)	-0.0433229	-0.02475322	-0.006183539

attr(,"label")
[1] "Fixed effects:"

Random Effects:
Level: Sample

	Lower	Est.	upper
sd((Intercept))	0.08349386	0.8402527	8.4560061
sd(time)	0.07531395	0.1878045	0.4683132

Variance function:

	Lower	Est.	upper
Col-0	0.1304086	0.2152903	0.3554206

attr(,"label")
[1] "Variance function:"
Within-group standard error:

Lower	Est.	upper
6.354409	9.030223	12.832811

LRT of fixed effects:

	numDF	denDF	F-value	p-value
(Intercept)	1	33	2794.9989	<.0001
plant	1	5	81.3761	0.0003
time	1	33	481.7686	<.0001
I(time^2)	1	33	7.3549	0.0105

plant within variability:

	Model	df	AIC	BIC	logLik	Test	L.Ratio	p-value
mod	1	8	259.0572	272.1578	-121.5286	1 vs 2	27.85039	<.0001
update(mod, weights = NULL)	2	7	284.9076	296.3707	-135.4538			

No signs of AR(1) correlation in residuals:

	Model	df	AIC	BIC	logLik	Test	L.Ratio	p-value
mod	1	8	259.0572	272.1578	-121.5286	1 vs 2	1.798303	0.1799
update(mod, correlation = corAR1())	2	9	259.2588	273.9971	-120.6294			

8. Linear mixed-effects model fit by REML Ein3-1 vs *ein30x*

"Best" fitted model:

Random effects:

Formula: ~1 | Sample

	(Intercept)	Residual
StdDev:	0.0005836563	9.535959

Correlation Structure: AR(1)

Formula: ~1 | Sample

Parameter estimate(s):

Phi

0.4477447

Variance function:

Structure: Different standard deviations per stratum

Formula: ~1 | plant

Parameter estimates:

ein3ox	ein3-1
1.0000000	0.5515923

Fixed effects: Curvature ~ time * plant + I(time^2)

	Value	Std.Error	DF	t-value	p-value
(Intercept)	-13.093605	3.867672	27	-3.385397	0.0022
time	8.162945	0.741553	27	11.007912	0.0000
plantein3ox	-9.671090	5.059821	4	-1.911350	0.1285
I(time^2)	-0.178343	0.024757	27	-7.203874	0.0000
time:plantein3ox	-0.757703	0.351702	27	-2.154390	0.0403

Approximate 95% confidence intervals

Fixed effects:

	Lower	Est.	upper
(Intercept)	-21.0294120	-13.0936054	-5.15779880
time	6.6414048	8.1629448	9.68448487
plantein3ox	-23.7194055	-9.6710903	4.37722496
I(time^2)	-0.2291389	-0.1783428	-0.12754660
time:plantein3ox	-1.4793362	-0.7577033	-0.03607036

attr(,"label")

[1] "Fixed effects:"

Random Effects:

Level: Sample

	Lower	Est.	upper
sd((Intercept))	6.098575e-165	0.0005836563	5.585808e+157

Correlation structure:

	Lower	Est.	upper
Phi	0.06714011	0.4477447	0.7145946

attr(,"label")

[1] "Correlation structure:"

Variance function:

	Lower	Est.	upper
ein3-1	0.3252931	0.5515923	0.935323

attr(,"label")

[1] "Variance function:"

Within-group standard error:

Lower	Est.	upper
6.224305	9.535959	14.609586

LRT of fixed effects:

plant within variability:

	Model	df	AIC	BIC	logLik	Test	L.Ratio	p-value
mod	1	9	250.0087	262.9146	-116.0043	1 vs 2	4.497777	0.0339
update(mod, weights = NULL)	2	8	252.5065	263.9783	-118.2532			

signs of AR(1) correlation in residuals:

	Model	df	AIC	BIC	logLik	Test	L.Ratio	p-value
mod	1	9	250.0087	262.9146	-116.0043	1 vs 2	4.009509	0.0452
update(mod, correlation = NULL)	2	8	252.0182	263.4901	-118.0091			

9. Linear mixed-effects model fit by REML *nia1* vs *ein3-1*

"Best" fitted model:

Random effects:

Formula: ~1 | Sample

	(Intercept)	Residual
StdDev:	2.350118	3.627519

Fixed effects: Curvature ~ time * plant + I(time^2)

	Value	Std.Error	DF	t-value	p-value
(Intercept)	-12.438029	2.2307891	32	-5.575618	0.0000
time	7.925749	0.3719387	32	21.309289	0.0000
plantein3-1	-2.877762	2.5508412	5	-1.128162	0.3105
I(time^2)	-0.203624	0.0130958	32	-15.548823	0.0000
time:plantein3-1	0.900970	0.1573574	32	5.725629	0.0000

Approximate 95% confidence intervals

Fixed effects:

	Lower	Est.	upper
(Intercept)	-16.9819976	-12.4380288	-7.8940600
time	7.1681344	7.9257487	8.6833630
plantein3-1	-9.4349078	-2.8777616	3.6793845
I(time^2)	-0.2302993	-0.2036241	-0.1769488
time:plantein3-1	0.5804438	0.9009704	1.2214971

attr(,"label")

[1] "Fixed effects:"

Random Effects:

Level: Sample

	Lower	Est.	upper
sd((Intercept))	0.9835342	2.350118	5.615521

Within-group standard error:

Lower	Est.	upper
2.839307	3.627519	4.634545

Approaching significance in differences of plant within variability:

	Model	df	AIC	BIC	logLik	Test	L.Ratio	p-value
mod	1	7	251.9185	263.1949	-118.9592	1 vs 2	3.835739	0.0502
update(mod, weights = varIdent(form = ~1 | plant))	2	8	250.0828	262.9701	-117.0414			

No signs of AR(1) correlation in residuals:

	Model	df	AIC	BIC	logLik	Test	L.Ratio	p-value
mod	1	7	251.9185	263.1949	-118.9592	1 vs 2	2.741499	0.0978
update(mod, correlation = corAR1())	2	8	251.1770	264.0643	-117.5885			

10. Linear mixed-effects model fit by REML *nia1* vs *ein3ox*

"Best" fitted model:

Random effects:
Formula: ~1 | Sample

	(Intercept)	Residual
StdDev:	1.194791	8.156669

Variance function:
Structure: Different standard deviations per stratum
Formula: ~1 | plant
Parameter estimates:

ein3ox	nia1
1.0000000	0.3504705

Fixed effects: Curvature ~ (time + I(time^2)) * plant

	Value	Std.Error	DF	t-value	p-value
(Intercept)	-13.047431	1.899705	31	6.868134	0.0000
time	8.072994	0.381317	31	21.171352	0.0000
I(time^2)	-0.209020	0.013652	31	-15.310231	0.0000
plantein3ox	-4.779698	6.275800	5	-0.761608	0.4807
time:plantein3ox	-2.352139	1.312924	31	-1.791527	0.0830
I(time^2):plantein30x	0.096884	0.047007	31	2.061070	0.0478

Approximate 95% confidence intervals
Approximate 95% confidence intervals

Fixed effects:

	Lower	Est.	upper
(Intercept)	-16.921905944	-13.04743106	-9.1729562
time	7.295292901	8.07299382	8.8506947
I(time^2)	-0.236863583	-0.20901957	-0.1811756
plantein30x	-20.912155351	-4.77969848	11.3527584
time:plantein30x	-5.029864972	-2.35213915	0.3255867
I(time^2):plantein30x	0.001013278	0.09688384	0.1927544

attr(,"label")
[1] "Fixed effects:"

Random Effects:

	Lower	Est.	upper
sd((Intercept))	0.266978	1.194791	5.346975

Variance function:

	Lower	Est.	upper
nia1	0.2152791	0.3504705	0.5705598

attr(,"label")
[1] "Variance function:"
Within-group standard error:

Lower	Est.	upper
5.684447	8.156669	11.704085

LRT of fixed effects:

significance in differences of plant within variability:

	Model	df	AIC	BIC	logLik	Test	L.Ratio	p-value
mod	1	9	270.7522	285.0039	-126.3761	1 vs 2	16.81562	<.0001
update(mod, weights = NULL)	2	8	285.5678	298.2360	-134.7839			

No signs of AR(1) correlation in residuals:

	Model	df	AIC	BIC	logLik	Test	L.Ratio	p-value
mod	1	9	270.7522	285.0039	-126.3761	1 vs 2	0.2691548	0.6039
update(mod, correlation = corAR1())	2	10	272.4831	288.3183	-126.2415			

11. Two way ANOVA for the effect of external application of NAA and cPTIO

Between-Subjects Factors

		Value Label	N
time interval	2	2hr	16
	4	4hr	16
	6	6hr	16
	8	8hr	16
	24	24hr	16
treatments	1	control	20
	2	cPTIO	20
	3	NAA	20
	4	cPTIO+NAA	20

Tests of Between-Subjects Effects

Dependent Variable: curvature

Source	Type III Sum of Squares	df	Mean Square	F	Sig.	Partial Eta Squared
Corrected Model	44084.950[a]	19	2320.261	63.824	.000	.953
Intercept	181260.800	1	181260.800	4985.970	.000	.988
timeinterval	38449.794	4	9612.448	264.411	.000	.946
treatment	1583.275	3	527.758	14.517	.000	.421
timeinterval * treatment	4051.881	12	337.657	9.288	.000	.650
Error	2181.250	60	36.354			
Total	227527.000	80				
Corrected Total	46266.200	79				

a. R Squared = .953 (Adjusted R Squared = .938)

Multiple Comparisons

Dependent Variable: curvature

Tukey HSD

(I) treatments	(J) treatments	Mean Difference (I-J)	Std. Error	Sig.	95% Confidence Interval	
					Lower Bound	Upper Bound
control	cPTIO	11.725*	1.9067	.000	6.687	16.763
	NAA	4.600	1.9067	.086	-.438	9.638
	cPTIO+NAA	8.975*	1.9067	.000	3.937	14.013
cPTIO	control	-11.725*	1.9067	.000	-16.763	-6.687
	NAA	-7.125*	1.9067	.002	-12.163	-2.087
	cPTIO+NAA	-2.750	1.9067	.478	-7.788	2.288
NAA	control	-4.600	1.9067	.086	-9.638	.438
	cPTIO	7.125*	1.9067	.002	2.087	12.163
	cPTIO+NAA	4.375	1.9067	.111	-.663	9.413
cPTIO+NAA	control	-8.975*	1.9067	.000	-14.013	-3.937
	cPTIO	2.750	1.9067	.478	-2.288	7.788
	NAA	-4.375	1.9067	.111	-9.413	.663

Based on observed means.

The error term is Mean Square(Error) = 36.354.

*. The mean difference is significant at the .05 level.

curvature

Tukey HSD[a,b]

treatments	N	Subset		
		1	2	3
cPTIO	20	42.200		
cPTIO+NAA	20	44.950	44.950	
NAA	20		49.325	49.325
control	20			53.925
Sig.		.478	.111	.086

Means for groups in homogeneous subsets are displayed.

Based on observed means.

The error term is Mean Square(Error) = 36.354.

a. Uses Harmonic Mean Sample Size = 20.000.

b. Alpha = .05.

Pairwise Comparisons

Dependent Variable: curvature

time interval	(I) treatments	(J) treatments	Mean Difference (I-J)	Std. Error	Sig.[b]	95% Confidence Interval for Difference[b]	
						Lower Bound	Upper Bound
2hr	control	cPTIO	13.875*	4.263	.011	2.242	25.508
		NAA	34.625*	4.263	.000	22.992	46.258
		cPTIO+NAA	34.625*	4.263	.000	22.992	46.258
	cPTIO	control	-13.875*	4.263	.011	-25.508	-2.242
		NAA	20.750*	4.263	.000	9.117	32.383
		cPTIO+NAA	20.750*	4.263	.000	9.117	32.383
	NAA	control	-34.625*	4.263	.000	-46.258	-22.992
		cPTIO	-20.750*	4.263	.000	-32.383	-9.117
		cPTIO+NAA	1.243E-14	4.263	1.000	-11.633	11.633
	cPTIO+NAA	control	-34.625*	4.263	.000	-46.258	-22.992
		cPTIO	-20.750*	4.263	.000	-32.383	-9.117
		NAA	-1.243E-14	4.263	1.000	-11.633	11.633
4hr	control	cPTIO	10.375	4.263	.108	-1.258	22.008
		NAA	4.000	4.263	1.000	-7.633	15.633
		cPTIO+NAA	4.875	4.263	1.000	-6.758	16.508
	cPTIO	control	-10.375	4.263	.108	-22.008	1.258
		NAA	-6.375	4.263	.841	-18.008	5.258
		cPTIO+NAA	-5.500	4.263	1.000	-17.133	6.133
	NAA	control	-4.000	4.263	1.000	-15.633	7.633
		cPTIO	6.375	4.263	.841	-5.258	18.008
		cPTIO+NAA	.875	4.263	1.000	-10.758	12.508
	cPTIO+NAA	control	-4.875	4.263	1.000	-16.508	6.758
		cPTIO	5.500	4.263	1.000	-6.133	17.133
		NAA	-.875	4.263	1.000	-12.508	10.758
6hr	control	cPTIO	11.500	4.263	.054	-.133	23.133
		NAA	-5.250	4.263	1.000	-16.883	6.383
		cPTIO+NAA	.750	4.263	1.000	-10.883	12.383
	cPTIO	control	-11.500	4.263	.054	-23.133	.133
		NAA	-16.750*	4.263	.001	-28.383	-5.117
		cPTIO+NAA	-10.750	4.263	.086	-22.383	.883
	NAA	control	5.250	4.263	1.000	-6.383	16.883
		cPTIO	16.750*	4.263	.001	5.117	28.383
		cPTIO+NAA	6.000	4.263	.987	-5.633	17.633
	cPTIO+NAA	control	-.750	4.263	1.000	-12.383	10.883

		cPTIO	10.750	4.263	.086	-.883	22.383
		NAA	-6.000	4.263	.987	-17.633	5.633
8hr	control	cPTIO	9.500	4.263	.178	-2.133	21.133
		NAA	-12.250*	4.263	.034	-23.883	-.617
		cPTIO+NAA	-.250	4.263	1.000	-11.883	11.383
	cPTIO	control	-9.500	4.263	.178	-21.133	2.133
		NAA	-21.750*	4.263	.000	-33.383	-10.117
		cPTIO+NAA	-9.750	4.263	.154	-21.383	1.883
	NAA	control	12.250*	4.263	.034	.617	23.883
		cPTIO	21.750*	4.263	.000	10.117	33.383
		cPTIO+NAA	12.000*	4.263	.040	.367	23.633
	cPTIO+NAA	control	.250	4.263	1.000	-11.383	11.883
		cPTIO	9.750	4.263	.154	-1.883	21.383
		NAA	-12.000*	4.263	.040	-23.633	-.367
24hr	control	cPTIO	13.375*	4.263	.016	1.742	25.008
		NAA	1.875	4.263	1.000	-9.758	13.508
		cPTIO+NAA	4.875	4.263	1.000	-6.758	16.508
	cPTIO	control	-13.375*	4.263	.016	-25.008	-1.742
		NAA	-11.500	4.263	.054	-23.133	.133
		cPTIO+NAA	-8.500	4.263	.304	-20.133	3.133
	NAA	control	-1.875	4.263	1.000	-13.508	9.758
		cPTIO	11.500	4.263	.054	-.133	23.133
		cPTIO+NAA	3.000	4.263	1.000	-8.633	14.633
	cPTIO+NAA	control	-4.875	4.263	1.000	-16.508	6.758
		cPTIO	8.500	4.263	.304	-3.133	20.133
		NAA	-3.000	4.263	1.000	-14.633	8.633

Based on estimated marginal means

*. The mean difference is significant at the .05 level.

b. Adjustment for multiple comparisons: Bonferroni.

12. Linear mixed-effects model fit by REML for the effect of external application of NAA and cPTIO

Linear mixed-effects model fit by REML
Data: xdata

AIC	BIC	logLik
534.7499	562.2354	-255.375

Random effects:
Formula: ~1 | Sample

	(Intercept)	Residual
StdDev:	2.435027	10.6079

Variance function:
Structure: Different standard deviations per stratum
Formula: ~1 | plant
Parameter estimates:

Col-0+NAA+cPTIO	Col 0+cPTIO	Col-0+NAA	Col-0
1.0000000	0.4667150	0.6346207	0.2115160

Fixed effects: Curvature ~ (time + I(time^2)) * NAA + CPTIO

	Value	Std.Error	DF	t-value	p-value
(Intercept)	24.98683	1.862832	60	13.413358	0e+00
time	4.57438	0.350245	60	13.060541	0e+00
I(time^2)	-0.08728	0.012549	60	-6.955322	0e+00
NAA	-45.03746	4.516679	13	-9.971365	0e+00
CPTIO	-9.59098	1.775461	13	-5.401965	1e-04
time:NAA	10.63074	1.035182	60	10.269441	0e+00
I(time^2):NAA	-0.36264	0.037089	60	-9.777474	0e+00

intervals(mod)
Approximate 95% confidence intervals
Fixed effects:

	lower	est.	upper
(Intercept)	21.2606114	24.98682970	28.71304802
time	3.8737893	4.57438261	5.27497593
I(time^2)	-0.1123820	-0.08728074	-0.06217946
NAA	-54.7951496	-45.03745769	-35.27976578
CPTIO	-13.4266327	-9.59098133	-5.75532997
time:NAA	8.5600697	10.63074237	12.70141507
I(time^2):NAA	-0.4368273	-0.36263799	-0.28844869

attr(,"label")
[1] "Fixed effects:"
Random Effects:
Level: Sample

	lower	est.	upper
sd((Intercept))	1.093699	2.435027	5.421382

Variance function:

	lower	est.	upper
Col 0+cPTIO	0.2829638	0.4667150	0.7697908
Col-0+NAA	0.3793524	0.6346207	1.0616604
Col-0	0.1267874	0.2115160	0.3528663

attr(,"label")
[1] "Variance function:"

Within-group standard error:

lower	est.	upper
7.402756	10.607902	15.200769

13. Two way ANOVA for the effect of external application of ACC and cPTIO

Between-Subjects Factors

		Value Label	N
time interval	2	2hr	16
	4	4hr	16
	6	6hr	16
	8	8hr	16
	24	24hr	16
treatments	1	control	20
	2	cPTIO	20
	3	ACC	20
	4	cPTIO+ACC	20

Tests of Between-Subjects Effects

Dependent Variable: curvature

Source	Type III Sum of Squares	df	Mean Square	F	Sig.	Partial Eta Squared
Corrected Model	35470.825[a]	19	1866.886	45.783	.000	.935
Intercept	171310.050	1	171310.050	4201.135	.000	.986
timeinterval	29236.513	4	7309.128	179.246	.000	.923
treatment	1919.275	3	639.758	15.689	.000	.440
timeinterval * treatment	4315.038	12	359.586	8.818	.000	.638
Error	2446.625	60	40.777			
Total	209227.500	80				
Corrected Total	37917.450	79				

a. R Squared = .935 (Adjusted R Squared = .915)

Multiple Comparisons

Dependent Variable: curvature

Tukey HSD

(I) treatments	(J) treatments	Mean Difference (I-J)	Std. Error	Sig.	95% Confidence Interval	
					Lower Bound	Upper Bound
control	cPTIO	11.725*	2.0193	.000	6.389	17.061
	ACC	12.125*	2.0193	.000	6.789	17.461
	cPTIO+ACC	6.750*	2.0193	.008	1.414	12.086
cPTIO	control	-11.725*	2.0193	.000	-17.061	-6.389
	ACC	.400	2.0193	.997	-4.936	5.736
	cPTIO+ACC	-4.975	2.0193	.076	-10.311	.361
ACC	control	-12.125*	2.0193	.000	-17.461	-6.789
	cPTIO	-.400	2.0193	.997	-5.736	4.936
	cPTIO+ACC	-5.375*	2.0193	.048	-10.711	-.039
cPTIO+ACC	control	-6.750*	2.0193	.008	-12.086	-1.414
	cPTIO	4.975	2.0193	.076	-.361	10.311
	ACC	5.375*	2.0193	.048	.039	10.711

Based on observed means.

The error term is Mean Square(Error) = 40.777.

*. The mean difference is significant at the .05 level.

curvature

Tukey HSD[a,b]

treatments	N	Subset		
		1	2	3
ACC	20	41.800		
cPTIO	20	42.200	42.200	
cPTIO+ACC	20		47.175	
control	20			53.925
Sig.		.997	.076	1.000

Means for groups in homogeneous subsets are displayed.

Based on observed means.

The error term is Mean Square(Error) = 40.777.

a. Uses Harmonic Mean Sample Size = 20.000.

b. Alpha = .05.

Pairwise Comparisons

Dependent Variable: curvature

treatments	(I) time interval	(J) time interval	Mean Difference (I-J)	Std. Error	Sig.[b]	95% Confidence Interval for Difference[b]	
						Lower Bound	Upper Bound
control	2hr	4hr	-8.500	4.515	.646	-21.660	4.660
		6hr	-15.375*	4.515	.012	-28.535	-2.215
		8hr	-21.625*	4.515	.000	-34.785	-8.465
		24hr	-51.000*	4.515	.000	-64.160	-37.840
	4hr	2hr	8.500	4.515	.646	-4.660	21.660
		6hr	-6.875	4.515	1.000	-20.035	6.285
		8hr	-13.125	4.515	.051	-26.285	.035
		24hr	-42.500*	4.515	.000	-55.660	-29.340
	6hr	2hr	15.375*	4.515	.012	2.215	28.535
		4hr	6.875	4.515	1.000	-6.285	20.035
		8hr	-6.250	4.515	1.000	-19.410	6.910
		24hr	-35.625*	4.515	.000	-48.785	-22.465
	8hr	2hr	21.625*	4.515	.000	8.465	34.785
		4hr	13.125	4.515	.051	-.035	26.285
		6hr	6.250	4.515	1.000	-6.910	19.410
		24hr	-29.375*	4.515	.000	-42.535	-16.215
	24hr	2hr	51.000*	4.515	.000	37.840	64.160
		4hr	42.500*	4.515	.000	29.340	55.660
		6hr	35.625*	4.515	.000	22.465	48.785
		8hr	29.375*	4.515	.000	16.215	42.535
cPTIO	2hr	4hr	-12.000	4.515	.101	-25.160	1.160
		6hr	-17.750*	4.515	.002	-30.910	-4.590
		8hr	-26.000*	4.515	.000	-39.160	-12.840
		24hr	-51.500*	4.515	.000	-64.660	-38.340
	4hr	2hr	12.000	4.515	.101	-1.160	25.160
		6hr	-5.750	4.515	1.000	-18.910	7.410
		8hr	-14.000*	4.515	.029	-27.160	-.840
		24hr	-39.500*	4.515	.000	-52.660	-26.340
	6hr	2hr	17.750*	4.515	.002	4.590	30.910
		4hr	5.750	4.515	1.000	-7.410	18.910
		8hr	-8.250	4.515	.727	-21.410	4.910
		24hr	-33.750*	4.515	.000	-46.910	-20.590
	8hr	2hr	26.000*	4.515	.000	12.840	39.160
		4hr	14.000*	4.515	.029	.840	27.160
		6hr	8.250	4.515	.727	-4.910	21.410
		24hr	-25.500*	4.515	.000	-38.660	-12.340

	24hr	2hr	51.500*	4.515	.000	38.340	64.660
		4hr	39.500*	4.515	.000	26.340	52.660
		6hr	33.750*	4.515	.000	20.590	46.910
		8hr	25.500*	4.515	.000	12.340	38.660
ACC	2hr	4hr	-46.500*	4.515	.000	-59.660	-33.340
		6hr	-49.625*	4.515	.000	-62.785	-36.465
		8hr	-50.625*	4.515	.000	-63.785	-37.465
		24hr	-62.250*	4.515	.000	-75.410	-49.090
	4hr	2hr	46.500*	4.515	.000	33.340	59.660
		6hr	-3.125	4.515	1.000	-16.285	10.035
		8hr	-4.125	4.515	1.000	-17.285	9.035
		24hr	-15.750*	4.515	.009	-28.910	-2.590
	6hr	2hr	49.625*	4.515	.000	36.465	62.785
		4hr	3.125	4.515	1.000	-10.035	16.285
		8hr	-1.000	4.515	1.000	-14.160	12.160
		24hr	-12.625	4.515	.069	-25.785	.535
	8hr	2hr	50.625*	4.515	.000	37.465	63.785
		4hr	4.125	4.515	1.000	-9.035	17.285
		6hr	1.000	4.515	1.000	-12.160	14.160
		24hr	-11.625	4.515	.125	-24.785	1.535
	24hr	2hr	62.250*	4.515	.000	49.090	75.410
		4hr	15.750*	4.515	.009	2.590	28.910
		6hr	12.625	4.515	.069	-.535	25.785
		8hr	11.625	4.515	.125	-1.535	24.785
cPTIO+ACC	2hr	4hr	-48.250*	4.515	.000	-61.410	-35.090
		6hr	-55.375*	4.515	.000	-68.535	-42.215
		8hr	-61.250*	4.515	.000	-74.410	-48.090
		24hr	-71.000*	4.515	.000	-84.160	-57.840
	4hr	2hr	48.250*	4.515	.000	35.090	61.410
		6hr	-7.125	4.515	1.000	-20.285	6.035
		8hr	-13.000	4.515	.055	-26.160	.160
		24hr	-22.750*	4.515	.000	-35.910	-9.590
	6hr	2hr	55.375*	4.515	.000	42.215	68.535
		4hr	7.125	4.515	1.000	-6.035	20.285
		8hr	-5.875	4.515	1.000	-19.035	7.285
		24hr	-15.625*	4.515	.010	-28.785	-2.465
	8hr	2hr	61.250*	4.515	.000	48.090	74.410

		4hr	13.000	4.515	.055	-.160	26.160
		6hr	5.875	4.515	1.000	-7.285	19.035
		24hr	-9.750	4.515	.348	-22.910	3.410
	24hr	2hr	71.000*	4.515	.000	57.840	84.160
		4hr	22.750*	4.515	.000	9.590	35.910
		6hr	15.625*	4.515	.010	2.465	28.785
		8hr	9.750	4.515	.348	-3.410	22.910

Based on estimated marginal means

*. The mean difference is significant at the .05 level.

b. Adjustment for multiple comparisons: Bonferroni.

14. Linear mixed-effects model fit by REML for the effect of external application of ACC and cPTIO

Linear mixed-effects model fit by REML
Data: xdata

AIC	BIC	logLik
568.6581	596.1436	-272.3291

Random effects:
Formula: ~1 | Sample

	(Intercept)	Residual
StdDev:	4.294053	13.06868

Variance function:
Structure: Different standard deviations per stratum
Formula: ~1 | plant
Parameter estimates:

Col-0+ACC+cPTIO	Col-0+ACC	Col 0+cPTIO	Col-0
1.0000000	0.9048999	0.3724916	0.1717896

Fixed effects: Curvature ~ (time + I(time^2)) * ACC + CPTIO

	Value	Std.Error	DF	t-value	p-value
(Intercept)	23.45498	2.473346	60	9.483096	0.0000
time	4.57935	0.349394	60	13.106549	0.0000
I(time^2)	-0.08747	0.012518	60	-6.987572	0.0000
ACC	-34.28600	6.805243	13	-5.038174	0.0002
CPTIO	-6.57859	2.729322	13	-2.410339	0.0315
time:ACC	8.40530	1.542868	60	5.447844	0.0000
I(time^2):ACC	-0.31505	0.055279	60	-5.699230	0.0000

Approximate 95% confidence intervals
Fixed effects:

	lower	est.	upper
(Intercept)	18.5075470	23.45497534	28.40240365
time	3.8804537	4.57934503	5.27823638
I(time^2)	-0.1125127	-0.08747242	-0.06243212
ACC	-48.9878307	-34.28599744	-19.58416420
CPTIO	-12.4749328	-6.57859127	-0.68224976
time:ACC	5.3191082	8.40530376	11.49149930
I(time^2):ACC	-0.4256207	-0.31504659	-0.20447252

attr(,"label")
[1] "Fixed effects:"
Random Effects:
Level: Sample

	lower	est.	upper
sd((Intercept))	1.840286	4.294053	10.01958

Variance function:

	lower	est.	upper
Col-0+ACC	0.52400733	0.9048999	1.5626573
Col 0+cPTIO	0.21531716	0.3724916	0.6443982
Col-0	0.09794928	0.1717896	0.3012953

attr(,"label")
[1] "Variance function:"
Within-group standard error:

lower	est.	upper
8.545841	13.068676	19.985195

15. Two way ANOVA for the effect of external application of SNAP and cPTIO

Between-Subjects Factors

		Value Label	N
time interval	2	2hr	16
	4	4hr	16
	6	6hr	16
	8	8hr	16
	24	24hr	16
treatments	1	control	20
	2	cPTIO	20
	3	SNAP	20
	4	cPTIO+SNAP	20

Tests of Between-Subjects Effects

Dependent Variable: curvature

Source	Type III Sum of Squares	df	Mean Square	F	Sig.	Partial Eta Squared
Corrected Model	29672.200[a]	19	1561.695	69.255	.000	.956
Intercept	225993.800	1	225993.800	10021.898	.000	.994
timeinterval	24458.231	4	6114.558	271.156	.000	.948
treatment	3536.875	3	1178.958	52.282	.000	.723
timeinterval * treatment	1677.094	12	139.758	6.198	.000	.553
Error	1353.000	60	22.550			
Total	257019.000	80				
Corrected Total	31025.200	79				

a. R Squared = .956 (Adjusted R Squared = .943)

Multiple Comparisons

Dependent Variable: curvature

Tukey HSD

(I) treatments	(J) treatments	Mean Difference (I-J)	Std. Error	Sig.	95% Confidence Interval	
					Lower Bound	Upper Bound
control	cPTIO	11.725*	1.5017	.000	7.757	15.693
	SNAP	-5.825*	1.5017	.001	-9.793	-1.857
	cPTIO+SNAP	-2.800	1.5017	.254	-6.768	1.168
cPTIO	control	-11.725*	1.5017	.000	-15.693	-7.757
	SNAP	-17.550*	1.5017	.000	-21.518	-13.582
	cPTIO+SNAP	-14.525*	1.5017	.000	-18.493	-10.557
SNAP	control	5.825*	1.5017	.001	1.857	9.793
	cPTIO	17.550*	1.5017	.000	13.582	21.518
	cPTIO+SNAP	3.025	1.5017	.194	-.943	6.993
cPTIO+SNAP	control	2.800	1.5017	.254	-1.168	6.768
	cPTIO	14.525*	1.5017	.000	10.557	18.493
	SNAP	-3.025	1.5017	.194	-6.993	.943

Based on observed means.

The error term is Mean Square(Error) = 22.550.

*. The mean difference is significant at the .05 level.

curvature

Tukey HSD[a,b]

treatments	N	Subset		
		1	2	3
cPTIO	20	42.200		
control	20		53.925	
cPTIO+SNAP	20		56.725	56.725
SNAP	20			59.750
Sig.		1.000	.254	.194

Means for groups in homogeneous subsets are displayed.

Based on observed means.

The error term is Mean Square(Error) = 22.550.

a. Uses Harmonic Mean Sample Size = 20.000.

b. Alpha = .05.

Pairwise Comparisons

Dependent Variable: curvature

time interval	(I) treatments	(J) treatments	Mean Difference (I-J)	Std. Error	Sig.[b]	95% Confidence Interval for Difference[b]	
						Lower Bound	Upper Bound
2hr	control	cPTIO	13.875*	3.358	.001	4.713	23.037
		SNAP	7.625	3.358	.161	-1.537	16.787
		cPTIO+SNAP	10.875*	3.358	.012	1.713	20.037
	cPTIO	control	-13.875*	3.358	.001	-23.037	-4.713
		SNAP	-6.250	3.358	.406	-15.412	2.912
		cPTIO+SNAP	-3.000	3.358	1.000	-12.162	6.162
	SNAP	control	-7.625	3.358	.161	-16.787	1.537
		cPTIO	6.250	3.358	.406	-2.912	15.412
		cPTIO+SNAP	3.250	3.358	1.000	-5.912	12.412
	cPTIO+SNAP	control	-10.875*	3.358	.012	-20.037	-1.713
		cPTIO	3.000	3.358	1.000	-6.162	12.162
		SNAP	-3.250	3.358	1.000	-12.412	5.912
4hr	control	cPTIO	10.375*	3.358	.018	1.213	19.537
		SNAP	-10.500*	3.358	.016	-19.662	-1.338
		cPTIO+SNAP	-8.125	3.358	.111	-17.287	1.037
	cPTIO	control	-10.375*	3.358	.018	-19.537	-1.213
		SNAP	-20.875*	3.358	.000	-30.037	-11.713
		cPTIO+SNAP	-18.500*	3.358	.000	-27.662	-9.338
	SNAP	control	10.500*	3.358	.016	1.338	19.662
		cPTIO	20.875*	3.358	.000	11.713	30.037
		cPTIO+SNAP	2.375	3.358	1.000	-6.787	11.537
	cPTIO+SNAP	control	8.125	3.358	.111	-1.037	17.287
		cPTIO	18.500*	3.358	.000	9.338	27.662
		SNAP	-2.375	3.358	1.000	-11.537	6.787
6hr	control	cPTIO	11.500*	3.358	.007	2.338	20.662
		SNAP	-13.750*	3.358	.001	-22.912	-4.588
		cPTIO+SNAP	-11.125*	3.358	.009	-20.287	-1.963
	cPTIO	control	-11.500*	3.358	.007	-20.662	-2.338
		SNAP	-25.250*	3.358	.000	-34.412	-16.088
		cPTIO+SNAP	-22.625*	3.358	.000	-31.787	-13.463
	SNAP	control	13.750*	3.358	.001	4.588	22.912
		cPTIO	25.250*	3.358	.000	16.088	34.412
		cPTIO+SNAP	2.625	3.358	1.000	-6.537	11.787

	cPTIO+SNAP	control	11.125*	3.358	.009	1.963	20.287
		cPTIO	22.625*	3.358	.000	13.463	31.787
		SNAP	-2.625	3.358	1.000	-11.787	6.537
8hr	control	cPTIO	9.500*	3.358	.038	.338	18.662
		SNAP	-17.125*	3.358	.000	-26.287	-7.963
		cPTIO+SNAP	-12.375*	3.358	.003	-21.537	-3.213
	cPTIO	control	-9.500*	3.358	.038	-18.662	-.338
		SNAP	-26.625*	3.358	.000	-35.787	-17.463
		cPTIO+SNAP	-21.875*	3.358	.000	-31.037	-12.713
	SNAP	control	17.125*	3.358	.000	7.963	26.287
		cPTIO	26.625*	3.358	.000	17.463	35.787
		cPTIO+SNAP	4.750	3.358	.974	-4.412	13.912
	cPTIO+SNAP	control	12.375*	3.358	.003	3.213	21.537
		cPTIO	21.875*	3.358	.000	12.713	31.037
		SNAP	-4.750	3.358	.974	-13.912	4.412
24hr	control	cPTIO	13.375*	3.358	.001	4.213	22.537
		SNAP	4.625	3.358	1.000	-4.537	13.787
		cPTIO+SNAP	6.750	3.358	.293	-2.412	15.912
	cPTIO	control	-13.375*	3.358	.001	-22.537	-4.213
		SNAP	-8.750	3.358	.069	-17.912	.412
		cPTIO+SNAP	-6.625	3.358	.319	-15.787	2.537
	SNAP	control	-4.625	3.358	1.000	-13.787	4.537
		cPTIO	8.750	3.358	.069	-.412	17.912
		cPTIO+SNAP	2.125	3.358	1.000	-7.037	11.287
	cPTIO+SNAP	control	-6.750	3.358	.293	-15.912	2.412
		cPTIO	6.625	3.358	.319	-2.537	15.787
		SNAP	-2.125	3.358	1.000	-11.287	7.037

Based on estimated marginal means

*. The mean difference is significant at the .05 level.

b. Adjustment for multiple comparisons: Bonferroni.

16. Linear mixed-effects model fit by REML for the effect of external application of SNAP and cPTIO

Data: xdata

AIC	BIC	logLik
506.0241	533.5096	-241.012

Random effects:
Formula: ~1 | Sample

	(Intercept)	Residual
StdDev:	3.216746	4.906842

Variance function:
Structure: Different standard deviations per stratum
Formula: ~1 | plant
Parameter estimates:

Col-0+ACC+cPTIO	Col-0+SNAP	Col-0+SNAP+cPTIO	Col-0
1.0000000	1.1178255	1.0063424	0.4573264

Fixed effects: Curvature ~ (time + I(time^2)) * SNAP + CPTIO

	Value	Std.Error	DF	t-value	p-value
(Intercept)	24.111074	2.052088	60	11.749534	0.0000
time	4.576941	0.349745	60	13.086514	0.0000
I(time^2)	-0.087380	0.012531	60	-6.973146	0.0000
SNAP	-11.148867	3.432663	13	-3.247877	0.0064
CPTIO	-7.754643	1.898413	13	-4.084804	0.0013
time:SNAP	6.129684	0.719649	60	8.517602	0.0000
I(time^2):SNAP	-0.235755	0.025784	60	-9.143452	0.0000

Approximate 95% confidence intervals

	lower	est.	upper
(Intercept)	20.0062875	24.11107410	28.21586075
time	3.8773475	4.57694146	5.27653542
I(time^2)	-0.1124450	-0.08737958	-0.06231411
SNAP	-18.5646837	-11.14886663	-3.73304952
CPTIO	-11.8559144	-7.75464349	-3.65337263
time:SNAP	4.6901713	6.12968357	7.56919582
I(time^2):SNAP	-0.2873306	-0.23575488	-0.18417918

attr(,"label")
[1] "Fixed effects:"

Random Effects:
Level: Sample

	lower	est.	upper
sd((Intercept))	1.842989	3.216746	5.614499

Variance function:

	lower	est.	upper
Col-0+SNAP	0.6675413	1.1178255	1.8718452
Col-0+SNAP+cPTIO	0.5997378	1.0063424	1.6886131
Col-0	0.2719230	0.4573264	0.7691422

attr(,"label")
[1] "Variance function:"
Within-group standard error:

lower	est.	upper
3.402177	4.906842	7.076966

17. Sequence analysis for single copy transgenic line selection

>C2+3.5-1_IGFP-F -- 17..823 of sequence

GAGACCACATGGTCCTTCTTGAGTTTGTAACAGCTGCTGGGATTACACATGGCATGGATGAACTATACAAAT
AA*GCGGCCGCCA*CCGCGGTGGAGCTCCAGCTTTTGTTCCCTTTAGTGAGGGTTAATTGCGCGCTTGGCGTAA
TCATGGTCATAGCTGTTTCCTGTGTGAAATTGTTATCCGCTCACAATTCCACACAACATACGAGCCGGAAGCA
TAAAGTGTAAAGCCTGGGGTGCCTAATGAGTGAGCTAACTCACATTAATTGCGTTGCGCTCACTGCCCGCTT
TCCAGTCGGGAAACCTGTCGTGCCAGCTGCATTAATGAATCGGCCAACGCGCGGGGAGAGGCGGTTTGCGT
ATTGGGCGCTCTTCCGCTTCCTCGCTCACTGACTCGCTGCGCTCGGTCGTTCGGCTGCGGCGAGCGGTATCA
GCTCACTCAAAGGCGGTAATACGGTTATCCACAGAATCAGGGGATAACGCAGGAAAGAACATGAAGGCCTT
GATTAGCCTTCGGGTTCTGCAAGAGCTTTTGCTTCAGCTCCTTTCCATTTCCATCTAGGCGCCATGGAATTGA
GCTGCATATATAGCACTAAAAATCAAACCTTTTGACCAAAAGATGTAAAAGCTTTTCTTAGTCTATTACCAAC
CTACAACTCTTATAATCTAGGAAATCAGATAAACATTGTCACTACGACATAGTTGTTTAACGTTTAAGGTATC
TTGAAGAACCAAGTAGGAATTGGAAATGAGCAAAACCAGAGCTTTTTGATTCTTTTCCCACTTTTGTATTCAA
AAATCAAATCTC

Arabidopsis thaliana chromosome 5, complete sequence
Sequence ID: gb|CP002688.1|Length: 26975502Number of Matches: 1

Range 1: 24250885 to 24251168

Score	Expect	Identities	Gaps	Strand
499 bits(270)	3e-140	283/288(98%)	5/288(1%)	Plus/Plus

```
Query  11        GGTTCTGCAAGAGCTTTTGCTTCAGCTCCTTTCCATTTCCATCTAGGCGCCATGGAATTG  70
                  ||||||||||||||||||||||||||||||||||||||||||||||||||||||||||||
Sbjct  24250885  GGTTCTGCAAGAGCTTTTGCTTCAGCTCCTTTCCATTTCCATCTAGGCGCCATGGAATTG  24250944

Query  71        AGCTGCATATATAGCACTAAAAATCAAACCTTTTGACCAAAAGATGTAAAAGCTTTTCTT  130
                  ||||||||||||||||||||||||||||||||||||||||||||||||||||||||||||
Sbjct  24250945  AGCTGCATATATAGCACTAAAAATCAAACCTTTTGACCAAAAGATGTAAAAGCTTTTCTT  24251004

Query  131       AGTCTATTACCAACCTACAACTCTTATAATCTAGGAAATCAGATAAACATTGTCACTACG  190
                  |||||||||||||| ||||||||||||||||||||||||||||||||||||||||||||
Sbjct  24251005  AGTCTATTACCAA-CTACAACTCTTATAATCTAGGAAATCAGATAAACATTGTCACTACG  24251063

Query  191       ACATAGTTGTTTAACGTTTAAGGTATCTTGAAGAACCAAGTAGGAATTGGAAATGAGCAA  250
                  ||||||||| |||||||||||||||||||||||||||||||||||| |||||||||
Sbjct  24251064  ACATAGTTG-TTAACGTTTAAGGTATCTTGAAGAACCAAGTAGGAATTGG-AATGAGCAA  24251121

Query  251       AACCA-GAGCTTTTTGATTCTTTTCCCACTTTTGTATTCAAAAATCAA  297
                  ||||| |||| ||||||||||||||||||||||||||||||||||||
Sbjct  24251122  AACCAAGAGC-TTTTGATTCTTTTCCCACTTTTGTATTCAAAAATCAA  24251168
```

In Col-0 NIA1Pro-NIA1-mGFP4 tranagenic line-2, T-DNA was inserted in chromosome five at 24,250,885 position.